

ADSORPTION OF ACETALDEHYDE, PROPIONALDEHYDE,  
AND BUTYRALDEHYDE ON SILICA GEL AND  
MOLECULAR SIEVE-13X

By

TUSHAR KANTI GHOSH

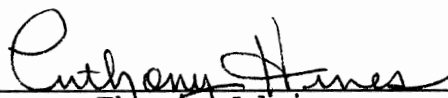
Bachelor of Chemical Engineering  
University of Jadavpur  
Jadavpur, Calcutta, India  
1980

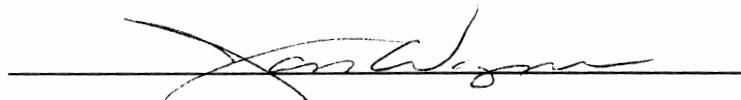
Master of Science in Chemical Engineering  
University of Calgary  
Calgary, Alberta, Canada  
1985

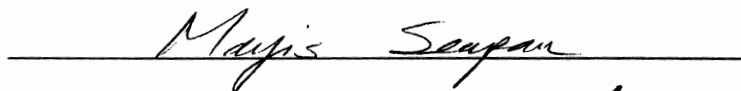
Submitted to the Faculty of the  
Graduate College of the  
Oklahoma State University  
in partial fulfillment of  
the requirements for  
the Degree of  
DOCTOR OF PHILOSOPHY  
July, 1989

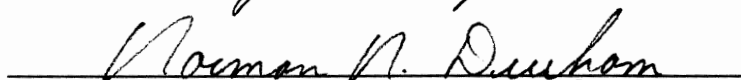
ADSORPTION OF ACETALDEHYDE, PROPIONALDEHYDE,  
AND BUTYRALDEHYDE ON SILICA GEL AND  
MOLECULAR SIEVE-13X

Thesis Approved:

  
\_\_\_\_\_  
Thesis Adviser

  
\_\_\_\_\_  
William F. McFarman

  
\_\_\_\_\_  
Majis Seapan

  
\_\_\_\_\_  
Dean of the Graduate College

## PREFACE

Pure component adsorption isotherms of acetaldehyde, propionaldehyde, and butyraldehyde on silica gel and molecular sieve-13X were determined gravimetrically by using a Cahn R-2000 electrobalance. The adsorption isotherms of acetaldehyde, propionaldehyde, and butyraldehyde on silica gel were of Type I isotherms and gave hysteresis upon desorption. The adsorption isotherms of these aldehydes on molecular sieve appeared to be of type I at higher temperatures but were of type II at lower temperatures and also produced hysteresis upon desorption. The heat of adsorption data suggested that both the adsorbents were heterogeneous in nature and strong lateral interaction existed between the adsorbed molecules.

The Langmuir and the BET equations gave a poor correlation of the data on both the adsorbents when entire pressure range was considered. However the BET equations provided a good fit to the data in the relative pressure range of  $0.05 \leq P/P_s \leq 0.2$ . Although the equations, developed by Sircar and Kuo and Hines for heterogeneous surfaces, provided a good correlation of the data for Type I isotherms, gave a large deviation for Type II isotherms in the high pressure region.

An isotherm for multilayer adsorption on heterogeneous surface was developed using the Jovanovic isotherm for multilayer coverage as the local isotherm. The energy distribution of a site was described by the combination of two distribution functions. The new model provided an excellent fit to the experimental data for both Type I and Type II isotherms.

The new isotherm was extended to binary mixture and was combined with the adsorption solution theory to predict the binary adsorption equilibrium data. The mole fractions in the adsorbed phase predicted by the present method for binary mixtures of hydrocarbons on activated carbons were in close agreement with the experimental data but showed some deviation for activity coefficients.

Silica gel was found to be more suitable for separation of the aldehydes and molecular sieve could be used to remove these aldehydes together from a gas stream. The lighter aldehydes were displaced by the heavier ones from the adsorbent surfaces. The concentrations of lighter aldehydes became higher than their inlet concentrations and later decreased to the inlet concentrations. The displacement of the lighter aldehydes by the heavier ones was more pronounced in the silica gel bed than was observed in a molecular sieve bed.

## ACKNOWLEDGEMENT

The author wishes to express his deepest sense of gratitude and respect to Dr. A.L. Hines for his continuous inspiration and guidance in this project.

The author also wishes to convey his sincere thanks to his co-advisor Dr. J. Wagner and Dr. Johnson for their interest, constructive criticism and valuable suggestions in the course of this work. The assistance and encouragement of the other committee members, Dr. M. Seapan, and Dr. W.F. Mcternan are gratefully recognized and appreciated. The continuous encouragement and inspiration of Dr. E.L. Tollefson, University of Calgary, Alberta, Canada, are gratefully appreciated.

The author is deeply indebted to the School of Chemical Engineering, Oklahoma State University, for the financial support provided during the course of this study.

The author would like to thank Mr. Charles Baker, Mrs. Dee Maule, Mrs. M. Kitchens, and other secretaries of the School of Chemical Engineering for their assistance and timely help. The author also appreciates the friendship and co-operation of Mousa Abu-Arabi and fellow graduate students of this department.

The author would like to express a special thanks to

Nancy, University of Missouri-Columbia, for her assistance in preparing this manuscript.

The author wishes to express his deepest respect and gratitude to his parents, brother, and sisters for their constant encouragement and support.

## TABLE OF CONTENTS

Chapter	Page
I. ADSORPTION OF ACETALDEHYDE, PROPIONALDEHYDE, AND BUTYRALDEHYDE ON SILICA GEL .....	1
Abstract .....	2
Introduction .....	3
Experimental Section .....	4
Materials and Apparatus .....	4
Procedure .....	5
Results and Discussions .....	6
Equilibrium Data .....	6
Data Correlation .....	8
Nomenclature .....	13
References .....	14
List of Tables .....	15
List of Figures .....	16
II. ADSORPTION OF ACETALDEHYDE, PROPIONALDEHYDE, AND BUTYRALDEHYDE ON MOLECULAR SIEVE 13X .....	30
Abstract .....	31
Introduction .....	32
Experimental Section .....	33
Materials and Apparatus .....	33
Procedure .....	34
Results and Discussions .....	35
Equilibrium Data .....	35
Data Correlation .....	37
Nomenclature .....	42
References .....	43
List of Tables .....	45
List of Figures .....	46
III. AN ISOTHERM FOR MULTILAYER ADSORPTION ON HETEROGENEOUS SURFACES .....	60
Abstract .....	61
Introduction .....	62
Theory .....	65
Test of the New Model .....	73
Nomenclature .....	77
References .....	78

Chapter	Page
List of Tables .....	80
List of Figures .....	81
VI.    PREDICTION OF BINARY ADSORPTION EQUILIBRIA FROM PURE COMPONENT DATA .....	96
Abstract .....	97
Introduction .....	98
Theory .....	102
Testing of the Model .....	107
Nomenclature .....	110
References .....	112
List of Tables .....	114
V.    ADSORPTION OF MULTICOMPONENT MIXTURES IN FIXED BEDS: AN EXPERIMENTAL INVESTIGATION .....	122
Abstract .....	123
Introduction .....	124
Experimental Section .....	126
Material and Apparatus .....	126
Results and Discussions .....	129
Pure Component Breakthrough Curves ...	129
Binary and Ternary Breakthrough Curves .....	132
Conclusions .....	136
References .....	137
List of Tables .....	138
List of Figures .....	139
VI.    CONCLUSIONS AND RECOMMENDATIONS .....	163
Conclusions .....	164
Recommendations .....	165
APPENDICES .....	166
APPENDIX A    CALCULATION FOR BUOYANCY EFFECTS ON WEIGHT MEASUREMENTS .....	167
APPENDIX B    CALCULATION FOR ISOTHERIC HEAT OF ADSORPTION .....	168
APPENDIX C    PLOTS OF THE EXPERIMENTAL DATA ACCORDING TO THE LANGMUIR, THE BET, AND THE FREUNDLICH EQUATION .....	170
APPENDIX D    CALCULATION OF MONOLAYER COVERAGES AND SURFACE AREAS FROM EQUILIBRIUM ISOTHERM DATA .....	175



APPENDIX E	ESTIMATIONS OF THE CONSTANTS IN THE KYO-HINES AND THE SIRCAR MODEL .....	179
APPENDIX F	CALCULATION FOR ENERGY DISTRIBUTION FUNCTION .....	182
APPENDIX G	PROPERTIES OF THE NEW ISOTHERM EQUATION AND CALCULATION OF THE HENRY'S LAW CONSTANT FROM THE NEW ISOTHERM .....	183
APPENDIX H	EXPERIMENTAL DATA FOR BINARY MIXTURES OF ALDEHYDES .....	186

## LIST OF TABLES

### CHAPTER I

Table		Page
I.	Monolayer Coverages and Calculated Surface Areas of Silica Gel .....	17
II.	Henry's Law Constants and Best Fit Parameters for the Kuo-Hines Model .....	18
III.	Comparison of Model Correlations .....	19

### CHAPTER II

I.	Monolayer Coverages and Calculated Surface Areas of Molecular Sieve-13X .....	47
II.	Best Fit Parameters for the Sircar and the Kuo-Hines Model .....	48
III.	Comparison of Model Correlations .....	49

### CHAPTER III

I.	Model Parameters for Methane, Ethylene, Ethane, and Propylene Adsorption on Activated Carbon at 293.2 K .....	82
II.	Best Fit Parameters of the New Model for Acetaldehyde, Propionaldehyde, and Butyraldehyde Adsorption on Molecular Sieve-13X .....	83

Table	Page
III. Best Fit Parameters of the New Model for Carbon Dioxide, Ethane, Ethylene, and Isobutane Adsorption on Molecular Sieve-13X .....	84
IV. Best Fit Parameters of the New Model for Carbon Dioxide, Hydrogen Sulfide, and Propane Adsorption on H-Mordenite at 283.2 K .....	85

#### CHAPTER IV

I. Parameters of the Pure Component Isotherm Equation (3) and of the Spreading Pressure Equation (18) for Methane, Ethylene, Ethane, and Propylene Adsorption on Activated Carbon at 293.2K .....	115
II. Mole Fraction in the Adsorbed Phase, Total Amount Adsorbed, and Activity Coefficients for the Methane(1)-Ethylene(2) Mixture .....	116
III. Mole Fraction in the Adsorbed Phase, Total Amount Adsorbed, and Activity Coefficients for the Methane(1)-Ethane(2) Mixture .....	116
IV. Mole Fraction in the Adsorbed Phase, Total Amount Adsorbed, and Activity Coefficients for the Ethylene(1)-Ethane(2) Mixture .....	117
V. Mole Fraction in the Adsorbed Phase, Total Amount Adsorbed, and Activity Coefficients for the Ethylene(1)-Propylene(2) Mixture .....	117
VI. Mole Fraction in the Adsorbed Phase, Total Amount Adsorbed, and Activity Coefficients for the Ethane(1)-Propylene(2) Mixture .....	118
VII. Spreading Pressure ( $\Pi_m A/RT$ ) of the Mixture and the Equilibrium Pressure ( $P_i$ ) of the Individual Component in the Binary Mixture ...	119

#### CHAPTER V

I. Description of the Adsorption Columns and Properties of the Adsorbents .....	141
---	-----

Table	Page
II. Operating Conditions for Gas Chromatograph ...	142

#### APPENDICES

D.I	Data for Calculation of Monolayer Coverage and Surface Area of Silica Gel Occupied by Acetaldehyde at 298.2 K .....	176
H.I	Experimental Data for Acetaldehyde Adsorption on Silica Gel .....	206
H.II	Experimental Data for Propionaldehyde Adsorption on Silica Gel .....	207
H.III	Experimental Data for Butyraldehyde Adsorption on Silica Gel .....	208
H.IV	Experimental Data for Acetaldehyde Adsorption on Molecular Sieve-13X .....	209
H.V	Experimental Data for Propionaldehyde Adsorption on Molecular Sieve-13X .....	210
H.VI	Experimental Data for Butyraldehyde Adsorption on Molecular Sieve-13X .....	211
H.VII	Experimental Data for Breakthrough Curves of Acetaldehyde on Silica Gel .....	212
H.VIII	Experimental Data for Breakthrough Curves of Propionaldehyde on Silica Gel .....	213
H.IX	Experimental Data for Breakthrough Curves of Butyraldehyde on Silica Gel .....	214
H.X	Experimental Data for Breakthrough Curves of Acetaldehyde on Molecular Sieve-13X .....	215
H.XI	Experimental Data for Breakthrough Curves of Propionaldehyde on Molecular Sieve-13X ..	216
H.XII	Experimental Data for Breakthrough Curves of Butyraldehyde on Molecular Sieve-13X ....	217
H.XIII	Experimental Data for Breakthrough Curves : Binary Mixtures of Acetaldehyde and Propionaldehyde on Silica Gel .....	218

Table	Page
H.XIV	Experimental Data for Breakthrough Curves : Binary Mixtures of Propionaldehyde and Butyraldehyde on Silica Gel ..... 219
H.XV	Experimental Data for Breakthrough Curves : Binary Mixtures of Acetaldehyde and Butyraldehyde on Silica Gel ..... 220
H.XVI	Experimental Data for Breakthrough Curves : Ternary Mixtures of Aldehydes on Silica Gel ..... 222
H.XVII	Experimental Data for Breakthrough Curves : Binary Mixtures of Acetaldehyde and Butyraldehyde on Molecular Sieve-13X ..... 224
H.XVIII	Experimental Data for Breakthrough Curves : Binary Mixtures of Acetaldehyde and Propionaldehyde on Molecular Sieve-13X ..... 225
H.XIX	Experimental Data for Breakthrough Curves : Binary Mixtures of Propionaldehyde and Butyraldehyde on Molecular Sieve-13X ..... 226
H.XX	Experimental Data for Breakthrough Curves : Ternary Mixtures of Aldehydes on Molecular Sieve-13X ..... 227

## LIST OF FIGURES

Figure		Page
1.	Adsorption and Desorption Curves for Acetaldehyde on Silica Gel (6-12 mesh) .....	20
2.	Adsorption and Desorption Curves for Propionaldehyde on Silica Gel (6-12 mesh) ...	21
3.	Adsorption and Desorption Curves for Butyraldehyde on Silica Gel (6-12 mesh) .....	22
4.	Heat of Adsorption at Different Loadings for Aldehydes on Silica Gel (6-12 mesh) .....	23
5.	Characteristic Curve for Acetaldehyde on Silica Gel (6-12 mesh) .....	24
6.	Characteristic Curve for Propionaldehyde on Silica Gel (6-12 mesh) .....	25
7.	Characteristic Curve for Butyraldehyde on Silica Gel (6-12 mesh) .....	26
8.	Comparison of the Experimental Data with the Kuo-Hines Model for Acetaldehyde-Silica Gel System .....	27
9.	Comparison of the Experimental Data with the Kuo-Hines Model for Propionaldehyde-Silica Gel System .....	28
10.	Comparison of the Experimental Data with the Kuo-Hines Model for Butyraldehyde-Silica Gel System .....	29

## CHAPTER II

1.	Adsorption and Desorption Curves for Acetaldehyde on Molecular Sieve-13X .....	50
----	--	----

Figure		Page
2.	Adsorption and Desorption Curves for Propionaldehyde on Molecular Sieve-13X .....	51
3.	Adsorption and Desorption Curves for Butyraldehyde on Molecular Sieve-13X .....	52
4.	Heat of Adsorption at Different Loadings for Aldehydes on Molecular Sieve-13X .....	53
5.	Characteristic Curve for Acetaldehyde on Molecular Sieve-13X .....	54
6.	Characteristic Curve for Propionaldehyde on Molecular Sieve-13X .....	55
7.	Characteristic Curve for Butyraldehyde on Molecular Sieve-13X .....	56
8.	Comparison of the Experimental Data with the Sircar and the Kuo-Hines Model for Acetaldehyde-Molecular Sieve-13X System .....	57
9.	Comparison of the Experimental Data with the Sircar and the Kuo-Hines Model for Propionaldehyde-Molecular Sieve-13X System ..	58
10.	Comparison of the Experimental Data with the Sircar and the Kuo-Hines Model for Butyraldehyde-Molecular Sieve-13X System .....	59

### CHAPTER III

1.	Energy Distribution on the Adsorbent Surface in $q_A/RT$ Domain for Constant $b_O$ , $\epsilon_M$ , $q_B/RT$ , and $A_2$ .....	86
2.	Equilibrium Isotherms of Methane, Ethane, Ethylene, and Propylene on Activated Carbon at 293.2 K (Experimental Data of Costa, et. al., 1981) .....	87
3.	Equilibrium Isotherms of Acetaldehyde on Molecular Sieve-13X (Experimental Data of Ghosh, 1989) .....	88
4.	Equilibrium Isotherms of Propionaldehyde on Molecular Sieve-13X (Experimental Data of Ghosh, 1989) .....	89

Figure		Page
5.	Equilibrium Isotherms of Butyraldehyde on Molecular Sieve-13X (Experimental Data of Ghosh, 1989) .....	90
6.	Equilibrium Isotherms of Carbon Dioxide on Molecular Sieve-13X (Experimental Data of Hyun and Danner, 1982) .....	91
7.	Equilibrium Isotherms of Ethane on Molecular Sieve-13X (Experimental Data of Hyun and Danner, 1982) .....	92
8.	Equilibrium Isotherms of Ethylene on Molecular Sieve-13X (Experimental Data of Hyun and Danner, 1982) .....	93
9.	Equilibrium Isotherms of Isobutane on Molecular Sieve-13X (Experimental Data of Hyun and Danner, 1982) .....	94
10.	Equilibrium Isotherms of Carbon Dioxide, Hydrogen Sulfide, and Propane on H-Mordenite at 283.2 K (Experimental Data of Talu and Zwiebel, 1986) .....	95

## CHAPTER V

1.	A Schematic Flow Diagram of the Experimental Apparatus .....	143
2.	Calculation of Total Amount Adsorbed from a Breakthrough Curve .....	144
3.	Effects of Flow Rate on Breakthrough Curves for Acetaldehyde in a Silica Gel Bed .....	145
4.	Effects of Flow Rate on Breakthrough Curves for Acetaldehyde in a Molecular sieve-13X Bed .....	146
5.	Effects of Inlet Concentration on Breakthrough Curves for Propionaldehyde in a Silica Gel Bed .....	147
6.	Effects of Inlet Concentration on Breakthrough for Propionaldehyde in a Molecular Sieve-13X Bed .....	148



Figure		Page
7.	Effects of Temperature on Breakthrough Curves for Butyraldehyde in a Silica Gel Bed	149
8.	Effects of Temperature on Breakthrough Curves for Butyraldehyde in a Molecular Sieve-13X Bed .....	150
9.	Effects of Flow Rate on Breakthrough Curves for Acetaldehyde and Propionaldehyde in their Binary Mixture in a Silica Gel Bed .....	151
10.	Effects of Flow Rate on Breakthrough Curves for Acetaldehyde, Propionaldehyde, and Butyraldehyde in their Ternary Mixture in a Silica Gel Bed .....	152
11.	Effects of Inlet Concentration on Breakthrough Curves for Acetaldehyde and Butyraldehyde in their Binary Mixture in a Silica Gel Bed .....	153
12.	Effects of Inlet Concentration on Breakthrough Curves for Acetaldehyde, Propionaldehyde, and Butyraldehyde in their Ternary Mixture in a Silica Gel Bed .....	154
13.	Effects of Temperature on Breakthrough Curves for Propionaldehyde and Butyraldehyde in their Binary Mixture in a Silica Gel Bed .....	155
14.	Effects of Temperature on Breakthrough Curves for Acetaldehyde, Propionaldehyde, and Butyraldehyde in their Ternary Mixture in a Silica Gel Bed .....	156
15.	Effects of Flow Rate on Breakthrough Curves for Acetaldehyde and Propionaldehyde in their Binary Mixture in a Molecular Sieve-13X Bed .....	157
16.	Effects of Flow Rate on Breakthrough Curves for Acetaldehyde, Propionaldehyde, and Butyraldehyde in their Ternary Mixture in a Molecular Sieve-13X Bed .....	158
17.	Effects of Inlet Concentration on Breakthrough Curves for Acetaldehyde and Butyraldehyde in their Binary Mixture in a Molecular Sieve-13X Bed .....	159

Figure		Page
18.	Effects of Inlet Concentration on Breakthrough Curves for Acetaldehyde, Propionaldehyde, and Butyraldehyde in their Ternary Mixture in a Molecular Sieve-13x Bed	160
19.	Effects of Temperature on Breakthrough Curves for Propionaldehyde and Butyraldehyde in their Binary Mixture in a Molecular Sieve-13X Bed ...	161
20.	Effects of Temperature on Breakthrough Curves for Acetaldehyde, Propionaldehyde, and Butyraldehyde in their Ternary Mixture in a Molecular Sieve-13X Bed .....	162

#### APPENDICES

B.1	Plots to Calculate Isotheric Heats of Adsorption at Different Loadings for Acetaldehyde-Silica Gel System .....	169
C.1	The Langmuir Plots for Propionaldehyde-Silica Gel System .....	171
C.2	The BET Plots for Butyraldehyde-Silica Gel System .....	173
C.3	The Freundlich Plots for Butyraldehyde-Molecular Sieve System .....	174
H.1	Effects of Inlet Concentration on Breakthrough Curves for Acetaldehyde in a Silica Gel Bed .....	187
H.2	Effects of Inlet Concentration on Breakthrough Curves for Acetaldehyde in a Molecular sieve-13X Bed .....	188
H.3	Effects of Temperature on Breakthrough Curves for Acetaldehyde in a Silica Gel Bed .....	189
H.4	Effects of Temperature on Breakthrough Curves for Acetaldehyde in a Molecular Sieve-13X Bed	190
H.5	Effects of Flow Rate on Breakthrough Curves for Propionaldehyde in a Silica Gel Bed .....	191

Figure	Page
H.6 Effects of Flow Rate on Breakthrough Curves for Propionaldehyde in a Molecular Sieve-13X Bed .....	192
H.7 Effects of Temperature on Breakthrough Curves for Propionaldehyde in a Silica Gel Bed .....	193
H.8 Effects of Temperature on Breakthrough Curves for Propionaldehyde in a Molecular sieve-13X Bed	194
H.9 Effects of Flow Rate on Breakthrough Curves for Butyraldehyde in a Silica Gel Bed .....	195
H.10 Effects of Flow Rate on Breakthrough Curves for Butyraldehyde in a Molecular Sieve-13X Bed	196
H.11 Effects of Inlet Concentration on Breakthrough Curves for Butyraldehyde in a Silica Gel Bed ...	197
H.12 Effects of Inlet Concentration on Breakthrough Curves for Butyraldehyde in a Molecular Sieve-13X .....	198
H.13 Effects of Inlet Concentration on Breakthrough Curves for Acetaldehyde and Propionaldehyde in their Binary Mixture in a Silica Gel Bed .....	199
H.14 Effects of Temperature on Breakthrough Curves for Acetaldehyde and Propionaldehyde in their Binary Mixtures in a Silica Gel Bed .....	200
H.15 Effects of Flow Rate on Breakthrough Curves for Acetaldehyde and Butyraldehyde in their Binary Mixtures in a Silica Gel Bed .....	201
H.16 Effects of Temperature on Breakthrough Curves for Acetaldehyde and Butyraldehyde in their Binary Mixture in a Silica Gel Bed .....	202
H.17 Effects of Flow Rate on Breakthrough Curves for Propionaldehyde and Butyraldehyde in their Binary Mixtures in a Silica Gel Bed .....	203
H.18 Effects of Inlet Concentration on Breakthrough Curves for Propionaldehyde and Butyraldehyde in their Binary Mixtures in a Silica Gel Bed ...	204
H.19 Reproducibility of the Experimental Data (Butyraldehyde Adsorption on Silica Gel at 288.2 K) .....	205

CHAPTER I

ADSORPTION OF ACETALDEHYDE, PROPIONALDEHYDE, AND  
BUTYRALDEHYDE ON SILICA GEL

**ADSORPTION OF ACETALDEHYDE, PROPIONALDEHYDE,  
AND BUTYRALDEHYDE ON SILICA GEL**

**Tushar K. Ghosh and Anthony L. Hines**

**School of Chemical Engineering  
Oklahoma State University  
Stillwater, Oklahoma 74078**

**ABSTRACT**

Adsorption isotherms of acetaldehyde, propionaldehyde, and butyraldehyde on Davison Silica gel were determined gravimetrically at three temperatures. The isotheric heat of adsorption initially increased at low loading and then decreased monotonously with an increase in loading. The equilibrium adsorption data were successfully correlated by the Polanyi's potential theory. The equilibrium data were also correlated with the Langmuir, BET, Freundlich, and the Kuo-Hines models. The Freundlich and the Kuo-Hines models provided the best fit to the data, while the BET equation was found to be applicable only for a relative pressure range of 0.05 to 0.2. The monolayer surface coverages of silica gel by all of the aldehydes estimated by the Langmuir equation were found to be consistently higher than those calculated from the BET equation, except for acetaldehyde at 306.5 K.

## INTRODUCTION

The aldehydes have been recognized as outdoor air pollutants for some time. Although formaldehyde is usually the most prevalent, in some areas the combined concentrations of the higher molecular weight aldehydes i.e., acetaldehyde, propionaldehyde and butyraldehyde may be higher than formaldehyde alone [1]. Aldehydes are introduced into the atmosphere from a variety of sources including: gasoline-powered, propane-powered, or diesel-powered engines, incinerator smoke, and stack gases from the combustion of various organic substances [2].

It has been long believed that indoor air, i.e. air inside homes, offices etc. is cleaner than the outside air. Recently, researchers have found that the indoor air may be more polluted than the outdoor air [3], and the aldehydes are major pollutants. Primary sources of aldehydes in indoor air include the products of combustion of natural gas (used for cooling and heating), tobacco smoke, and urine. The most common effect of aldehydes on humans is the irritation of eyes and mucous membranes. Other possible health problems are headaches, narcotic action on the nervous system, and a rise in blood pressure [4].

Growing public concern about the health hazards that might be caused by these chemicals is creating a challenge for the researcher to remove them effectively and economically from indoor and outdoor air. One way to remove the

aldehydes from air is to adsorb them on porous materials, such as silica gel, activated carbon, and molecular sieve. However, the design of any adsorption system requires pure component adsorption data.

In the present work, the adsorption behavior of acetaldehyde, propionaldehyde, and butyraldehyde on silica gel was studied at three temperatures. Experimental data were correlated by applying the potential theory proposed by Polanyi to check the consistency of the data. Different adsorption models were employed to fit the equilibrium adsorption data, including the Langmuir, the BET, the Freundlich, and the Kuo-Hines model. The isotheric heats of adsorption were calculated at different loadings to evaluate the surface characteristics of the silica gel for these aldehydes.

## **EXPERIMENTAL SECTION**

### **Materials and Apparatus:**

The silica gel used in the present work was Grade 40, 6-12 mesh and was supplied by Davison Chemical, Baltimore, Maryland. Acetaldehyde and Butyraldehyde were obtained from Fluka AG and had purities of 99.9% and 99%+, respectively. Propionaldehyde was obtained from Aldrich Chemical Company, Milwaukee, Wisconsin and had a stated purity greater than 99%.

The adsorption study was carried out gravimetrically using a Cahn R-2000 electrobalance. The electrobalance was capable of measuring weights up to 3.5 g with a sensitivity



of 0.1  $\mu\text{g}$ . The description of the electrobalance and the flow diagram are given in detail in a paper by Kuo and Hines [3]. A vacuum of  $1 \times 10^{-4}$  mmHg could be obtained in the system prior to an adsorption run. The leak rate of the complete assembly was approximately 0.0054 mmHg/hr. The pressure was measured by a Wallace and Tiernan absolute pressure gauge to an accuracy of  $\pm 0.1$  mmHg. The temperature during the adsorption and desorption run was controlled within  $\pm 0.1$  K.

**Procedure:**

Prior to an adsorption run, the silica gel was heated to a temperature of  $373.15 \pm 2$  K under vacuum to remove the moisture and other gases that might be adsorbed on the surface. Heating was continued until a constant sample weight was obtained, which typically required about 4-10 h. To maintain consistency, a heating period of 10h was used for all runs. After regeneration of the silica gel, it was cooled to the adsorption temperature and the adsorbate was introduced into the system in steps. After each step, the system was allowed to reach equilibrium as indicated by the constant weight of the sample. The pressure and weight change were recorded after each equilibrium step. Following adsorption, desorption of the adsorbate was carried out by reducing the system pressure in steps. Fresh samples of silica gel were used for each run as a result of not being able to remove the adsorbate completely from the silica gel, in spite of several hours of heating under vacuum. Because

the amount adsorbed on the silica gel was found to be dependent on regeneration temperature, the temperature used during the regeneration of the silica gel sample was controlled within  $\pm 2$  K. The error introduced in the weight measurement due to the buoyancy effect was found to be negligible.

## **RESULTS AND DISCUSSION**

### **Equilibrium Data:**

Adsorption isotherms were obtained at 287, 298.2 and 306.5 K for acetaldehyde, at 282, 297, and 304.3 K for propionaldehyde and at 288.2, 299.3 and 308.2 K for butyraldehyde. All three aldehydes exhibited Type I adsorption isotherms and gave reproducible hysteresis loops upon desorption. The adsorption and the desorption data for all the aldehydes are shown in Figures 1 through 3. Nayar and Rao [5] also found that propionaldehyde and butyraldehyde gave Type I isotherms and hysteresis loops from their studies on silica gel at 303 K. In addition, they reported that the adsorbate was strongly attached to the silica gel and suggested that the aldehyde molecules were chemisorbed on the surface. Adsorption studies of aliphatic hydrocarbons [6] and chlorinated hydrocarbons [7] on 80-100 mesh silica gels showed no apparent hysteresis during desorption.

The isotheric heat of adsorption was calculated at constant loading of the adsorbate from the following relationship:

$$\Delta H_{iso} = -R \left[ \frac{\partial \ln P}{\partial (1/T)} \right]_q \quad (1)$$

The heats of adsorption at different loadings are plotted in Figure 4 for all three aldehydes. The heats of adsorption of acetaldehyde and butyraldehyde increased with an increase in loading up to a certain point then started to decrease. Due to the lack of adsorption data at lower loadings, the heat of adsorption for propionaldehyde could not be calculated in that region. However, the curve for propionaldehyde showed a trend similar to that of acetaldehyde. The initial increase in the heat of adsorption curves can be attributed to lateral interactions between the adsorbed aldehydes, which are known to form associated molecules on a solid surface. The subsequent decrease in the curves can be attributed to heterogeneity of the surface and multilayer coverage. Brunauer [8] reported a similar type of observation for both water and methanol, which are highly polar and exhibit a strong tendency toward association.

Although silica gel generally provides a homogeneous surface for adsorption, some sites might become more energetic than others following regeneration. The heat of adsorption for adsorbates on silica gel surfaces have been frequently found to decrease as the loading increases and then remain practically constant. For all of the aldehydes, the hysteresis loop decreased with increasing temperature. This may be attributed to a sieving effect on the expanded adsorbate at the higher temperature. The surface areas predicted from the adsorption data also decreased with

increasing temperature. This suggests that some of the micropores were inaccessible at the higher temperatures because the adsorbate had expanded.

#### **DATA CORRELATION:**

The potential theory of Polanyi was applied to the systems studied in this work to check the consistency of the data. The polanyi theory assumes that the adsorbent exerts long range attractive forces on the gas or vapor surrounding it. These attractive forces generate a potential field which decreases as the distance between the gas and adsorbent surface increases. The adsorption potential ( $\epsilon$ ) in its original form is given by

$$\epsilon = RT \ln(P_g/P) \quad (2)$$

where  $P_g$  is the saturation pressure of the adsorbate at the adsorption temperature. Thus a plot of the volume adsorbed versus the adsorption potential should produce a single characteristic curve independent of temperature as shown in Figures 5 through 7.

The equilibrium data were next correlated by the Langmuir, the BET, and the Freundlich equations, in addition to a new isotherm proposed by Kuo and Hines [9] for heterogeneous surfaces.

The Langmuir equation was developed using the assumption that the adsorbent surface is homogeneous and the surface is covered by a single layer of molecules. The Langmuir

equation is given by

$$q = \frac{q_m KP}{1+KP} \quad (3)$$

where  $q_m$  is a constant and is defined as the amount of adsorbate that will be adsorbed on the surface in a monolayer. As shown in Table III, the Langmuir equation did not provide a good fit to the data. This may be due to the combined effects of surface heterogeneity, multilayer adsorption and the formation of associated molecules on the silica gel surface.

Although the BET equation was developed based on the assumption of multilayer adsorption, the heterogeneity of the adsorbent surface was not considered. The BET equation can be written as

$$\frac{P}{q(P_S - P)} = \frac{1}{q_m C} + \frac{(C-1)P}{Cq_m P_S} \quad (4)$$

The BET equation provided a good correlation of the data for the range  $0.05 \leq P/P_S \leq 0.2$ . A large deviation between the calculated values and the experimental data was observed at pressures higher than  $P/P_S > 0.2$ . This type of behavior has also been observed by other researchers [10]. Because the BET model is more suitable for Type II and III isotherms, the failure of the BET model to predict the Type I behavior observed in the present study is not surprising.

Low pressure data (where the Langmuir and the BET equations provided a straight line) were used to calculate the monolayer coverage and the surface area of silica gel;

the results are presented in Table I. The area occupied by a molecule was estimated by assuming hexagonal close packing of the aldehydes on the surface. The surface area predicted by the Langmuir equation was consistently higher than that predicted by the BET equation, except for acetaldehyde at 306.5 K. The surface areas obtained by using propionaldehyde and butyraldehyde are in close agreement with the values reported by Nayar and Rao [5] at 303 K. However, aldehydes occupy less than the total surface area, which is  $760 \text{ m}^2/\text{g}$  as measured by an Orr Surface Area-Pore Volume Analyzer (Model 2100D, Micromeritics Instrument Corporation) using  $\text{N}_2$  as the adsorbent at 77.3 K. The low coverage by the aldehydes may be due in part to their inability to enter the pores of the silica gel and their orientation on the surface. Tanada [12] found that the amount of acetaldehyde that was adsorbed on several adsorbents depended on the pore radius rather than on the total pore volume.

The Freundlich equation provided a better fit to the experimental data than either the Langmuir or the BET equation. The Freundlich equation can be written as

$$q = a(P)^b \quad (5)$$

where  $a$  and  $b$  are constants. The results are compared in Table III. Kuo and Hines [9] developed an isotherm considering the heterogeneity of the surface. In developing the isotherm, Kuo and Hines assumed that the surface consisted of energetically heterogeneous sites and the distribution of

such sites could be described by a probability density function. The adsorption of the adsorbate on a particular site was described by the Jovanovic [11] equation for monolayer coverage. The resulting overall adsorption isotherm has the form

$$q = m \left[ 1 - \left( \frac{K_3}{K_3 - K_1 K_2} \right) \left( \frac{K_1}{P + K_1} - \frac{K_1 K_2}{P + K_3} \right) \right] \quad (6)$$

where  $m$ ,  $K_1$ ,  $K_2$ , and  $K_3$  were related to the Henry's law constant by the expression

$$m \left[ \frac{K_3^2 - K_1^2 K_2}{K_1 K_3 (K_3 - K_1 K_2)} \right] = K_L \text{ as } P \rightarrow 0 \quad (7)$$

As suggested by Kuo and Hines,  $K_3$  was set to unit pressure while the parameters  $m$ ,  $K_1$ , and  $K_2$  were determined by a trial and error procedure. The Henry's law constant,  $K_L$ , was obtained from the initial slope of the isotherm. A value of  $m$  was chosen and  $K_2$  was calculated from Equation (7) for different values of  $K_1$ . The entire isotherm was then generated by Equation (6). This trial and error procedure was continued until a satisfactory fit of the experimental data was obtained. In the present study, the trial and error procedure continued until the calculated data were within  $\pm 2\%$  of the experimental data. The Henry's law constant and the best fit values for the constants  $K_1$  and  $K_2$  are shown in Table II.

The best fit curves generated by the Kuo-Hines model and the experimental data are plotted in Figures 8 through 10. The Kuo-Hines model provided an excellent fit for most of the aldehyde-silica gel data. However, a larger deviation was observed for propionaldehyde and butyraldehyde at low temperatures (282 K for propionaldehyde and 288.2 K for butyraldehyde) and high pressures.

A comparison of the Langmuir, BET, Freundlich, and Kuo-Hines models are given in Table III for all the experimental runs. The average absolute percent error, maximum positive error, and maximum negative error over the complete pressure range are given in the table. The Kuo-Hines and the Freundlich models provided a better correlation of the data than did the Langmuir and the BET models when the entire pressure range was considered.



**NOMENCLATURE**

a	Constant in the Freundlich equation
b	Constant in the Freundlich equation
C	Constant in the BET equation
$\epsilon$	Adsorption Potential
$\Delta H_{iso}$	Isoteric heat of adsorption
K	Constant in the Langmuir equation
$K_L$	Henry's law constant
$K_1$	Constant in the Kuo-Hines equation
$K_2$	Constant in the Kuo-Hines equation
$K_3$	Constant in the Kuo-Hines equation
m	Constant in the Kuo-Hines equation
P	System pressure
$P_s$	Saturation pressure at system temperature
q	Uptake of the adsorbate
$q_m$	Equilibrium uptake of the adsorbate as defined by the Langmuir and the BET equation
R	Gas Constant
T	System temperature

**REFERENCES**

1. P.L. Magill, F.R. Holden, and C. Ackley, Air Pollution Handbook, McGraw Hill Book Company, Inc., New York (1956).
2. M.B. Jacobs, The Chemical Analysis of Air Pollutants, Interscience Publishers, Inc., New York (1960).
3. S.L. Kuo and A.L. Hines, "Adsorption of Chlorinated Hydrocarbon Pollutants on Silica Gel," Separation Science and Technology, Vol.23, No.(4&5), p 293,(1988).
4. R.E. Kirk and D.F. Othmer, Encyclopedia of Chemical Technology, 2nd ed. The Interscience Encyclopedia, Inc., New York, Vol. 1 (1963).
5. B.C. Nayar and U. Subba Rao, "Contact Angle and Oriented Adsorption of Aliphatic Amines and Aldehydes on Silica Gel and Silica Aerogel," Indian J. of Chemistry, Vol. 20A, pp 551-555 (1981).
6. T.A. Al-Sahhf, E.D. Sloan and A.L. Hines, "Application of the Modified Potential Theory to the Adsorption of Hydrocarbon Vapors on Silica Gel," I & EC Process Design and Development, Vol. 20, pp 698 (1981).
7. S.L. Kuo, "Adsorption of Chlorinated Hydrocarbon on Silica Gel," PhD Dissertation, Oklahoma State University, (1988).
8. S. Brunauer, The Adsorption of Gases and Vapor, Vol. 1, Princeton University Press, Princeton (1945).
9. S.L. Kuo and A.L. Hines, "New Theoretical Isotherm for Adsorption on Heterogeneous Adsorbents," submitted to Separation Science and Technology.
10. D.M. Young and A.D. Crowell, Physical Adsorption of Gases, Butterworths, Washington (1962).
11. D.S. Jovanovic, "Physical Adsorption of Gases, I: Isotherms for Monolayer and Multilayer Adsorption," Colloid and Polymer Science, pp. 1203, (1969).
12. S. Tanada, "Studies on Adsorption Removal of Odorous Pollutants (Acetaldehyde and Methyl Mercaptan), Adsorption of Acetaldehyde on Porous Adsorbents," Japanese J. of Hygiene, Vol. 32, No. 9, pp 671, (1977).

**LIST OF TABLES**

- I. Monolayer Coverages and Calculated Surface Areas of Silica Gel
- II. Henry's Law Constants and Best Fit Parameters for the Kuo-Hines Model
- III. Comparison of Model Correlations

**LIST OF FIGURES**

1. Adsorption and Desorption Curves for Acetaldehyde on Silica Gel (6-12 mesh)
2. Adsorption and Desorption Curves for Propionaldehyde on Silica Gel (6-12 mesh)
3. Adsorption and Desorption Curves for Butyraldehyde on Silica Gel (6-12 mesh)
4. Heat of Adsorption at Different Loadings for Aldehydes on Silica Gel (6-12 mesh)
5. Characteristic Curve for Acetaldehyde on Silica Gel (6-12 mesh)
6. Characteristic Curve for Propionaldehyde on Silica Gel (6-12 mesh)
7. Characteristic Curve for Butyraldehyde on Silica Gel (6-12 mesh)
8. Comparison of the Experimental Data with the Kuo-Hines Model for Acetaldehyde-Silica Gel System
9. Comparison of the Experimental Data with the Kuo-Hines Model for Propionaldehyde-Silica Gel System
10. Comparison of the Experimental Data with the Kuo-Hines Model for Butyraldehyde-Silica Gel System

Table I. Monolayer Coverages and the Calculated Surface Areas of Silica Gel

SYSTEM	TEMP. (K)	MOLECULAR CROSS SECTION $\text{\AA}^2$	MONOLAYER COVERAGE ( $\text{cm}^3/\text{g}$ )		SURFACE AREA ( $\text{m}^2/\text{g}$ )	
			LANGMUIR	BET	LANGMUIR	BET
Acetaldehyde Silica Gel	287.0	22.38	95.2	90.7	573	546
	298.2	22.67	88.7	87.8	541	535
	306.5	22.89	71.5	84.3	440	519
Propionaldehyde Silica Gel	282.0	26.41	76.1	65.5	541	466
	297.0	26.79	70.8	64.3	510	463
	304.3	26.98	67.3	63.6	489	461
Butyraldehyde Silica Gel	288.2	30.57	62.0	54.5	510	448
	299.3	30.88	61.2	53.3	508	442
	308.2	31.11	57.5	52.4	481	438

Table II. Henry's Law Constant and Best Fit Parameters for the Kuo-Hines Model

SYSTEM	TEMP. (K)	HENRY'S LAW CONSTANT (mmol/g-mmHg)	m (mmol/g)	K <sub>1</sub>	K <sub>2</sub>
Acetaldehyde* Silica Gel	287.0	2.873	7.983	174.9	-3.164x10 <sup>-3</sup>
	298.2	2.510	6.512	154.1	-4.002x10 <sup>-3</sup>
	306.5	2.277	5.736	141.2	-4.579x10 <sup>-3</sup>
Propionaldehyde** Silica Gel	282.0	11.450	5.192	4.626x10 <sup>-3</sup>	-195.4
	297.0	10.281	4.729	4.286x10 <sup>-3</sup>	-253.2
	304.3	9.933	4.477	4.113x10 <sup>-3</sup>	-274.7
Butyraldehyde** Silica Gel	288.2	12.346	4.602	4.804x10 <sup>-3</sup>	-166.2
	299.3	11.333	4.328	4.796x10 <sup>-3</sup>	-182.2
	308.2	11.127	4.065	4.455x10 <sup>-3</sup>	-207.3

\* K<sub>1</sub> in mmHg and K<sub>3</sub>=1 mmHg

\*\* K<sub>1</sub> in psia and K<sub>3</sub>=1 psia

Table III. Comparison of Model Correlations

SYSTEM	TEMP (K)	ABS. AVERAGE ERROR* (%)				MAX. POSITIVE ERROR* (%)				MAX. NEGATIVE ERROR* (%)			
		Kuo-Hines	Langmuir	BET	Freundlich	Kuo-Hines	Langmuir	BET	Freundlich	Kuo-Hines	Langmuir	BET	Freundlich
Acetaldehyde Silica Gel	287.0	0.58	12.49	15.40	1.71	2.06	72.69	8.78	7.98	1.17	9.25	105.95	2.37
	298.2	0.40	8.51	5.62	0.93	0.87	65.04	54.62	2.58	2.49	6.23	4.07	1.53
	306.5	0.46	9.82	6.50	0.89	1.01	59.69	50.67	3.23	1.20	9.00	5.44	1.34
Propionaldehyde Silica Gel	282.0	1.73	5.15	142.36	1.27	2.10	42.92	1753.71	1.72	4.30	3.08	190.95	3.37
	297.0	0.26	6.61	8.23	0.88	0.62	52.01	3.83	5.66	0.82	5.64	54.33	1.54
	304.3	0.87	6.54	1.96	1.00	1.15	39.88	1.71	4.42	1.46	7.01	5.73	1.53
Butyraldehyde Silica Gel	288.2	1.55	6.07	94.38	1.19	2.81	49.02	743.21	1.69	2.77	4.63	222.09	3.74
	299.3	0.66	3.44	10.01	0.61	0.88	23.68	5.64	1.99	1.78	2.57	70.58	1.28
	308.2	0.27	5.12	5.57	0.82	0.48	36.92	4.31	3.05	0.85	3.37	33.69	1.52

$$* \text{ ERROR} = \frac{\text{Experimental} - \text{Calculated}}{\text{Experimental}} \times 100$$

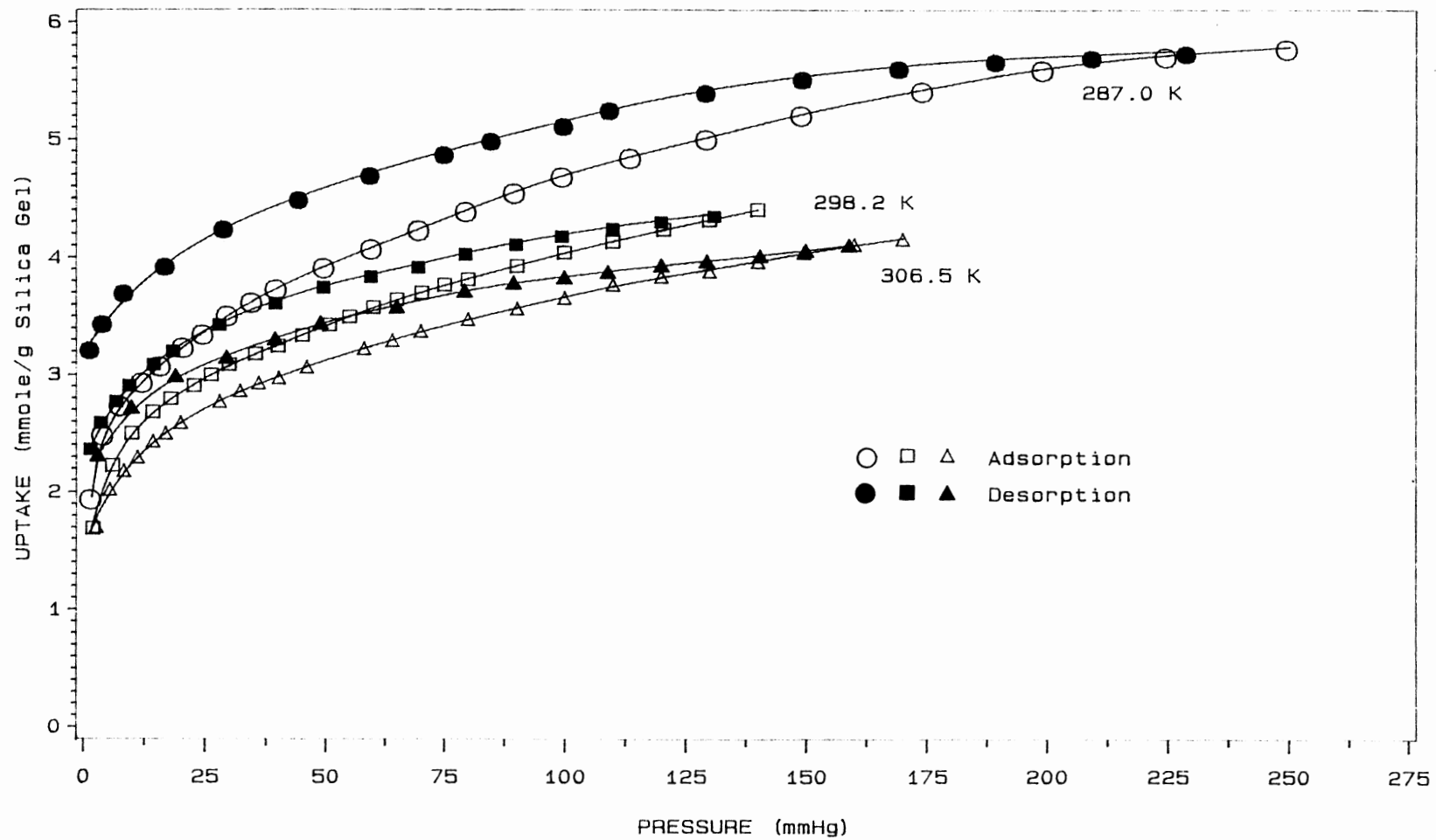


Figure 1. Adsorption and Desorption Curves for Acetaldehyde on Silica Gel (6-12 mesh)



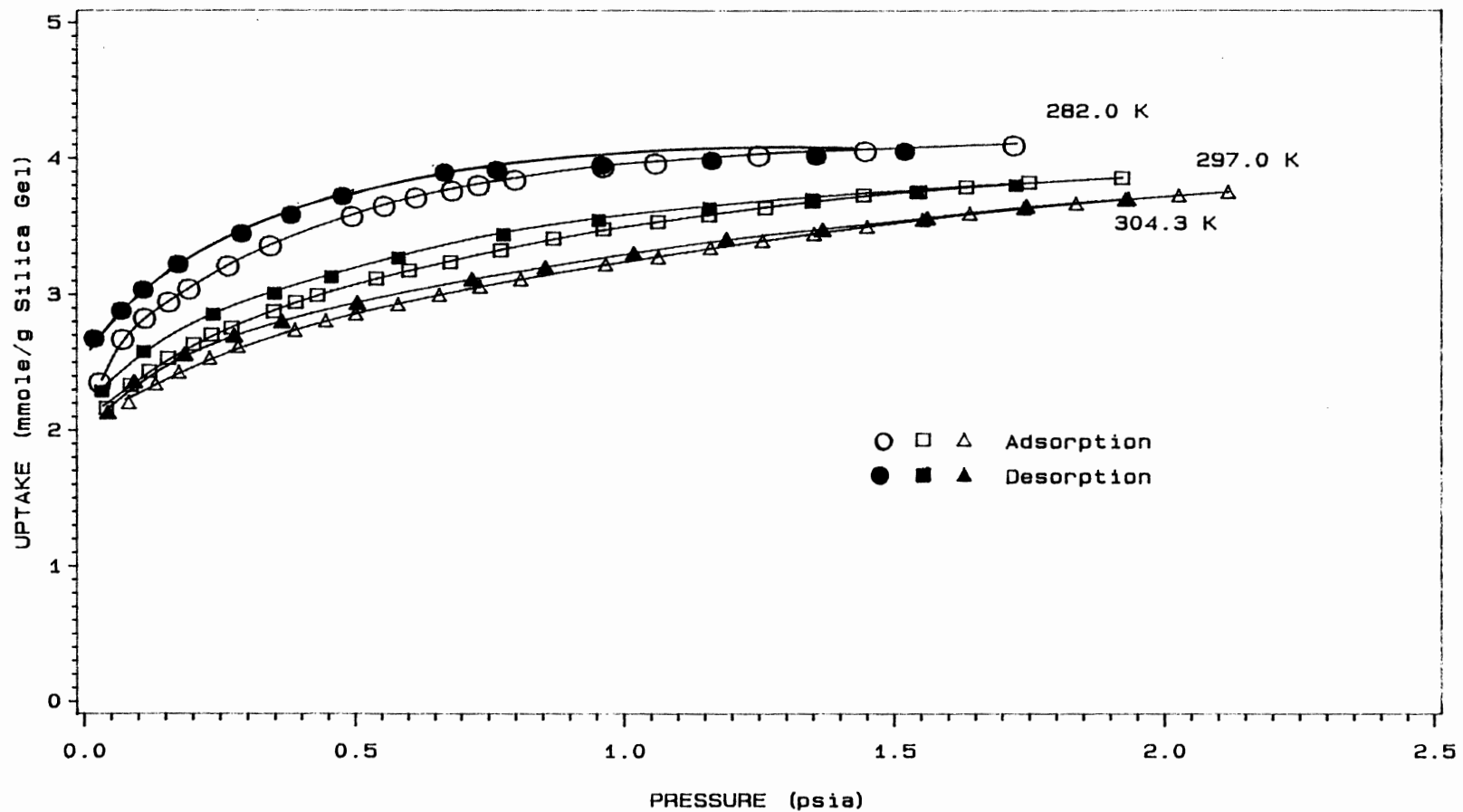


Figure 2. Adsorption and Desorption Curves for Propionaldehyde on Silica Gel (6-12 mesh)

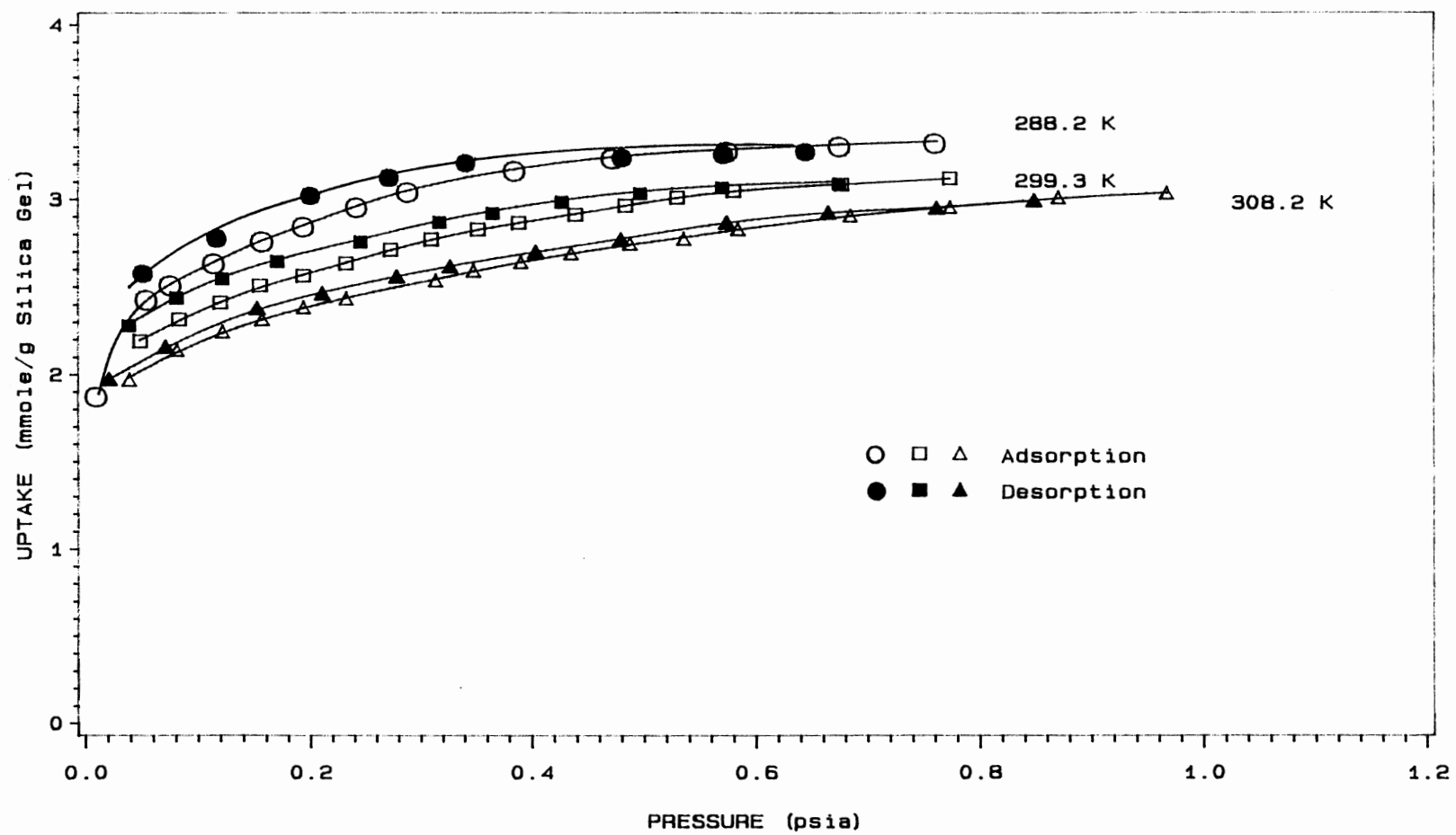


Figure 3. Adsorption and Desorption Curves for Butyraldehyde on Silica Gel (6-12 mesh)

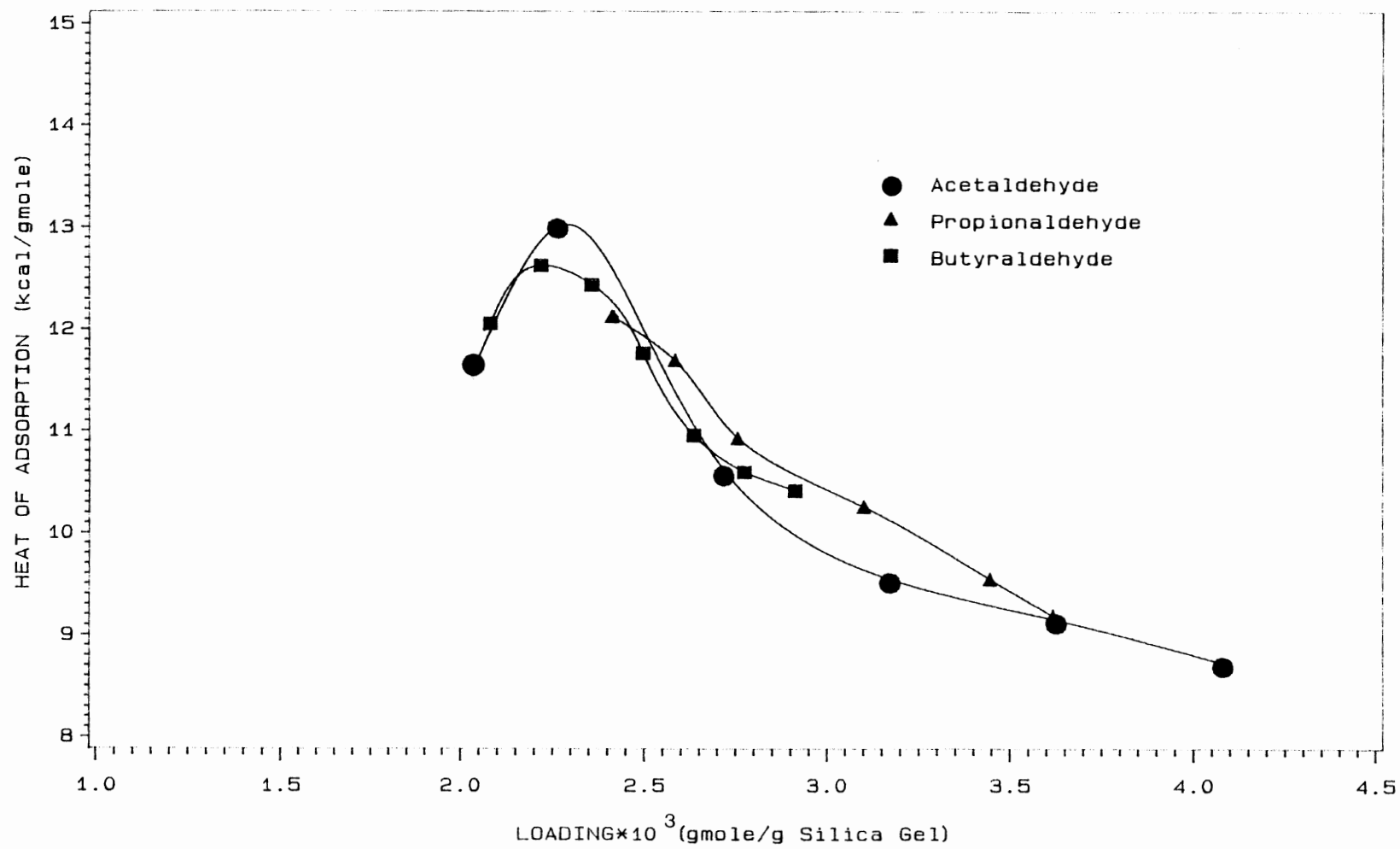


Figure 4. Heat of Adsorption at Different Loadings for Aldehydes on Silica Gel (6-12 mesh)

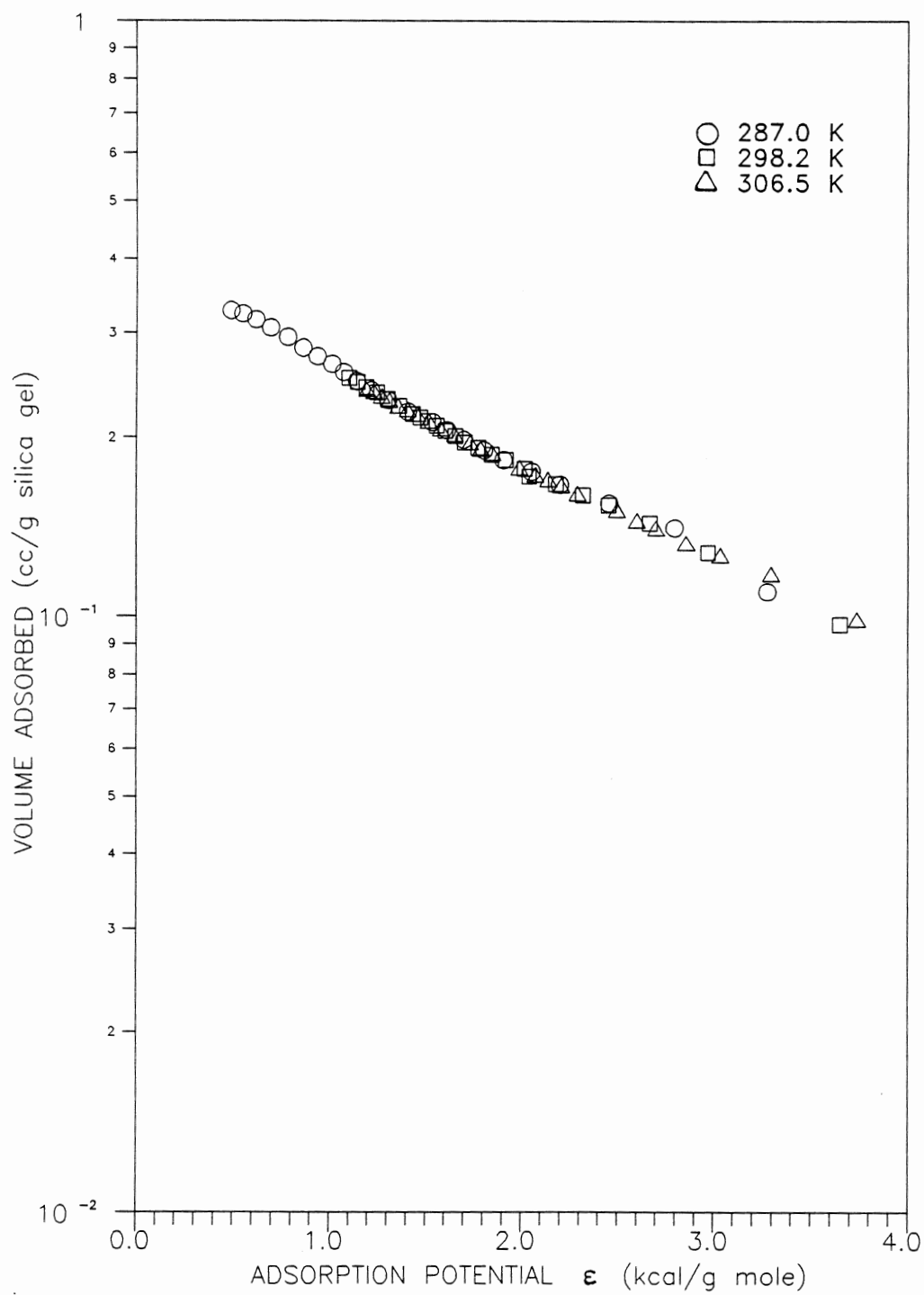


Figure 5. Characteristic Curve for Acetaldehyde on Silica Gel (6-12 mesh)

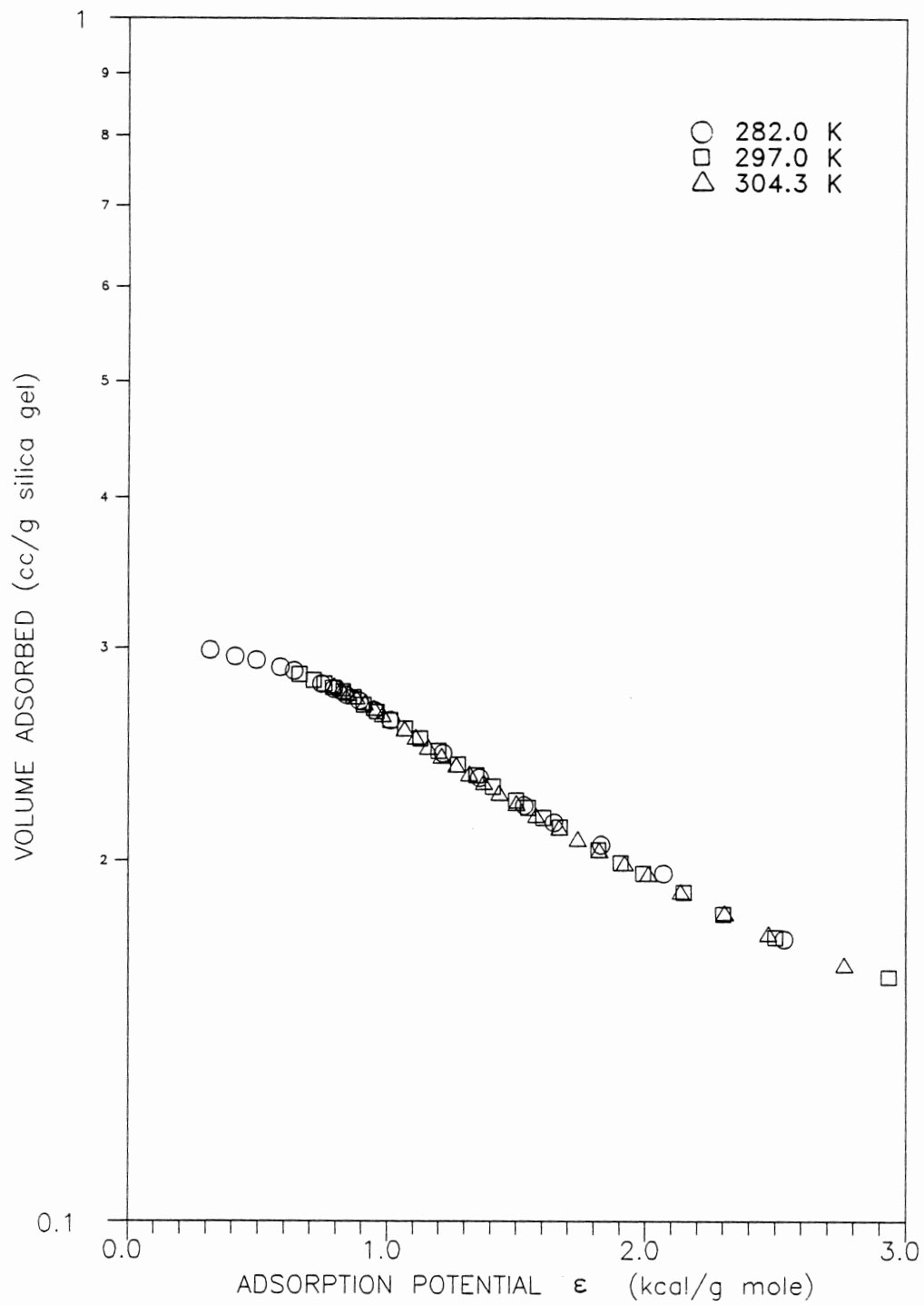


Figure 6. Characteristic Curve for Propionaldehyde on Silica Gel (6-12 mesh)

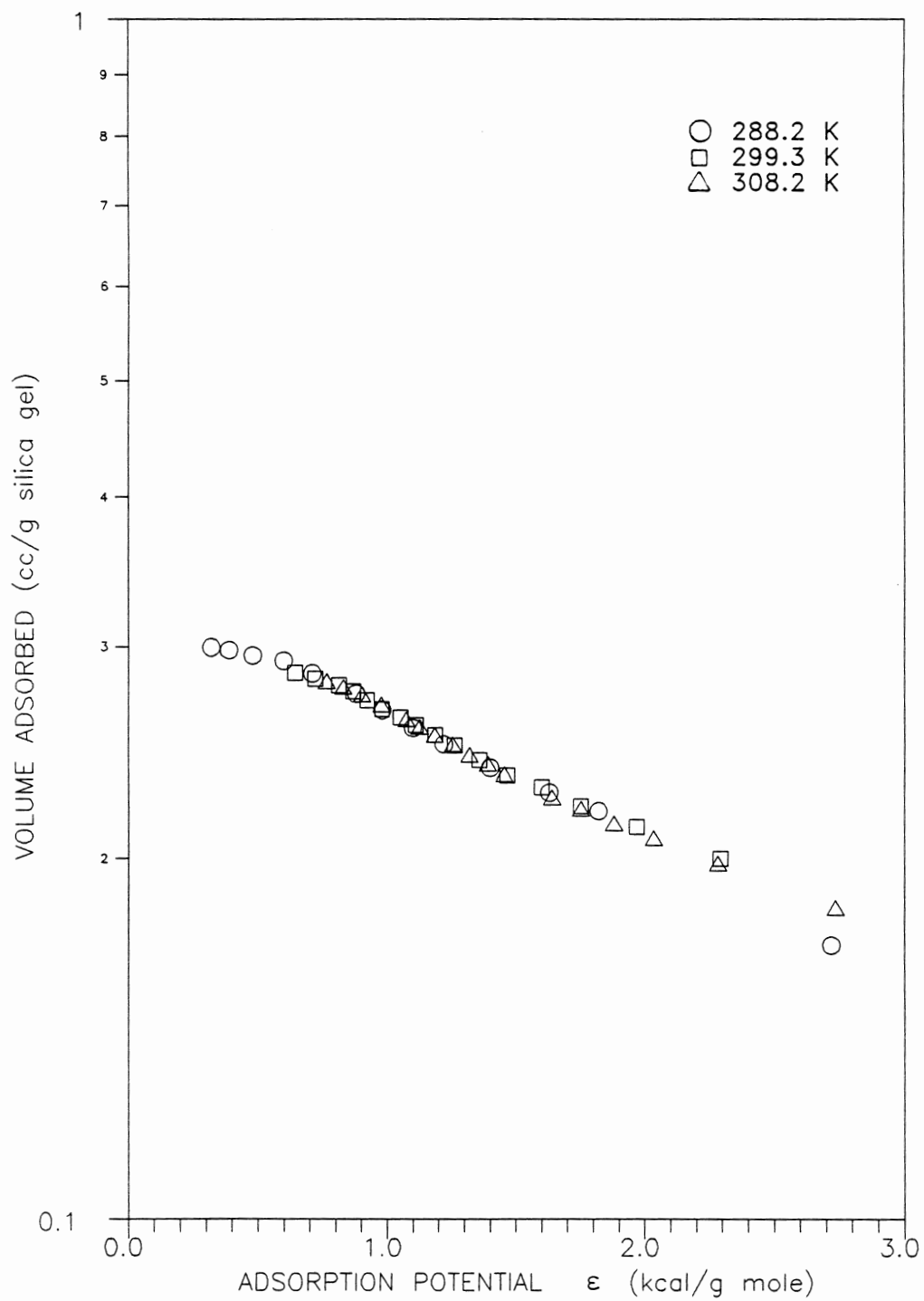


Figure 7. Characteristic Curve for Butyraldehyde on Silica Gel (6-12 mesh)

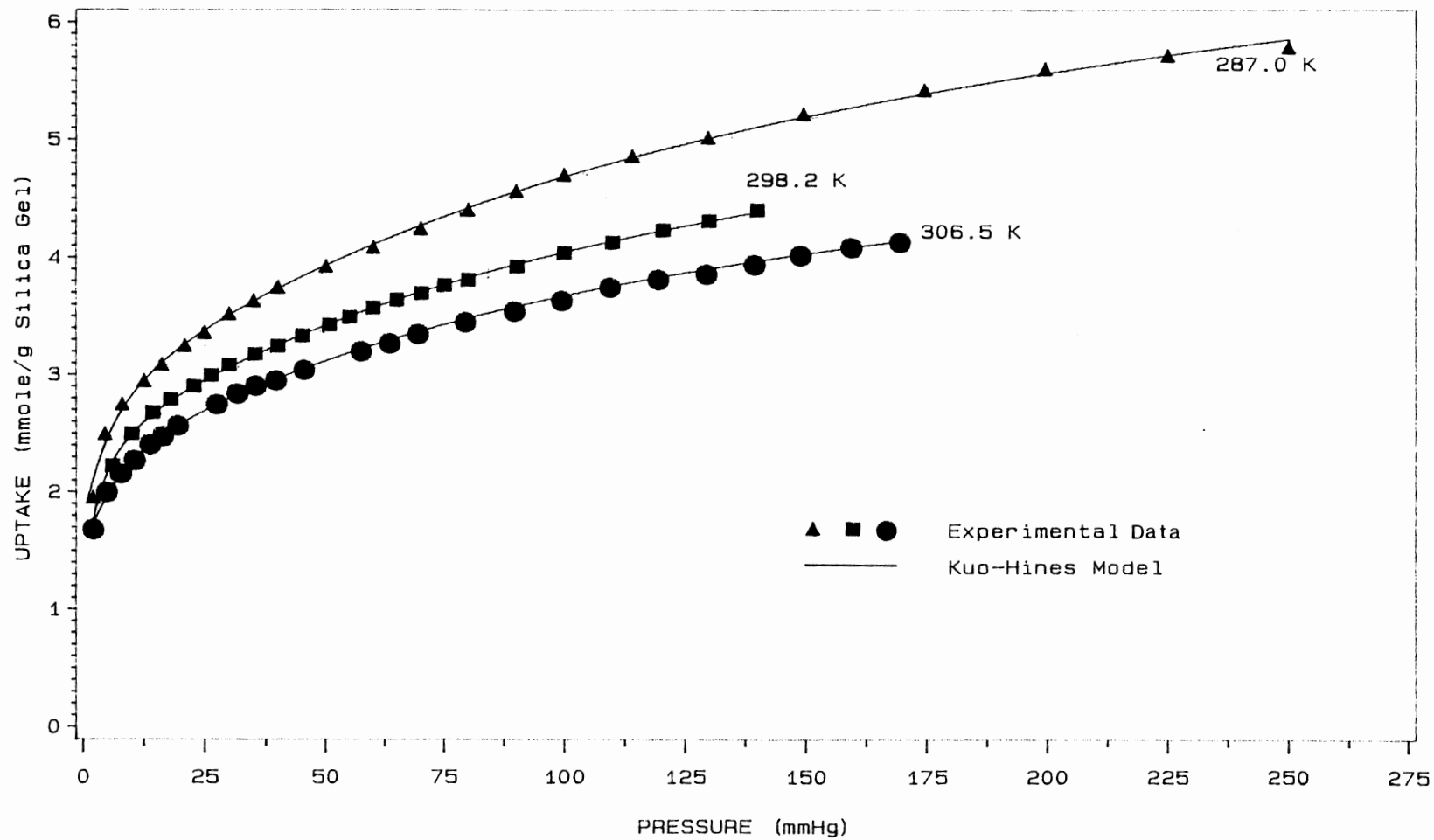


Figure 8. Comparison of Experimental Data With the Kuo-Hines Model for Acetaldehyde-Silica Gel System

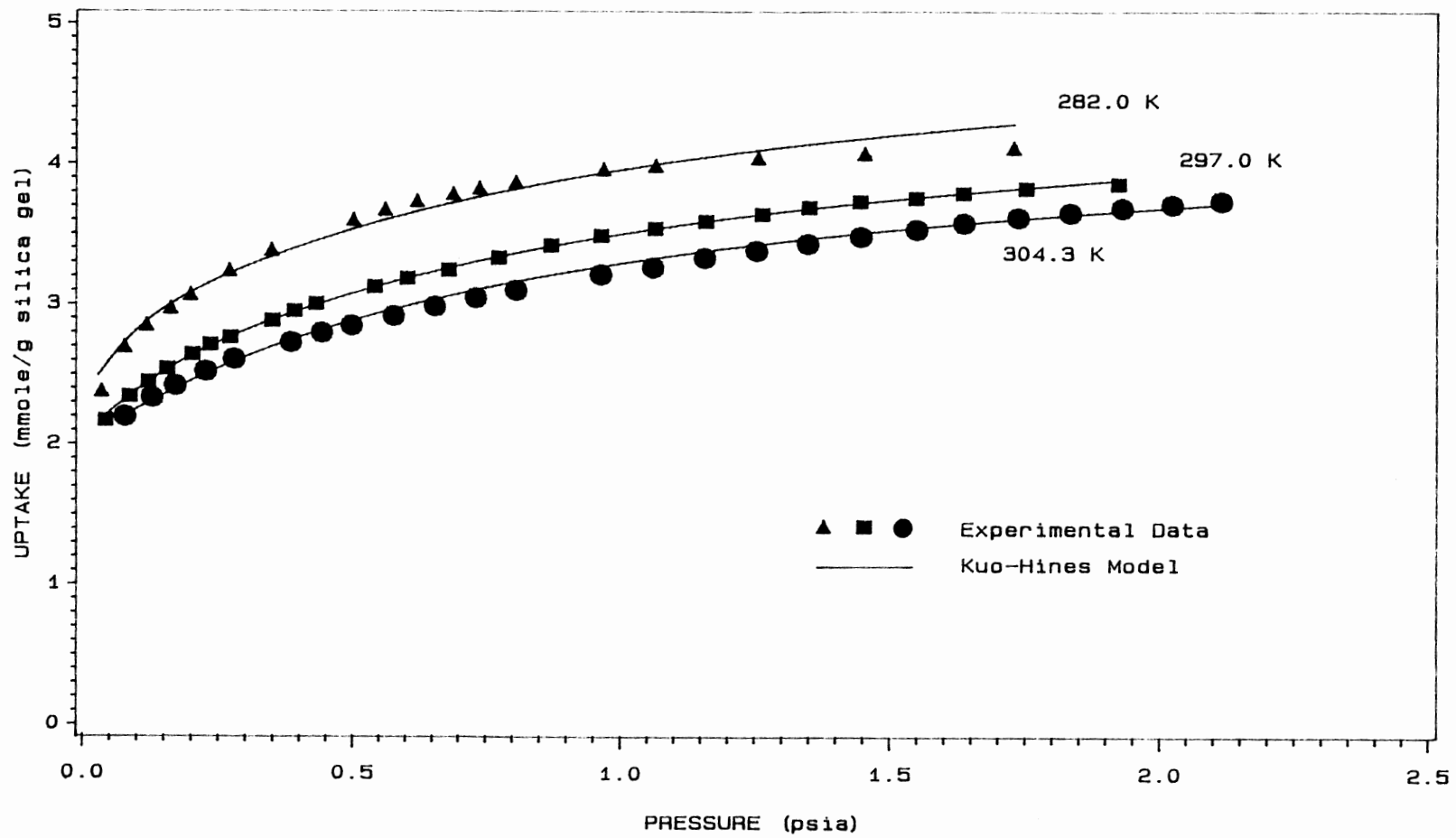


Figure 9. Comparison of Experimental Data With the Kuo-Hines Model for Propionaldehyde-Silica Gel System



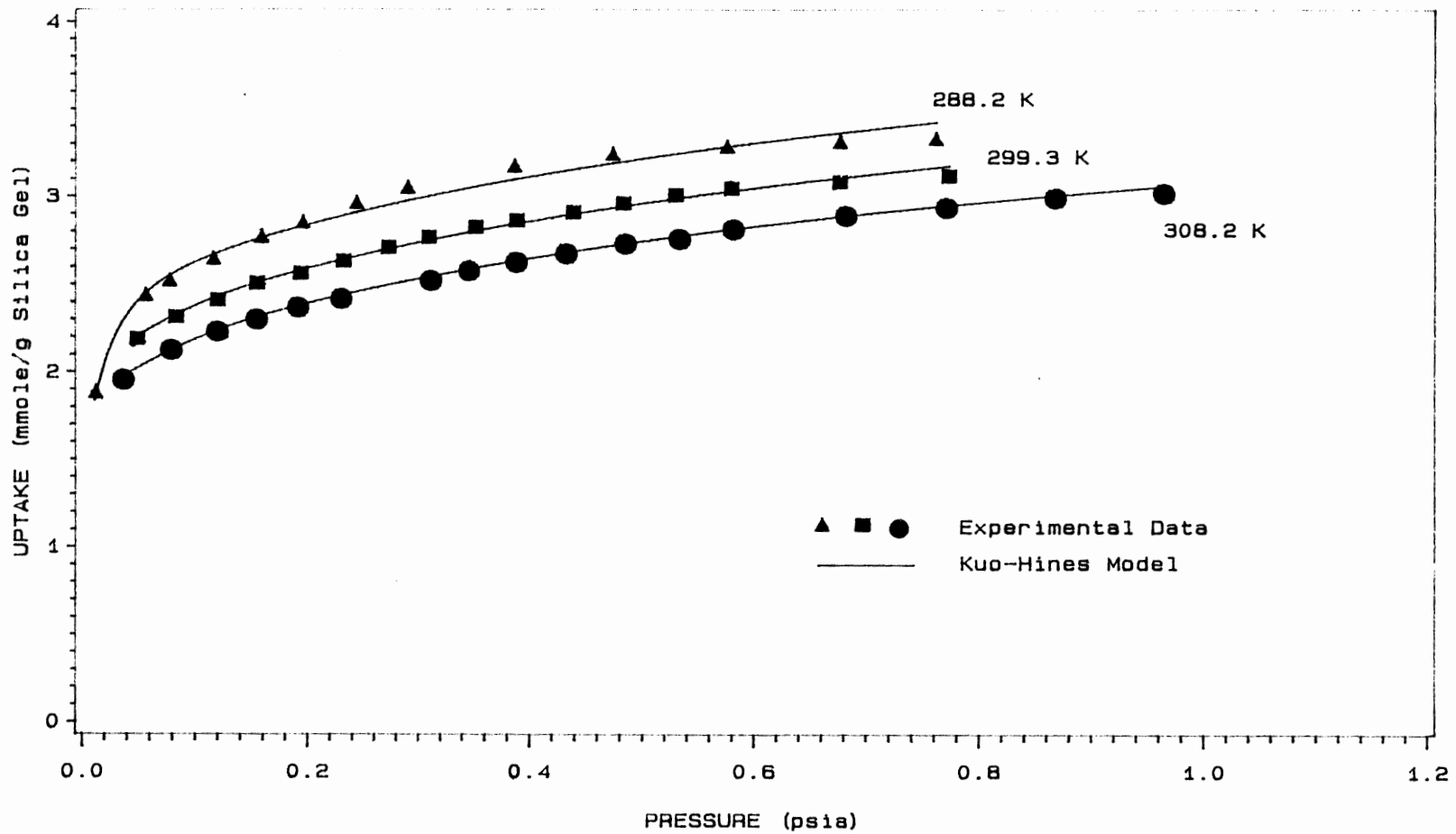


Figure 10. Comparison of Experimental Data With the Kuo-Hines Model for Butyraldehyde-Silica Gel System

CHAPTER II

ADSORPTION OF ACETALDEHYDE, PROPIONALDEHYDE, AND  
BUTYRALDEHYDE ON MOLECULAR SIEVE-13X

**ADSORPTION OF ACETALDEHYDE, PROPIONALDEHYDE, AND  
BUTYRALDEHYDE ON MOLECULAR SIEVE-13X**

**Tushar K. Ghosh and Anthony L. Hines**

**School of Chemical Engineering  
Oklahoma State University  
Stillwater, Oklahoma 74078**

**ABSTRACT**

Adsorption isotherms for acetaldehyde, propionaldehyde, and butyraldehyde on Davison molecular sieve-13X were determined gravimetrically at three temperatures. The isotheric heat of adsorption of acetaldehyde and propionaldehyde decreased initially with the increase in loading, then increased up to a certain point after which it decreased again. For butyraldehyde the heat of adsorption initially increased then decreased with increased loading. The equilibrium adsorption data reduce to a single characteristic curve when correlated according to the Polanyi's potential theory. Recently proposed isotherm equations for heterogeneous surfaces by Sircar and Kuo and Hines provided a better fit of the data than did the BET equation. The BET equation gave a good correlation of the data for a relative pressure range of  $0.05 \leq P/P_s \leq 0.25$ . The monolayer surface coverage and surface area were calculated by the Langmuir and the BET equations. The Langmuir equation consistently provided a larger estimate of the surface area than did the BET equation.

## INTRODUCTION

one method of removing air pollutants from both indoor and outdoor air is to adsorb them in porous materials, such as silica gel, molecular sieve, and activated carbon. Besides having offensive odors, pollutants such as the aldehydes may cause a number of health problems. The most common effects are headaches, narcotic action on the nervous system, and a rise in blood pressure [1,2].

The design of an adsorption process to remove these compounds from air requires pure component equilibrium data as a function of temperature and pressure. Very little experimental work on the adsorption of aldehydes on porous materials has been reported in the literature. Nayar and Rao [3] studied the adsorption of propionaldehyde and butyraldehyde on silica gel and silica aerogel at one temperature only (303 K). Tanada [4] examined the adsorption of acetaldehyde by 20 different adsorbents. Most of the adsorbents studied by Tanada were varieties of activated carbons, although that study did include silica gel and molecular sieve. His experiments were designed to determine the maximum adsorption capacities of the adsorbent at various concentrations of acetaldehyde, rather than determining the complete adsorption isotherm. None of the data in the previous studies were correlated with theoretical adsorption models.

In the present work, adsorption isotherms of acetaldehyde

propionaldehyde, and butyraldehyde on molecular sieve-13X were obtained at three temperatures. The equilibrium adsorption data were correlated according to the Polanyi's potential theory to check the consistency of the experimental data. Data were also correlated with several different theoretical models. The isotheric heat of adsorption was calculated as a function of loading to determine the heterogeneity of the molecular sieve-13X surface.

### EXPERIMENTAL SECTION

#### **Materials and Apparatus:**

Grade 542, 8 mesh bead molecular sieve-13X was supplied by the Davison Chemical Co., Baltimore, Maryland. Acetaldehyde and Butyraldehyde were obtained from Fluka AG and had stated purities of 99.5% and 99%+, respectively. Propionaldehyde which was obtained from Aldrich Chemical Company, Milwaukee, Wisconsin, had a minimum purity of 99%.

A Cahn R-2000 electrobalance with a sensitivity of 0.1  $\mu\text{g}$  was used for the adsorption study. The description of the electrobalance and the flow diagram of the experimental apparatus were described in a paper by Kuo and Hines [5]. A vacuum of  $1 \times 10^{-4}$  mmHg was obtained in the system prior to the adsorption run. The leak rate of the complete experimental set-up was approximately 0.0054 mmHg/hr. The system pressure was measured with a Wallace and Tiernan absolute pressure gauge to an accuracy of  $\pm 0.1$  mmHg. The temperature during adsorption and desorption run was

controlled within  $\pm 0.1$  K.

**Procedure:**

Prior to each adsorption run the molecular sieve was heated at a temperature of  $423 \pm 2$  K under vacuum to remove the moisture and other gases that might have been adsorbed on the surface; heating under vacuum was continued until a constant sample weight was obtained. Although approximately 8 hours were required to attain constant weight, a heating period of 12 hours was used for all the runs. During regeneration, the temperature was controlled within  $\pm 2$  K. The amount that could be adsorbed on the molecular sieve was found to be a function of regeneration temperature up to 423 K. After regeneration of the sample, the adsorption chamber and the molecular sieve were cooled to a predetermined temperature. The adsorbate vapor was introduced into the system in steps and the system was allowed to attain equilibrium as indicated by the constant weight of the sample. The system pressure and sample weight were recorded after each equilibrium step. Following adsorption, desorption was carried out by reducing the system pressure in small pressure increments. A fresh sample of molecular sieve was used in each run because of the inability to remove the adsorbate completely from the molecular sieve, in spite of several hours of heating under vacuum. The error introduced in the weight measurement due to the buoyancy effect was negligible.

## RESULTS AND DISCUSSION

### **Equilibrium Data:**

Adsorption isotherms for acetaldehyde, propionaldehyde, and butyraldehyde on molecular sieve-13X were obtained at three temperatures. Temperatures employed were 286.5, 293.2, and 301.0 K for acetaldehyde; 283.2, 293.2, and 303.2 K for propionaldehyde, and 282.6, 293.2 and 302.0 K for butyraldehyde. The adsorption isotherms for acetaldehyde, propionaldehyde, and butyraldehyde at the higher temperatures appeared to be of Type I, but were of Type II at the lower temperatures. The adsorption and desorption curves for the aldehydes are shown in Figures 1 through 3. Adsorption curves begin to increase more rapidly at adsorption pressures greater than half of the saturation pressure. From Figures 2 and 3, it can be seen that at low temperatures multilayer adsorption and pore filling become more pronounced as the adsorption pressure approaches the saturation pressure. The maximum adsorption pressure for propionaldehyde was 0.909 of the saturation pressure at 283.2 K. At 293.2 and 303.2 K,  $P/P_g$  was 0.66 and 0.565, respectively. For butyraldehyde,  $P/P_g$  was 0.98, 0.813, and 0.55 at temperatures of 282.6, 293.2, and 302.0 K, respectively. During the desorption runs, hysteresis was observed to decrease for all of the aldehydes as the temperature increased. Above 300 K, hysteresis was not present for either propionaldehyde or butyraldehyde. This is probably due to the sieving action of the adsorbent on



the expanded molecules. Ponec et al. [6] noted that at a certain pressure capillary condensation can occur following the multilayer adsorption in the same pore. Cohan [7] pointed out that condensation and evaporation from pores occur at different relative pressures and results in hysteresis. Because the diameter of the acetaldehyde molecule is smaller than either the propionaldehyde or butyraldehyde molecules, more acetaldehyde will enter the pores of the molecular sieve. As a consequence, the size of the hysteresis loop should be expected to be larger. This was indeed the case as noted in Figure 1 through 3.

The isotheric heat of adsorption was calculated at constant loading from the relationship given below:

$$\Delta H_{\text{iso}} = -R \left[ \frac{\partial \ln P}{\partial (1/T)} \right]_q \quad (1)$$

Plots of the heats of adsorption at different loadings are presented in Figure 4. Both acetaldehyde and propionaldehyde showed a minimum and maximum point in the curve, while butyraldehyde showed a maximum only. The heat of adsorption at lower loading could not be calculated due to the lack of adsorption data in the low pressure region.

Beebe and Young [8] observed behavior similar to that shown in Figure 4 for argon on nonporous spheron carbon blacks. The isotherms for the argon-spheron system are also of Type II. Typically the heat of adsorption should be expected to increase on a molar basis approximately as the molecular weight of the aldehydes increase. Due to the

sieving of the adsorbate, however, this is not true here and should not be expected. The decrease in the heat of adsorption in the initial period with increasing coverage is the typical behavior for adsorption on a heterogeneous surface. As the higher energy sites are gradually filled, the heat of adsorption starts to decrease. The aldehydes are also known to form associated molecules on a solid surface. Therefore, as the coverage increases the lateral interaction between the molecules increases which causes the heat of adsorption to increase. When the multilayer adsorption starts, the energy released by the second layer and the subsequent layers is much lower than the first layer. Therefore the overall heat of adsorption starts to decrease as observed in the present work. This is described by Adamson [9] and Joyner and Emmett [10] for the adsorption of nitrogen on carbon black.

#### **Data Correlation:**

The consistency of the adsorption data was checked by correlating the data according to the potential theory of Polanyi. This theory was initially developed for multilayer gas adsorption and assumes that a potential field exists at the solid surface which exerts long range attractive forces on the surrounding gas or vapor phase. The potential field decreases as the distance between the gas phase and solid surface increases. The potential theory of Polanyi can be expressed as

$$\epsilon = RT \ln(P_s/P) \quad (2)$$

where  $\epsilon$  is the adsorption potential and  $P_s$  is the saturation pressure of the adsorbate at the system temperature,  $T$ . Polanyi further assumed that the adsorption potential given by Equation (2) is independent of temperature. Therefore, a plot of adsorption potential ( $\epsilon$ ) versus the volume adsorbed on the solid surface should yield a single characteristic curve. Such plots for acetaldehyde, propionaldehyde, and butyraldehyde are presented in Figures 5, 6, and 7, respectively. The shape of the characteristic curves is typical of that found for multilayer gas adsorption.

The equilibrium adsorption data were also correlated by applying the BET model and the heterogeneous surface models developed by Sircar [11] and Kuo and Hines [12]. Although multilayer adsorption was considered in developing the BET equation, the heterogeneity of the solid surface and lateral interaction of the molecules were not included. The BET equation in its original form is given by

$$\frac{P}{q(P_s - P)} = \frac{1}{q_m C} + \frac{(C-1)P}{Cq_m P} \quad (3)$$

A good correlation of the data was obtained for the pressure range of  $0.05 \leq P/P_s \leq 0.25$ . This is the pressure range over which the BET equation typically gives the best correlation of experimental data as observed by other researchers [13,14]. Larger deviations from the calculated data were observed both at low pressures  $P/P_s < 0.05$  and higher pressures  $P/P_s > 0.25$ . Although the BET equation is best

suites for Type II isotherms, the failure of the equation to predict the aldehydes-molecular sieve data may be due in part to the heterogeneity of the solid surface and the lateral interaction between the aldehyde molecules.

Both the Langmuir and the BET equations were used to calculate the surface area and the monolayer coverage of the molecular sieve. The area occupied by an aldehyde molecule on the solid surface was calculated by assuming the hexagonal close packing of the aldehyde molecules on the solid surface. Estimated surface areas and the monolayer coverages at different temperatures are presented in Table I. Surface areas predicted by the Langmuir equation are found to be consistently higher than those estimated from the BET equation. The aldehyde molecules covered less than the available surface area of the molecular sieve, which is 456 m<sup>2</sup>/g (measured by an Orr Surface Area-Pore Volume Analyzer, Model 2100D Micromeritics Instrument Corporation, using N<sub>2</sub> as the adsorbate at 77.3 K). Such a low coverage of the surface can be attributed to the inability of the aldehyde molecules to penetrate the pores of the molecular sieve.

Sircar [11] and Kuo and Hines [12] proposed isotherms which took into consideration the heterogeneity of the solid surface. They assumed that the solid surface consisted of energetically different heterogeneous sites which could be described by a probability density function. Sircar used a gamma probability density function while Kuo and Hines used a probability density function obtained by modifying the

Morse Potential. Sircar described the local adsorption with the Langmuir isotherm, whereas Kuo and Hines employed the Jovanovic [15] isotherm for monolayer coverage to model the adsorption on a specific site. The adsorption isotherm of Sircar can be expressed as

$$\left. \begin{aligned} q &= m \left( 1 - \theta e^{\theta} E_{n+1}(\theta) \right) ; \quad n = 0, 1, 2, \dots \\ q &= \frac{K_L P}{1 + (K_L/m) P} ; \quad n = \alpha \\ \theta &= \frac{\alpha}{P} \\ K_L &= \frac{(n+1)m}{\alpha} \end{aligned} \right\} \quad (4)$$

where  $\alpha$ ,  $n$ , and  $m$  are the unknown parameters.  $E_{n+1}(\theta)$  is the exponential integral and its value can be obtained from the Handbook of Mathematical Functions [15].

The Kuo and Hines equation can be written as

$$q = m \left[ 1 - \frac{K_3}{K_3 - K_1 K_2} \left( \frac{K_1}{P + K_1} - \frac{K_1 K_2}{P + K_3} \right) \right] \quad (5)$$

where  $m$ ,  $K_1$ ,  $K_2$ , and  $K_3$  are functions of temperature only and are related to the Henry's Law constant by the equation given below

$$K_L = m \left[ \frac{K_3^2 - K_1^2 K_2}{K_1 K_3 (K_3 - K_1 K_2)} \right] \text{ as } P \rightarrow 0 \quad (6)$$

The parameters of Equations (4) and (5) are obtained by a trial and error procedure, as described by Sircar and Kuo and Hines in their respective paper. The best fit values of the parameters are given in Table II. The best fit curves provided by the Sircar and the Kuo and Hines equations are shown along with the experimental data in Figures 8 through 10. As can be seen from the figures, the Kuo and Hines model provided a better fit of the experimental data than did Sircar's model. When the multilayer adsorption becomes more prominent, a large deviation between the calculated and the experimental values was observed. Although, Sircar and Kuo and Hines considered the surface heterogeneity in the model, multilayer adsorption was not considered. Both the Jovanovic and the Langmuir isotherms used to describe the local adsorption are for monolayer adsorption only. Therefore, the failure of these models when multilayer adsorption is occurring is not surprising. A comparison of the experimental data with the calculated values were made for all of the experimental runs. The average absolute percent error, maximum positive error, and maximum negative error over the complete pressure range are given in Table III. In general the Kuo-Hines and the Sircar equations provided a better fit than did the BET equation.

**NOMENCLATURE**

C	Constant in the BET equation
$\epsilon$	Adsorption Potential
$\Delta H_{iso}$	Isoteric heat of adsorption
$K_L$	Henry's Law constant
$K_1, K_2, K_3$	Constants in the Kuo-Hines equation
m	Constant in the Sircar and the Kuo and Hines equations
$n, \theta, \alpha$	Constants in the Sircar equation.
P	System pressure
$P_s$	Saturation pressure of the adsorbate at the system temperature
q	Uptake of the adsorbate
$q_m$	Equilibrium uptake of the adsorbate as defined by the BET equation
R	Gas constant
T	System temperature

**REFERENCES**

1. P.L. Magill, F.R. Holden, and C. Ackley, Air Pollution Handbook, McGraw Hill Book Company, Inc., New York (1956).
2. R.E. Kirk and D.F. Othmer, Encyclopedia of Chemical Technology, 2nd ed. The Interscience Encyclopedia, Inc., New York, Vol. 1 (1963).
3. B.C. Nayar and U. Subba Rao, "Contact Angle and Oriented Adsorption of Aliphatic Amines and Aldehydes on Silica Gel and Silica Aerogel," Indian J. of Chemistry, Vol. 20A, p 551-555 (1981).
4. S. Tanada, "Studies on Adsorption Removal of Odorous Pollutants (Acetaldehyde and Methyl Mercaptan), Adsorption of Acetaldehyde on Porous Adsorbents," Japanese J. of Hygiene, Vol. 32, No.9, p 671 (1977).
5. S.L. Kuo and A.L. Hines, "Adsorption of Chlorinated Hydrocarbon Pollutants on Silica Gel," Separation Science and Technology, Vol.23, No.(4&5), p 293, (1988).
6. V.Ponec, Z. Knor, and S.Cerny, "Adsorption on Solids" Butterworth & Co. Ltd., (1974)
7. L.H. Cohan, "Sorptions Hysteresis and the Vapor Pressure of Concave Surfaces," J. Amer. Chem. Soc., Vol.60, p. 433, (1938).
8. R.A. Beebe and D.M. Young, "Heats of Adsorption of Argon on a Series of Carbon Black's Graphitized at Successively Higher Temperatures," J. Phys. Chem., Vol.58, p 93, (1954).
9. A.W. Adamson, "Physical Chemistry of Surfaces," 3rd Ed., John Wiley & Sons, (1976).
10. L.G. Joyner and P.H. Emmett, "Differential Heats of Adsorption of Nitrogen on Carbon Blacks," J. Amer. Chem. Soc., Vol. 70, p 2353, (1948).
11. S. Sircar, "New Adsorption Isotherm for Energetically Heterogeneous Adsorbents," J. Colloid. Inter. Sci., Vol. 98, No. 2, p 523, (1984).
12. S.L. Kuo and A.L. Hines, "New Theoretical Isotherm for Adsorption on Heterogeneous Adsorbents," submitted to Separation Science and Technology.



13. S.J. Gregg and K.S.W. Sing, "Adsorption, Surface Area and Porosity," 2nd Ed., Academic Press, (1982).
14. D.M. Young and A.D. Crowell, "Physical Adsorption of Gases," Butterworth & Co. Ltd., Washsington, (1962).
15. D.S. Jovanovic, "Physical Adsorption of Gases, I: Isotherms for Monolayer and Multilayer Adsorption," Colloid and Polymer Science, p. 1203, (1969).
16. M. Abramowitz and I.A. Stegun, "Handbook of Mathematical Functions," Dover Publications Inc., New York, (1965).

**LIST OF TABLES**

- I. Monolayer Coverages and Calculated Surface Areas of Molecular Sieve-13X
- II. Best Fit Parameters for the Sircar and the Kuo-Hines Model
- III. Comparison of Model Correlations

**LIST OF FIGURES**

1. Adsorption and Desorption Curves for Acetaldehyde on Molecular Sieve-13X
2. Adsorption and Desorption Curves for Propionaldehyde on Molecular Sieve-13X
3. Adsorption and Desorption Curves for Butyraldehyde on Molecular Sieve-13X
4. Heat of Adsorption at Different Loadings for Aldehydes on Molecular Sieve-13X
5. Characteristic Curve for Acetaldehyde on Molecular Sieve-13X
6. Characteristic Curve for Propionaldehyde on Molecular Sieve-13X
7. Characteristic Curve for Butyraldehyde on Molecular Sieve-13X
8. Comparison of Experimental Data with the Kuo-Hines and the Sircar Model for Acetaldehyde-Molecular Sieve-13X System
9. Comparison of Experimental Data with the Kuo-Hines and the Sircar Model for Propionaldehyde-Molecular Sieve-13X System
10. Comparison of Experimental Data with the Kuo-Hines and the Sircar Model for Butyraldehyde-Molecular Sieve-13X System

Table I. Monolayer Coverages and Calculated Surface Areas of Molecular Sieve-13X

SYSTEM	TEMP. (K)	MOLECULAR CROSS SECTION $\text{\AA}^2$	MONOLAYER COVERAGE ( $\text{cm}^3/\text{g}$ )		SURFACE AREA ( $\text{m}^2/\text{g}$ )	
			LANGMUIR	BET	LANGMUIR	BET
Acetaldehyde Molecular Sieve	286.5	22.38	65.13	54.67	392	329
	293.2	22.55	64.40	52.34	390	317
	301.0	22.75	62.79	51.14	384	312
Propionaldehyde Molecular Sieve	283.2	26.44	52.48	40.91	373	291
	293.2	26.69	49.72	39.46	357	283
	303.2	26.96	47.71	38.44	346	279
Butyraldehyde Molecular Sieve	282.6	30.43	45.08	31.83	369	260
	293.2	30.70	42.31	30.26	349	251
	302.0	30.95	41.50	30.16	345	250

Table II. Best Fit Parameters for the Sircar and the Kuo-Hines Model.

SYSTEM	TEMP. (K)	HENRY'S LAW CONSTANT (mmol/g-mmHg)	KUO-HINES MODEL			SIRCAR MODEL		
			m (mmol/g)	$K_1$ (mmHg)	$K_2$	m (mmol/g)	n	$\alpha$ (mmHg)
Acetaldehyde Molecular Sieve	286.5	12.6	3.157	0.1969	- 72.707	2.923	0	0.2324
	293.2	12.4	3.138	0.1898	- 89.438	2.891	0	0.2321
	301.0	12.2	2.975	0.1907	- 74.815	2.742	0	0.2241
Propionaldehyde Molecular Sieve	283.2	20.6	2.953	0.0868	-390.285	2.404	0	0.1169
	293.2	18.0	2.517	0.1037	-174.174	2.200	0	0.1220
	303.2	14.5	2.363	0.1255	-122.772	2.142	0	0.1478
Butyraldehyde Molecular Sieve	282.6	24.1	3.334	0.0649	-906.654	2.171	0	0.008998
	293.2	22.3	2.540	0.0733	-392.574	2.001	0	0.008970
	302.0	18.0	2.176	0.0907	-187.926	1.863	0	0.010310

$K_3 = 1$  psia (51.7 mmHg)

Table III. Comparison of Model Correlations

SYSTEM	TEMP. (K)	ABS. AVERAGE ERROR* (%)			Max. POSITIVE ERROR (%)			Max. NEGATIVE ERROR (%)		
		Kuo-Hines	Sircar	BET	Kuo-Hines	Sircar	BET	Kuo-Hines	Sircar	BET
Acetaldehyde Molecular Sieve	286.5	0.65	3.45	112.82	1.79	6.53	351.44	1.05	6.00	1010.63
	293.2	0.87	4.57	117.44	2.70	8.32	1116.88	1.53	8.93	164.75
	301.0	0.34	3.51	183.60	1.36	6.85	212.09	0.59	6.31	2332.46
Propionaldehyde Molecular Sieve	283.2	3.74	8.42	170.05	7.55	16.83	125.16	5.27	13.37	1773.46
	293.2	1.33	4.29	60.01	4.61	11.78	213.25	2.08	6.65	76.54
	303.2	1.10	3.89	65.62	2.92	8.16	238.70	1.46	6.66	310.69
Butyraldehyde Molecular Sieve	282.6	3.74	11.12	105.81	7.11	18.59	103.17	6.31	16.42	153.02
	293.2	2.49	6.21	108.38	5.53	13.38	654.54	3.48	9.10	39.71
	302.0	0.80	2.98	277.09	1.64	7.19	128.60	1.12	4.73	1741.97

\* Error =  $\frac{\text{Experimental} - \text{Calculated}}{\text{Experimental}} * 100.0$

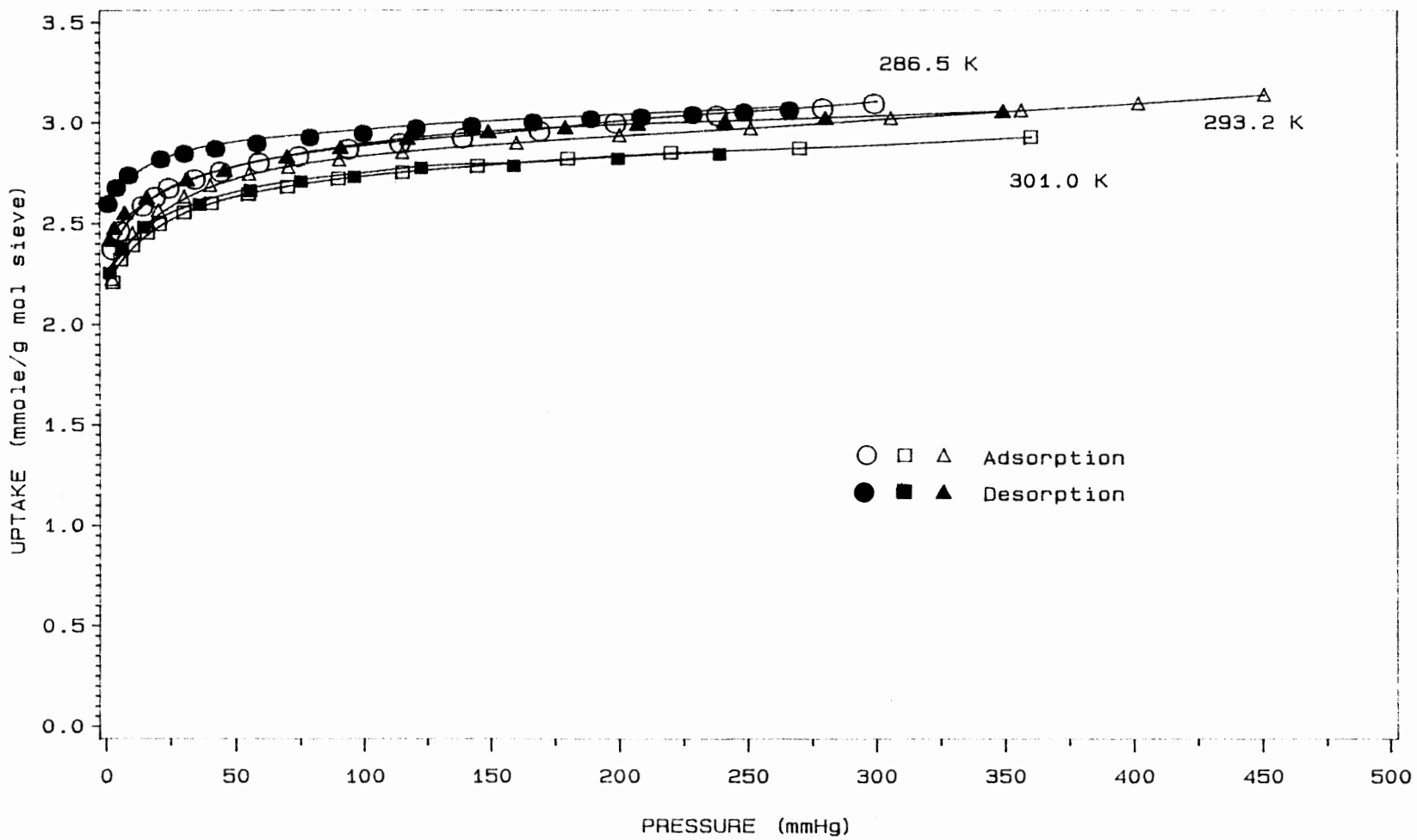


Figure 1. Adsorption and Desorption Curves for Acetaldehyde on Molecular Sieve-13x

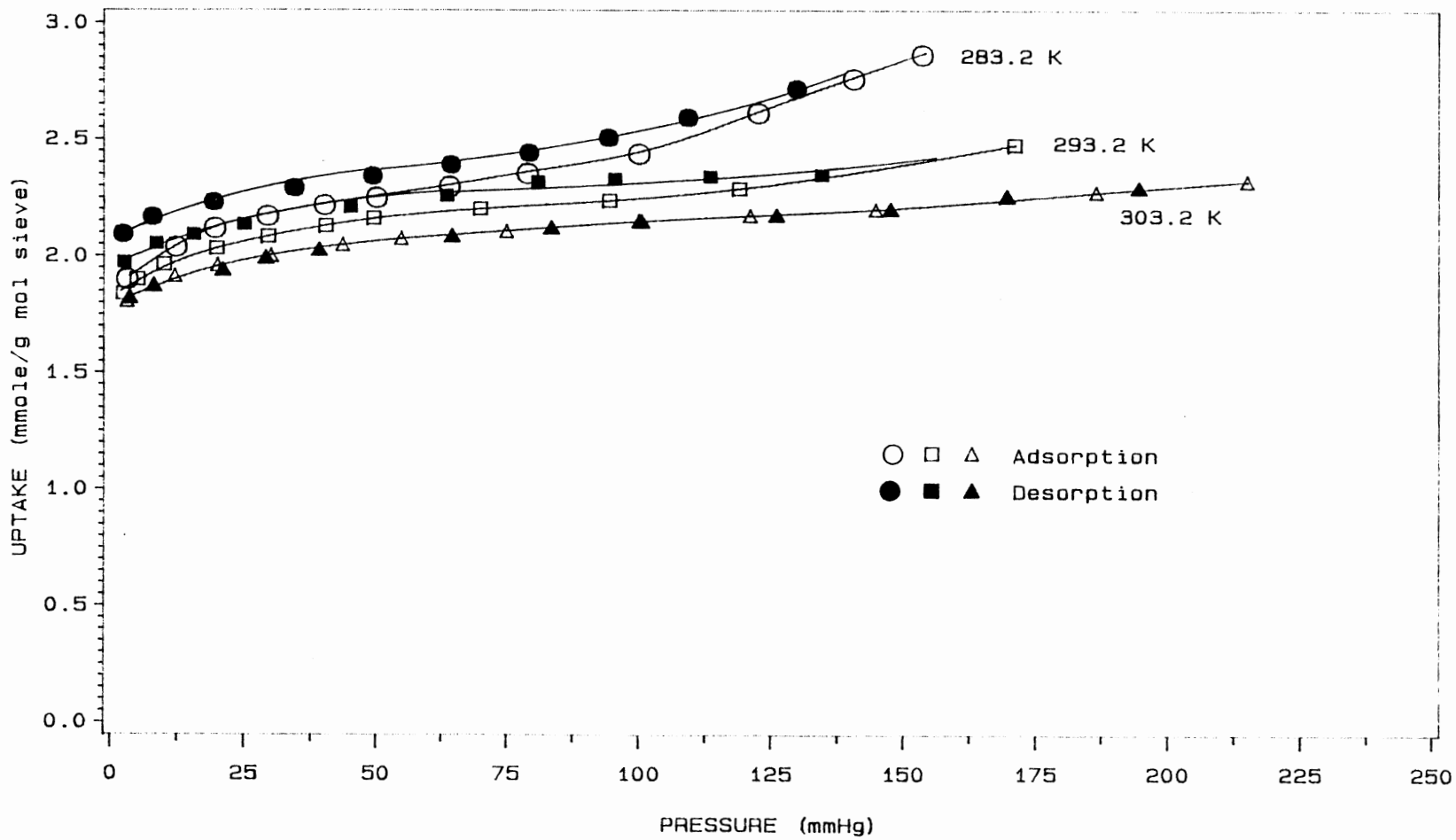


Figure 2. Adsorption and Desorption Curves for Propionaldehyde on Molecular Sieve-13x



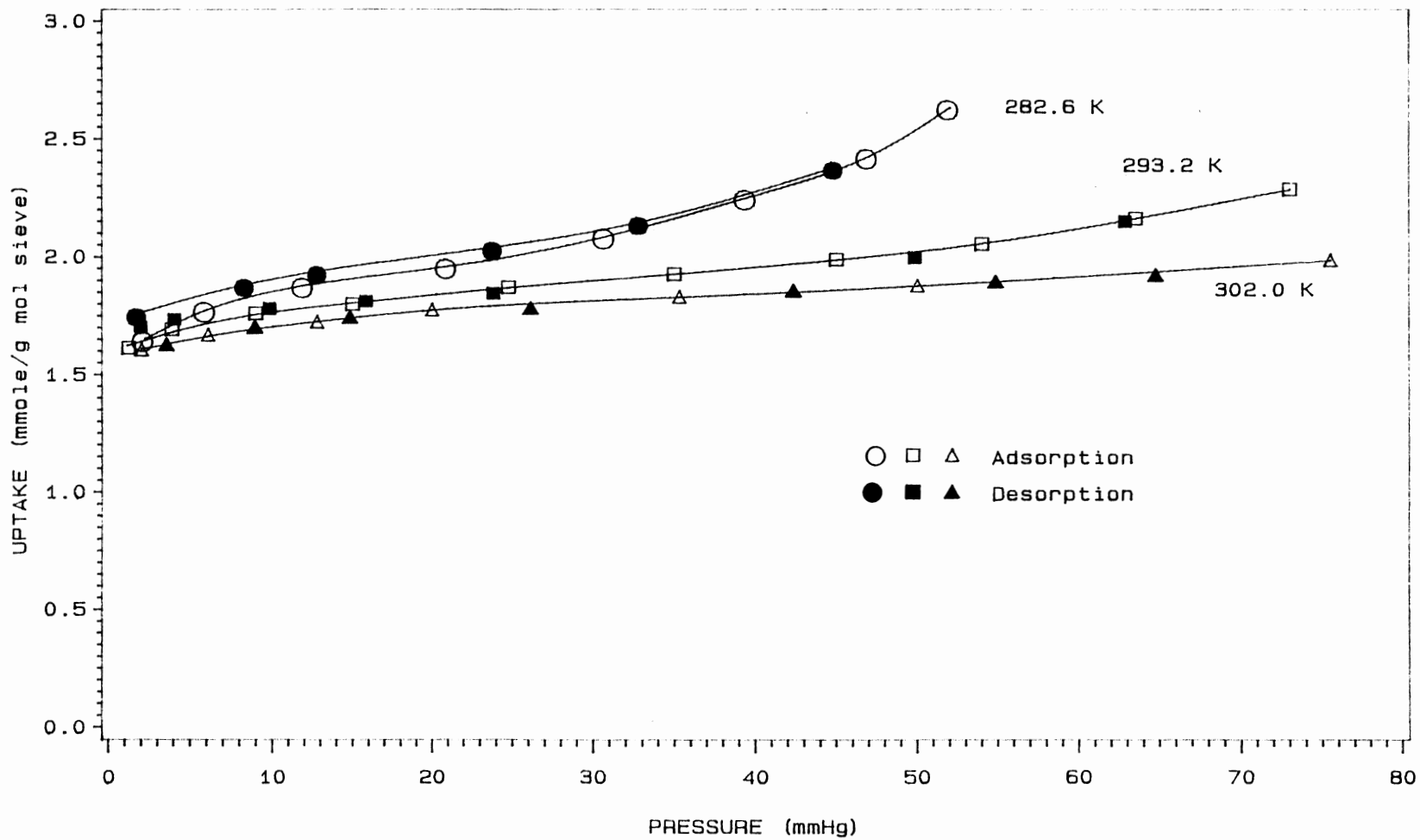


Figure 3. Adsorption and Desorption Curves for Butyraldehyde on Molecular Sieve-13X

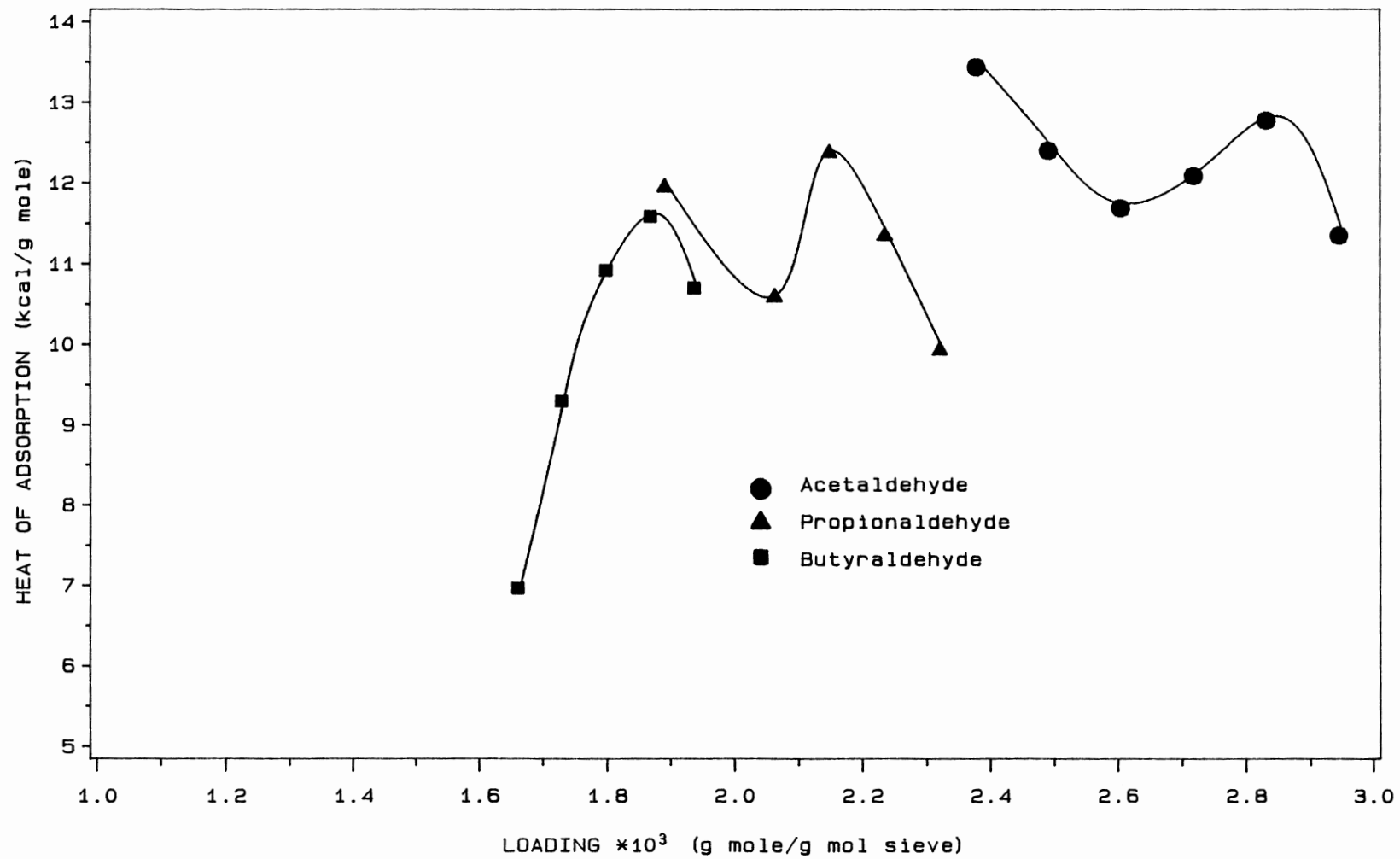


Figure 4. Heat of Adsorption at Different Loadings for Aldehydes on Molecular Sieve-13X

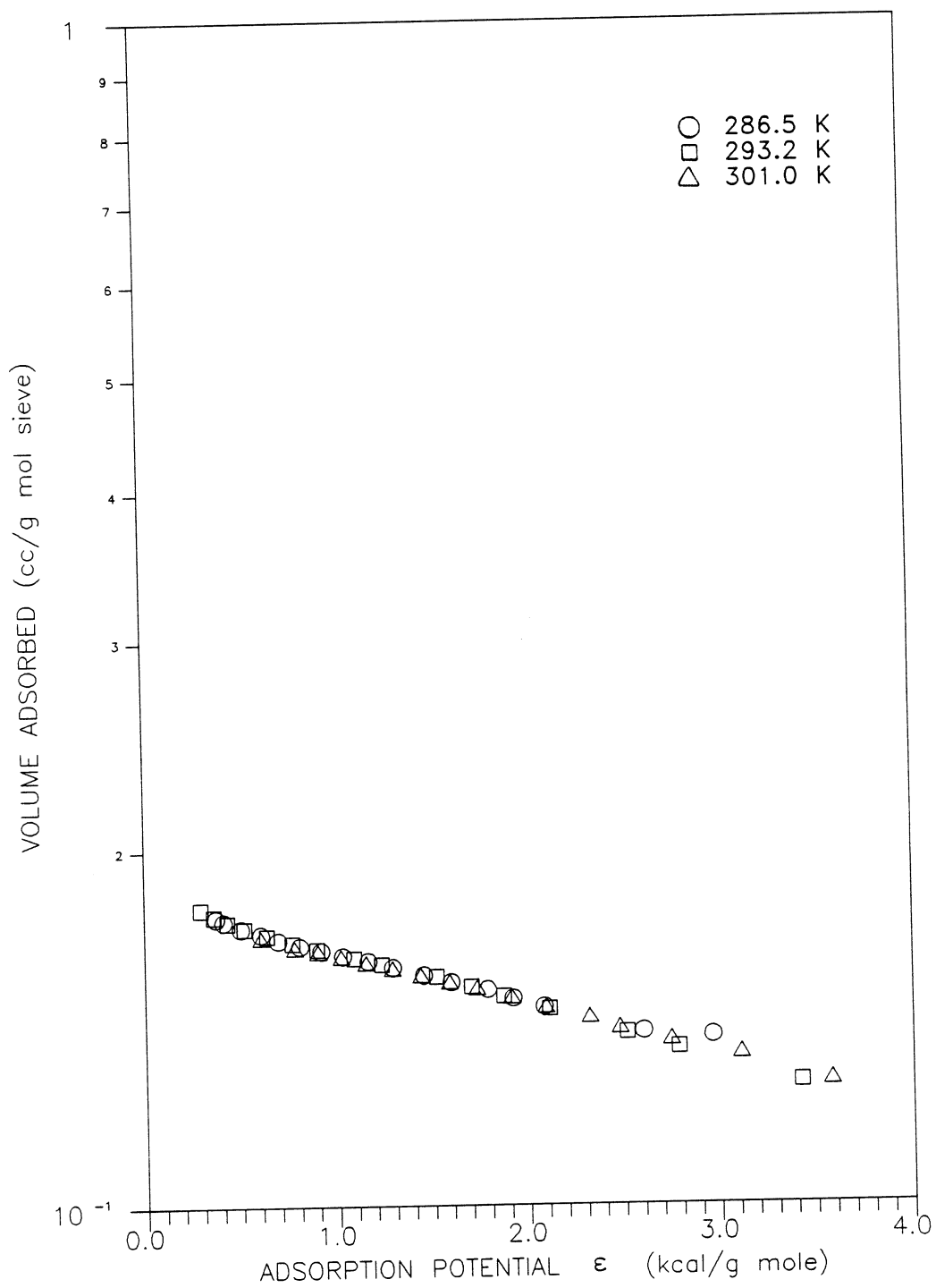


Figure 5. Characteristic Curve for Acetaldehyde on Molecular Sieve-13X

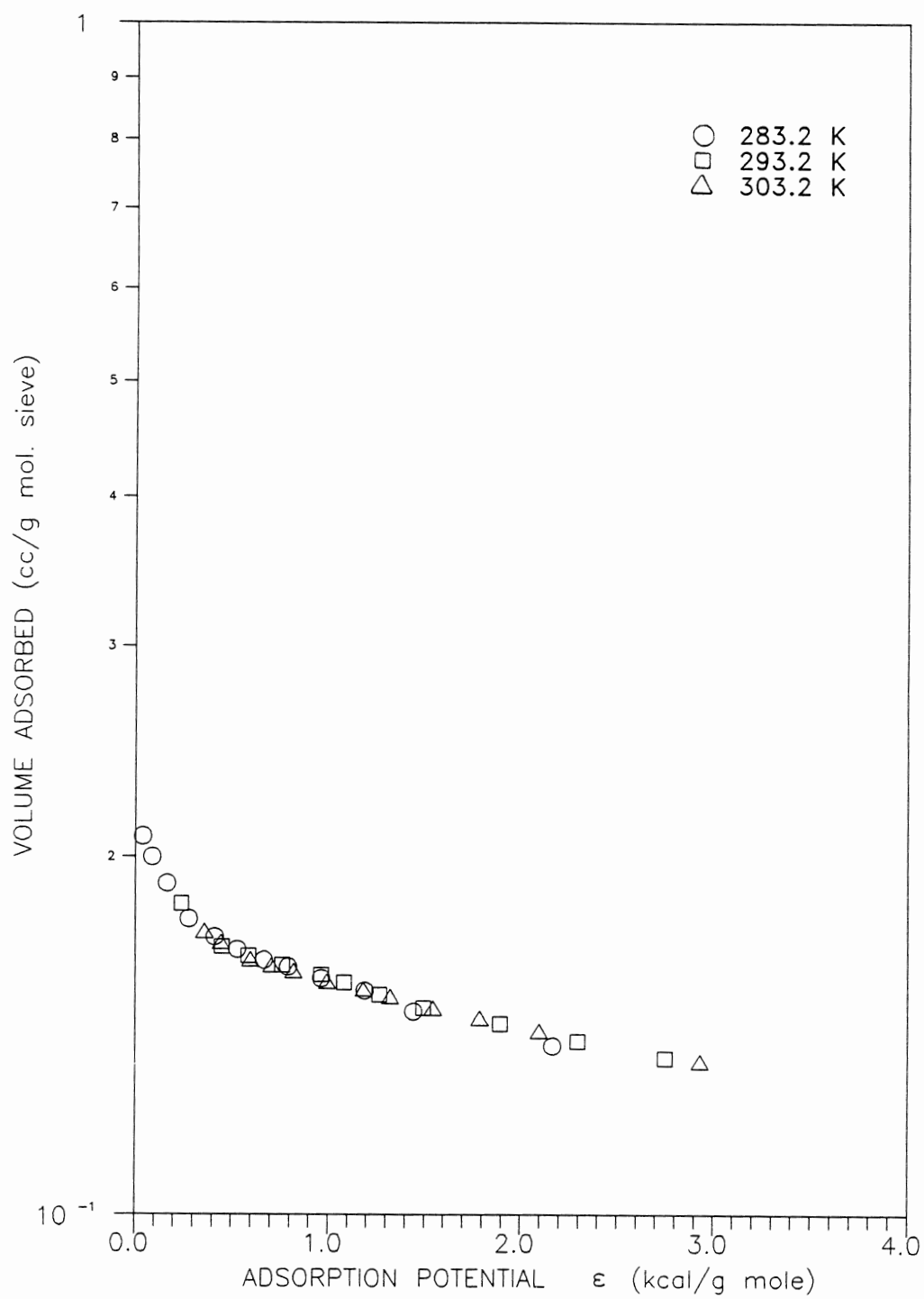


Figure 6. Characteristic Curve for Propionaldehyde on Molecular Sieve-13X

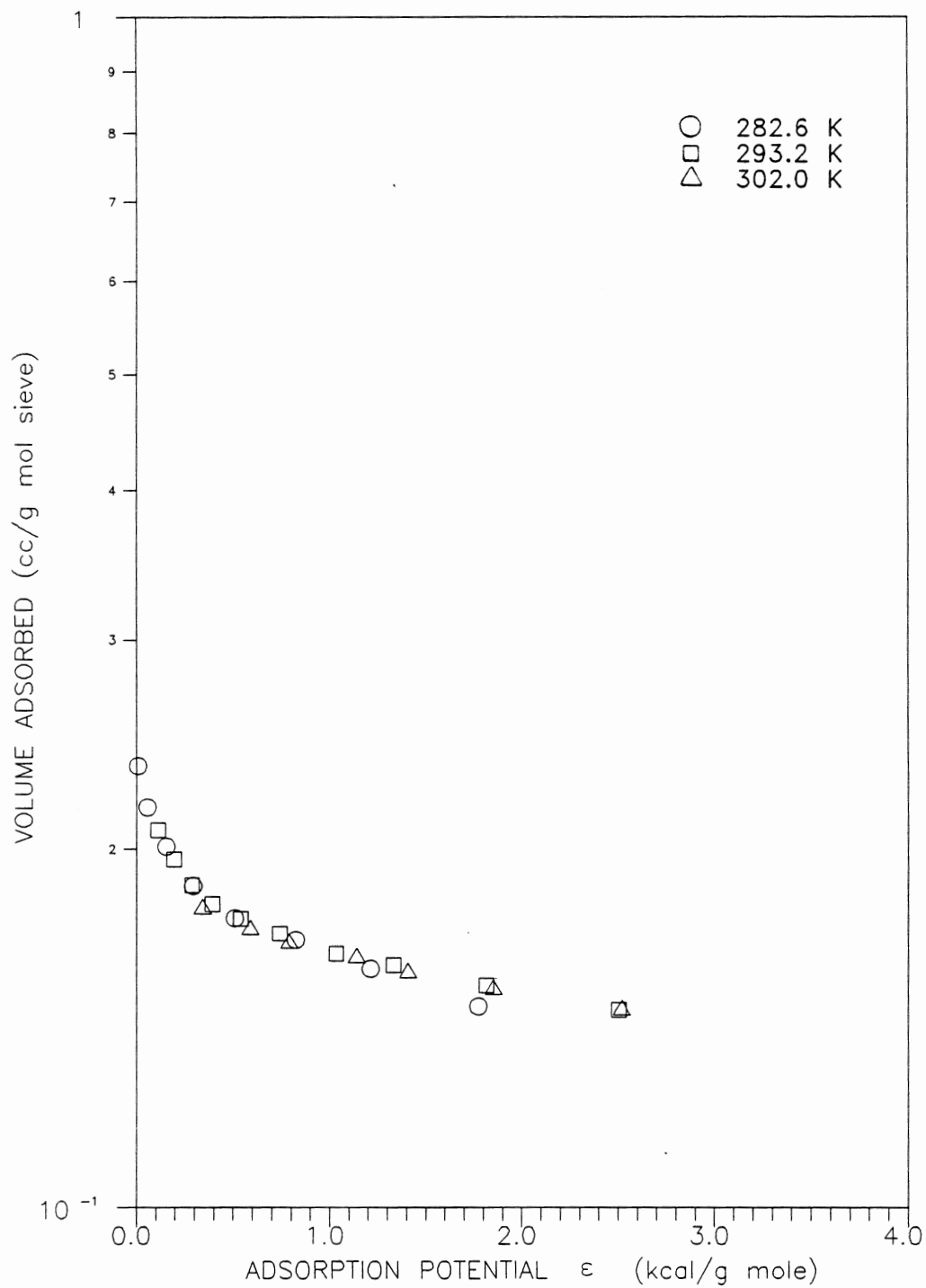


Figure 7. Characteristic Curve for Butyraldehyde on Molecular Sieve-13X

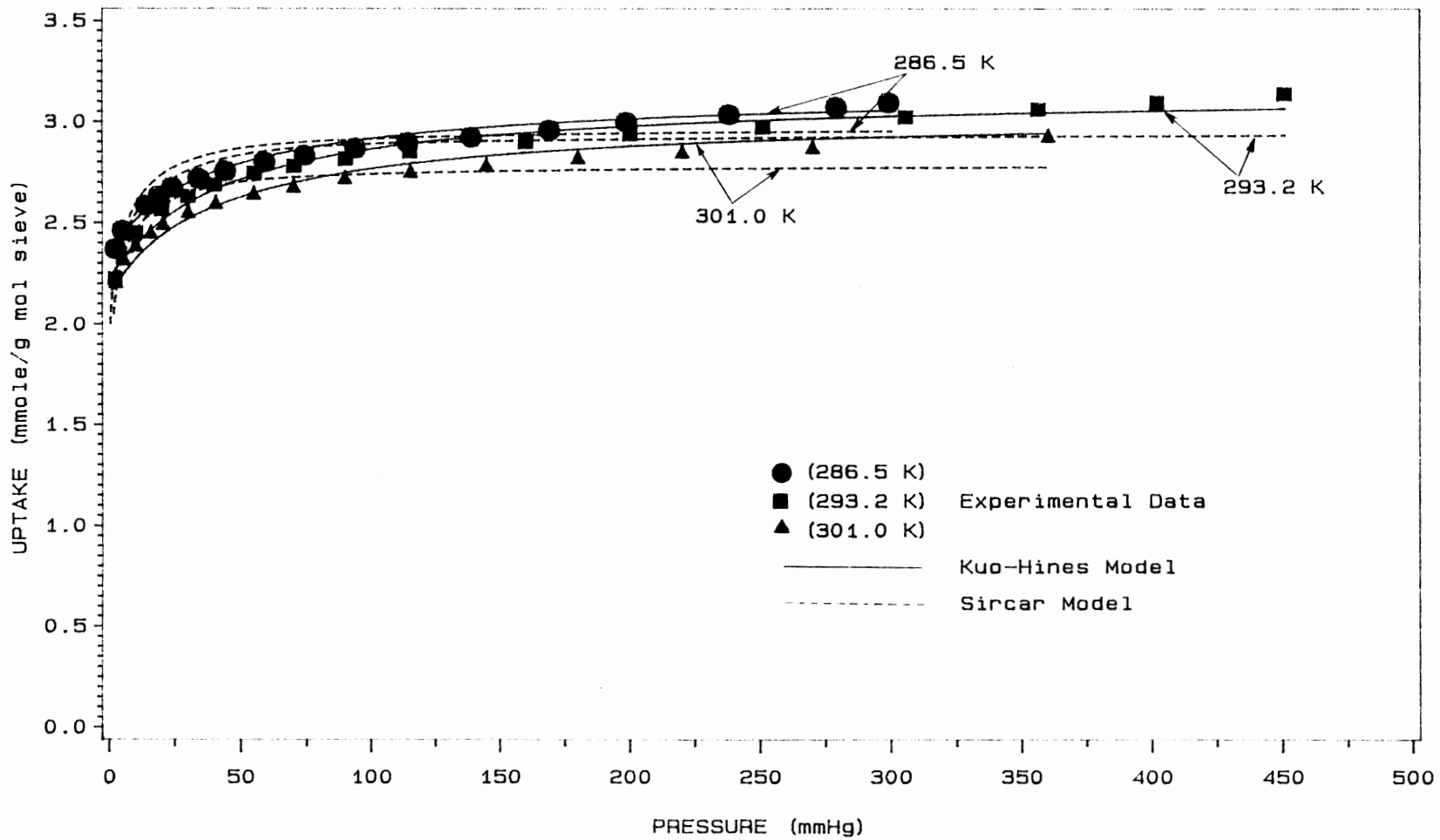


Figure 8. Comparison of Experimental Data With the kuo-Hines and the Sircar Model for Acetaldehyde-Molecular Sieve-13x System

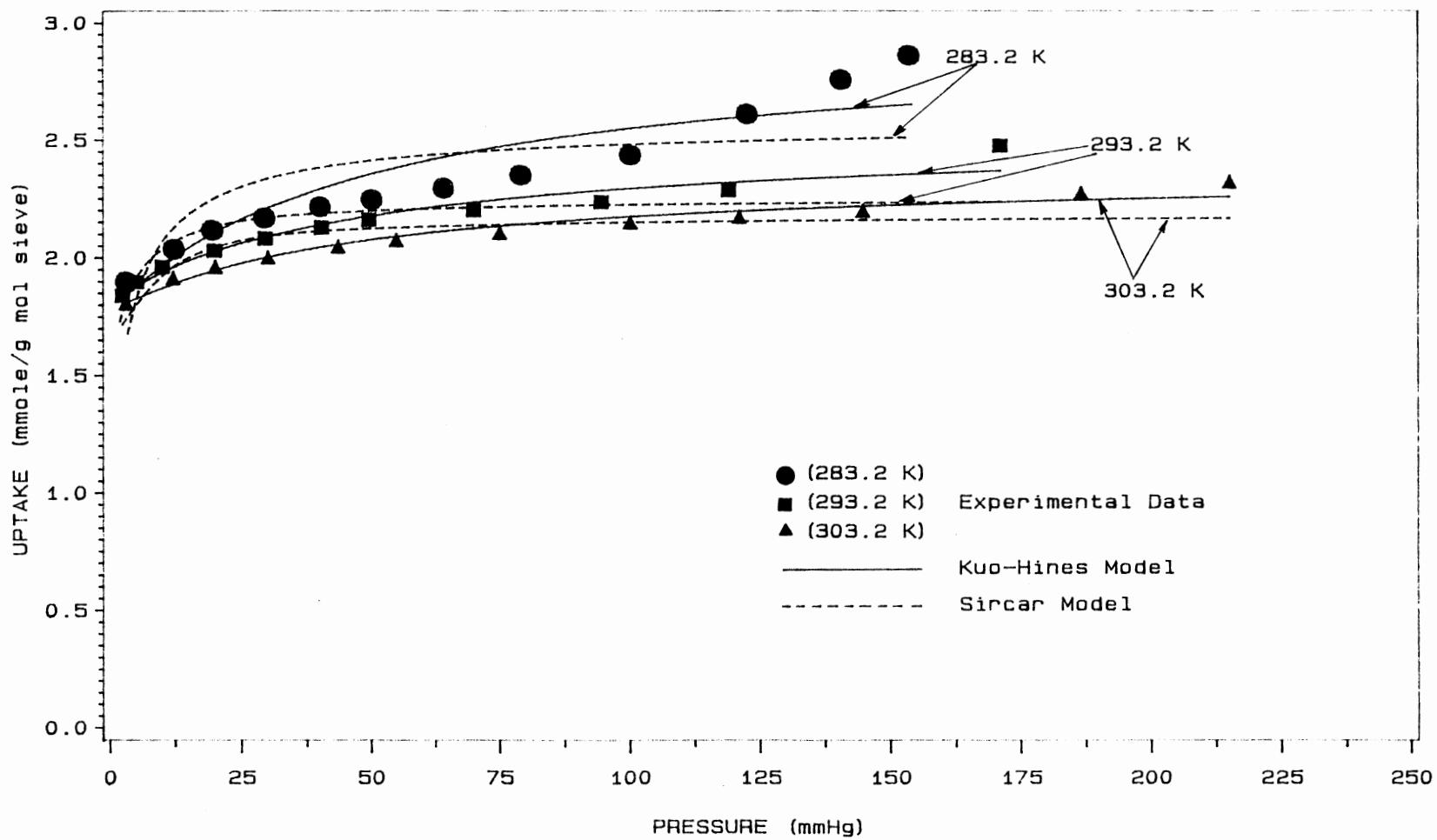


Figure 9. Comparison of Experimental Data With the kuo-Hines and the Sircar Model for Propionaldehyde-Molecular Sieve-13x System

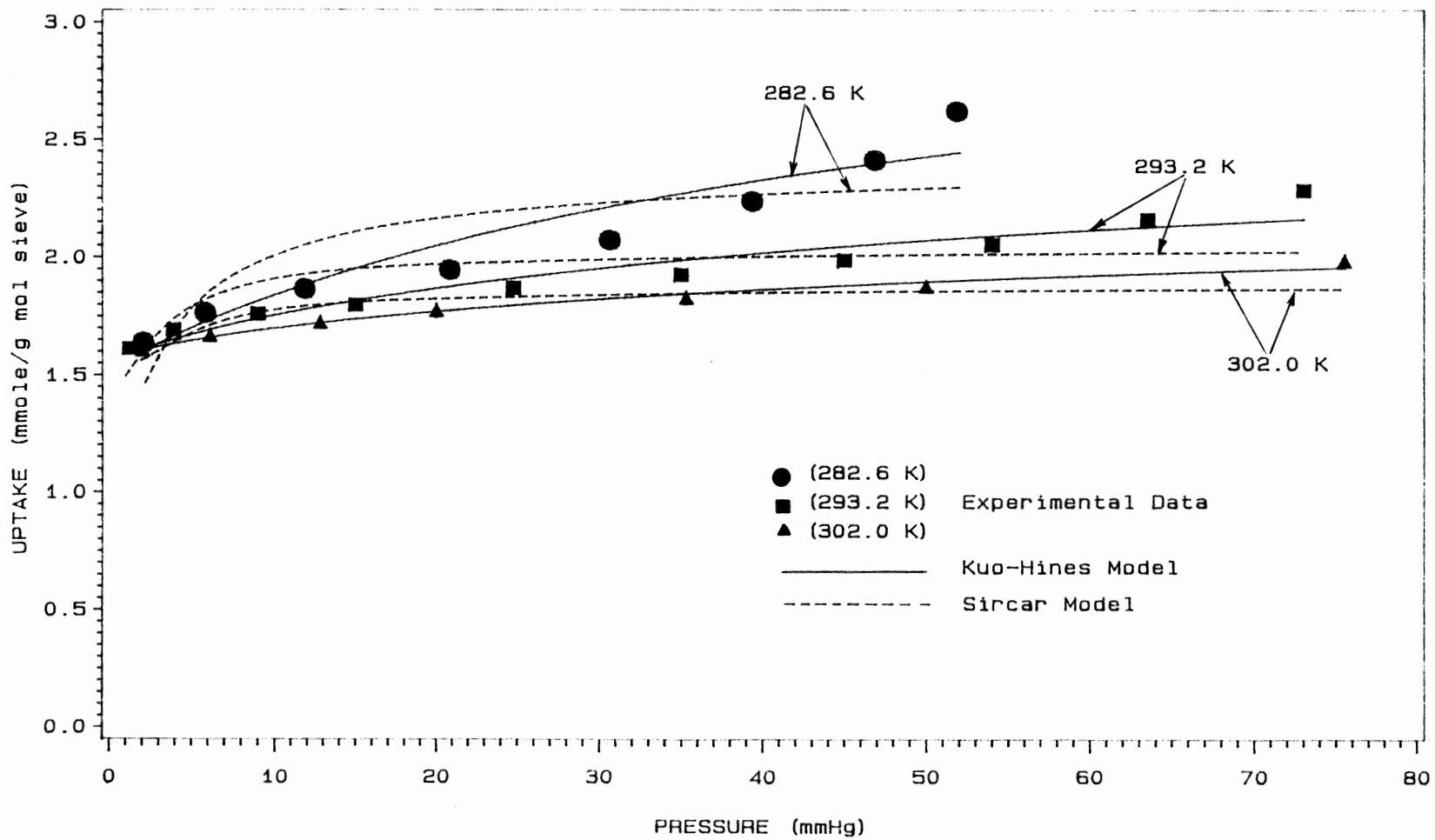


Figure 10. Comparison of Experimental Data With the kuo-Hines and the Sircar Model for Butyraldehyde-Molecular Sieve-13x System



CHAPTER III

AN ISOTHERM FOR MULTILAYER ADSORPTION ON  
HETEROGENEOUS SURFACES

**AN ISOTHERM FOR MULTILAYER ADSORPTION ON  
HETEROGENEOUS ADSORBENTS**

**Tushar K. Ghosh and Anthony L. Hines**

**School of Chemical Engineering  
Oklahoma State University  
Stillwater, Oklahoma 74078**

**ABSTRACT**

A new analytical expression is derived to describe the multilayer adsorption process of a single gas on energetically heterogeneous solid surfaces. The distribution of energy on the solid surface is described by a combination of two distribution functions. The energy distribution of the surface adjacent to the first layer of adsorbate is assumed to be given by a modified Morse type probability distribution function, while that of the second and subsequent layers are considered to have a constant distribution function. The adsorption on a particular site is given by the Jovanovic equation for multilayer coverage. The model has five adjustable parameters which can be obtained easily from the pure component experimental data by using a non-linear regression method.

The proposed isotherm reduces to the Henry's Law constant as the pressure approaches zero. The new model provides excellent correlation for Type I isotherms. The prediction capability for Type II and Type IV isotherms are better than other existing isotherm equations.

## INTRODUCTION

A number of adsorption isotherm models for energetically heterogeneous adsorbents have been proposed in the literature [Misra, 1969, 1973; Cerofolini et al., 1978; Jaroniec and Toth, 1978; House and Jaycock, 1978; Ross and Morrison, 1973; Sircar, 1984; Kuo and Hines, 1989]. Jaroniec et al. (1981) provided a detail review of the subject. The basic assumption in the derivation of isotherm models is that the solid surface consists of a number of energetic sites, the distribution of which can be described from a probability density function. The overall adsorption isotherm is obtained by summing the contribution of each site and is given by

$$N(P, T) = \int_0^{\infty} \theta(P, T, \epsilon) f(\epsilon) d\epsilon \quad (1)$$

where  $N(P, T)$  is the overall adsorption isotherm on the heterogeneous surface. In the above equation,  $\theta(P, T, \epsilon)$  is the local adsorption isotherm on a site having energy between  $\epsilon$  and  $\epsilon + d\epsilon$ ,  $f(\epsilon)$  represents the probability density function for  $\epsilon$ , and  $P$  and  $T$  are the equilibrium pressure and temperature of the system. Both  $N$  and  $\theta$  represent the amount adsorbed per unit mass of adsorbate. The probability density function  $f(\epsilon)$  should satisfy the following condition:

$$\int_0^{\infty} f(\epsilon) d\epsilon = 1.0 \quad (2)$$

In Equation (1), both  $\theta(P, T, \epsilon)$  and  $f(\epsilon)$  are unknown

functions.

House and Jaycock (1978) and Ross and Morrison (1973) assumed different isotherms for  $\theta$  and then numerically estimated the energy function  $f(\epsilon)$ . Misra (1969) and Jaroniec (1975) obtained an analytical function for  $f(\epsilon)$  considering that the overall adsorption isotherm  $N(P,T)$  can be represented by the generalized Freundlich, the Dubnin-Radushkevich or the Toth isotherms. The local isotherm  $\theta(P,T,\epsilon)$  is assumed to be either the Langmuir equation or a step-like isotherm.

Most of the recent studies employed different types of probability density functions to describe the energy distribution of the adsorbent and either the Langmuir or the Jovanovic isotherm to describe the monolayer coverage. Misra (1970, 1973) used an exponential form as well as a constant probability density function. Neither of the equations derived by Misra were tested with experimental data. As noted by Sircar (1984), the resulting isotherms of Misra do not have a defined Henry's Law region. Cerofolini et al. (1978) applied the Langmuir equation to calculate the local uptake in conjunction with a condensation approximation for the adsorption energy distribution to derive the overall isotherm. Although, their isotherm reduces to the linear isotherm at low pressures as required by the physics of adsorption, it has not been tested with experimental data.

Sircar (1984) derived his isotherm considering that the energy distribution is given by a gamma probability density

function and the local adsorption is described by the Langmuir equation. His isotherm does comply with the constraints imposed by the physics of adsorption. He tested the isotherm successfully with various systems such as,  $\text{CH}_4$ -BPL carbon,  $\text{CO}_2$ -BPL carbon,  $\text{CO}_2$ -MSCV carbon, and  $\text{N}_2$ -5A zeolite. However, a larger deviation between the predicted values and the experimental data was reported for the  $\text{CO}_2$ -BPL carbon system in the high pressure region. Kuo and Hines (1989) improved the prediction capabilities for  $\text{CO}_2$ -BPL carbon system as well as for the other systems by developing a similar type of isotherm. They used the Jovanovic isotherm to describe the local uptake along with a modified Morse type probability density function. The parameters in the Kuo and Hines model are easier to evaluate than those in Sircar's model. The Kuo and Hines equation also reduces to a linear isotherm in the low pressure region.

O'Brien and Myers (1984) suggested a different approach for deriving an isotherm for heterogeneous adsorbents. They expanded the right hand side of Equation (1) as an infinite series. The terms of the series needed not only the derivatives of the local isotherm with respect to  $\epsilon$  evaluated at the mean of the energy distribution but also the central moments of the distribution. The Langmuir equation and the normal distribution function were used as the local isotherm and the energy distribution function, respectively. The isotherm was tested with the equilibrium data for the  $\text{CO}_2$ -carbon system at three different temperatures. The deviation

between the predicted values and the experimental data was greater at higher pressures, particularly at low temperature.

All the models mentioned above showed varying degrees of success for Type I isotherms. However, a larger deviation between the predicted value and the experimental data was observed at higher pressures when multilayer adsorption occurs. In all of the above models, the local isotherms were for monolayer adsorption.

In the present study, the Jovanovic (1969) model for multilayer coverage was used to describe local adsorption. The energy distribution of the adsorbent surface was divided into two functions. The energy distribution of the surface adjacent to the first layer was assumed to be given by a Morse type distribution function. The energy distribution of the second and higher layers was assumed to be constant. The proposed isotherm is tested with experimental data and compared with the Kuo and Hines model.

### THEORY

For multilayer adsorption, it can be assumed that the adsorption process in the higher layer proceeds in the same way as on the adsorbent surface. The amount of available surface for the second and subsequent layers is equal to the exposed surface of the first adsorbed layer of molecules. The energy of attraction for these layers should be lower than that of the solid surface. Every site on the heterogeneous surface therefore can be visualized as having two

adsorption energies  $\epsilon_A$  and  $\epsilon_B$ . The fraction of the surface adjacent to the first layer has energies between  $\epsilon_A$  and  $\epsilon_A+d\epsilon_A$ , while that of the second and higher layers have energies between  $\epsilon_B$  and  $\epsilon_B+d\epsilon_B$ . The overall energy of the site can be described by  $f(\epsilon_A, \epsilon_B)d\epsilon_A d\epsilon_B$ . The function  $f(\epsilon_A, \epsilon_B)$  represents the energy of the whole surface. The overall adsorption isotherm, therefore, is written as

$$N(P, T) = \int_0^{\infty} \int_0^{\infty} \theta(P, T, \epsilon_A, \epsilon_B) f(\epsilon_A, \epsilon_B) d\epsilon_A d\epsilon_B \quad (3)$$

In the above expression,  $\theta$  represents the local isotherm for the multilayer adsorption and  $f(\epsilon_A, \epsilon_B)$  is the energy distribution function which should be normalized as

$$\int_0^{\infty} \int_0^{\infty} f(\epsilon_A, \epsilon_B) d\epsilon_A d\epsilon_B = 1.0 \quad (4)$$

The local isotherm  $\theta(P, T, \epsilon_A, \epsilon_B)$  is assumed to be given by the Jovanovic (1969) isotherm for multilayer adsorption, which can be expressed as

$$\theta = \theta_m \{1 - \exp(-aP)\} \exp(bP) \quad (5)$$

where  $\theta_m$  is the adsorption capacity at saturation, and  $a$  and  $b$  are constants which are given by

$$a = a_0 \exp\left(\frac{q_A}{RT}\right) \quad (6a)$$



and

$$b = b_0 \exp\left(\frac{q_B}{RT}\right) \quad (6b)$$

The constants  $a_0$  and  $b_0$  represent the limiting value of  $a$  and  $b$ , respectively, as temperature approaches infinity. The heats of adsorption,  $q_A$  and  $q_B$ , are associated with the first layer and the second and higher layers, respectively. The Jovanovic isotherm given by Equation (5) reduces to the Henry's Law constant as pressure approaches zero and is given by

$$\left\{ \frac{\partial \theta}{\partial P} \right\}_T \lim_{P \rightarrow 0} = \theta_m a \quad (7)$$

As mentioned earlier, the energy function,  $f(\epsilon_A, \epsilon_B)$ , describes the energy distribution of a complete site, which consists of a number of layers of the adsorbate. Thus  $f(\epsilon_A, \epsilon_B)$  is divided into two functions, one for first layer and another for the second and higher layers as follows:

$$f(\epsilon_A, \epsilon_B) = f(\epsilon_A) \cdot f(\epsilon_B) \quad (8)$$

A solid surface generally has variations of energies resulting from cracks, lattice defects, edges, etc. The distribution of adsorptive potentials on the surface adjacent to the first layer of adsorbate was assumed to be given by the same distribution function that was used by Kuo and Hines (1989). Therefore,

$$f(\epsilon_A) = A_0 \left\{ \exp(-A_1 \epsilon_A) - A_2 \exp(-A_3 \epsilon_A) \right\} \quad (9)$$

where the parameters  $A_0$ ,  $A_1$ , and  $A_2$  are functions of temperature only. Further, the parameter  $A_0$  can be interpreted as the energy required to bring an adsorbate molecule from infinity to an adsorptive site,  $A_1$  is associated with the short range repulsive potential,  $A_3$  is associated with the energy of attraction and  $A_2$  is an empirical constant. In the above equation,  $\epsilon_A$  represents an energy parameter associated with the distance between an adsorbate molecule in the gas phase and an adsorptive site. The parameter,  $\epsilon_A$ , is related to the heats of adsorption of the first layer by the expression suggested by Sircar (1984).

$$\epsilon_A = a_0 \left[ \exp\left(\frac{q_A}{RT}\right) - 1 \right] \quad (10)$$

Since  $q_A$  can have any value between zero and infinity for a heterogeneous adsorbent,  $\epsilon_A$  can also vary between zero and infinity.

The distribution of energy for second and higher layers is assumed constant.

$$f(\epsilon_B) = \lambda \text{ (constant)} \quad (11)$$

However, the energy parameter  $\epsilon_B$  is related to the Jovanovic constant  $b$  by the following expression:

$$\epsilon_B = b_0 \left[ \exp\left(\frac{q_B}{RT}\right) + 1 \right] \quad (12)$$

It should be noted that when there is no second and higher layers, the constant  $b_0$  is equal to zero and  $\epsilon_B$  becomes zero also. However, when second or higher layers form,  $\epsilon_B$  should assume a constant value which is denoted here as  $\epsilon_M$ . The constant  $\epsilon_M$ , can be interpreted as the average of the heats of adsorption due to the second and higher layers. Upon substitution of Equation (8) into Equation (4) and with the new limits of integration, Equation (4) becomes

$$\int_{\epsilon_A=0}^{\epsilon_A=\infty} f(\epsilon_A) \left[ \int_{\epsilon_B=0}^{\epsilon_B=\infty} f(\epsilon_B) d\epsilon_B \right] d\epsilon_A = 1.0 \quad (13)$$

The constants  $A_0$  and  $\lambda$  can be expressed in terms of the other constants,  $A_1$ ,  $A_2$ , and  $\epsilon_M$  by substituting Equations (9) and (11) into Equation (13). Integration gives

$$A_0 \lambda = \frac{1}{\epsilon_M} \left[ \frac{A_1 A_3}{A_3 - A_1 A_2} \right] \quad (14)$$

The energy distribution function can be obtained by combining Equations (9)-(13) as

$$\int_0^{\infty} \int_0^{\epsilon_M} A_0 \left( \exp(-A_1 \epsilon_A) - A_2 \exp(-A_3 \epsilon_A) \right) (\epsilon_A + a_0) \lambda (\epsilon_B - b_0) \cdot d\left(\frac{q_A}{RT}\right) d\left(\frac{q_B}{RT}\right) = 1 \quad (15)$$

Substitution of Equation (14) into Equation (15) gives

$$\int_0^{\infty} \int_0^{\epsilon_M} \frac{A_1 A_3}{A_3 - A_1 A_2} \left\{ \exp(-A_1 \epsilon_A) - A_2 \exp(-A_3 \epsilon_A) \right\} (\epsilon_A + a_0) \left\{ \frac{\epsilon_B - b_0}{\epsilon_M} \right\} \circ$$

$$d\left(\frac{q_A}{RT}\right) d\left(\frac{q_B}{RT}\right) = 1 \quad (16)$$

Equation (16) suggests that the overall energy distribution function  $f(\epsilon_A, \epsilon_B)$  can be expressed as

$$f\left(\frac{q_A}{RT}, \frac{q_B}{RT}\right) = \frac{A_1 A_3}{A_3 - A_1 A_2} \left\{ \exp(-A_1 \epsilon_A) - A_2 \exp(-A_3 \epsilon_A) \right\} (\epsilon_A + a_0) \left\{ \frac{\epsilon_B - b_0}{\epsilon_M} \right\} \quad (17)$$

and  $f(q_A/RT)$  and  $f(q_B/RT)$  can be written respectively as

$$f\left(\frac{q_A}{RT}\right) = \frac{A_1 A_3}{A_3 - A_1 A_2} \left\{ \exp(-A_1 \epsilon_A) - A_2 \exp(-A_3 \epsilon_A) \right\} (\epsilon_A + a_0) \quad (18)$$

and

$$f\left(\frac{q_B}{RT}\right) = \frac{\epsilon_B - b_0}{\epsilon_M} \quad (19)$$

It is interesting to note that the energy distribution of the first layer given by Equation (18) is the same as that obtained by Kuo and Hines (1989). Kuo and Hines showed that  $f(q_A/RT)$  has a skewed Gaussian-like shape for certain values of  $A_1$  when plotted against  $(q_A/RT)$ . However,  $f(q_A/RT)$  does not reduce to zero when  $\epsilon_A$  approaches zero. The function of  $f(q_B/RT)$  is a constant if  $q_B$  remains constant for the second

and higher layers. Theoretically,  $q_B$  should approach the heat of condensation as more and more layers form on the adsorbent surface. A bimodel type energy distribution of the adsorbent surface is found for certain values of  $A_1$ . The distribution is shown in Figure (1) for different values of  $A_1$ . During data correlation it was observed that  $A_1$  can vary from a very high number ( $>10^3$ ) to a very low number ( $<10^{-3}$ ). The shape of the energy distribution curve is strongly dependent on the value of  $A_1$ .

The overall isotherm,  $N(P,T)$ , is obtained by using Equation (3) as follows:

$$N(P,T) = \int_0^{\infty} \int_0^{\epsilon_M} \theta_m \left\{ 1 - \exp(-aP) \right\} \exp(bP) A_0 \left\{ \exp(-A_1 \epsilon_A) - A_2 \exp(-A_3 \epsilon_A) \right\} \lambda d\epsilon_A d\epsilon_B \quad (20)$$

To integrate, Equation (20) is rearranged as follows :

$$N(P,T) = \theta_m A_0 \lambda \int_0^{\infty} \left\{ 1 - \exp(-aP) \right\} \left\{ \exp(-A_1 \epsilon_A) - A_2 \exp(-A_3 \epsilon_A) \right\} \cdot \left[ \int_0^{\epsilon_M} \exp(bP) d\epsilon_B \right] d\epsilon_A \quad (21)$$

Integration of Equation (21) provides the overall isotherm as shown below:

$$N(P,T) = \theta_m \left\{ 1 - \exp(-a_0 P) \frac{A_1 A_3}{A_3 - A_1 A_2} \left( \frac{1}{A_1 + P} - \frac{A_2}{A_3 + P} \right) \right\} \frac{\exp(-b_0 P)}{\epsilon_M^P} \cdot \left( \exp(\epsilon_M P) - 1 \right) \quad (22)$$

Kuo and Hines (1989) pointed out that  $a_0$  is generally very small ( $1 \times 10^{-4}$ ). Therefore, for pressures up to 1 atm the term  $a_0 P$  is very small and  $\exp(-a_0 P) \approx 1.0$ . Hence, Equation (22) can be rewritten as follows:

$$N(P, T) = \theta_m \left\{ 1 - \frac{A_1 A_3}{A_3 - A_1 A_2} \left( \frac{1}{A_1 + P} - \frac{A_2}{A_3 + P} \right) \right\} \frac{\exp(-b_0 P)}{\epsilon_M P} \cdot \left( \exp(\epsilon_M P) - 1 \right) \quad (23)$$

By expanding the term  $\exp(\epsilon_M P)$  in a power series, it can be shown that

$$N(P, T) = 0 \quad \text{as } P \rightarrow 0 \quad (24)$$

and

$$N(P, T) \rightarrow \infty \quad \text{as } P \rightarrow \infty \quad \text{for } (\epsilon_M - b_0) > 0 \quad (25)$$

Equation (23) therefore retains the same properties as the original Jovanovic isotherm for multilayer adsorption. The Henry's Law constant is given as follows:

$$\left( \frac{\partial N(P, T)}{\partial P} \right)_{T \lim P \rightarrow 0} = \theta_m \left[ \frac{A_3^2 - A_1^2 A_2}{A_1 A_3 (A_3 - A_1 A_2)} \right] \quad (26)$$

Equation (26) shows that the adsorption isotherm given by Equation (23) reduces to a linear isotherm as pressure approaches zero, thus satisfying the physics of adsorption. Equation (23) also reduces to the isotherm proposed by Kuo and Hines (1989), provided  $\epsilon_M$  and  $b_0$  are zero. The parame-

ters  $\epsilon_M$  and  $b_0$  are associated with multilayer adsorption and are therefore expected to be zero for monolayer coverage. The new model can be used to correlate the equilibrium adsorption data for both Type I and Type II isotherms for heterogeneous adsorbents. Although Equation (23) has five adjustable parameters, ( $\theta_m$ ,  $A_1$ ,  $A_2$ ,  $b_0$ , and  $\epsilon_M$ )  $A_3$  can be set to unit pressure for any system. The parameters  $\theta_m$ ,  $A_1$ , and  $A_2$  are related to the Henry's Law constant by Equation (26), which can reduce the number of adjustable parameters to four provided the Henry's Law constant is known from the pure component equilibrium data. To determine the Henry's Law constant, however, good low pressure equilibrium data are required, which are frequently difficult to obtain experimentally.

#### **TEST OF THE NEW MODEL**

The new model given in Equation (23) was evaluated by using published literature data for several different systems. The five adjustable parameters were obtained by using a nonlinear regression analysis (Marquardt-S method) for all experimental data. The systems tested included the adsorption of methane, ethane, ethylene and propylene on activated carbon (Costa et al., 1981);  $\text{CO}_2$ , isobutane, ethane, and ethylene on molecular sieve-13X (Hyun and Danner, 1982); acetaldehyde, propionaldehyde, and butyraldehyde on molecular sieve-13X (Ghosh, 1989);  $\text{CO}_2$ ,  $\text{H}_2\text{S}$ , and propane on H-mordenite (Talu and Ziewebel, 1986). These

systems were selected because the adsorbents were not only microporous, but the experimental equilibrium data could not be accurately described with existing homogeneous isotherm equations. The above observation suggested that the adsorbents were heterogeneous in nature. The prediction capability of Equation (23) is compared with the Flory-Huggins Vacancy Solution model and with the model of Kuo and Hines.

Figure (2) shows a comparison of the experimental data for methane, ethane, ethylene and propylene on activated carbon at 293.2 K (Costa et al., 1981) with the prediction made from the Kuo and Hines model and Equation (23). The best fit parameters for both models are given in Table I. The activated carbon used by Costa et al. had a surface area of  $750 \text{ m}^2/\text{g}$  and a porosity of 0.715. The system temperature was above the critical temperature for methane and ethylene while it was below the critical temperature for ethane and propylene. It can be seen from Figure (2) that both models provided very good correlation of the data.

Figures (3), (4) and (5) show the best fit of the data by the above models for the adsorption of acetaldehyde, propionaldehyde, and butyraldehyde on molecular sieve-13X at three temperatures (Ghosh, 1989). The system temperatures in all cases were below the critical values. As shown butyraldehyde and propionaldehyde exhibited Type II isotherms at low temperatures. The isotherms, however, appeared to be of Type I at the higher temperatures. As noted by Ghosh and



Hines (1989), the heat of adsorption data for these systems indicated that the adsorbent surface was not only heterogeneous, but the adsorbate molecules on the adsorbent surface had strong interactions. The new model appears to correlate the experimental data better than the Kuo-Hines equation under these circumstances. Since the local isotherm used in the Kuo and Hines equation is for monolayer adsorption, the failure of their model is not surprising. As expected, the Kuo-Hines equation predicted the data well in the low pressure region. The best fit parameters for the new model are presented in Table II.

The experimental equilibrium data for carbon dioxide, ethane, and ethylene on molecular sieve-13X are compared in Figures 6 through 8 with prediction made from Equation (23) and from the Flory-Huggins Vacancy Solution Model (Cochran et al, 1985). As shown the predictions made with Equation (23) and the Flory-Huggins-Vacancy Solution Model are comparable.

The best fit curves for isobutane on molecular sieve-13X and for  $\text{CO}_2$ ,  $\text{H}_2\text{S}$ , and propane on H-mordenite at 293.2 K are shown in Figures (9) and (10), respectively. As can be seen from these figures an excellent fit of the data was obtained. The best fit parameters of the new model for the above systems are given in Tables III and VI.

From Tables I through VI it can be seen that the five parameters of the new model are functions of temperature. The constant  $A_2$  of the acetaldehyde-molecular sieve-13X

system, however, did not show a definite trend. This may be due to the adsorption temperature, 293.2 K, being equal to the boiling point of acetaldehyde. Therefore, these parameters can be correlated with respect to temperature which will help in interpolating the data from one temperature to another.

**NOMENCLATURE**

$A_0$	Parameter in the energy distribution function
$A_1$	Parameter in the energy distribution function
$A_2$	Parameter in the energy distribution function
$A_3$	Parameter in the energy distribution function
$a$	Constant in the Jovanovic equation
$a_0$	Limiting value of $a$
$b$	Constant in the Jovanovic equation
$b_0$	Limiting value of $b$
$N$	Overall adsorption isotherm
$P$	System pressure
$q$	Heat of adsorption
$T$	System temperature

**Greek Letters**

$\epsilon$	Energy of a particular site
$\epsilon_M$	Parameter in the energy distribution function
$\theta$	Local adsorption isotherm
$\theta_m$	Adsorption capacity at saturation
$\lambda$	Constant

**Subscripts**

A	First adsorbate layer
B	Second and higher adsorbate layer

**REFERENCES**

- Cerofolini, G.F., M. Jaroniec, and S. Sokolowski, "A Theoretical Isotherm for Adsorption on Heterogeneous Surfaces," *J. Colloid and Polymer Sci.*, **256**, 471, (1978)
- Cochran, T.W., R.L. Kabel, and R.P. Danner, "Vacancy Solution Theory of Adsorption Using Flory-Huggins Coefficient Equations," *AIChEJ*, **31**(2), 268, (1985)
- Costa, E., J.L. Sotelo, G. Calleja, and C. Marron, "Adsorption of Binary and Ternary Hydrocarbon Gas Mixtures on Activated Carbon : Experimental Determination and Theoretical Prediction of the Ternary Equilibrium Data," *AIChEJ*, **27**(1), 5, (1981)
- Ghosh, T.K., Ph.D. Dissertation, Oklahoma State University, (1989)
- Ghosh, T.K. and A.L. Hines, " Adsorption of Acetaldehyde, Propionaldehyde, and Butyraldehyde on Molecular Sieve-13X," Submitted to *Separation Science and Technology* (1989)
- House, W.A. and M.J. Jaycock, " A Numerical Algorithm for the Determination of the Adsorptive Energy Distribution from Isotherm Data," *J. Colloid Polym. Sci.*, **256**, 52(1978)
- Hyun, S.H. and R.P. Danner, " Equilibrium Adsorption of Ethane, Ethylene, Isobutane, Carbon Dioxide, and Their Binary Mixtures on 13X Molecular Sieves," *J. Chem. Eng. Data*, **27**, 196, (1982)
- Jaroniec, M., " Adsorption of Gas Mixtures on Heterogeneous Solid Surfaces. Analytical Solution of Integral Equation for Jovanovic Adsorption Isotherm," *J. Colloid Inter. Sci.*, **53**(3), 422, (1975)
- Jaroniec, M. and J. Toth, " Adsorption of Gas Mixture on Heterogeneous Solid Surfaces. III. Extension of Toth Isotherm on Multilayer Adsorption of Gas Mixtures," *Colloid & Polym. Sci.*, **256**, 690, (1978)
- Jaroniec, M., A. Patrykiewicz, and M. Borowko, " Progress in Surface and Membrane Science," Vol 14, Academic Press, New York (1981)
- Jovanovic, D.S., " Physical Adsorption of Gases. I. Isotherms for Monolayer and Multilayer Adsorption," *Kolloid-Z. Z. Polym.*, **235**, 1203, (1969)

- Kuo, S.L. and A.L. Hines, " New Theoretical Isotherm for Adsorption on Heterogeneous Adsorbents," Submitted to Separation Science and Technology, (1989).
- Misra, D.N., " Adsorption on Heterogeneous Surfaces : A Dubinin-Rudushkevich Equation," Surface Sci., **18**, 367, (1969)
- Misra, D.N., " New Adsorption Isotherm for Heterogeneous Surface," J. Chem. Phys., **52**, 5499, (1970)
- Misra, D.N., " Jovanovic Adsorption Isotherm for Heterogeneous Surfaces," J. Colloid Inter. Sci., **43**, 85, (1973)
- O'Brien, J.A. and A.L. Myers, "Physical Adsorption of Gases on Heterogeneous Surfaces," J Chem. Soc. Faraday Trans.1, **80**, 1467, (1984)
- Ross, S. and I.D. Morrison, " Computed Adsorptive Energy Distribution in the Monolayer (Caedmon)," Surface Sci., **52**, 103, (1978)
- Sircar, S., " New Adsorption Isotherm for Energetically Heterogeneous Adsorbents," J. Colloid Inter. Sci., **98**(2), 306, (1984)
- Talu, O. and I. Zwiebel, " Multicomponent Adsorption Equilibria of Nonideal Mixtures," AIChEJ, **32**(8), 1263 (1986)

**LIST OF TABLES**

- I. Model Parameters for Methane, Ethylene, Ethane, and Propylene Adsorption on Activated Carbon at 293.2 K
- II. Best Fit Parameters of the New Model for Acetaldehyde, Propionaldehyde, and Butyraldehyde Adsorption on Molecular Sieve-13X
- III. Best Fit Parameters of the New Model for Carbon Dioxide, Ethane, Ethylene, and Isobutane Adsorption on Molecular Sieve-13X
- IV. Best Fit Parameters of the New Model for Carbon Dioxide, Hydrogen Sulfide, and Propane Adsorption on H-Mordenite at 283.2 K

**LIST OF FIGURES**

1. Energy Distribution on the Adsorbent Surface in  $q_A/RT$  Domain for Constant  $b_0$ ,  $\epsilon_M$ ,  $q_B/RT$ , and  $A_2$ .
2. Equilibrium Isotherms of Methane, Ethane, Ethylene, and Propylene on Activated Carbon at 293.2 K (Experimental Data of Costa, et al., 1981)
3. Equilibrium Isotherms of Acetaldehyde on Molecular Sieve-13X (Experimental Data of Ghosh, 1989)
4. Equilibrium Isotherms of Propionaldehyde on Molecular Sieve-13X (Experimental Data of Ghosh, 1989)
5. Equilibrium Isotherms of Butyraldehyde on Molecular Sieve-13X (Experimental Data of Ghosh, 1989)
6. Equilibrium Isotherms of Carbon Dioxide on Molecular Sieve-13X (Experimental Data of Hyun and Danner, 1982)
7. Equilibrium Isotherms of Ethane on Molecular Sieve-13X (Experimental Data of Hyun and Danner, 1982)
8. Equilibrium Isotherms of Ethylene on Molecular Sieve-13X (Experimental Data of Hyun and Danner, 1982)
9. Equilibrium Isotherms of Isobutane on Molecular Sieve-13X (Experimental Data of Hyun and Danner, 1982)
10. Equilibrium Isotherms of Carbon Dioxide, Hydrogen Sulfide, and Propane on H-Mordenite at 283.2 K (Experimental Data of Talu and Zwiebel, 1986)

Table I. Model Parameters for Methane, Ethylene, Ethane, and Propylene Adsorption on Activated Carbon at 293.2 K.

(a) Parameters for the New Model (Equation 23)

ADSORBATE	$\theta_m$ (mmol/g)	$A_1$ (atm)	$A_2$	$\epsilon_M$ (atm) <sup>-1</sup>	$b_0$ (atm) <sup>-1</sup>
Methane <sup>*</sup>	1.100	1.0099	0.7799	0.7800	0.2042
Ethylene <sup>*</sup>	3.464	$2.4535 \cdot 10^{-2}$	-216.8950	$1.2143 \cdot 10^{-3}$	$1.4739 \cdot 10^{-2}$
Ethane <sup>*</sup>	4.415	$1.4406 \cdot 10^{-2}$	-447.3608	$4.5990 \cdot 10^{-3}$	0.1223
Propylene <sup>**</sup>	2.798	$3.5598 \cdot 10^{-4}$	-758.2483	0.8335	0.2190

\*  $A_3 = 1 \text{ atm}$     \*\*  $A_3 = 1 \text{ psia (0.068 atm)}$

(b) Parameters for the Kuo and Hines Model

ADSORBATE	$m$ (mmol/g)	$K_1$ (atm)	$K_2$
Methane	2.416	3.7345	$-007.1651 \cdot 10^{-2}$
Ethylene	3.402	$2.5759 \cdot 10^{-2}$	-195.3889
Ethane	3.774	$2.2501 \cdot 10^{-2}$	-184.0894
Propylene	4.919	$1.1652 \cdot 10^{-2}$	-146.5824



Table II. Best Fit Parameters of the New Model for Acetaldehyde, Propionaldehyde, and Butyraldehyde Adsorption on Molecular Sieve-13X.

ADSORBATE	TEMP. (K)	$\theta_m$ (mmol/g)	$A_1$ (mmHg)	$A_2$	$\epsilon_M$ (mmHg) <sup>-1</sup>	$b_0$ (mmHg) <sup>-1</sup>
Acetaldehyde	286.5	3.170	0.1983	-71.1931	$4.7551 \cdot 10^{-3}$	$2.6053 \cdot 10^{-3}$
	293.2	3.095	0.1923	-78.8059	$3.1423 \cdot 10^{-3}$	$1.6651 \cdot 10^{-3}$
	301.0	2.940	0.1917	-68.2685	$2.0356 \cdot 10^{-3}$	$1.0152 \cdot 10^{-3}$
Propionaldehyde	283.2	3.250	0.0925	-397.9541	$2.5748 \cdot 10^{-2}$	$1.6730 \cdot 10^{-2}$
	293.2	2.600	0.1052	-183.5066	$1.3673 \cdot 10^{-2}$	$8.0238 \cdot 10^{-3}$
	303.2	2.300	0.1281	-95.8925	$7.0011 \cdot 10^{-3}$	$3.7067 \cdot 10^{-3}$
Butyraldehyde	282.6	7.501	0.0667	-2860.3759	0.1292	0.1032
	293.2	2.500	0.0764	-317.9758	$3.8401 \cdot 10^{-2}$	$2.2728 \cdot 10^{-2}$
	302.0	2.000	0.0922	-113.9271	$1.3550 \cdot 10^{-2}$	$6.4930 \cdot 10^{-3}$

$A_3 = 1 \text{ psia (51.70 mmHg)}$

Table III. Best Fit Parameters of the New Model for Carbon Dioxide, Ethane, Ethylene, and Isobutane Adsorption on Molecular Sieve-13X.

ADSORBATE	TEMP. (K)	$\theta_m$ (mmol/g)	$A_1$ (kpa)	$A_2$	$\epsilon_M$ (kpa) <sup>-1</sup>	$b_o$ (kpa) <sup>-1</sup>
Carbon Dioxide	298.2	3.712	0.0509	-1085.8610	$3.7748 \cdot 10^{-3}$	$1.0198 \cdot 10^{-3}$
	323.2	2.500	0.2440	- 486.3553	$1.0881 \cdot 10^{-2}$	$3.0458 \cdot 10^{-3}$
Ethane	298.2	2.800	16.1594	0.1620	$1.8655 \cdot 10^{-6}$	$2.9800 \cdot 10^{-4}$
	323.2	1.900	26.5893	$6.3294 \cdot 10^{-2}$	$6.5825 \cdot 10^{-3}$	$1.7363 \cdot 10^{-3}$
	373.2	0.870	66.1895	$7.8269 \cdot 10^{-3}$	$8.8497 \cdot 10^{-3}$	$1.5959 \cdot 10^{-3}$
Ethylene*	298.2	4.520	1.8520	-68.1873	$7.2591 \cdot 10^{-5}$	$1.4657 \cdot 10^{-3}$
	323.2	4.250	4.0236	-45.6778	$6.9147 \cdot 10^{-5}$	$1.3513 \cdot 10^{-3}$
	373.2	2.800	10.1032	-38.9325	$2.0404 \cdot 10^{-5}$	$2.6072 \cdot 10^{-4}$
Isobutane	298.2	1.776	0.1594	-13.5211	$2.1762 \cdot 10^{-3}$	$5.5565 \cdot 10^{-4}$
	323.2	1.568	0.3432	- 5.4554	$2.0311 \cdot 10^{-3}$	$4.4722 \cdot 10^{-4}$
	373.2	1.300	4.7614	0.7953	$1.4508 \cdot 10^{-3}$	$2.9903 \cdot 10^{-4}$

\*  $A_3 = 1 \text{ atm (101.325 kpa)}$ ; for others  $A_3 = 1 \text{ psia (6.893 kpa)}$

Table IV. Best Fit Parameters of the New Model for Carbon Dioxide, Hydrogen Sulfide, and Propane Adsorption on H-Mordenite at 283.2 K.

ADSORBATE	$\theta_m$ (mmol/g)	$A_1$ (kpa)	$A_2$	$\epsilon_M$ (kpa) <sup>-1</sup>	$b_0$ (kpa) <sup>-1</sup>
Carbon Dioxide	1.980	0.1200	-201.3686	$1.6684 \cdot 10^{-2}$	$4.4974 \cdot 10^{-3}$
Propane	1.110	0.1382	- 39.5105	$5.4404 \cdot 10^{-3}$	$1.4073 \cdot 10^{-3}$
Hydrogen Sulfide	2.500	0.2198	- 17.3397	$2.9016 \cdot 10^{-2}$	$7.4722 \cdot 10^{-3}$

$$A_3 = 1 \text{ psia (6.893 kpa)}$$

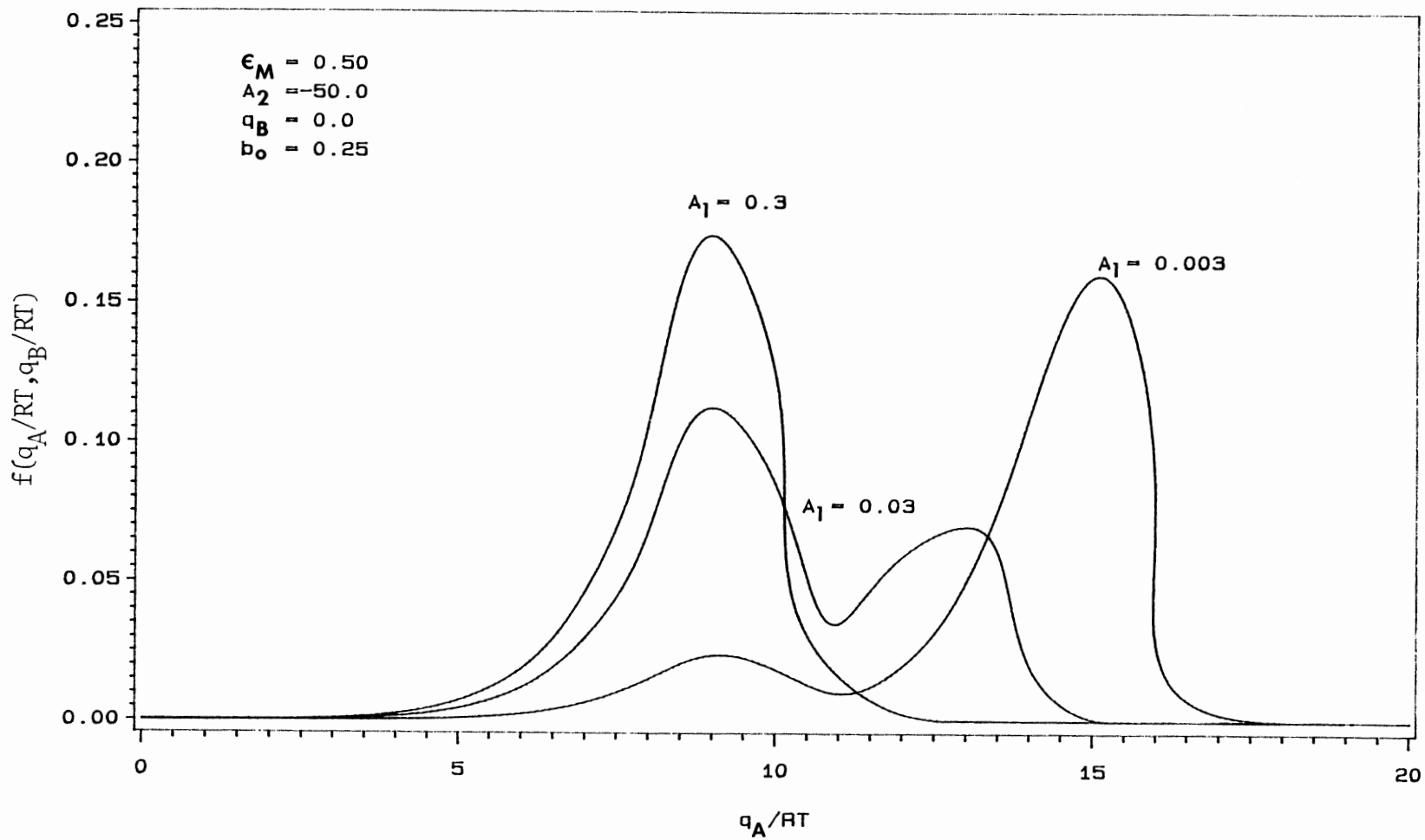


Figure 1. Energy Distribution on the Adsorbent Surface in  $q_A/RT$  Domain for Constant  $b_0$ ,  $\epsilon_M$ ,  $q_B/RT$ , and  $A_2$ .

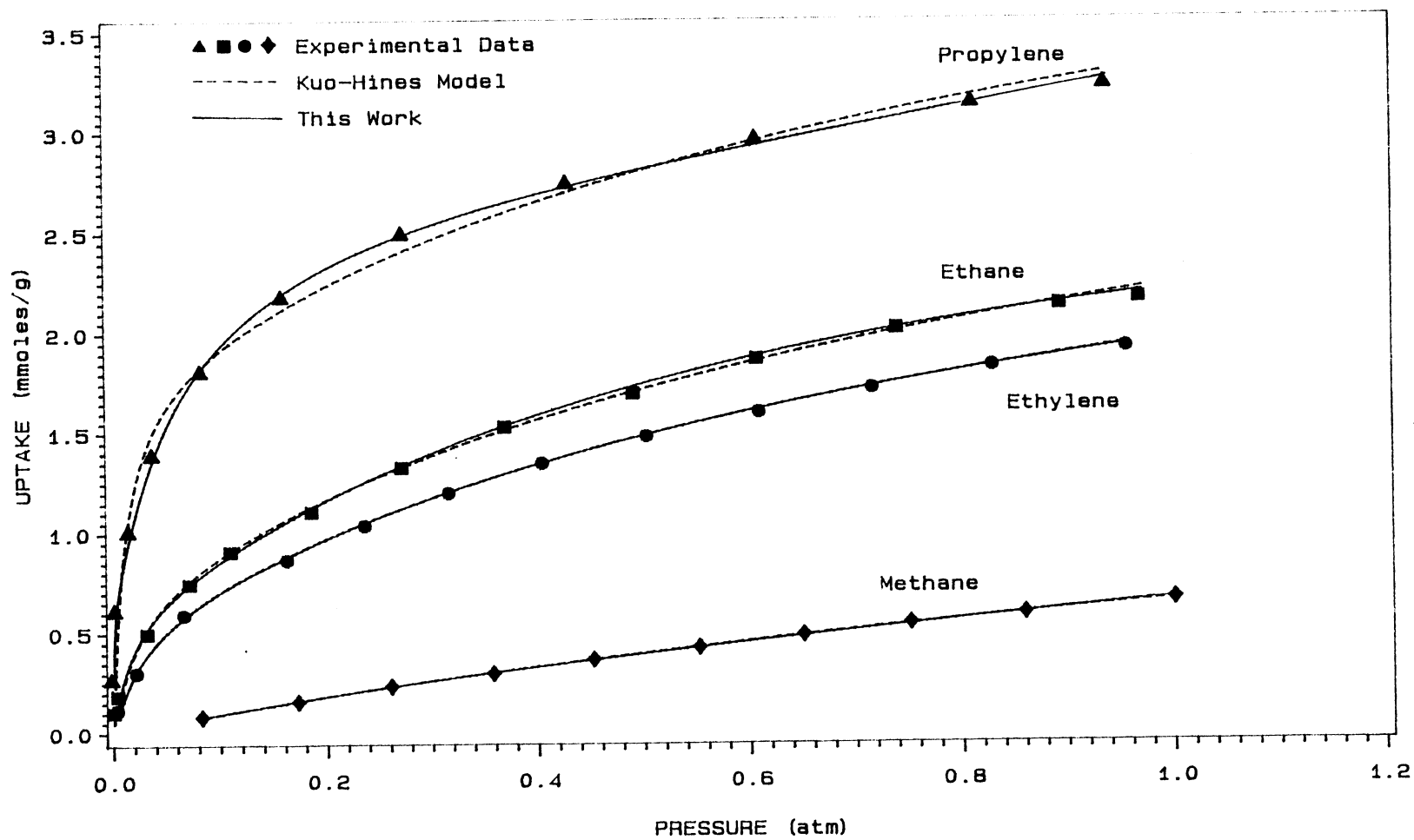


Figure 2. Equilibrium Isotherms of Methane, Ethane, Ethylene, and Propylene on Activated Carbon at 293.2 K (Experimental Data of Costa et. al., 1981)

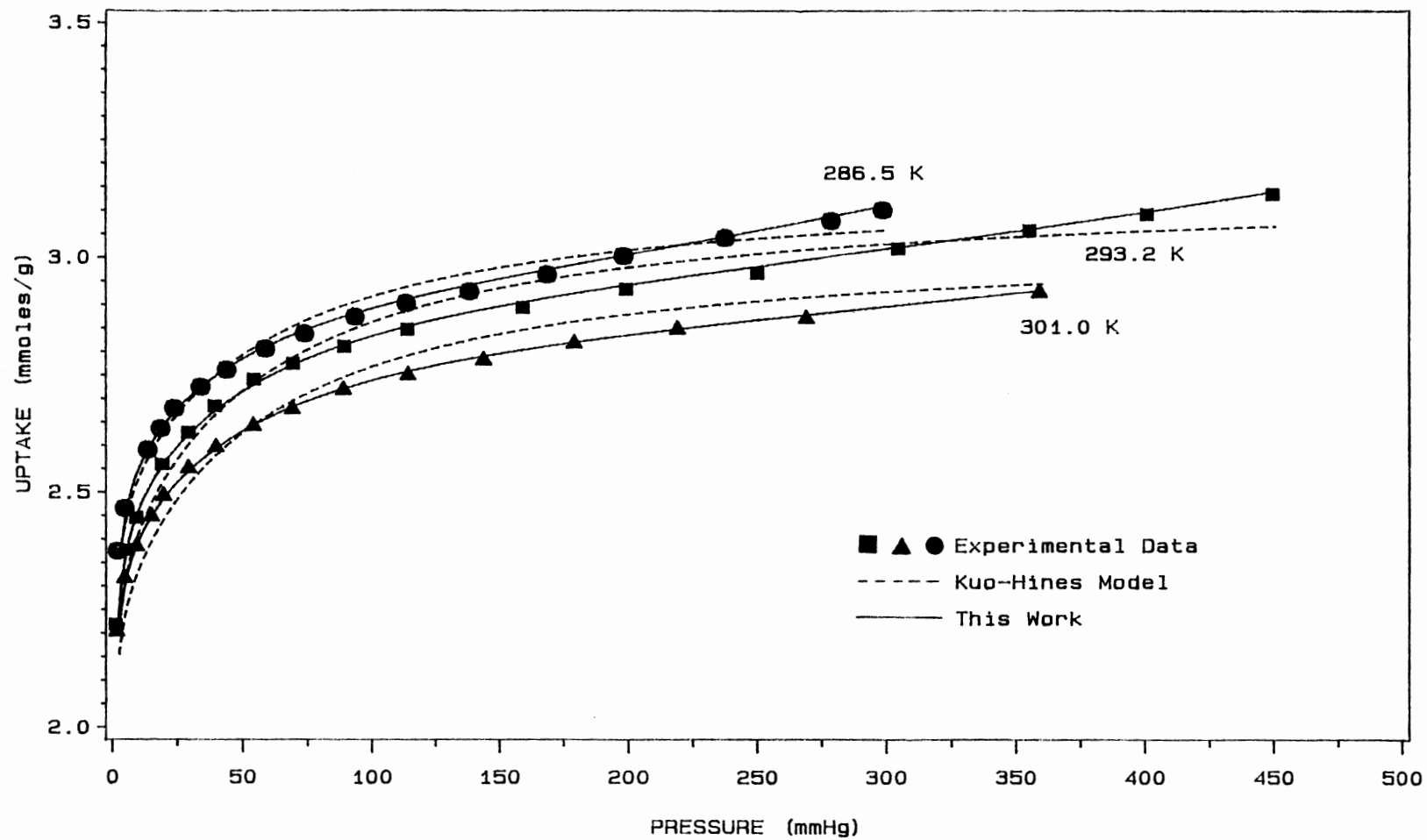


Figure 3. Equilibrium Isotherms of Acetaldehyde on Molecular Sieve-13X  
(Experimental Data of Ghosh, 1989)

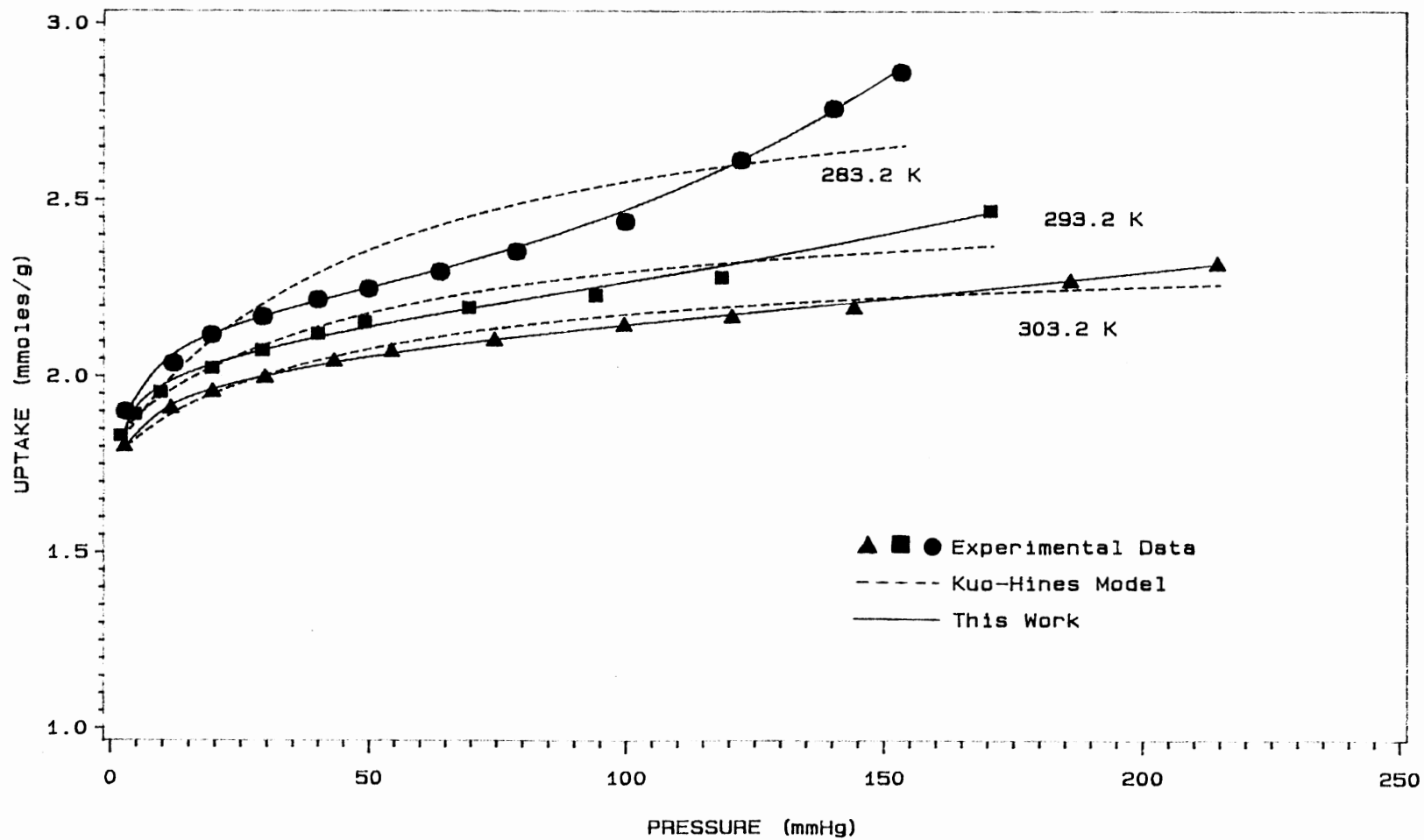


Figure 4. Equilibrium Isotherms of Propionaldehyde on Molecular Sieve-13x  
(Experimental Data of Ghosh, 1989)

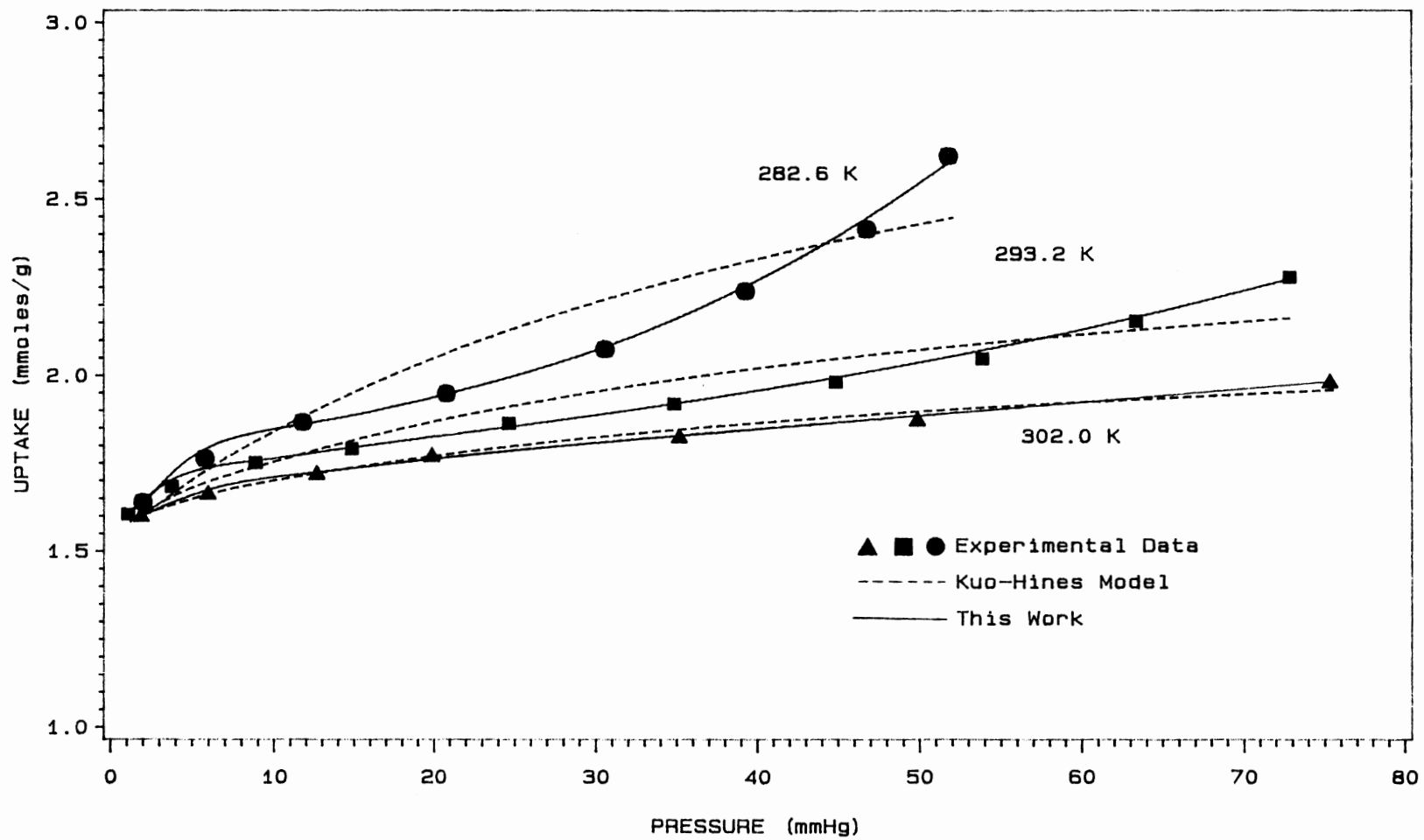


Figure 5. Equilibrium Isotherms of Butyraldehyde on Molecular Sieve-13X  
(Experimental Data of Ghosh, 1989)



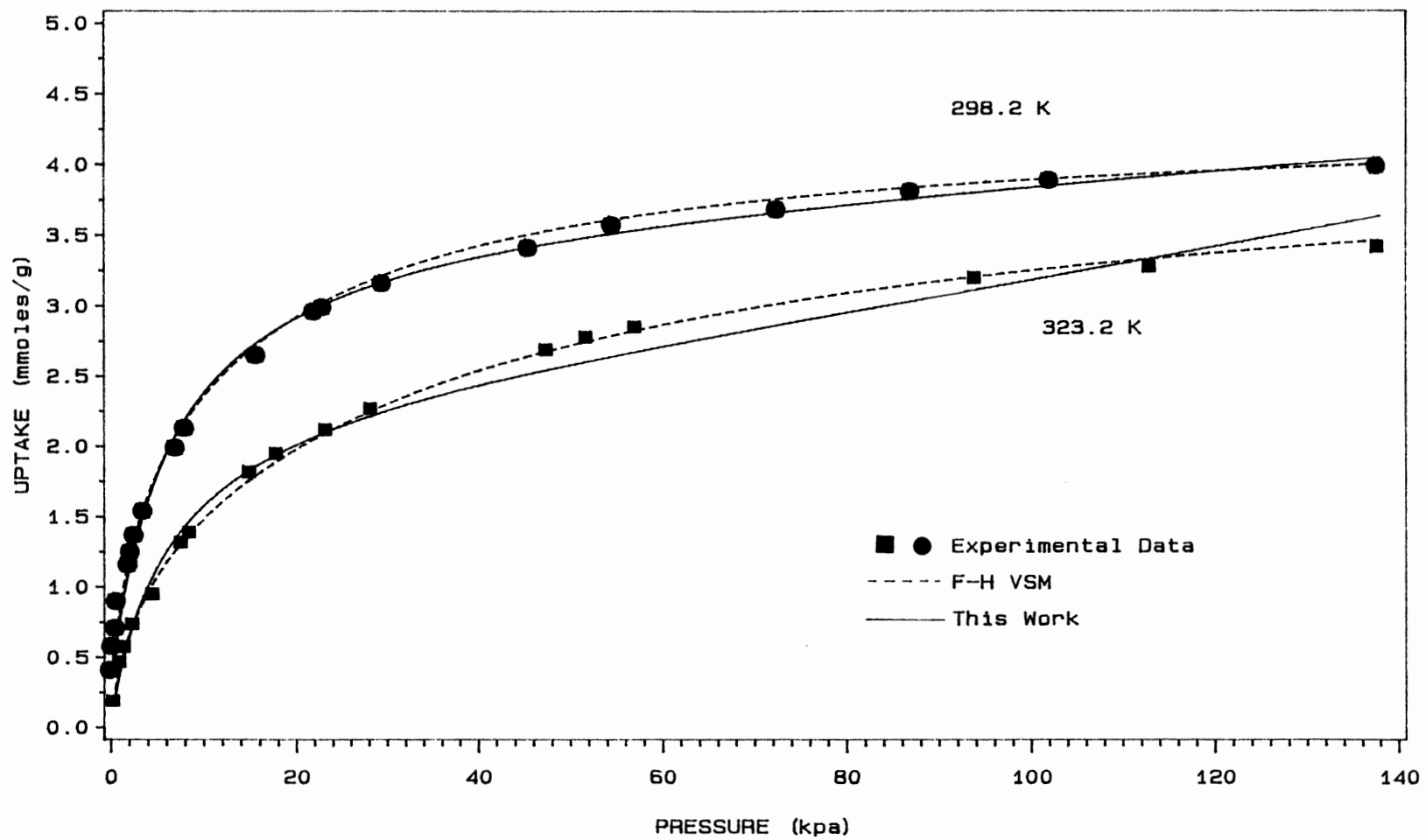


Figure 6. Equilibrium Isotherms of Carbon Dioxide on Molecular Sieve-13X  
(Experimental Data of Hyun and Danner, 1982)

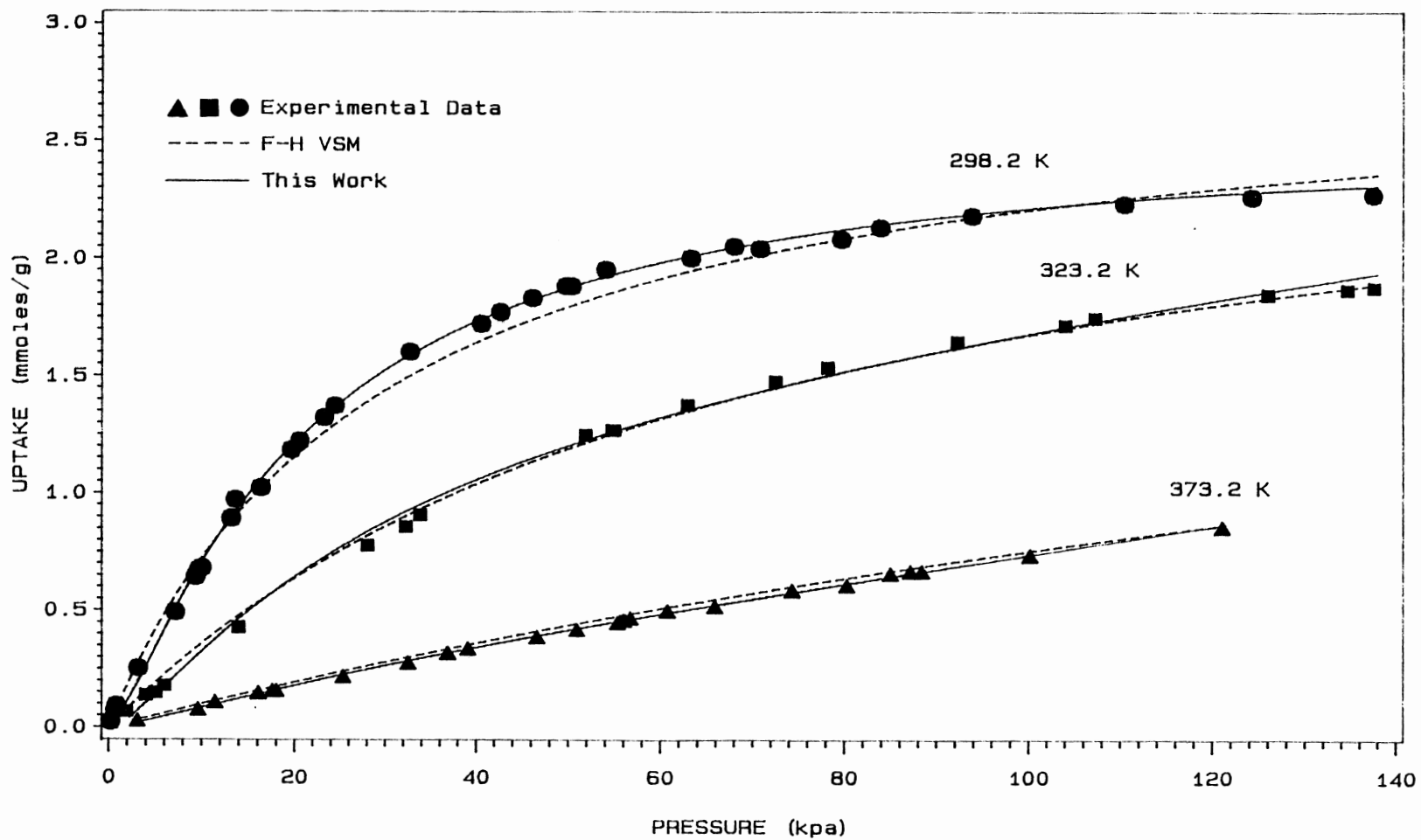


Figure 7. Equilibrium Isotherms of Ethane on Molecular Sieve-13X  
(Experimental Data of Hyun and Danner, 1982)

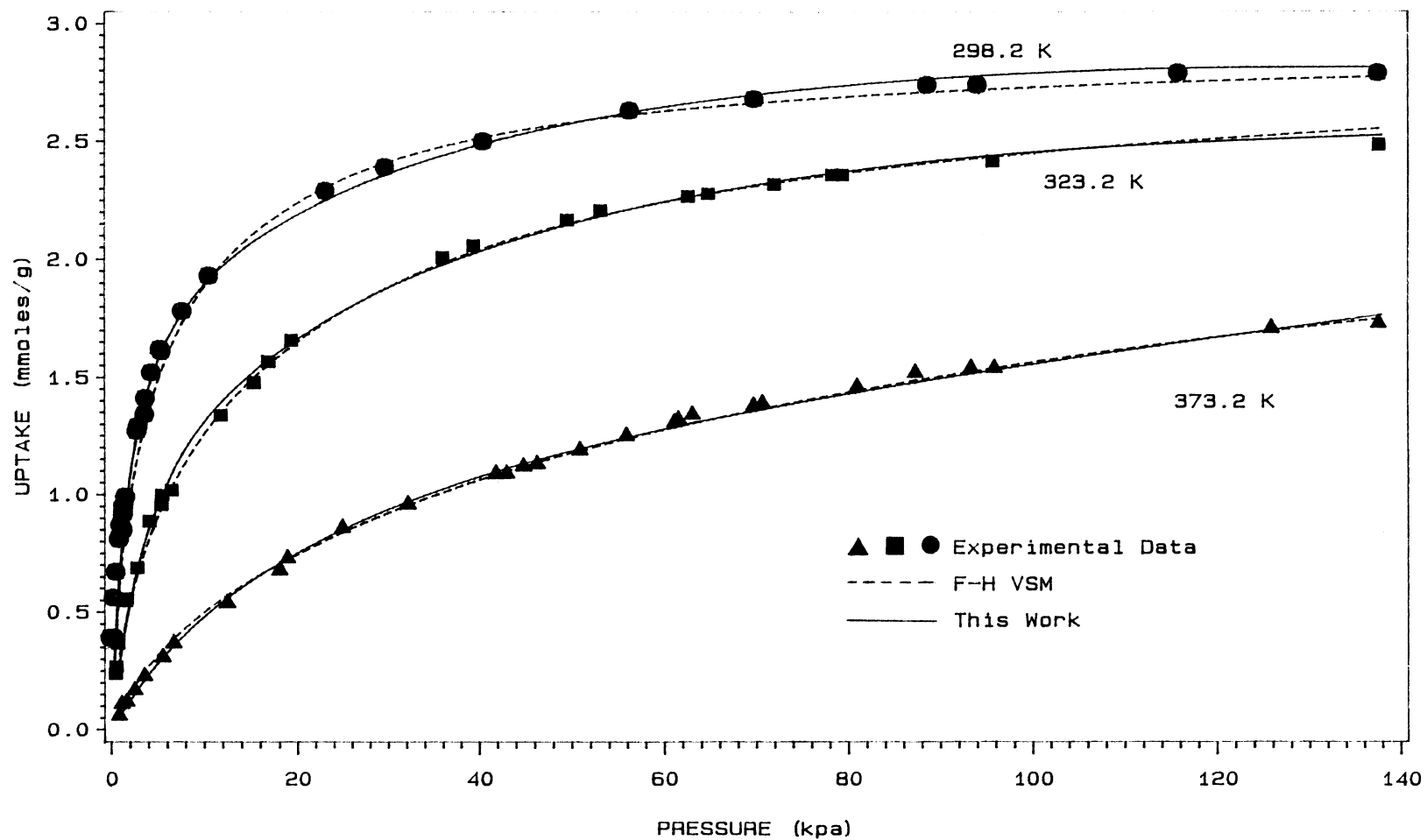


Figure 8. Equilibrium Isotherms of Ethylene on Molecular Sieve-13X  
(Experimental Data of Hyun and Danner, 1982)

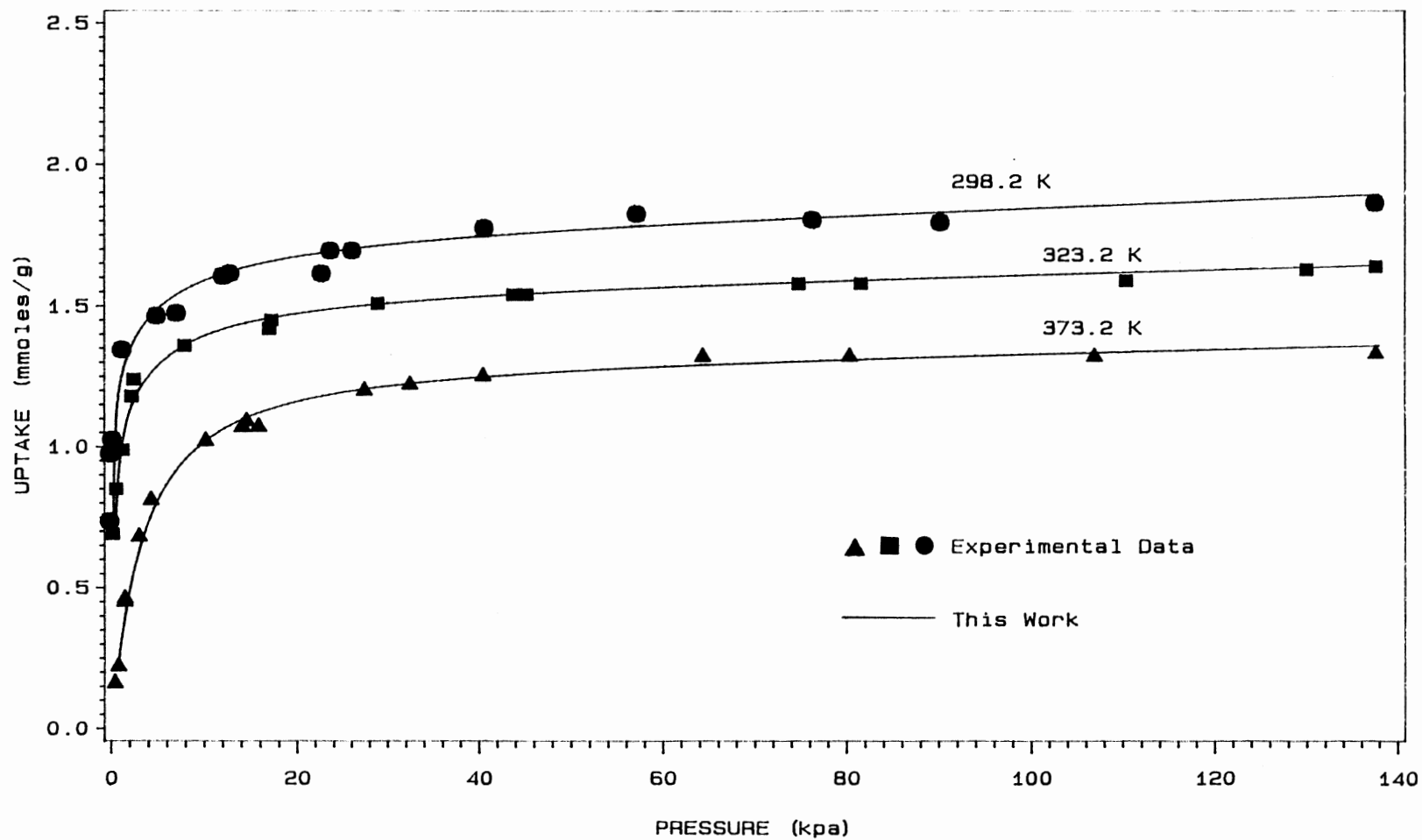


Figure 9. Equilibrium Isotherms of Iso-Butane on Molecular Sieve-13X  
(Experimental Data of Hyun and Danner, 1982)

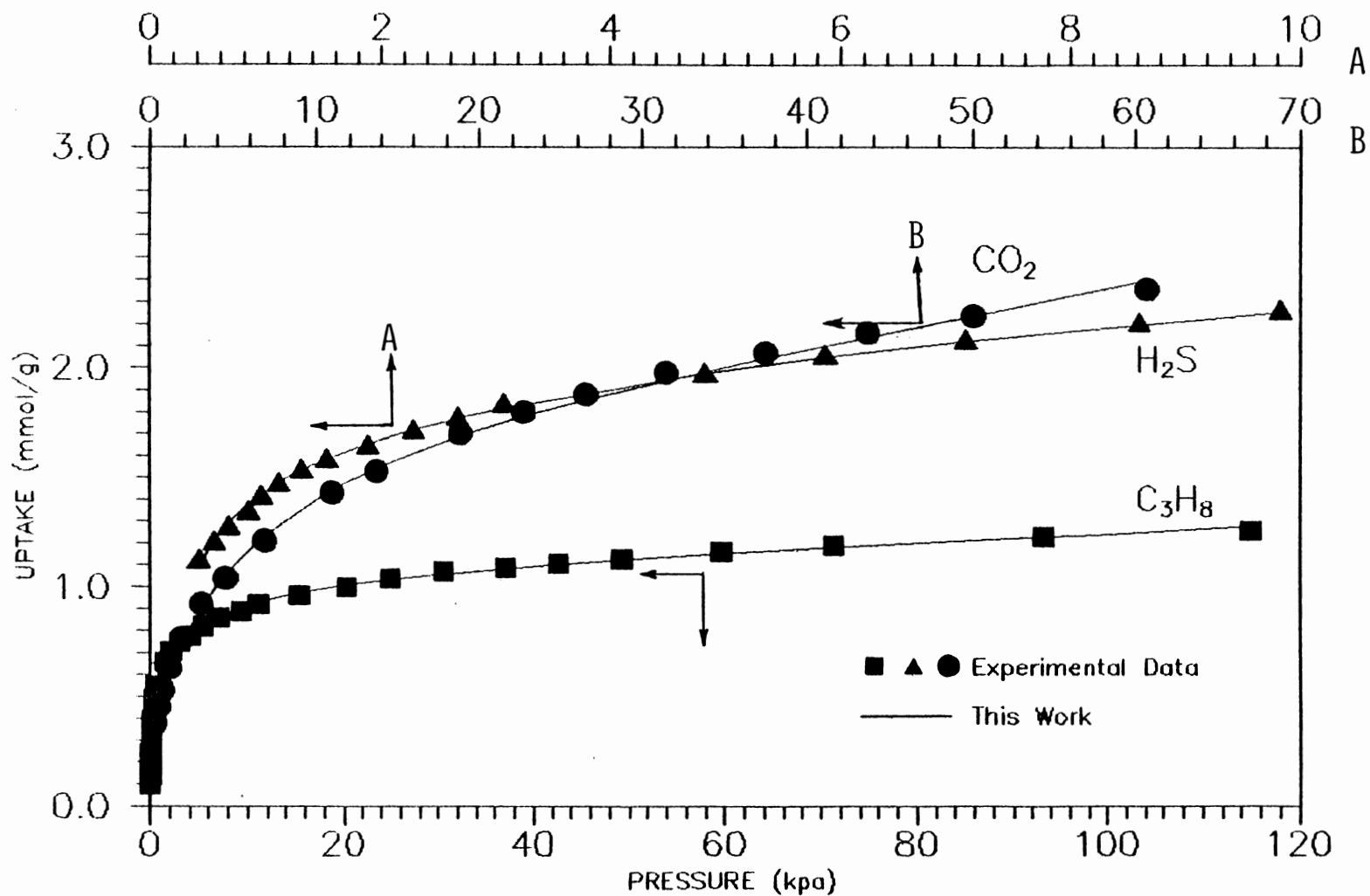


Figure 10. Equilibrium Isotherms of Carbon Dioxide, Hydrogen Sulfide, and Propane on H-Mordenite at 283.2 K (Experimental Data of Talu and Zwiebel, 1986)

## CHAPTER IV

### PREDICTION OF BINARY ADSORPTION EQUILIBRIA FROM PURE COMPONENT DATA

**PREDICTION OF BINARY ADSORPTION EQUILIBRIA FROM  
PURE COMPONENT DATA**

**Tushar K. Ghosh and Anthony L. Hines**

**School of Chemical Engineering  
Oklahoma State University  
Stillwater, Oklahoma 74078**

**ABSTRACT**

A new method for calculating the binary adsorption equilibrium data on the solid surface from the pure component isotherm data is presented. An adsorption isotherm previously proposed by Ghosh and Hines (1989) is extended to binary mixture by estimating the binary mixture parameters from the pure component data. The new isotherm model for a binary mixture is combined with the adsorption solution theory to predict the mole fraction in the adsorbed phase. The nonideality of the adsorbed phase is taken into account by introducing the activity coefficient in the adsorbed solution theory. The present method can be used to predict the mole fractions and the activity coefficients in the adsorbed phase. The method is tested successfully with the literature data for several hydrocarbon mixtures.



## INTRODUCTION

Adsorption processes are rapidly gaining importance in various industries as a means of removing chemical contaminants from gases. The design of an adsorber to remove two or more components, however, requires multicomponent adsorption equilibrium data. The experimental measurement of multicomponent data can be very complicated and time consuming, depending on the number of components. A review of the different methods to predict multicomponent adsorption has been provided by Sircar and Myers (1973).

Jaroniec (1980) reviewed the kinetics and the equilibrium state of adsorption for multicomponent systems. Jaroniec (1978, 1977, 1975) and Jaroniec and Toth (1976, 1978) developed partial isotherms for the individual components in a binary gas mixture when adsorbed on a heterogeneous solid surface. Various pure component isotherm equations, such as the Jovanovic, the Freundlich, the Langmuir, and the Toth model, were used along with a combination of different energy distribution functions. The predictive capabilities of these isotherms are rather limited and are tested for only a few systems. Jaroniec and Toth (1976) successfully predicted the partial isotherms of  $C_2H_4$  from the  $C_2H_4-C_2H_6$  mixture and  $C_2H_6$  from the  $C_2H_6-C_2H_4$  mixture both on Nuxit-AL at 293 K. However, a large deviation was reported for  $C_3H_6$  from the  $C_3H_6-C_3H_8$  mixture on the same adsorbent at the same temperature. Their treatment was also limited to binary systems and

was not extended to ternary or higher order mixtures.

Earlier, a number of researchers (Arnold, 1949; Lewis et al., 1950; Myers and Prausnitz, 1965; Cook and Basmadjian, 1965) developed models for multicomponent adsorption assuming that the adsorbed phase formed an ideal solution on the solid surface. The basic assumption of the Ideal Adsorbed Solution (IAS) theory is that equilibrium exists between the gas phase and the adsorbed phase for each component of the mixture and is given by

$$P y_i = P_i^{\circ} x_i \quad (1)$$

where  $P_i^{\circ}$  is a function of the spreading pressure ( $\Pi$ ) and is interpreted as the equilibrium pressure that a pure component  $i$  should have in the gas phase to produce the same spreading pressure as that of the mixture ( $\Pi_m$ ) at the same temperature, when adsorbed on the solid surface. The term  $P$  is the total pressure and  $y_i$  and  $x_i$  are mole fractions in the gas phase and on the solid surface, respectively.

Sircar and Myers (1973) showed that the models developed by the previous researchers differed from each other in their choice of standard states. All of the models performed poorly for multilayer adsorption. Sircar and Myers (1973) developed a model based on surface potential theory of multilayer adsorption. They also considered the adsorbed phase to be ideal and was successful in predicting the data for  $O_2-N_2$  on anatase and for benzene-2,4, dimethylpentane on silica gel.

O'Brien and Myers (1985) developed an algorithm based on

the IAS theory to predict the adsorbed phase mole fractions from pure component isotherm data. They required an isotherm equation to represent accurately the pure component data which, at the same time, was analytically integrable to obtain the spreading pressure. Otherwise, their model required repeated numerical integrations which increased the computation time. Later, Moon and Tien (1987) tried to improve the algorithm by reformulating the equations of O'Brien and Myers. Substantial improvement in CPU time was reported for mixtures having more than five components. Moon and Tien compared the predictive capability of their model with the algorithm of O'Brien and Myers (1985).

Many researchers (Costa et al., 1981; Hyun and Danner, 1982; Talu and Zwiebel, 1986) pointed out that a few systems behave ideally in the adsorbed phase. The nonideality of the adsorbed phase is taken into account by introducing the activity coefficient in Equation (1). The gas phase is still considered to be ideal. Equation (1) is written as

$$pY_i = \gamma_i P_i^0 x_i \quad (2)$$

where  $\gamma_i$  is the activity coefficient. The activity coefficients of the components were calculated from the binary mixture data. Costa et al. (1981) used the Wilson and the UNIQUAC type activity coefficient models to estimate the activity coefficient of a component in the mixture. The binary interaction parameters of these models were obtained from the binary mixture data. Talu and Zwiebel (1986)

developed an expression from the Superlattice Model and followed the approach of Maurer and Prausnitz (1978) to calculate the activity coefficients. Paludetto et al. (1987) used an approach similar to the one followed by Costa et al. to predict the adsorption equilibrium data of ternary mixtures of xylenes on a zeolite. Paludetto et al. used a different approach to calculate the spreading pressure of the mixture. However, one of their assumptions, that there was no area change upon mixing at constant  $\Pi$  and  $T$ , might not be valid for other systems. Paludetto et al. employed the Wilson and the Hilderband equation to estimate the activity coefficients. Good agreement between the experimental data and the predicted values for ternary mixtures was reported by the above researchers. Other methods used to predict binary and multicomponent adsorption data have been discussed in detail by Ruthven (1984) and Yang (1987).

The aim of the present work was to develop a method to calculate binary adsorption equilibrium data from pure component data, taking into consideration the nonideality of the system. The mole fractions, activity coefficients, and the total amount adsorbed were predicted by this method. The method was tested with experimental data for several binary mixtures of hydrocarbons on activated carbon.

## THEORY

The pure component isotherm equation developed by Ghosh and Hines (1989) for multilayer adsorption is extended to binary mixture to calculate the total amount adsorbed per unit mass of the adsorbent. The isotherm equation for a component  $i$  is expressed as

$$n_i = \theta_i \left[ 1 - \frac{A_{1i}A_{3i}}{A_{3i} - A_{1i}A_{2i}} \left\{ \frac{1}{P+A_{1i}} - \frac{A_{2i}}{P+A_{3i}} \right\} \right] \frac{\exp(-b_{oi}P)}{\epsilon_{Mi}P} \cdot \left[ \exp(\epsilon_{Mi}P) - 1 \right] \quad (3)$$

where the parameters,  $\theta_i$ ,  $A_{1i}$ ,  $A_{2i}$ ,  $A_{3i}$ ,  $b_{oi}$ , and  $\epsilon_{Mi}$  are estimated from pure component data by using a nonlinear regression analysis (Marquardt-S method). The Extension of Equation (3) to binary mixtures can be written as

$$n_t = \theta_m \left[ 1 - \frac{A_{1m}A_{3m}}{A_{3m} - A_{1m}A_{2m}} \left\{ \frac{1}{P+A_{1m}} - \frac{A_{2m}}{P+A_{3m}} \right\} \right] \frac{\exp(-b_{om}P)}{\epsilon_{Mm}P} \cdot \left[ \exp(\epsilon_{Mm}P) - 1 \right] \quad (4)$$

where  $\theta_m$ ,  $A_{1m}$ ,  $A_{2m}$ ,  $A_{3m}$ ,  $b_{om}$ , and  $\epsilon_{Mm}$  are mixture parameters and are evaluated from pure component parameters by applying appropriate mixing rules. The following mixing rules are used in the present study:

$$\left. \begin{aligned}
 \frac{1}{\theta_m} &= \frac{x_1}{\theta_1} + \frac{x_2}{\theta_2} \\
 \frac{1}{A_{1m}} &= \frac{y_1}{A_{11}} + \frac{y_2}{A_{12}} \\
 A_{2m} &= y_1 A_{21} + y_2 A_{22} \\
 b_{om} &= y_1 b_{o1} + y_2 b_{o2} \\
 \epsilon_{Mm} &= y_1 \epsilon_{M1} + y_2 \epsilon_{M2}
 \end{aligned} \right\} \quad (5)$$

In the above equation  $x_1$  and  $x_2$  are mole fractions in the adsorbed phase and  $y_1$  and  $y_2$  are mole fractions in the gas phase. For a binary mixture,

$$x_1 + x_2 = 1 \quad (6)$$

Therefore, the unknowns in Equation (4) are  $n_t$  and either  $x_1$  or  $x_2$ . To solve for  $n_t$  and, say  $x_1$ , another expression relating these two variables is required. According to Yang (1987), the total amount adsorbed from a mixture can be obtained from the Adsorbed Solution theory and is given as

$$\frac{1}{n_t} = \sum \frac{x_i}{n_i^{\circ}} + \frac{RT}{A} \sum x_i \left\{ \frac{\partial \ln \gamma_i}{\partial \Pi_m} \right\} x_i \quad (7)$$

In the above equation,  $n_i^{\circ}$  is the amount of  $i$  that would have been adsorbed from a pure gas at pressure  $P_i^{\circ}$  and the system temperature.  $P_i^{\circ}$  was defined earlier in Equation (1). The terms  $\gamma_i$  and  $\Pi_m$  are the activity coefficient of component  $i$  in the adsorbed phase and the mixture spreading pressure, respectively. In the above equation,  $A$  is the surface area

of the adsorbent. The mixture spreading pressure and equilibrium pressure are calculated as follows.

According to Myers and Prausnitz (1965), the total Gibbs free energy for both the adsorbed and gas phase can be written as

$$dG^g = -SdT + VdP + \sum \mu_i^g dn_i^g \quad (\text{gas phase}) \quad (8)$$

$$dG^a = -SdT + Ad\Pi + \sum \mu_i^a dn_i^a \quad (\text{adsorbed phase}) \quad (9)$$

If equilibrium exists between the ideal gas phase and the adsorbed phase ( $\mu_i^g = \mu_i^a$ ), the following relationship can be obtained by combining Equations (8) and (9) at constant T for each component.

$$Ad\Pi_i = n_i RT d \ln P \quad (10)$$

Equation (10) is known as the Gibbs Adsorption equation. Integration of Equation (10) results in the following expression :

$$\frac{\Pi_i A}{RT} = \int_0^P \frac{n_i}{P} dP \quad \text{at constant T} \quad (11)$$

For a mixture, Equation (11) can be written as

$$\frac{\Pi_m A}{RT} = \int_0^P \frac{n_t}{P} dP$$

where  $n_t$  can be replaced by Equation (4). From the definition of  $P_i^0$  it follows that for a binary mixture,

$$\Pi_1 = \Pi_2 = \Pi_m$$

or

$$\frac{\Pi_1 A}{RT} = \frac{\Pi_2 A}{RT} = \frac{\Pi_m A}{RT} \quad (13)$$

where  $\Pi_1$  and  $\Pi_2$  are the spreading pressure of components 1 and 2 corresponding to equilibrium pressures  $P_1^{\circ}$  and  $P_2^{\circ}$ , respectively. Once  $\Pi_m$  is known, Equations (11) and (13) can be used to calculate  $P_1^{\circ}$  and  $P_2^{\circ}$ .

To evaluate the term  $(\partial \ln \gamma_i / \partial \Pi_m)$  of Equation (7),  $\gamma_i$  should be expressed as a function of mole fraction and mixture spreading pressure. In the present method the above term is approximated as

$$\left( \frac{\partial \ln \gamma_i}{\partial \Pi_m} \right)_{x_i} = \left( \frac{\ln \gamma_i^s - \ln \gamma_i}{\Pi_m^s - \Pi_m} \right)_{x_i} \quad (14)$$

where  $\gamma_i^s$  and  $\Pi_m^s$  are values of activity coefficient and mixture spreading pressure at some standard state. The standard state can be defined as

$$P \rightarrow 0 ; \Pi_m^s \rightarrow 0 ; \gamma_i^s \rightarrow 1 \quad (15)$$

Therefore Equation (14) becomes

$$\left( \frac{\partial \ln \gamma_i}{\partial \Pi_m} \right)_{x_i} \approx \left( \frac{\ln \gamma_i}{\Pi_m} \right) \quad (16)$$

and Equation (7) can be written as



$$\frac{1}{n_t} = \sum \frac{x_i}{n_i} + \frac{RT}{A\Pi_m} \sum x_i \ln \gamma_i \quad (17)$$

The step by step calculation procedure to obtain  $x_1$ ,  $x_2$ ,  $\gamma_1$ , and  $\gamma_2$  using Equations (2) through (6) and Equations (11), (12), and (17) is summarized below. The mole fractions,  $y_1$  and  $y_2$ , and the system pressure are known from the experimental data. The calculations proceed as follows:

- (1) A value of  $x_1$  is assumed.
- (2) The total amount adsorbed is calculated from Equation (4) by substituting mixture parameters from Equation (5).
- (3) The spreading pressure of the mixture corresponding to total pressure  $P$  is calculated from Equation (12).
- (4) Equilibrium pressures  $P_1^0$  and  $P_2^0$  are obtained by solving Equation (11).
- (5) The amount adsorbed,  $n_1^0$  and  $n_2^0$ , corresponding to equilibrium pressures  $P_1^0$  and  $P_2^0$ , respectively are calculated by using a pure component isotherm [Equations (3)].
- (6) The activity coefficient  $\gamma_1$  and  $\gamma_2$  are calculated from Equation (2).
- (7) The total amount adsorbed,  $n_t$ , is calculated from Equation (17).
- (8) If the values of  $n_t$  calculated in step [2] and [7] do not agree with each other within  $\pm 5\%$ , a new value of  $x_1$  is assumed and the calculation is continued from step [2].

Step (4) requires repeated integration of Equation (11) with

different values of  $P_1^{\circ}$  and  $P_2^{\circ}$  until the spreading pressures of the individual components ( $\Pi_i$ ) are equal to that of the mixture spreading pressure. To avoid the repeated integration of Equation (11), the values of  $\Pi_i$  at different  $P_i^{\circ}$  are obtained in a separate calculation and are expressed as a function of  $P_i^{\circ}$  as shown below:

$$\frac{\Pi_i A}{RT} = K_{1i} \left\{ 1 - \frac{K_{2i}}{1 - K_{2i} K_{3i}} \left[ \frac{1}{P_i^{\circ} + K_{2i}} + \frac{K_{3i}}{P_i^{\circ} + 1} \right] \right\} \exp(-K_{5i} P_i^{\circ}) \left[ \frac{\exp(K_{4i} P_i^{\circ})}{K_{4i} P_i^{\circ}} \right] \quad (18)$$

The constants,  $K_{1i}$ ,  $K_{2i}$ ,  $K_{3i}$ ,  $K_{4i}$ , and  $K_{5i}$ , are obtained by a nonlinear regression method using the values obtained by the method just mentioned. The values of  $P_i^{\circ}$  corresponding to the mixture spreading pressure is obtained by solving Equation (18) by a root searching method.

#### TESTING OF THE MODEL

The present method was tested using the binary adsorption data of Costa et al. (1981) at 293.2 K. The binary mixtures were methane-ethane, methane-ethylene, ethane-ethylene, ethylene-propylene and ethane-propylene, and the adsorbent was activated carbon. The best fit parameters for pure component equilibrium data and the spreading pressure are presented in Table I. The experimental and calculated mole fractions of the adsorbed phase for five binary mixtures are shown in Tables II through VI. Good agreement was obtained

for all five mixtures. In the same tables, the values of the activity coefficients and the total amount adsorbed calculated by this method are compared with the values reported by Costa et al. The difference between the two values of the activity coefficients may be in part due to the error in calculating the equilibrium pressure  $P_i^0$ . The values of  $P_i^0$  and the mixture spreading pressure estimated by the present method are shown in Table VII, along with the values given by Costa et al. Good agreement was obtained for all the components except for methane in the methane-ethane mixtures at low concentrations of methane. When the concentration of methane in the mixture was low, a large spreading pressure resulted because of greater ethane adsorption. Since experimental data were not available for methane in the high pressure region, the interpolation of data in that region predicted lower values for the equilibrium pressure for methane. The values of the activity coefficients suggested a significant deviation from ideality for these mixtures, except for the ethane-ethylene mixture. As suggested by Costa et al., this ideal behavior of ethane and ethylene in their mixture may be due to their same molecular size and similar adsorption capacity. The departure from ideality for other mixtures may be due to the surface heterogeneity, interaction between the adsorbed molecules, and the formation of multilayers on the surface. In the derivation of Equation (4), all of these factors are considered. In Equation (16), however, the influence of

these factors are taken into account through the activity coefficient. As a result, good agreement between these two equations is observed when calculating the number of moles adsorbed on the solid surface.

**NOMENCLATURE**

A	Surface area
$A_1, A_2, A_3, b_0$	Parameters of the pure component isotherm
G	Gibbs free energy
$K_1, K_2, K_3$ $K_4, K_5$	Constants in Equation (17)
n	Amount adsorbed on the adsorbent
$n^0$	Amount adsorbed at pressure $p^0$
P	System pressure
$p^0$	Equilibrium pressure as defined in Equation (1)
R	Gas constant
S	Entropy
T	System temperature
V	Volume
x	Mole fraction in the adsorbed phase
y	Mole fraction in the gas phase

**Greek Letters**

$\Pi$	Spreading pressure
$\epsilon_M$	Parameter in the pure component isotherm
$\theta$	Adsorption capacity at saturation
$\mu$	Chemical potential
$\gamma$	Activity coefficient

**Subscripts**

i	Component i
m	Referred to mixture
t	Total amount adsorbed from a binary mixture

**Superscripts**

s	Standard state
g	Gas phase
a	Adsorbed phase

**REFERENCES**

- Arnold, J.R., "Adsorption of Gas Mixtures, Nitrogen-Oxygen on Anatase," J. Am. Chem. Soc., **71**, 104, (1949)
- Cook, W.H. and D. Basmadjian, " The Prediction of Binary Adsorption Equilibrium From Pure Component Isotherm," Can. J. Chem. Eng., **43**, 78, (1965)
- Costa, E., J.L. Sotelo, G. Calleja, and C. Marron, "Adsorption of Binary and Ternary Hydrocarbon Gas Mixtures on Activated Carbon : Experimental Determination and Theoretical Prediction of the Ternary Equilibrium Data," AIChEJ, **27**(1), 5, (1981)
- Ghosh, T.K. and A.L. Hines, "An Isotherm for Multilayer Adsorption on Heterogeneous Solid Surface" Submitted to AIChEJ (1989)
- Hyun, S.H. and R.P. Danner, " Equilibrium Adsorption of Ethane, Ethylene, Isobutane, Carbon Dioxide, and Their Binary Mixtures on 13X Molecular Sieves," J. Chem. Eng. Data, **27**, 196, (1982)
- Jaroniec, M., " Adsorption of Gas Mixtures on Heterogeneous Solid Surfaces. Analytical Solution of Integral Equation for Jovanovic Adsorption Isotherm," J. Colloid Inter. Sci., **53**(3), 422, (1975)
- Jaroniec, M., "Adsorption of Gas Mixtures on Heterogeneous Solid Surfaces. II. Adsorption Isotherms for Gaseous Mixtures Whose Pure Component Isotherms Show the Freundlich, Toth, and Langmuir Behaviors," Colloid & Polym. Sci., **255**, 32, (1977)
- Jaroniec, M., " Description of Kinetics and Equilibrium State of Adsorption from Multicomponent Gas Mixtures on Solid Surfaces," Thin Solid Films, **71**, 273, (1980)
- Jaroniec, M. and J. Toth, "Adsorption of Gas Mixtures on Heterogeneous Solid Surfaces : I. Extension of Toth Isotherm on Adsorption from Gas Mixture," Colloid & Polym. Sci., **256**, 643 (1976)
- Jaroniec, M. and J. Toth, " Adsorption of Gas Mixture on Heterogeneous Solid Surfaces. III. Extension of Toth Isotherm on Multilayer Adsorption of Gas Mixtures," Colloid & Polym. Sci., **256**, 690, (1978)

- Lewis, W.K., E.R. Gilliland, B. Chertow, and W.P. Cadogan, "Adsorption Equilibria Hydrocarbon Mixtures", *Ind. Eng. Chem.*, **42**, 1319, (1950)
- Maurer, G., and J.M. Prausnitz, "On the Derivation Extension of the UNIQUAC Equation," *Fluid Phase Equilibria*, **2**, 91 (1978)
- Moon, H. and C. Tien, "Further Work on Multicomponent Adsorption Equilibria Calculation Based on the Ideal Adsorbed Solution Theory," *Ind. Eng. Chem. Res.*, **26**, 2042, (1987)
- Myers, A.L. and J.M. Prausnitz, "Thermodynamics of Mixed Gas Adsorption," *AICHEJ*, **19**, 453, (1965)
- O'Brien, J.A. and A.L. Myers, "Physical Adsorption of Gases on Heterogeneous Surfaces," *J Chem. Soc. Faraday Trans.1*, **80**, 1467, (1984)
- Paludetto, R., G. Storti, G. Gamba, S. Carra, and M. Morbidelli, "On Multicomponent Adsorption Equilibria of Xylene Mixtures on Zeolite," *Ind. Eng. Chem. Res.*, **26**, 2250 (1987)
- Ruthven, D.M., "Principles of Adsorption and Adsorption Processes", John Wiley & Sons Inc., New York, (1974)
- Sircar, S. and A.L. Myers, "Surface Potential Theory of Multilayer Adsorption from Gas Mixtures," *Chem. Eng. Sci.*, **28**, 489, (1973)
- Talu, O. and I. Zwiebel, " Multicomponent Adsorption Equilibria of Nonideal Mixtures," *AICHEJ*, **32**(8), 1263
- Yang, R.T., "Gas Separation by Adsorption Processes," Butterworth Publishers, Boston, (1987)



**List of Tables**

- I. Parameters for the Pure Component Isotherm Equation (3) and the Spreading Pressure Equation (18) for Methane, Ethylene, Ethane, and Propylene Adsorption on Activated Carbon at 293.2 K.
- II. Mole Fraction in the Adsorbed Phase, Total Amount Adsorbed, and Activity Coefficients for the Methane(1)-Ethylene(2) Mixture.
- III. Mole Fraction in the Adsorbed Phase, Total Amount Adsorbed, and Activity Coefficients for the Methane(1)-Ethane(2) Mixture.
- IV. Mole Fraction in the Adsorbed Phase, Total Amount Adsorbed, and Activity Coefficients for the Ethylene(1)-Ethane(2) Mixture.
- V. Mole Fraction in the Adsorbed Phase, Total Amount Adsorbed, and Activity Coefficients for the Ethylene(1)-Propylene(2) Mixture.
- VI. Mole Fraction in the Adsorbed Phase, Total Amount Adsorbed, and Activity Coefficients for the Ethane(1)-Propylene(2) Mixture.
- VII. Spreading Pressure ( $\Pi_m A/RT$ ) of the Mixture and the Equilibrium Pressure ( $P_i^0$ ) of the Individual Components in the Binary Mixture.

Table I. Parameters for the Pure Component Isotherm Equation (3) and the Spreading Pressure Equation (18) for Methane, Ethane, Ethylene, and Propylene Adsorption on Activated Carbon at 293.2 K

(a) Parameters for the Isotherm Equation (3)

ADSORBATE	$\theta$ (mmol/g)	$A_1$ (atm)	$A_2$	$\epsilon_M$ (atm) <sup>-1</sup>	$b_0$ (atm) <sup>-1</sup>
Methane	1.100	1.0099	0.7799	0.7800	0.2042
Ethylene	3.464	2.4535 10 <sup>-2</sup>	-216.8950	1.2143 10 <sup>-3</sup>	1.4739 10 <sup>-2</sup>
Ethane	4.415	1.4406 10 <sup>-2</sup>	-447.3608	4.5990 10 <sup>-3</sup>	0.1223
Propylene	10.000	2.7965 10 <sup>-3</sup>	-2608.8310	-3.0508	-0.6213

$$A_3 = 1 \text{ atm}$$

(b) Parameters for the Spreading Equation (18)

ADSORBATE	$K_1$	$K_2$	$K_3$	$K_4$	$K_5$
Methane	1.040	0.9870	0.9225	2.7436 10 <sup>-5</sup>	-0.3120
Ethylene	7.178	4.1579 10 <sup>-2</sup>	-1.8731 10 <sup>2</sup>	-1.0944	-0.5027
Ethane	12.662	1.1904 10 <sup>-2</sup>	-1.6303 10 <sup>3</sup>	-3.4758	-0.9953
Propylene	45.161	4.0295 10 <sup>-3</sup>	-4.8762 10 <sup>3</sup>	-5.8940	-1.0487

$$P_i^0 \text{ in atm}$$

Table II. Mole Fraction in the Adsorbed Phase, Total Amount Adsorbed, and Activity Coefficients for the Methane(1)-Ethylene(2) Mixture

$y_1$	Data of Costa et al.				Values predicted by present method			
	$x_1$	$n_t$ (mmol/g)	$\gamma_1$	$\gamma_2$	$x_1$	$n_t$ (mmol/g)	$\gamma_1$	$\gamma_2$
0.998	0.939	0.110	0.938	0.585	0.919	0.116	0.969	0.480
0.991	0.818	0.130	0.918	0.741	0.825	0.133	0.922	0.855
0.974	0.632	0.190	0.876	0.815	0.625	0.175	0.908	0.872
0.787	0.144	0.390	0.788	0.933	0.128	0.405	0.846	0.907
0.539	0.063	0.540	0.760	0.961	0.063	0.560	0.839	0.921

Table III. Mole Fraction in the Adsorbed Phase, Total Amount Adsorbed, and Activity Coefficients for the Methane(1)-Ethane(2) Mixture

$y_1$	Data of Costa et al.				Values predicted by present method			
	$x_1$	$n_t$ (mmol/g)	$\gamma_1$	$\gamma_2$	$x_1$	$n_t$ (mmol/g)	$\gamma_1$	$\gamma_2$
0.998	0.848	0.120	0.981	0.858	0.836	0.126	0.972	0.502
0.996	0.728	0.135	0.977	0.799	0.749	0.140	0.967	0.582
0.987	0.546	0.185	0.960	0.930	0.504	0.192	0.989	0.647
0.975	0.380	0.200	0.943	0.960	0.384	0.238	0.988	0.751
0.790	0.116	0.400	0.676	0.979	0.086	0.574	0.935	0.819
0.580	0.051	0.600	0.600	0.991	0.059	0.676	0.682	0.925

Table IV. Mole Fraction in the Adsorbed Phase, Total Amount Adsorbed, and Activity Coefficients for the Ethylene(1)-Ethane(2) Mixture

$y_1$	Data of Costa et al.				Values Predicted by present method			
	$x_1$	$n_t$ (mmol/g)	$\gamma_1$	$\gamma_2$	$x_1$	$n_t$	$\gamma_1$	$\gamma_2$
0.931	0.880	0.700	0.992	0.980	0.883	0.713	0.981	0.905
0.857	0.770	0.720	0.982	0.961	0.771	0.727	0.985	0.912
0.762	0.649	0.730	0.984	0.991	0.644	0.745	0.988	0.920
0.620	0.478	0.740	0.998	0.963	0.482	0.764	0.990	0.928
0.444	0.314	0.780	0.992	1.013	0.314	0.795	0.994	0.933
0.243	0.153	0.805	1.013	0.993	0.156	0.820	0.999	0.940

Table V. Mole Fraction in the Adsorbed Phase, Total Amount Adsorbed, and Activity Coefficients for the Ethylene(1)-Propylene(2) Mixture

$y_1$	Data of Costa et al.				Values predicted by present method			
	$x_1$	$n_t$ (mmol/g)	$\gamma_1$	$\gamma_2$	$x_1$	$n_t$	$\gamma_1$	$\gamma_2$
0.993	0.800	0.780	0.960	0.656	0.815	0.790	0.946	0.841
0.980	0.614	0.810	0.919	0.720	0.626	0.910	0.916	0.857
0.858	0.253	1.150	0.796	0.864	0.249	1.320	0.818	0.917
0.696	0.141	1.300	0.733	0.931	0.132	1.530	0.756	0.886
0.436	0.055	1.520	0.702	0.973	0.053	1.696	0.732	0.901
0.248	0.028	1.700	0.649	0.992	0.023	1.760	0.790	0.929

Table VI. Mole Fraction in the Adsorbed Phase, Total Amount Adsorbed, and Activity Coefficients for the Ethane(1)-Propylene(2) Mixture

$y_1$	Data of Costa et al.				Values predicted by present method			
	$x_1$	$n_t$ (mmol/g)	$\gamma_1$	$\gamma_2$	$x_1$	$n_t$ (mmol/g)	$\gamma_1$	$\gamma_2$
0.989	0.807	0.900	0.999	0.777	0.841	0.932	0.932	0.875
0.954	0.619	0.960	0.940	0.862	0.600	1.098	0.904	0.939
0.798	0.277	1.230	0.841	0.892	0.283	1.400	0.820	0.932
0.565	0.126	1.480	0.792	0.962	0.128	1.610	0.753	0.913
0.363	0.064	1.620	0.764	0.983	0.067	1.700	0.710	0.944
0.156	0.021	1.700	0.758	1.012	0.024	1.760	0.693	0.973

Table VII. Spreading Pressure ( $\Pi_m A/RT$ ) of the Mixture and the Equilibrium Pressure ( $P_i^0$ ) of the Individual Components in the Binary Mixture

Methane(1) - Ethylene(2)

$y_1$	Data of Costa et al.			Values predicted by present method		
	$\Pi_m A/RT$ (gmo1)	$P_1^0$ (mmHg)	$P_2^0$ (mmHg)	$\Pi_m A/RT$ (gmo1)	$P_1^0$ (mmHg)	$P_2^0$ (mmHg)
0.998	$6.010 \cdot 10^{-3}$	85.0	4.2	$6.07 \cdot 10^{-3}$	84.03	3.87
0.991	$7.008 \cdot 10^{-3}$	99.0	5.0	$6.97 \cdot 10^{-3}$	97.66	4.50
0.974	$9.088 \cdot 10^{-3}$	132.0	6.5	$8.95 \cdot 10^{-3}$	128.88	5.96
0.787	$2.900 \cdot 10^{-2}$	520.0	20.0	$2.63 \cdot 10^{-2}$	468.66	22.75
0.539	$4.252 \cdot 10^{-2}$	844.3	38.4	$3.87 \cdot 10^{-2}$	768.08	40.05

Methane(1) - Ethane(2)

0.998	$6.370 \cdot 10^{-3}$	90.0	1.15	$6.611 \cdot 10^{-3}$	92.20	1.82
0.996	$7.373 \cdot 10^{-3}$	105.0	1.38	$7.330 \cdot 10^{-3}$	103.24	2.04
0.987	$9.999 \cdot 10^{-3}$	141.2	2.31	$1.015 \cdot 10^{-2}$	148.49	3.03
0.975	$1.364 \cdot 10^{-2}$	204.0	3.15	$1.274 \cdot 10^{-2}$	192.79	4.05
0.790	$4.050 \cdot 10^{-2}$	755.0	18.20	$3.717 \cdot 10^{-2}$	730.43	21.05
0.580	$5.450 \cdot 10^{-2}$	1421.0	33.50	$5.042 \cdot 10^{-2}$	1069.20	36.18

Table VII (continued)

## Ethylene(1) - Ethane(2)

$y_1$	Data of Costa et. al.			Values predicted by present method		
	$\pi_m A/RT$ (gmol)	$P_1^0$ (mmHg)	$P_2^0$ (mmHg)	$\pi_m A/RT$ (gmol)	$P_1^0$ (mmHg)	$P_2^0$ (mmHg)
0.931	$6.382 \cdot 10^{-2}$	80.0	44.0	$5.960 \cdot 10^{-2}$	80.70	48.68
0.857	$6.640 \cdot 10^{-2}$	85.0	48.5	$6.138 \cdot 10^{-2}$	84.72	51.22
0.762	$6.924 \cdot 10^{-2}$	89.5	51.3	$6.350 \cdot 10^{-2}$	89.87	54.50
0.620	$7.224 \cdot 10^{-2}$	97.5	56.7	$6.667 \cdot 10^{-2}$	97.48	59.21
0.444	$7.584 \cdot 10^{-2}$	106.5	60.0	$7.035 \cdot 10^{-2}$	106.83	65.02
0.243	$7.967 \cdot 10^{-2}$	118.0	67.5	$7.429 \cdot 10^{-2}$	117.35	71.51

## Ethylene(1) - Propylene(2)

0.993	$7.200 \cdot 10^{-2}$	97.0	4.0	$6.631 \cdot 10^{-2}$	96.59	3.38
0.980	$8.426 \cdot 10^{-2}$	130.2	5.4	$7.820 \cdot 10^{-2}$	128.38	4.66
0.858	$1.352 \cdot 10^{-1}$	319.5	16.5	$1.298 \cdot 10^{-1}$	316.30	15.52
0.696	$1.701 \cdot 10^{-1}$	505.0	28.5	$1.673 \cdot 10^{-1}$	525.00	29.65
0.436	$2.072 \cdot 10^{-1}$	847.7	46.0	$2.084 \cdot 10^{-1}$	838.80	49.55
0.248	$2.271 \cdot 10^{-1}$	1024.8	58.5	$2.304 \cdot 10^{-1}$	1040.00	62.10

Table VII (Continued)

Ethane(1) - Propylene(2)

$y_1$	Data of Costa et al.			Values predicted by present method		
	$\pi_m A/RT$ (gmol)	$P_1^0$ (mmHg)	$P_2^0$ (mmHg)	$\pi_m A/RT$ (gmol)	$P_1^0$ (mmHg)	$P_2^0$ (mmHg)
0.989	$9.210 \cdot 10^{-2}$	92.0	5.5	$8.72 \cdot 10^{-2}$	94.66	3.90
0.954	$1.081 \cdot 10^{-1}$	123.0	10.5	$1.05 \cdot 10^{-1}$	131.9	9.19
0.798	$1.536 \cdot 10^{-1}$	257.0	23.5	$1.50 \cdot 10^{-1}$	257.0	22.66
0.565	$1.922 \cdot 10^{-1}$	424.5	38.8	$1.91 \cdot 10^{-1}$	437.0	40.97
0.363	$2.156 \cdot 10^{-1}$	557.0	51.9	$2.16 \cdot 10^{-1}$	573.9	54.26
0.156	$2.348 \cdot 10^{-1}$	735.0	63.9	$2.37 \cdot 10^{-1}$	692.2	66.69



CHAPTER V

ADSORPTION OF MULTICOMPONENT MIXTURES IN FIXED BEDS  
AN EXPERIMENTAL INVESTIGATION

**ADSORPTION OF MULTICOMPONENT MIXTURES IN FIXED BEDS  
AN EXPERIMENTAL INVESTIGATION**

**Tushar k. Ghosh and Anthony L. Hines**

**Oklahoma State University  
School of Chemical Engineering  
Stillwater, Oklahoma 74078**

**ABSTRACT**

Breakthrough curves for acetaldehyde, propionaldehyde, and butyraldehyde as single components and in their binary and ternary mixtures were obtained from an isothermal fixed bed adsorber. Silica gel and molecular sieve 13X were used as the adsorbent. Experiments with different flow rates suggested that the resistance to mass transfer due to the fluid film was significant below a superficial gas velocity of 6 cm/sec in the silica gel bed. A similar resistance was insignificant at superficial gas velocities higher than 5.5 cm/sec in the molecular sieve bed. The slope of the Breakthrough curves increased when the inlet concentrations of the aldehydes or the temperature of the bed was increased. In the silica gel bed, the heavier aldehydes displaced some of the previously adsorbed lighter aldehydes from the solid surface, thus raised the concentration of the lighter aldehydes in the fluid phase so much that the peak composition increased above the inlet concentration. The peak height and the profile of the breakthrough curve were found to be a function of the fluid phase concentration of the aldehydes. In the molecular sieve 13X bed, only a small amount of lighter aldehydes was displaced by heavier aldehydes and no such behavior was observed in binary mixtures of propionaldehyde and butyraldehyde.

## INTRODUCTION

Adsorption processes are finding increasing applications in the gas separation industries and as methods for removing pollutants from gas streams. Frequently, these streams contain more than one compound that may be adsorbed on the adsorbent surface. Most of the experimental work reported in the literature are limited to binary mixtures, and in very few cases the influence of various parameters, such as temperature, flow rate, concentration, and bed length are studied.

Gariepy and Zwiebel (1976) studied the breakthrough pattern of carbon dioxide, ethane, and ethylene from their binary mixtures in an activated carbon bed. They found that the displacement of a component from the adsorbent surface by another component depended on their adsorption capacity or relative affinity rather than on the molecular weight of the components. Both CO<sub>2</sub> and ethylene were displaced by ethane from the activated carbon bed. The concentration of the displaced compound in the fluid phase increased above the inlet concentration and the shape of breakthrough curves were found to be a function of the bed length and relative affinity. A similar phenomenon was also observed by Carter and Husain (1974) in their experiment with CO<sub>2</sub> and water adsorption on a molecular sieve 4A bed. The CO<sub>2</sub> was displaced by the more strongly adsorbed water from the bed. The breakthrough curve of water showed normal single

component adsorbate characteristics. Needham et al. (1966) reported the displacement of pentane by hexane from a nonisothermal silica gel bed. The shape of the breakthrough curves for pentane was a strong function of the inlet composition. A sharp peak followed by an elongated tail was exhibited by pentane for the highest inlet concentration of pentane. It had a prolonged plateau zone at low concentration. Thomas and Lombardi (1971) studied the breakthrough nature of benzene and toluene as single components and in binary mixtures of their vapor. An inert carrier gas, nitrogen, was saturated with benzene and toluene vapors by dispersing  $N_2$  through saturators filled with liquid benzene and toluene. They also studied the effect of flow rate, concentration, and bed length on the shape of the breakthrough curves and found constant pattern behavior for single components. Although the experimental data for various other binary mixtures are available in the literature, very few studies have been reported for ternary or higher mixtures, particularly for the gas phase. Balzli et al. (1978) and Sheindorf et al. (1983) investigated the adsorption of three components from an aqueous phase on activated carbon. Balzli et al. studied the adsorption of butanol, t-amyl alcohol, and phenol from water, whereas Sheindorf et al. investigated the adsorption of phenol, parabromophenol and benzenesulfonate from water.

The objective of the present work was to obtain the breakthrough curves for several single components and then

obtain breakthrough curves of individual components from their multicomponent mixtures. Silica gel and molecular sieve-13X were used as the adsorbents in this work. The influence of temperature, flow rate, and concentration on the breakthrough time and on the shape of the breakthrough curves were investigated as part of this study.

## **EXPERIMENTAL SECTION**

### **Materials and Apparatus:**

Silica gel, Grade 40 (6-12 mesh), was supplied by Davison Chemical, Baltimore, Maryland. It was crushed and particles in the size range 16 to 30 mesh were used in all of the experimental runs. Molecular sieve-13X, Grade 542 (8-12 mesh bead), was also supplied by Davison Chemical. The adsorbates used in the present work were acetaldehyde, propionaldehyde, and butyraldehyde. Acetaldehyde and butyraldehyde were obtained from Fluka AG and had stated purities of 99.5 % and 99 %+, respectively. Propionaldehyde had a minimum stated purity of 99 % and was obtained from Aldrich Chemical Company. Both silica gel and molecular sieve were regenerated in a fixed bed by heating them at 473 K, under a vacuum of about 1 mmHg for 24 hours. The regenerated material was kept in a dessicator for later use.

The experimental set up could be divided into four sections: flow controlling section, saturators, adsorption column, and gas analysis section. A schematic diagram of the setup is shown in Figure 1. Helium (the carrier gas) was

passed through a molecular sieve bed to remove any moisture and impurities before splitting it into four streams. Each helium stream was passed through an empty bottle before it was dispersed through a fritted disc into the saturators which contained the liquid aldehydes. The empty bottles were used to prevent the back flow of the liquids, if any, into the flow controller. The saturators were immersed in constant temperature water baths whose temperature was controlled within  $\pm 0.2$  K. Two saturators in series were used for each aldehyde to ensure the saturation of the helium stream by the respective aldehydes at the bath temperature. The helium gas stream became 80-90 % saturated with the aldehyde after the first saturator and was completely saturated after second one. In a separate test a third saturator was connected in series with the other two and no further change in concentration was noticed. The complete saturation of the helium stream ensured the constant inlet concentration of the aldehydes. The gas streams from the saturators were next passed through flasks packed with glass wool to eliminate entrained liquid droplets, if any. Separate vapor streams could either be mixed or admitted into the adsorption column as a single component. The fourth stream, which was pure helium, was then mixed with the streams containing the aldehydes to obtain the desired flow rate and concentration of aldehydes in the final gas mixture. The pressures in the saturators were measured by a mercury manometer.

The gas mixture was then admitted into the adsorption column after it had passed through a 10 ft, 1/4 inch steel coil. Both the steel coil and the adsorption bed were immersed in a second stirred water bath. The temperature was controlled within  $\pm 0.1$  K. The steel coil helped to ensure proper mixing of the gases and also to maintain the same inlet gas temperature as that of the adsorption bed. Two different columns, one for silica gel and another one for molecular sieve, were used in the present work. The description of the adsorption columns and the properties of the adsorbents are provided in Table I. The pressure and temperature at the inlet and outlet of the bed were measured by mercury manometers and thermocouples, respectively. The temperature of the water baths was measured both by a thermometer and a thermocouple. Regeneration was carried out at a temperature of 473 K by wrapping a heating tape around the column. A vacuum pump was used to maintain the vacuum in the bed during the regeneration of the adsorbents.

Both the inlet and outlet gas streams were analyzed by a gas chromatograph. The best conditions for the minimum column retention time of the heaviest component and at the same time a good peak resolution were obtained by a trial and error procedure. These conditions are given in Table II. During analysis of the gas sample it was found that approximately two minutes was necessary for complete analysis of the gas mixture when all three aldehydes were present in the stream. However, during experiments with multicomponent



mixtures, particularly in the silica gel bed, it was noted that the lighter aldehydes could breakthrough from the bed within a very short period of time. To obtain several data points along the breakthrough curve, a valve with 16 sample loops was used in combination with a 6-port valve to collect samples. The samples could be drawn from the gas streams at any time and could be stored for later analysis. A UV/VIS spectrophotometer was connected on-line to determine the time at which the adsorbate first appeared in the gas stream at the bed outlet. As soon as the adsorbate appeared in the bed outlet as indicated by the spectrophotometer, samples of the gas mixture were collected at specific time intervals and stored in the loops. Calibration of the chromatograph was achieved by injecting mixtures (of aldehydes) of known composition.

## **RESULTS AND DISCUSSIONS**

### **Pure Component Breakthrough Curves**

Single component breakthrough curves for acetaldehyde, propionaldehyde, and butyraldehyde were obtained both in a silica gel and in a molecular sieve-13X bed. The effect of temperature, flow rate, and concentration on the breakthrough time and on the profile were also studied.

The area behind a breakthrough curve as shown in Figure 2 provided the total amount adsorbed in the column. This represents a point on the equilibrium isotherm corresponding to the concentration or the partial pressure of the adsor-

bate in the inlet gas stream. The amount of adsorbed aldehydes, calculated from the shaded area as shown in Figure 2, was found to be higher than that obtained from equilibrium isotherm data determined gravimetrically on silica gel (6-12 mesh) and molecular sieve-13X (4-8 mesh bead). The increase in uptake by 16-30 mesh silica gel and 8-12 mesh molecular sieve are in part due to the greater surface area of these particles. Also some pores, which were inaccessible in larger size particles became available when the particle size was reduced. The BET surface area measured by using  $N_2$  as adsorbate at 77.3 K was found to increase from  $760 \text{ m}^2/\text{g}$  for 6-12 mesh silica gel to  $796 \text{ m}^2/\text{g}$  for 16-30 mesh particles. The surface area of molecular sieve increased from  $456 \text{ m}^2/\text{g}$  for 8-12 mesh to  $472 \text{ m}^2/\text{g}$  for 4-8 mesh bead. Based on a comparison of the surface areas measured by using aldehydes and  $N_2$  as adsorbates, Ghosh and Hines (1989a, 1989b) suggested that some pores are inaccessible to aldehydes in larger size particles.

In a series of runs, the flow rates through the bed were varied keeping the concentration of the aldehydes and temperature constant. In Figures 3 and 4, the dimensionless concentration  $C_i/C_o$  for acetaldehyde in the silica gel and the molecular sieve beds are plotted as a function of time. It can be seen from these figures that the constant pattern breakthrough curves were obtained when the superficial gas velocity was greater than 6 cm/sec in the silica gel bed and above 5.5 cm/sec in the molecular sieve bed. Similar

behavior was also observed for other aldehydes and the plots are presented in Appendix H. In these figures the curves at different flow rates are superimposed over each other by shifting the curves by a given amount of time to account for the flow rates. The deviation of the curve from constant pattern behavior at low flow rate suggested that the bed should be operated at a velocity higher than 6 cm/sec for a silica gel bed and above 5.5 cm/sec for a molecular sieve bed to avoid fluid film resistance to mass transfer.

The effects of inlet concentration on the breakthrough time and on the shape of the breakthrough curve for acetaldehyde are presented in Figures 5 and 6. (See Appendix H for plots of other aldehydes). The shape of a breakthrough curve is determined by the rate of mass transfer between the fluid and solid phases. As the concentration increased in the gas phase, breakthrough curves started to sharpen due to an increase in the rate of mass transfer and assumed constant patterns as shown in the above figures. The breakthrough curves for acetaldehyde at different temperatures are shown in Figures 7 and 8 for the silica gel and molecular sieve beds, respectively (plots for other aldehydes are given in Appendix H). The effect of temperature on the shape of the curves was negligible as illustrated by these figures. However, the breakthrough time was higher at lower temperature due to the the higher equilibrium capacity.

## BINARY AND TERNARY BREAKTHROUGH CURVES

During adsorption from binary and ternary mixtures of aldehydes it was observed that the breakthrough characteristics of individual aldehydes in a silica gel bed were different from that in a molecular sieve bed. The breakthrough behavior of the aldehydes in these adsorbents are discussed below.

In all experimental runs with the silica gel bed involving binary and ternary mixtures, it was observed that a competitive adsorption regime developed and low molecular weight aldehydes were displaced by the heavier aldehydes. The concentration of lighter aldehydes in the fluid phase increased so much that its concentration in the mixture became higher than the inlet composition. As mentioned earlier, this type of behavior was also observed by other researchers (Needham et al., 1966; Carter and Husain, 1982). In ternary mixtures of aldehydes, propionaldehyde first displaced the acetaldehyde, but later was displaced by butyraldehyde. Therefore, the concentrations of both acetaldehyde and propionaldehyde in the fluid phase became higher than the inlet concentrations. Although the heavier aldehydes displaced the lighter ones, the heavier one itself was not adsorbed at the same rate as could be adsorbed as a single component because of the counterdiffusion which decreased the driving force for the heavier aldehydes. As a result the breakthrough curves for heavier aldehydes were flatter compared to the pure component curves. However, the

heavier aldehydes did not completely displace the lighter ones from the adsorbent surface in any of the runs.

To determine the effect of fluid film resistance to the mass transfer, the flow rate through the bed was varied while the concentration and temperature were kept constant. The resulting breakthrough curves for a binary mixture of acetaldehyde and propionaldehyde and for a ternary mixture at two flow rates are shown in Figures 9 and 10. Breakthrough curves for other binary and ternary mixtures are presented in Appendix H. Nearly constant pattern behavior of the curves suggested that the fluid film resistance could be neglected if the velocity is maintained above 6 cm/sec. The small deviation of the curves in the region where the gas phase concentration was above the inlet concentration was due to the small variation in the inlet gas concentration.

From Figures 11 and 12, it can be seen that both in binary and ternary mixtures the shape of the breakthrough curves the peak height were a strong function of the inlet gas composition. When the inlet concentration of the heavier component was higher, the lighter component was displaced at a faster rate and its breakthrough curve rose sharply. The outlet concentration of the lighter component became very much higher than its inlet concentration and then dropped, rather quickly, to the inlet concentration. However, when the concentration of lighter aldehyde was higher, it exhibited a plateau zone where the concentration remained nearly constant for a while and then decreased slowly to the

inlet composition.

The breakthrough time increased as the bed temperature was decreased. This was due to the higher adsorption capacity at lower temperature. However the profile of the curves remained the same, which suggests no major change in the mass transfer mechanism due to a temperature change. Plots of the breakthrough curves at different temperatures for one binary mixture of butyraldehyde and propionaldehyde and for one ternary mixture are given in Figures 13 and 14.

The concentration profiles from a molecular sieve bed showed a different type of behavior than that observed for silica gel. In binary mixtures of aldehydes, both butyraldehyde and propionaldehyde displaced only a small amount of adsorbed acetaldehyde from the bed. Such phenomenon was not observed in binary mixtures of propionaldehyde and butyraldehyde. Butyraldehyde broke through at a faster rate than propionaldehyde did. It was also noticed in all experimental runs that both of the aldehydes in binary mixtures and all three aldehydes in ternary mixtures started to break out from the bed at the same time. This phenomenon and the fact that only a very small amount of acetaldehyde could be displaced by the heavier one suggest that all three aldehydes have similar affinities for molecular sieve and are strongly adsorbed on the surface. Therefore, molecular sieve is not suitable for separation of the aldehydes but can be used to remove them from a gas stream.

The constant pattern behavior was noticed both for binary and ternary mixtures when the superficial velocity through the bed was maintained above 5.5 cm/sec. The breakthrough curves for the acetaldehyde-propionaldehyde system and for the ternary mixture at various flow rates are given in Figures 15 and 16 (Plots for other aldehyde mixtures can be found in Appendix H). The shape of the breakthrough curve was very much dependent on the inlet gas composition as can be seen in Figures 17 and 18. Although acetaldehyde was displaced by propionaldehyde and butyraldehyde, the breakthrough curves for acetaldehyde did not rise as sharply as observed for the silica gel bed. In most of the cases a plateau zone was observed where the concentration remained constant for a while and then slowly approached the inlet concentration. Breakthrough curves at different temperatures are presented in Figures 19 and 20. As shown, the temperature did not change the profile significantly.

An interesting phenomenon was observed for all ternary mixtures when butyraldehyde concentration in the gas phase was lower than that of acetaldehyde or of propionaldehyde. Butyraldehyde was displaced by acetaldehyde and its concentration in the fluid phase increased above the inlet concentration. At the same time the concentration of acetaldehyde started to decrease. Eventually, both concentrations became the same as the inlet concentration indicating bed saturation.

## CONCLUSIONS

The experimental data from the present study suggest that the silica gel bed is more suitable for separation of the aldehydes, although the molecular sieve bed could be used to remove them all together from a gas stream.

An increase in the inlet concentration of the aldehydes both as a single component or in the multicomponent mixture sharpened the breakthrough curves. The concentration profile was found to be more dependent on the inlet gas composition than on the flow rates or the temperature of the bed.

The displacement of the lighter aldehydes by the heavier one was more pronounced in the silica gel bed than was observed for molecular sieve. Although all three aldehydes exhibited similar affinities towards molecular sieve, the affinity of the aldehydes for silica gel increased with the molecular weight.



**REFERENCES**

- Balzli, M.W., A.I. Liapis, and D.W.T. Rippin, "Application of Mathematical Modelling to the Simulation of Multi-Component Adsorption in Activated Carbon Columns", *Trans. Inst. Chem. Eng.*, **56**, 145 (1978).
- Carter, J.W. and H. Husain, "The Simultaneous Adsorption of Carbon Dioxide and Water Vapour by Fixed Beds of Molecular Sieves," *Chem. Eng. Sci.*, **29**, 267, (1974).
- Gariepy, R.L. and I. Zwiebel, "Adsorption of Binary Mixtures in Fixed Beds," *AIChE Sym. Series*, **67**, No 117, 17 (1976).
- Ghosh, T.K. and A.L. Hines, "Adsorption of Acetaldehyde, Propionaldehyde and Butyraldehyde on Silica Gel," submitted to *Separation Science and Technology*, (1989a).
- Ghosh, T.K. and A.L. Hines, "Adsorption of Acetaldehyde, Propionaldehyde and Butyraldehyde on Molecular Sieve 13X," submitted to *Separation Science and Technology*, (1989b).
- Needham, R.B., J.M. Campbell, and H.O. McLeod, "Critical Evaluation of Mathematical Models Used for Dynamic Adsorption of Hydrocarbons," *I&EC Proc. Des. Dev.*, **5**, 122, (1966).
- Sheindorf, C., M. Rebhun, and M. Sheintuch, "Prediction of Breakthrough Curves from Fixed-Bed Adsorber with Freundlich-Type Multisolute Isotherm," *Chem. Eng. Sci.*, **38**, No 2, 335, (1983).
- Thomas, W.J. and J.L. Lombardi, "Binary Adsorption of Benzene-Toluene Mixtures," *Trans. Instn. Chem. Engrs.* **49**, 240, (1971).

**LIST OF TABLES**

- I. Description of the Adsorption Column and Properties of the Adsorbents
- II. The Operating Conditions for Gas Chromatograph

**LIST OF FIGURES**

1. A Schematic Flow Diagram of the Experimental Apparatus
2. Calculation of the Total Amount Adsorbed from a Breakthrough Curve
3. Effects of Flow Rates on Breakthrough Curves for Acetaldehyde in a Silica Gel Bed
4. Effects of Flow Rates on Breakthrough Curves for Acetaldehyde in a Molecular Sieve 13X-Bed
5. Effects of Inlet Concentrations on Breakthrough Curves for Propionaldehyde in a Silica Gel Bed
6. Effects of Inlet Concentrations on Breakthrough Curves for Propionaldehyde in a Molecular Sieve-13X Bed
7. Effects of Temperatures on Breakthrough Curves for Butyraldehyde in a Silica Gel Bed
8. Effects of Temperatures on Breakthrough Curves for Butyraldehyde in a Molecular Sieve-13X Bed
9. Effects of Flow Rates on Breakthrough Curves for Acetaldehyde and Propionaldehyde in their Binary Mixtures in a Silica Gel Bed
10. Effects of Flow Rates on Breakthrough Curves for Acetaldehyde, Propionaldehyde, and Butyraldehyde in their Ternary Mixtures in a Silica Gel Bed
11. Effects of Inlet Concentrations on Breakthrough Curves for Acetaldehyde and Butyraldehyde in their Binary Mixtures in a Silica Gel Bed
12. Effects of Inlet Concentrations on Breakthrough Curves for Acetaldehyde, Propionaldehyde, and Butyraldehyde in their Ternary Mixtures in a Silica Gel Bed
13. Effects of Temperatures on Breakthrough Curves for Propionaldehyde and Butyraldehyde in their Binary Mixtures in a Silica Gel Bed
14. Effects of Temperatures on Breakthrough Curves for Acetaldehyde, Propionaldehyde, and Butyraldehyde in their Ternary Mixtures in a Silica Gel Bed
15. Effects of Flow Rates on Breakthrough Curves for Acetaldehyde and Propionaldehyde in their Binary Mixtures in a Molecular Sieve-13X Bed

16. Effects of Flow Rates on Breakthrough Curves for Acetaldehyde, Propionaldehyde, and Butyraldehyde in their Ternary Mixtures in a Molecular Sieve-13X Bed
17. Effects of Inlet Concentrations on Breakthrough Curves for Acetaldehyde and Butyraldehyde in their Binary Mixtures in a Molecular Sieve-13X Bed
18. Effects of Inlet Concentrations on Breakthrough Curves for Acetaldehyde, Propionaldehyde, and Butyraldehyde in their Ternary Mixtures in a Molecular Sieve-13X Bed
19. Effects of Temperatures on Breakthrough Curves for Propionaldehyde and Butyraldehyde in their Binary Mixtures in a Molecular Sieve-13X Bed
20. Effects of Temperatures on Breakthrough Curves for Acetaldehyde, Propionaldehyde, and Butyraldehyde in their Ternary Mixtures in a Molecular Sieve-13X Bed

Table I. Description of the Adsorption Columns and Properties of the Adsorbents

SILICA GEL BED		MOLECULAR SIEVE-13X BED	
Bed Length	15.0 cm	Bed Length	7.0 cm
Internal Bed Diameter	1.1 cm	Internal Bed Diameter	2.62 cm
Solid Weight	10.0 g	Solid Weight	20.0 g
Equivalent Diameter of Particles	0.039 cm	Equivalent Diameter of Particles	0.019 cm
Bed Void Fraction	0.378	Bed Void Fraction	0.527
Particle Void Fraction	0.483	Pore Volume	0.35 cm <sup>3</sup> /g
Solid Density	2.195 g/cm <sup>3</sup>		
Particle Density	1.129 g/cm <sup>3</sup>	Particle Density	1.12 g/cm <sup>3</sup>

Table II. Operating Conditions for Gas Chromatograph

Chromatograph	: Carle Chromatograph Series 100
Detector	: Thermal Conductivity
Column	: 274 X 0.254 cm I.D. (108 X 0.1inch) Stainless Steel Column, Packed with 10 % Carbowax on Chromosorb WHP
Oven Temperature	: 383.2 K
Bridge Current Setting	: 3
Carrier Gas	: Helium
Carrier Gas Flow Rate	: 30 ml/min

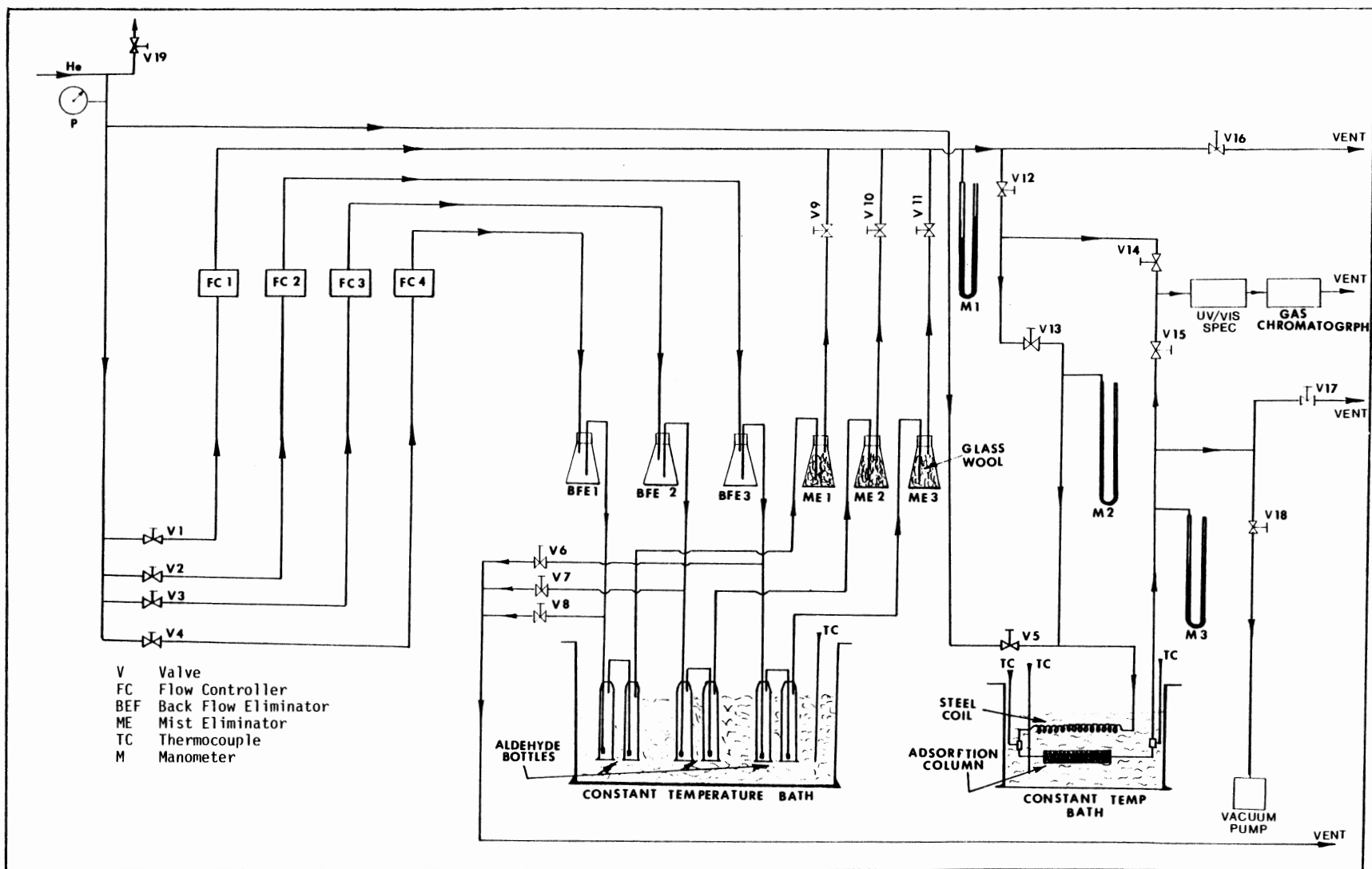


Figure 1. A Schematic Flow Diagram of the Experimental Apparatus

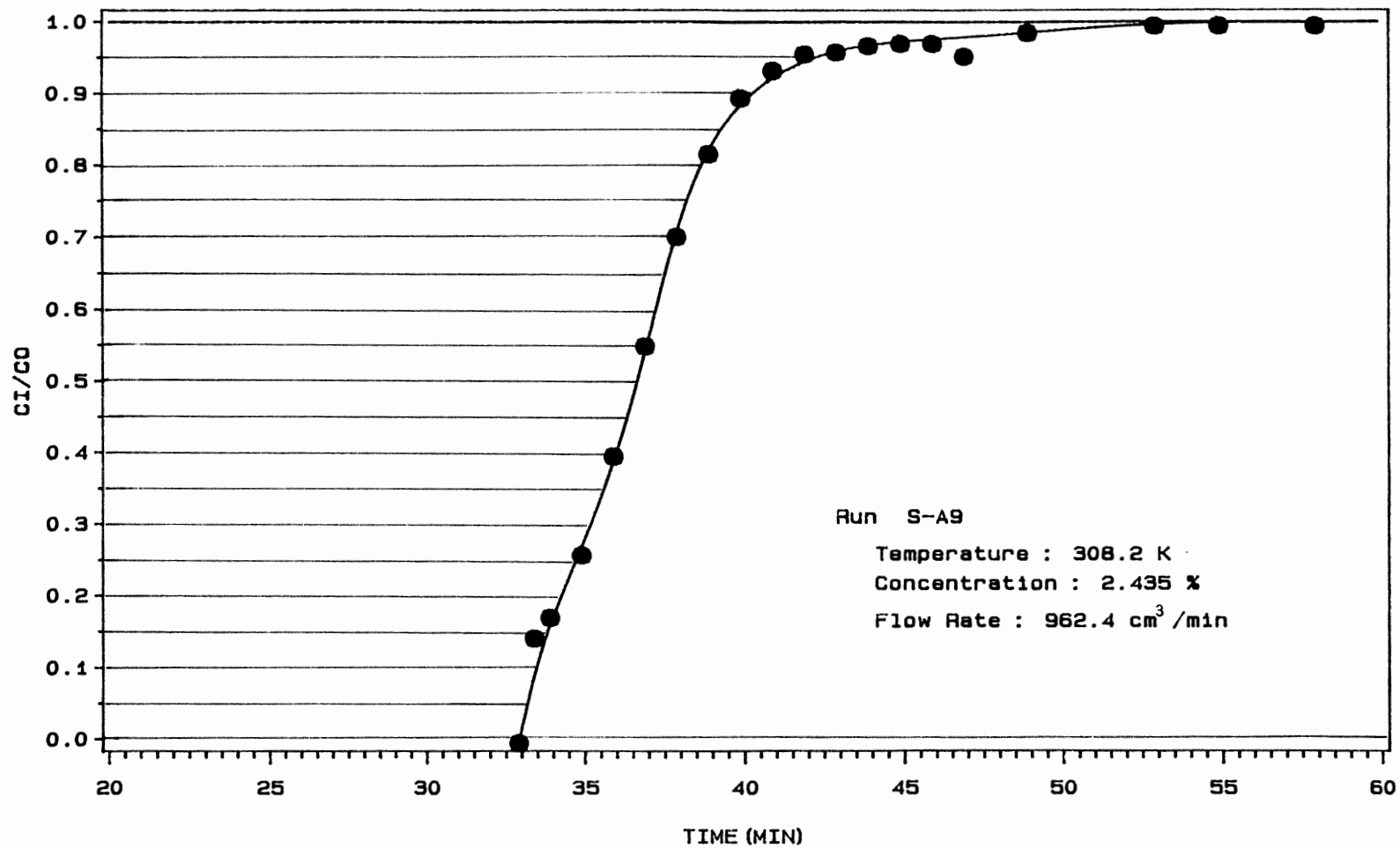


Figure 2. Calculation of Total Amount Adsorbed from A Breakthrough Curve



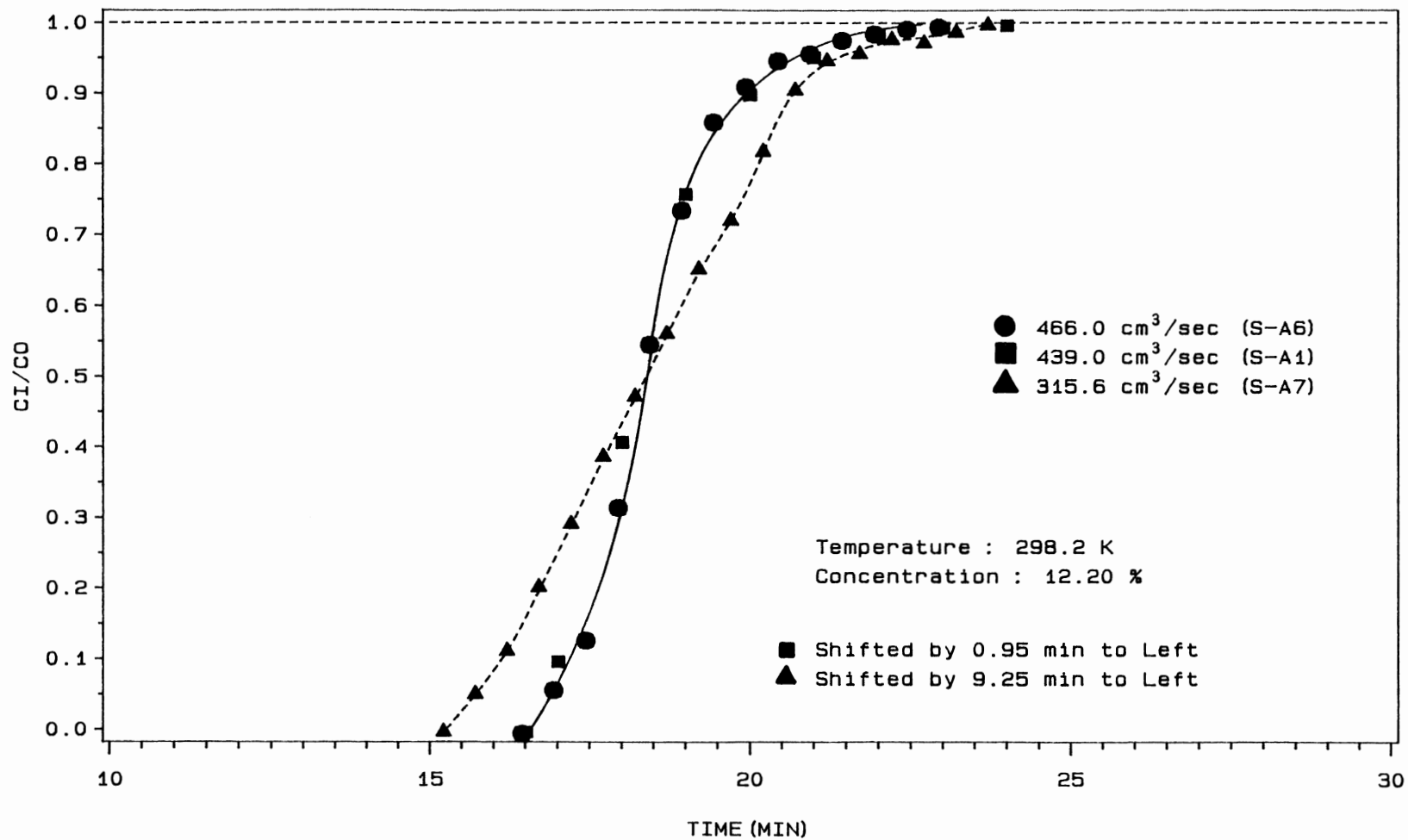


Figure 3. Effects of Flow Rate on Breakthrough Curves for Acetaldehyde in a Silica Gel Bed

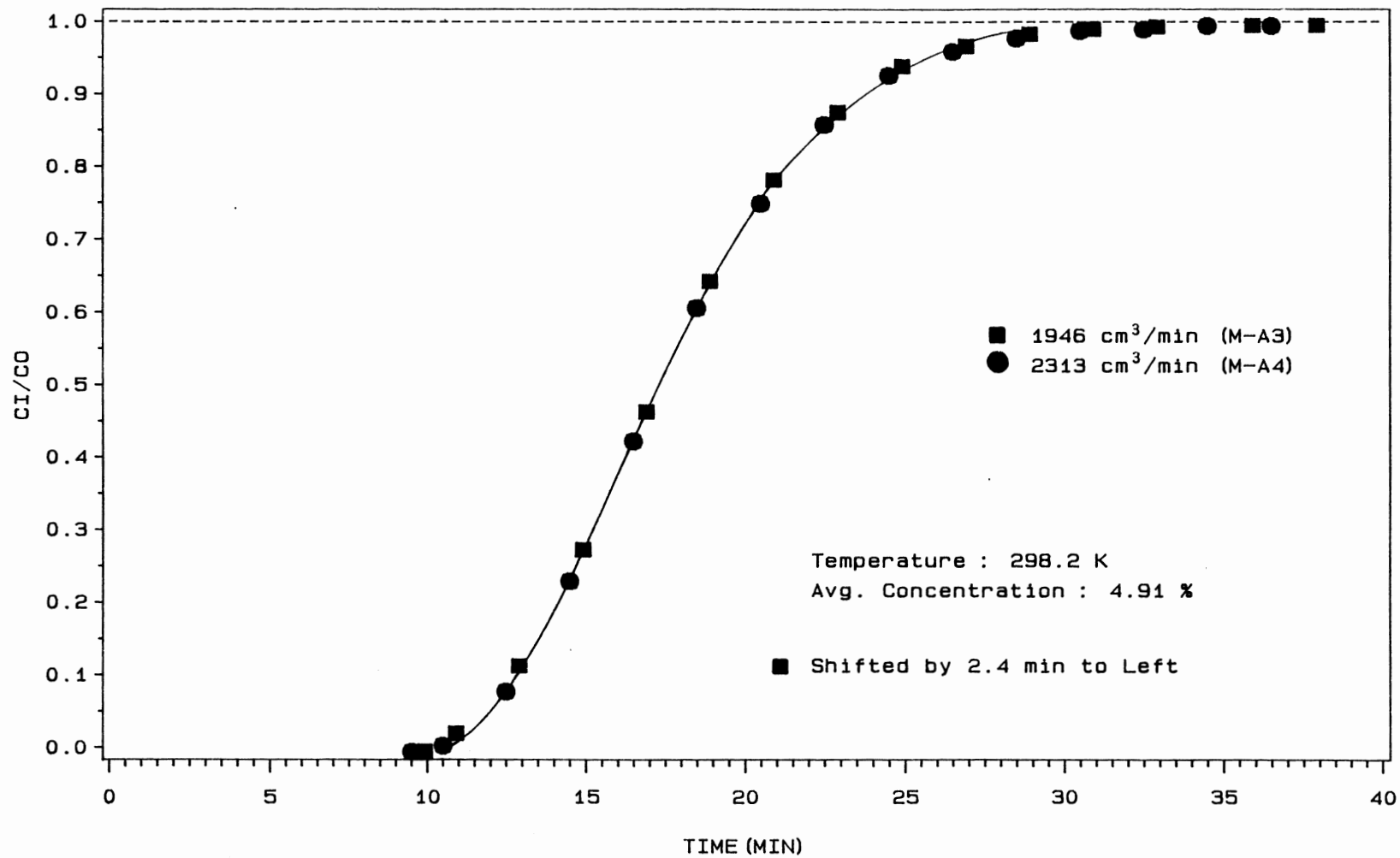


Figure 4. Effects of Flow Rate on Breakthrough Curves for Acetaldehyde in a Molecular Sieve-13X Bed

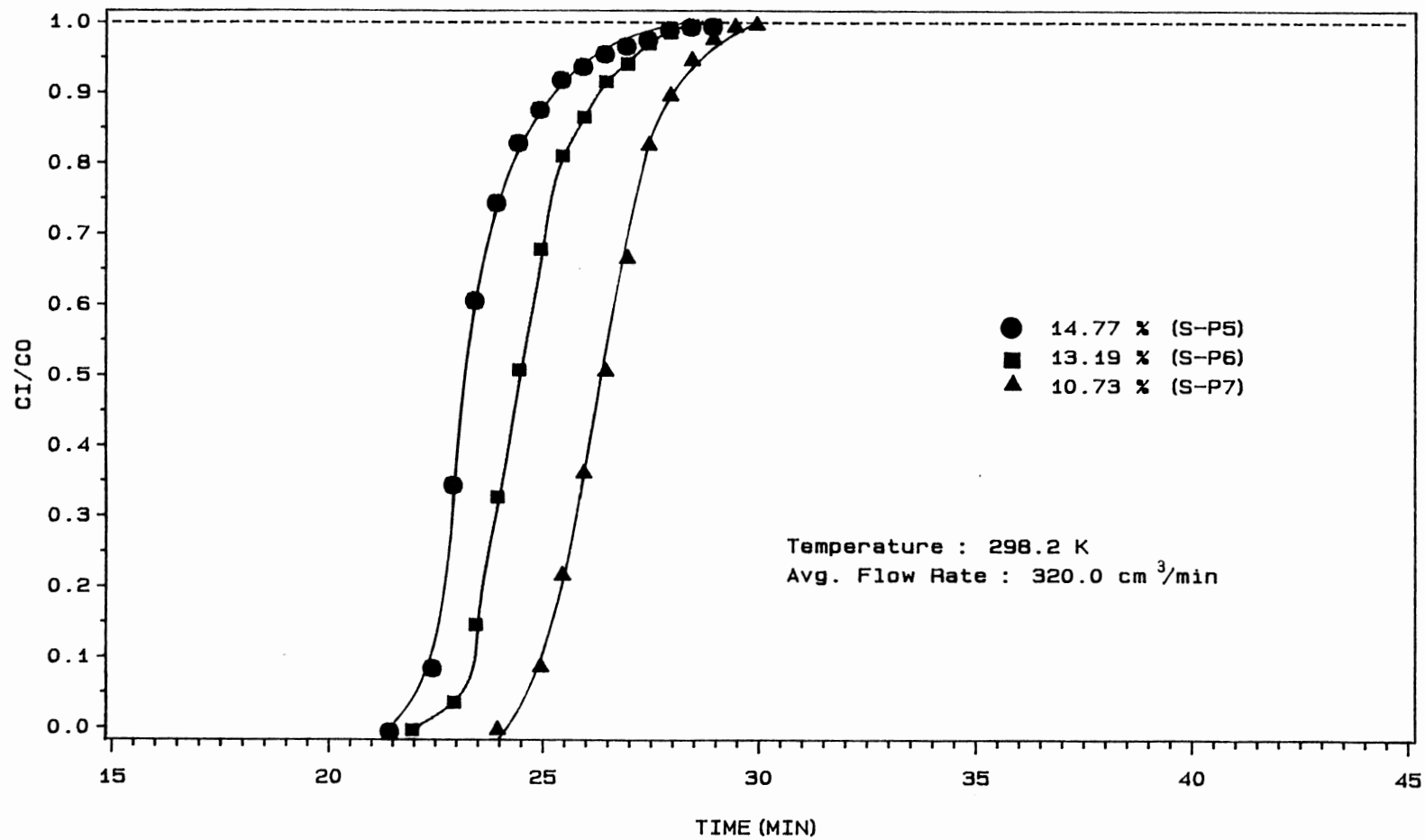


Figure 5. Effects of Inlet Concentration on Breakthrough Curves for Propionaldehyde in a Silica Gel Bed

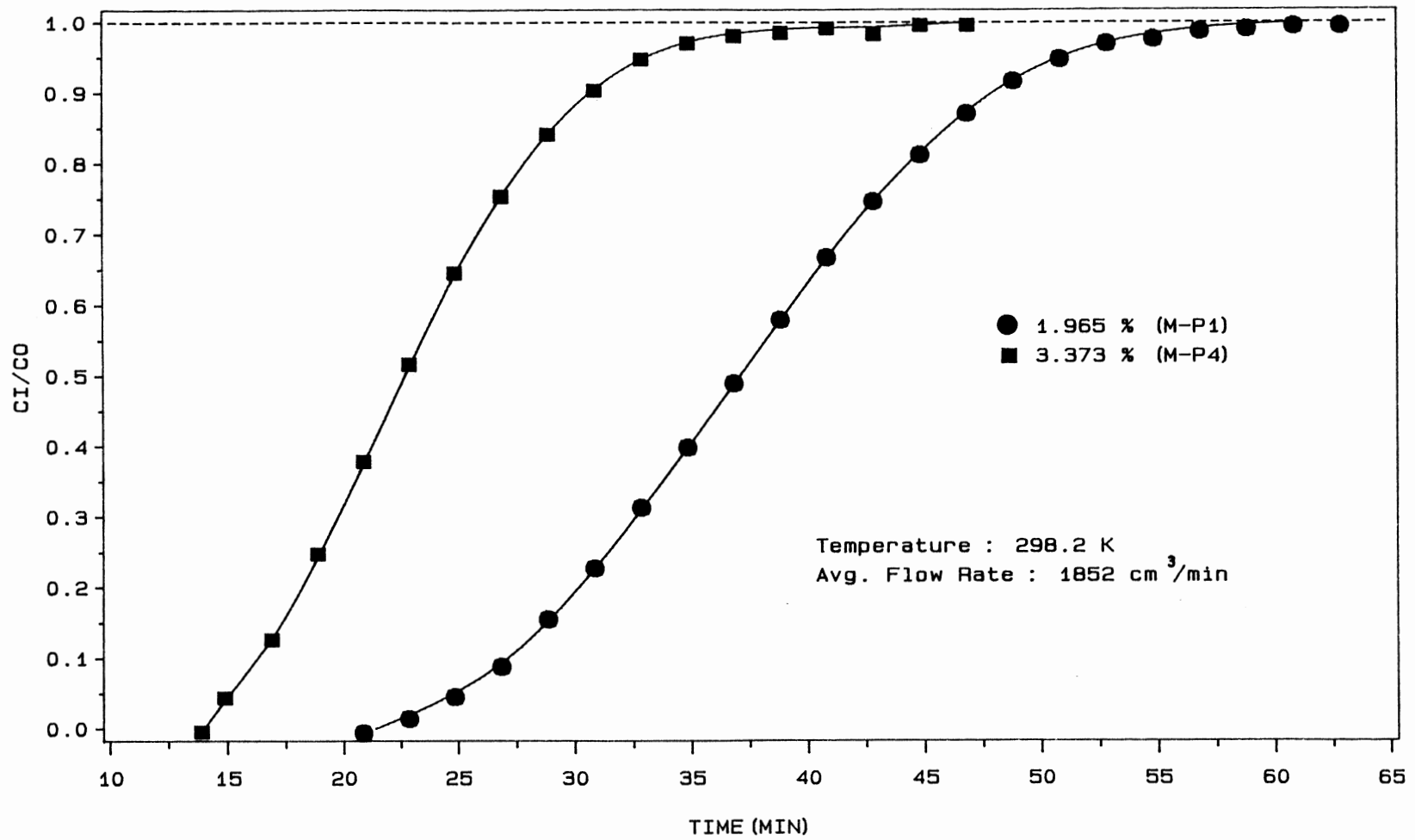


Figure 6. Effects of Inlet Concentration on Breakthrough Curves for Propionaldehyde in a Molecular Sieve-13X Bed

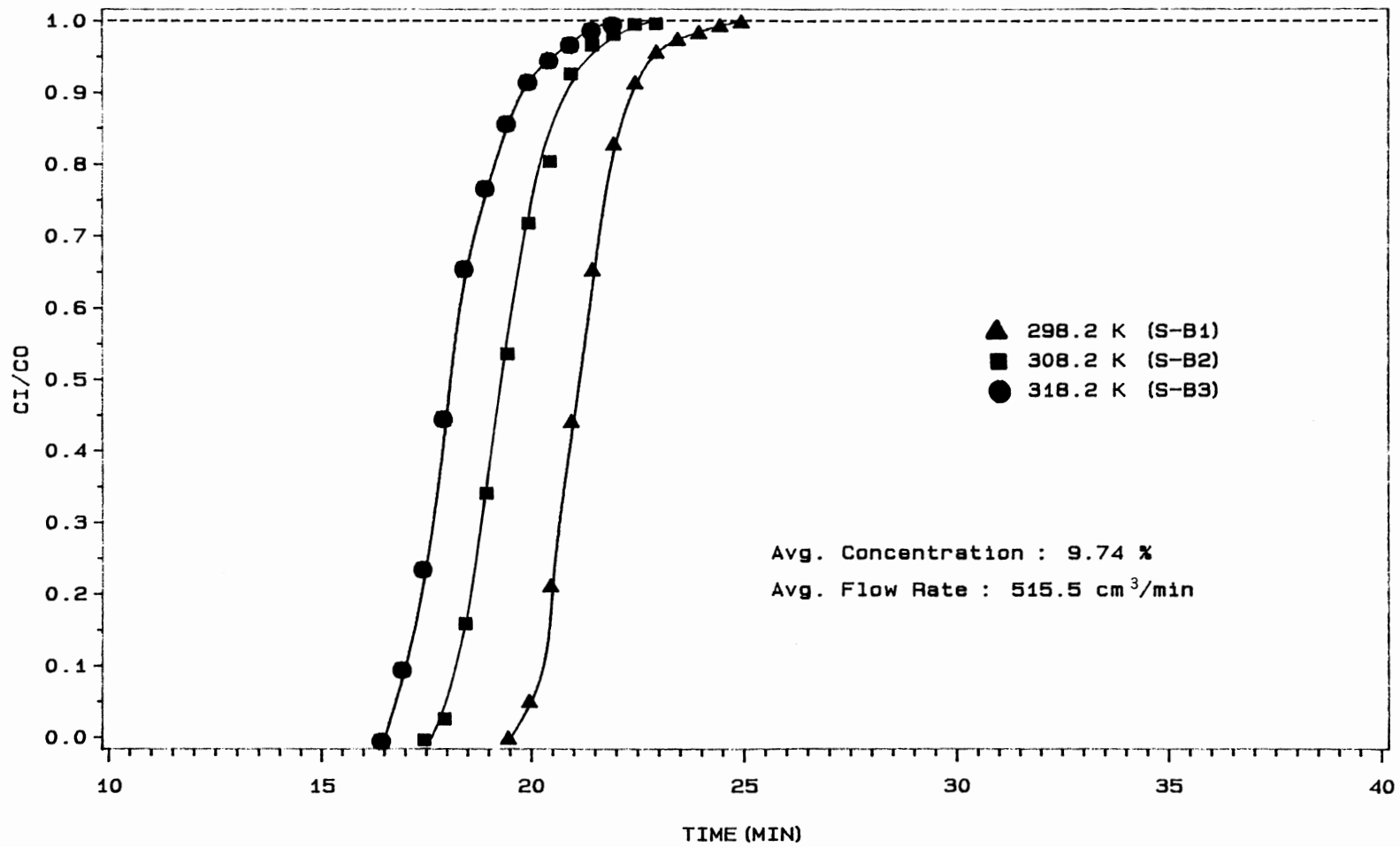


Figure 7. Effects of Temperature on Breakthrough Curves for Butyraldehyde in a Silica Gel Bed

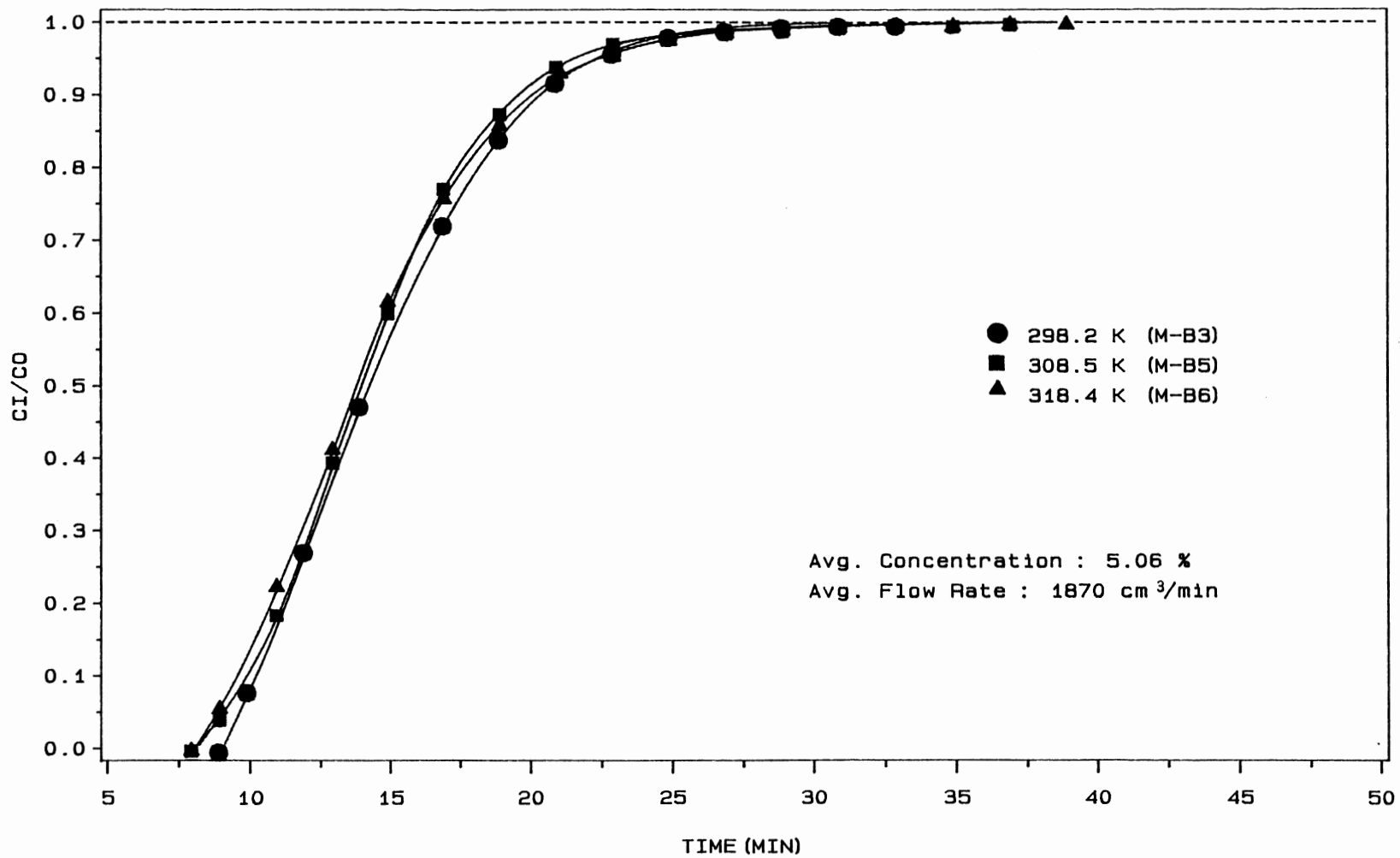


Figure 8. Effects of Temperature on Breakthrough Curves for Butyraldehyde in a Molecular Sieve-13X Bed

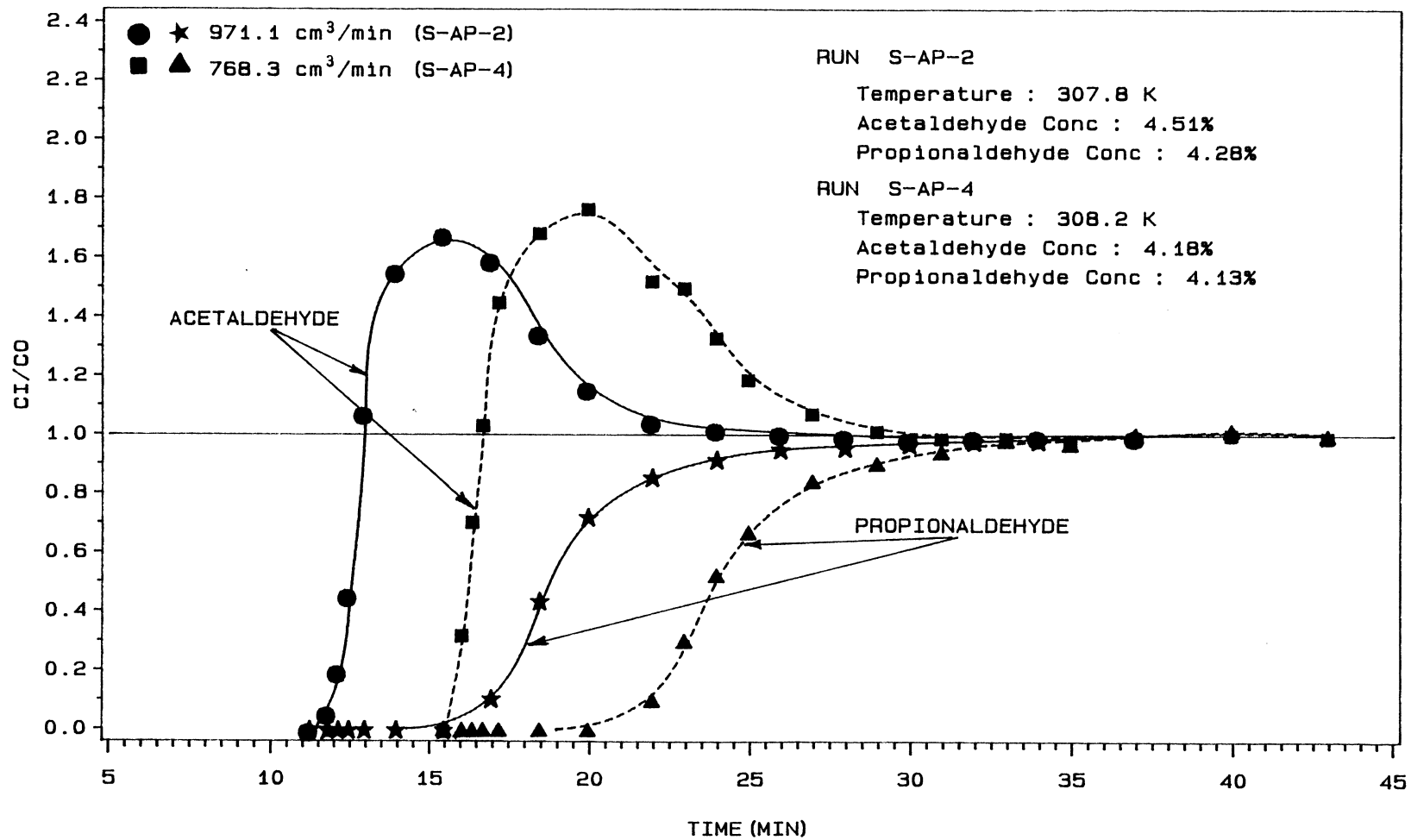


Figure 9. Effects of Flow Rate on Breakthrough Curves for Acetaldehyde and Propionaldehyde in their Binary Mixture in a Silica Gel Bed

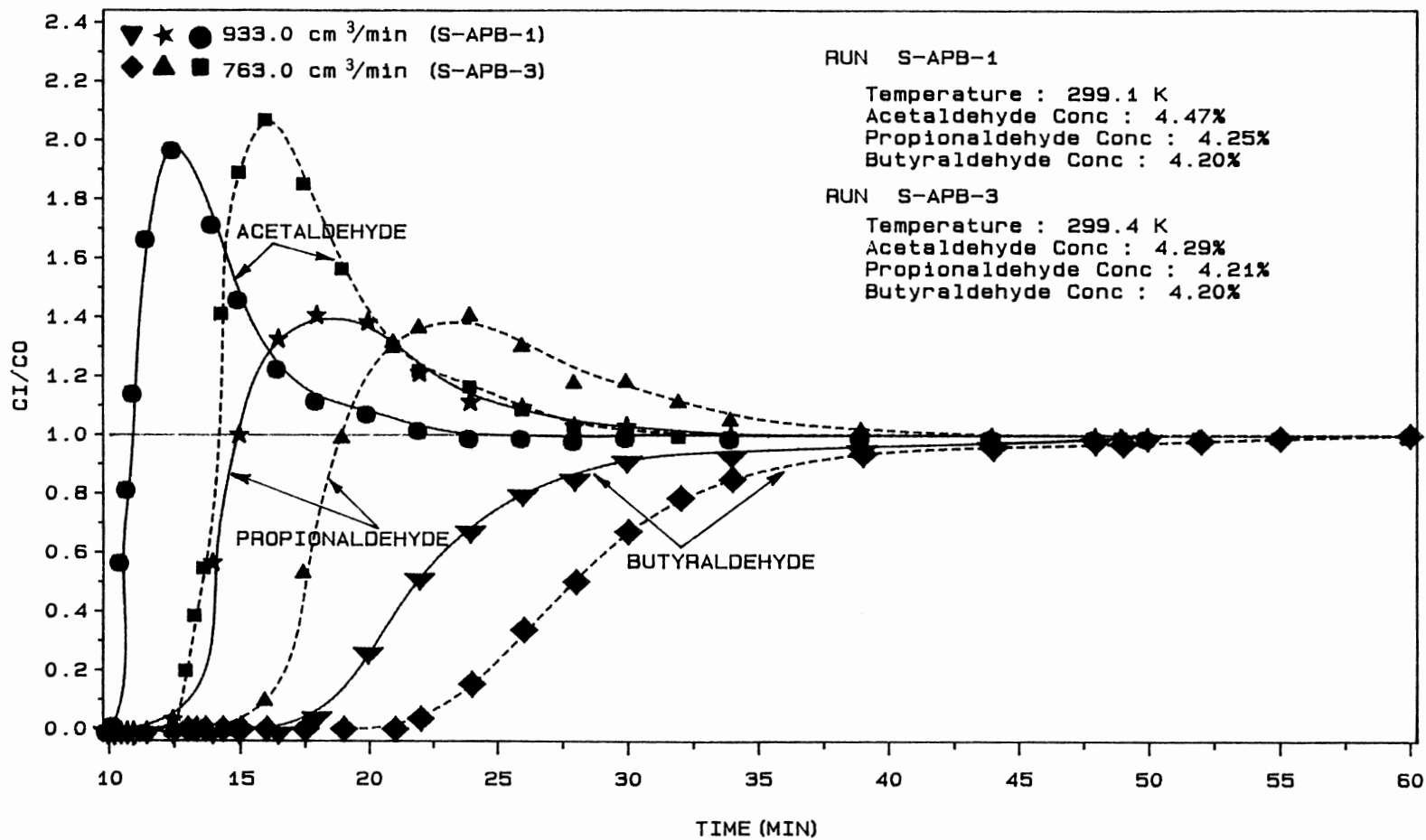


Figure 10. Effects of Flow Rate on Breakthrough Curves for Aldehydes in their Ternary Mixture in a Silica Gel Bed



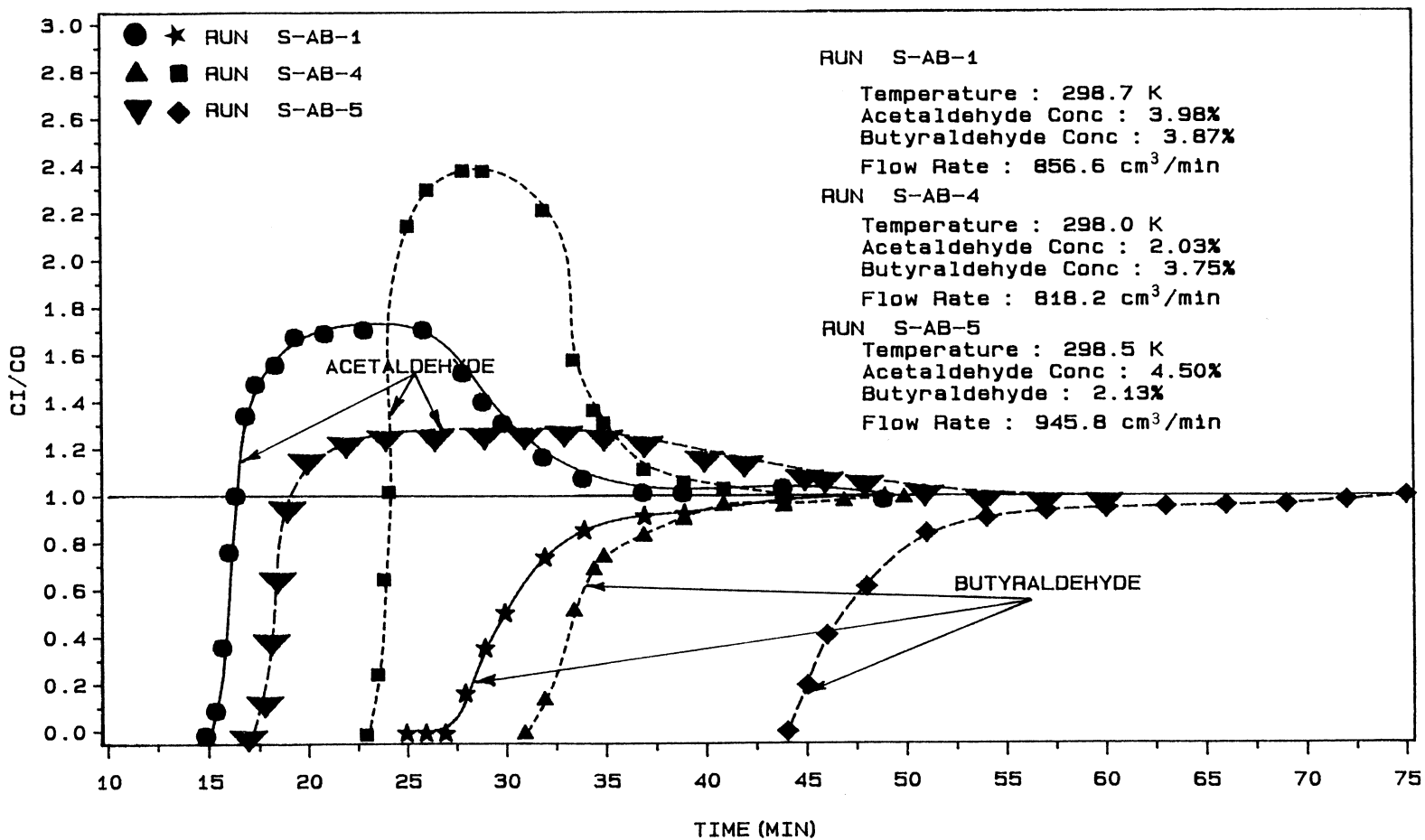


Figure 11. Effects of Inlet Concentration on Breakthrough Curves for Acetaldehyde and Butyraldehyde in their Binary Mixtures in a Silica Gel Bed

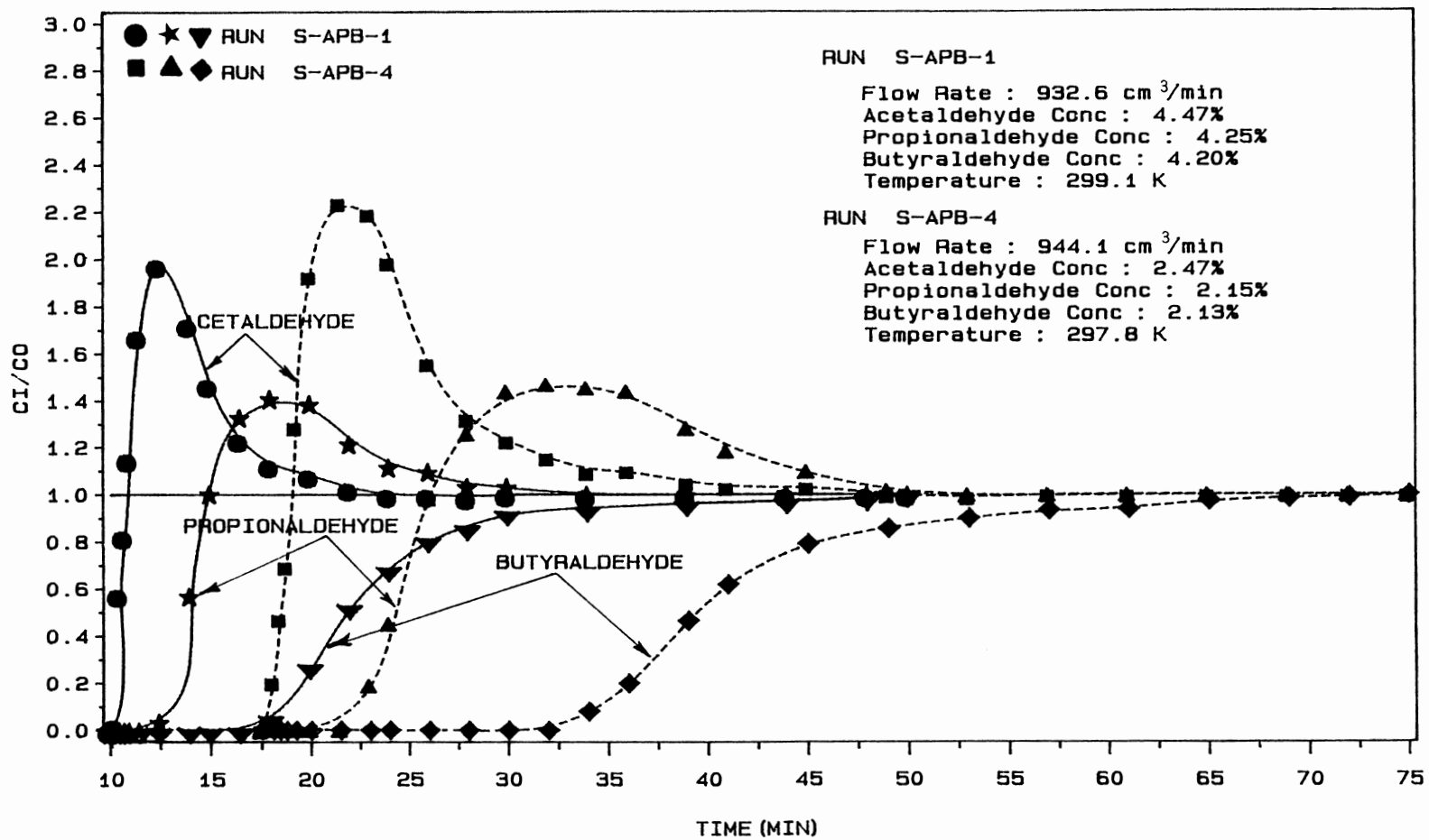


Figure 12. Effects of Inlet Concentration on Breakthrough Curves for Aldehydes in their Ternary Mixtures in a Silica Gel Bed

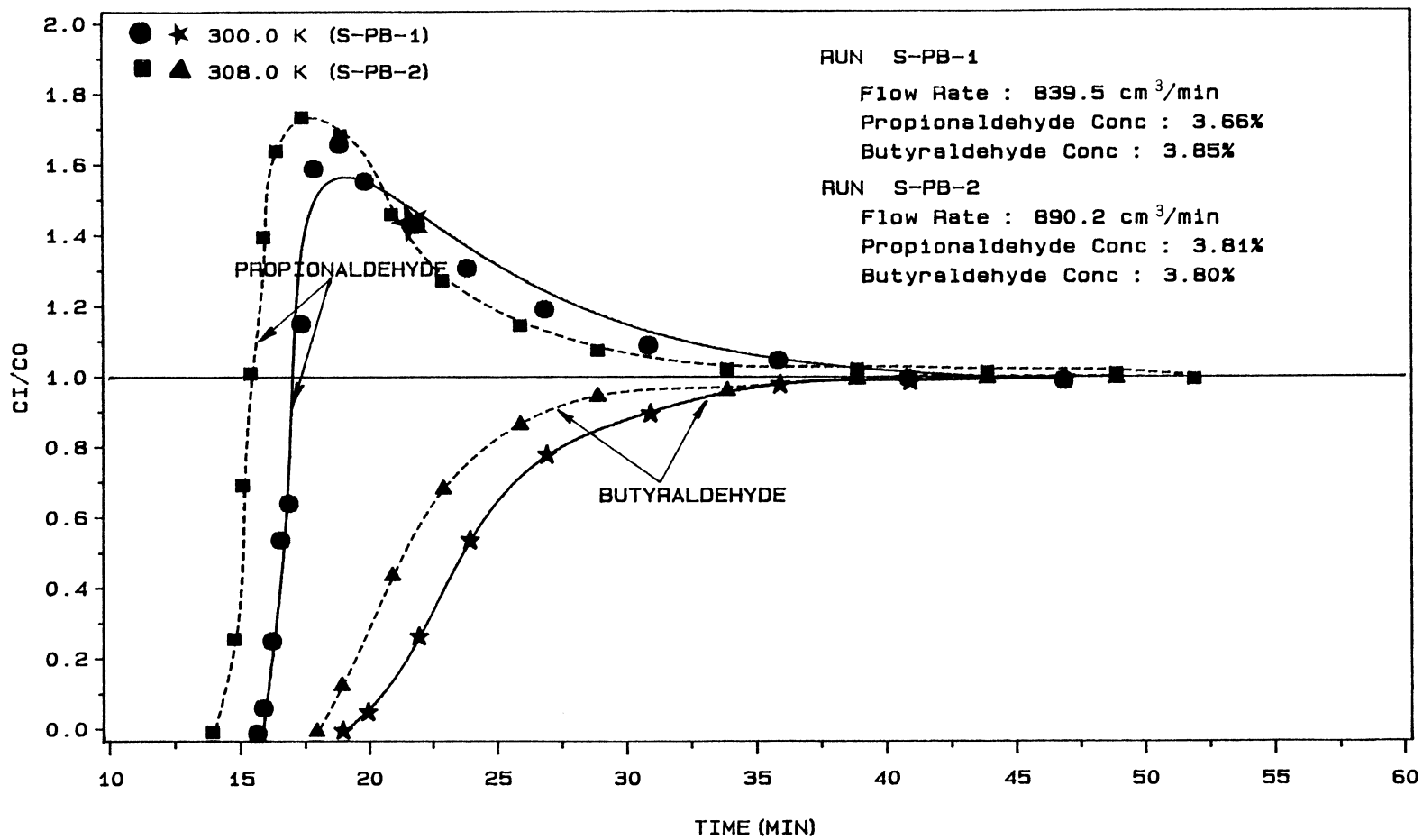


Figure 13. Effects of Temperature on Breakthrough Curves for Propionaldehyde and Butyraldehyde in their Binary Mixture in a Silica Gel Bed

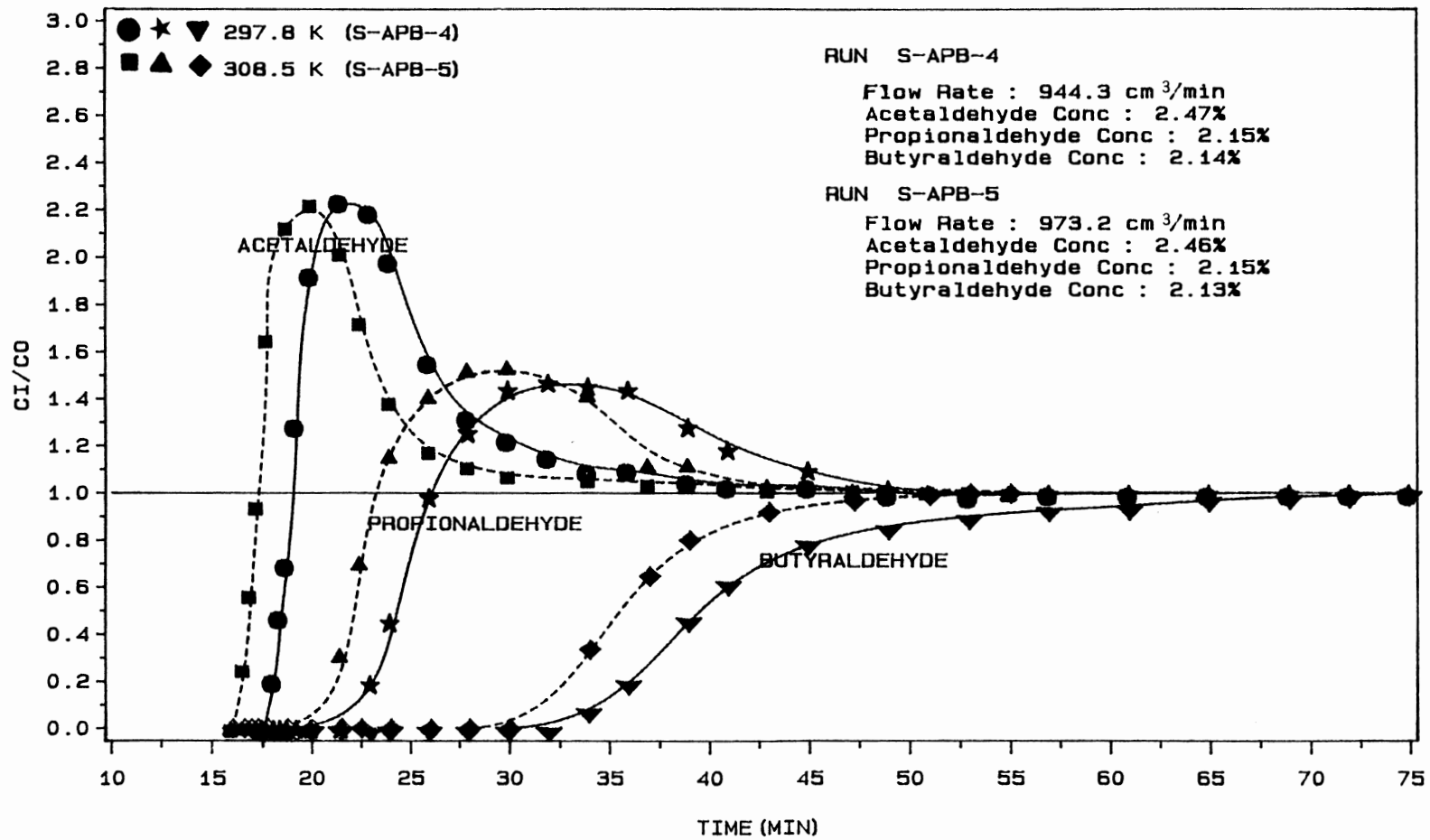


Figure 14. Effects of Temperature on Breakthrough Curves for Aldehydes in their Ternary Mixture in a Silica Gel Bed

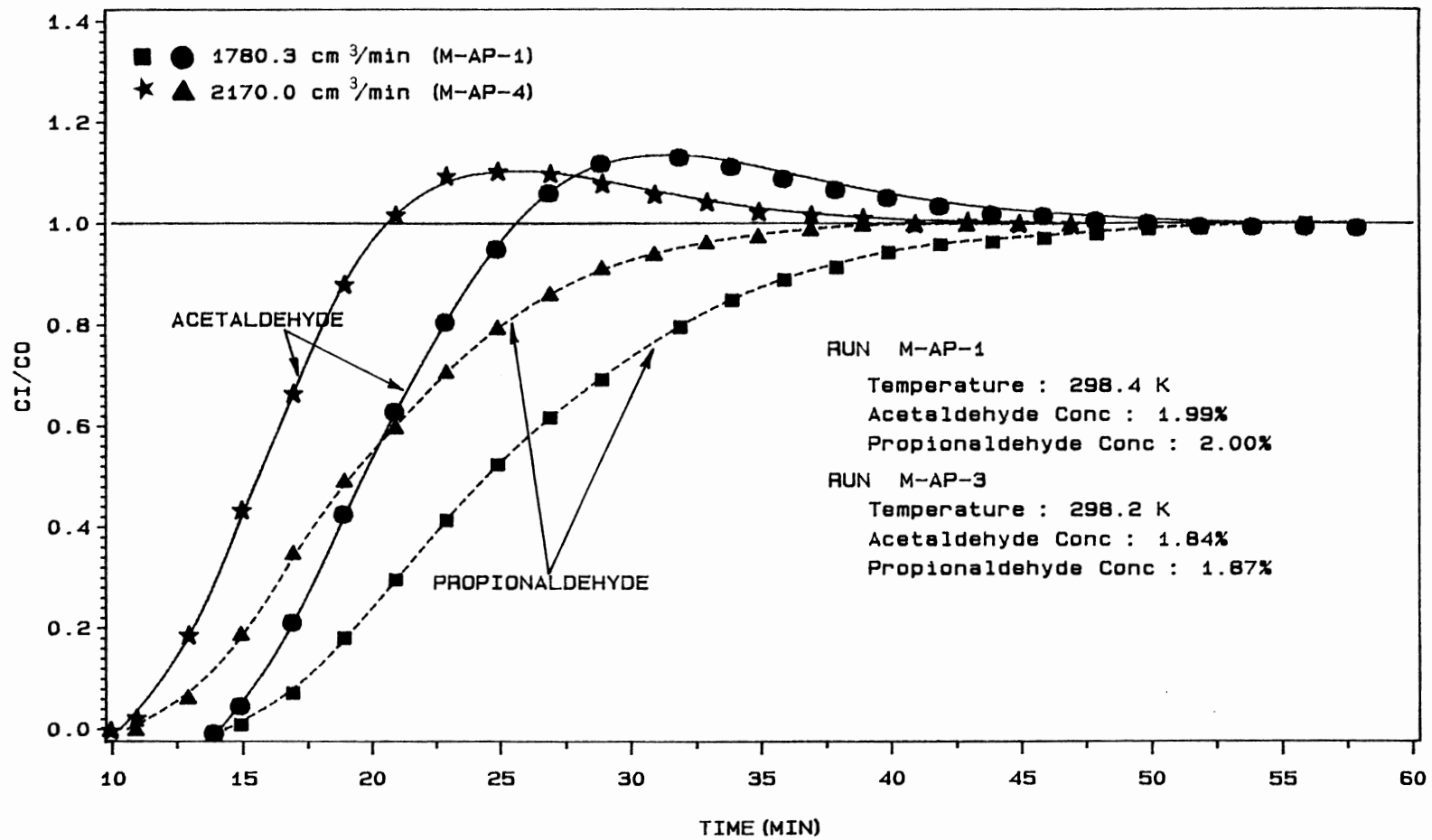


Figure 15. Effects of Flow Rate on Breakthrough Curves for Acetaldehyde and Propionaldehyde in their Binary Mixture in a Molecular Sieve-13X Bed

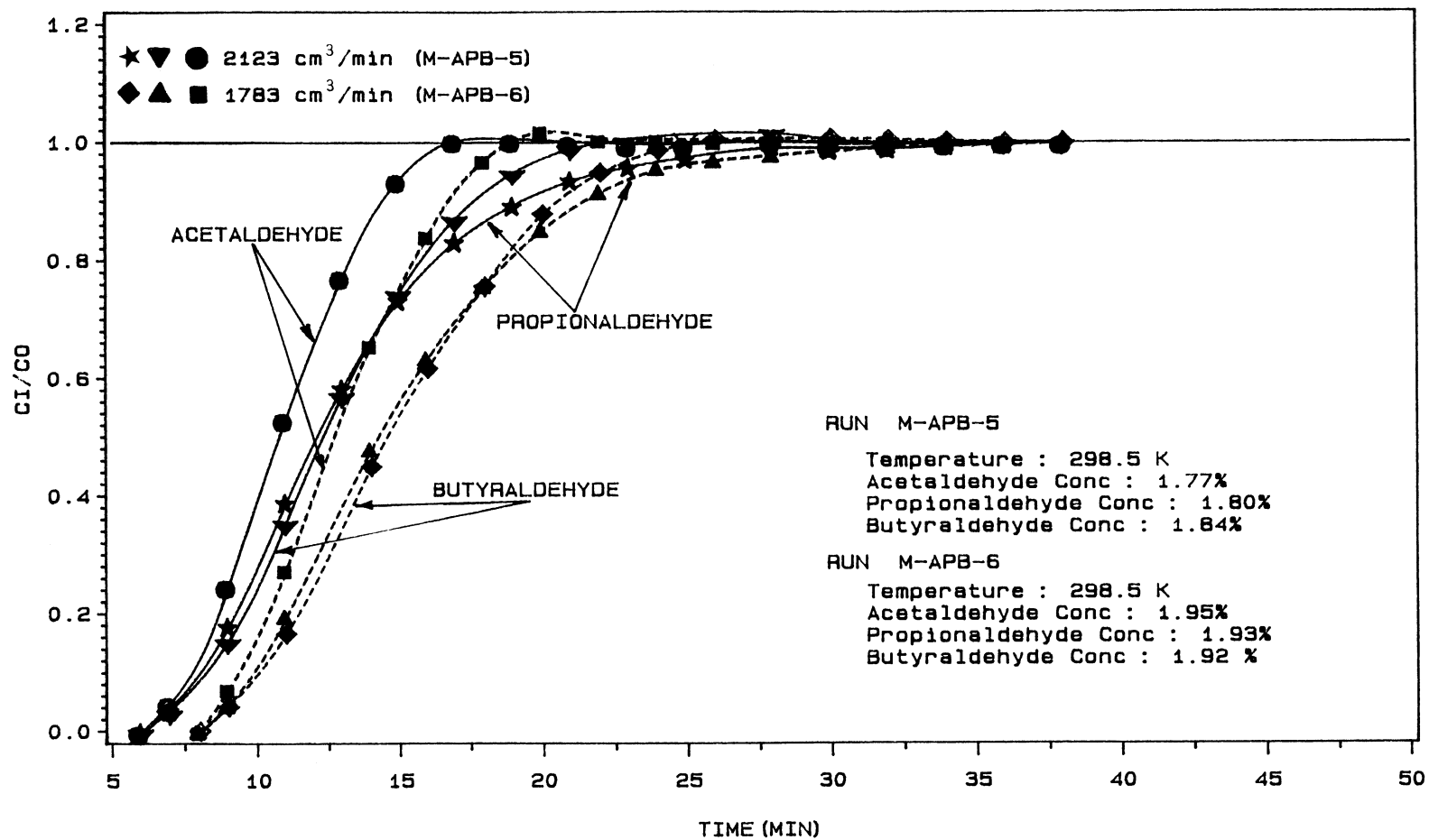


Figure 16. Effects of Flow Rate on Breakthrough Curves for Aldehydes in their Ternary Mixture in a Molecular Sieve-13X Bed

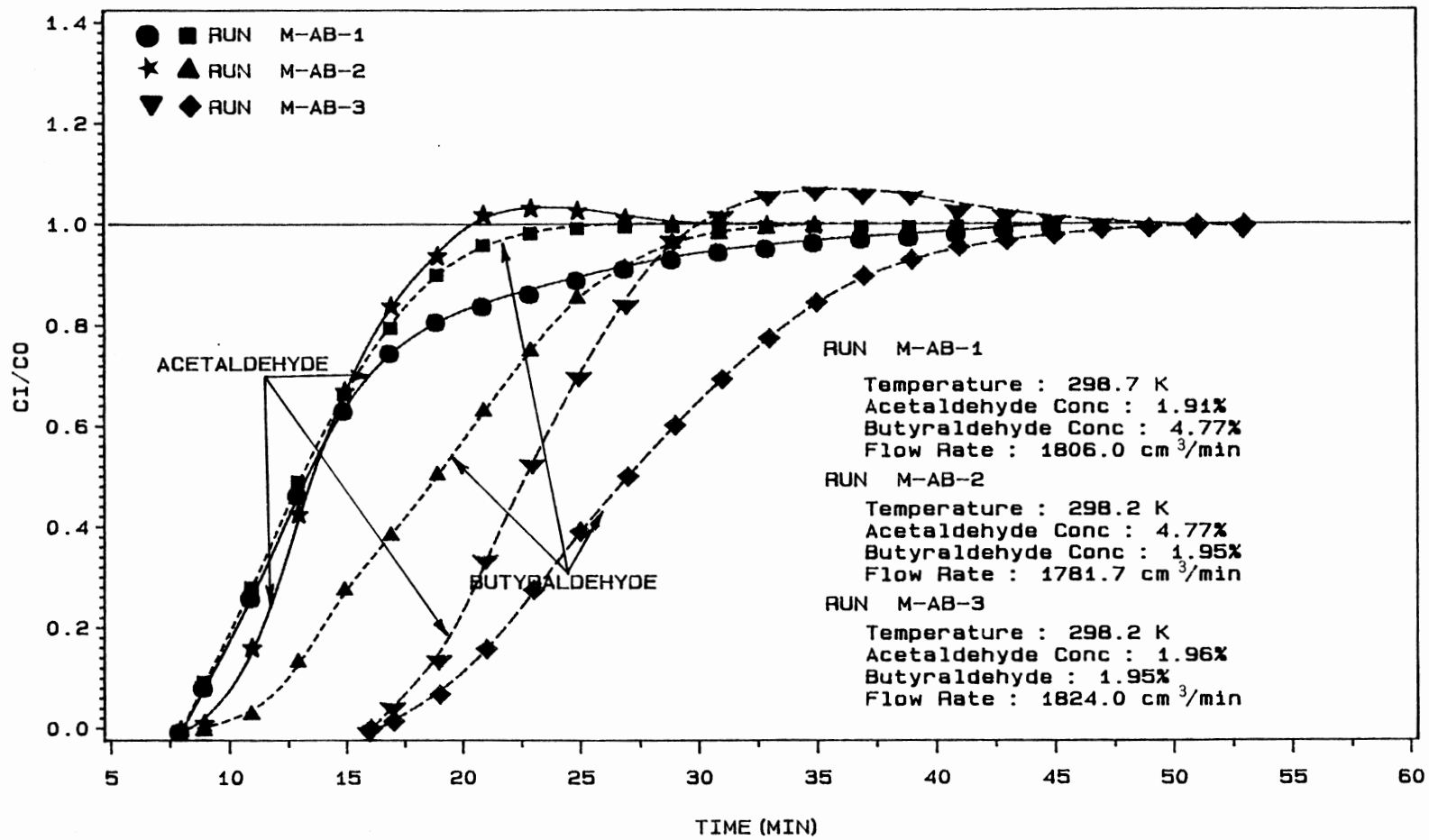


Figure 17. Effects of Inlet Concentration on Breakthrough Curves for Acetaldehyde and Butyraldehyde in their Binary Mixtures in a Molecular Sieve-13X Bed

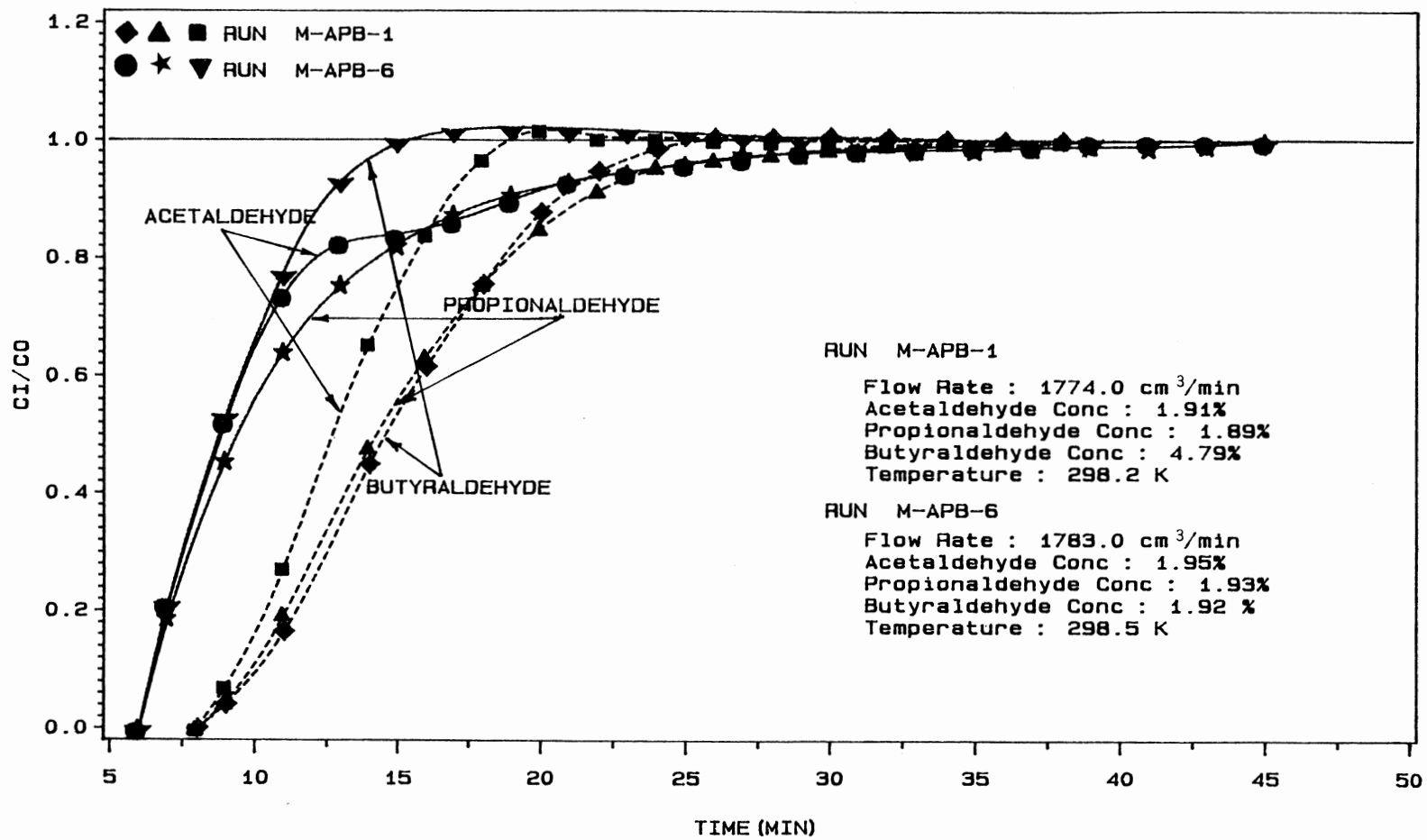


Figure 18. Effects of Inlet Concentration on Breakthrough Curves for Aldehydes in their Ternary Mixtures in a Molecular Sieve-13X Bed



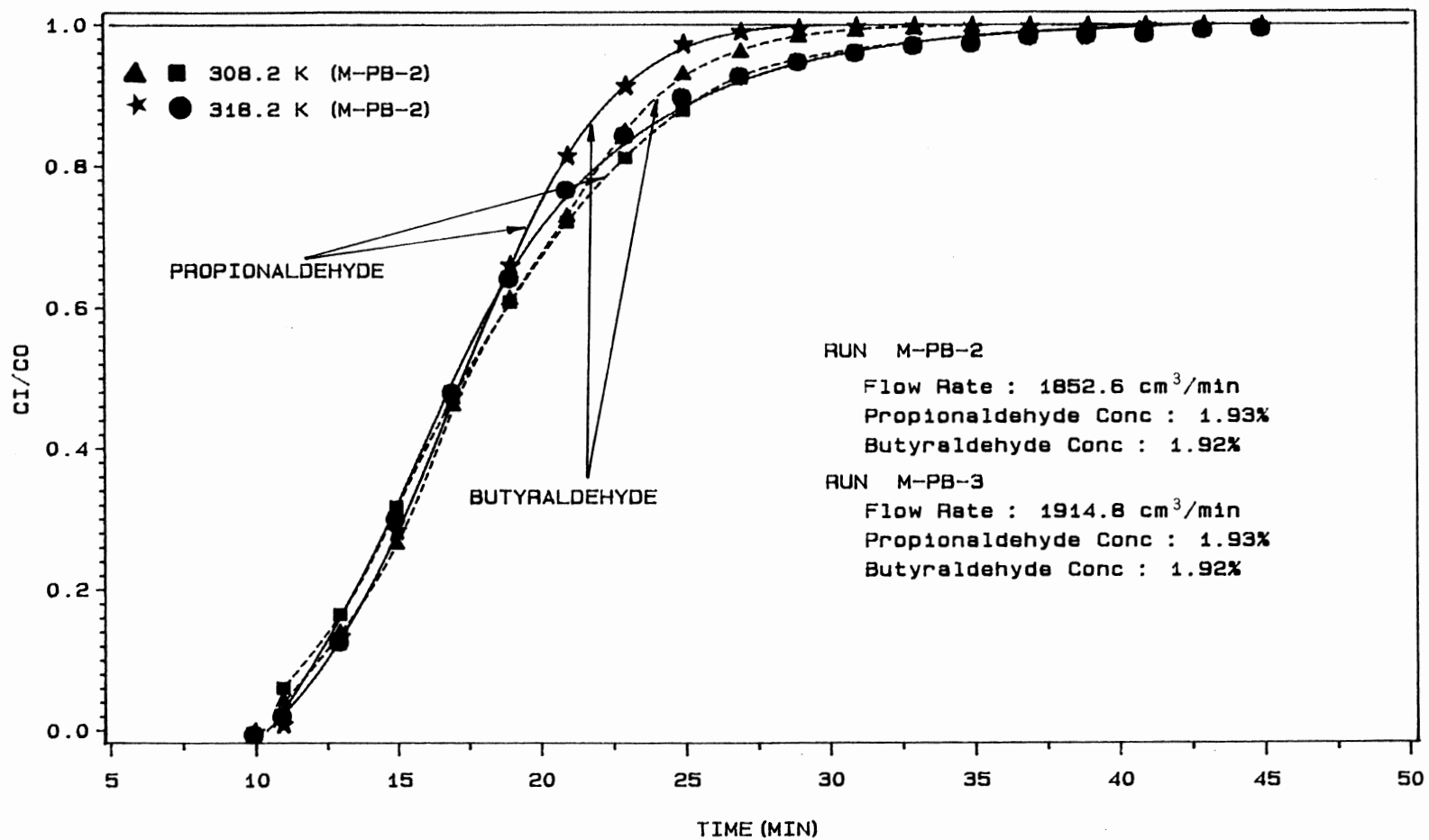


Figure 19. Effects of Temperature on Breakthrough Curves for Propionaldehyde and Butyraldehyde in their Binary Mixture in a Molecular Sieve-13X Bed

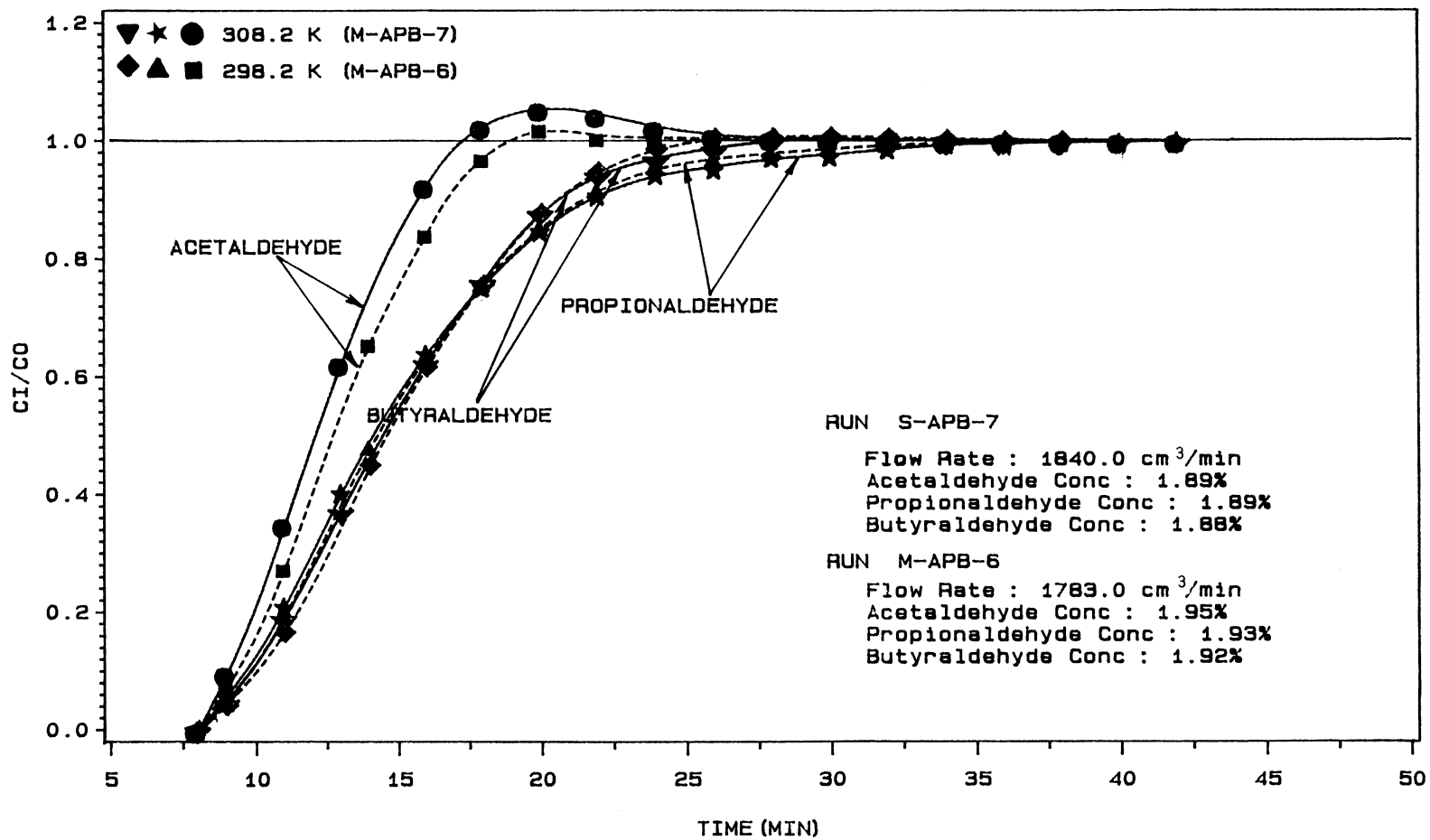


Figure 20. Effects of Temperature on Breakthrough Curves for Aldehydes in their Ternary Mixture in a Molecular Sieve-13X Bed

CHAPTER VI

CONCLUSIONS AND RECOMMENDATIONS

## CONCLUSIONS

The conclusions that can be drawn from the following study are summarized as follows :

1. Acetaldehyde, propionaldehyde, and butyraldehyde exhibited Type I isotherms on silica gel in the temperature range 282.0 to 308.2 K and gave hysteresis upon desorption. The adsorption isotherms of the same aldehydes on molecular sieve-13X appeared to be of Type I at higher temperature and were of Type II at lower temperature.

2. The heat of adsorption data of aldehydes on both the adsorbents suggested that the lateral interaction between the adsorbed molecule existed and the adsorbent surface was heterogeneous in nature.

3. The surface area covered by the aldehydes, calculated from the Langmuir equation was found to be consistently higher than the surface area estimated from the BET equation. Also, the aldehyde molecules occupied less surface than the total surface as measured by using  $N_2$  as adsorbate.

4. The isotherm equations for heterogeneous surfaces developed by Kuo and Hines and Sircar correlated the equilibrium data well for Type I isotherms, but gave a poor fit of the data for Type II isotherms when multilayer adsorption was more pronounced.

5. The energy distribution of a site was described by the combination of two probability density functions when multilayer adsorption was occurring. The new adsorption isotherm, developed based on above concept and using the

Jovanovic isotherm for multilayer coverage, provided excellent correlation for both Type I and Type II isotherms.

6. The mole fractions in the adsorbed phase predicted by the proposed method were in close agreement with the experimental data for hydrocarbon on activated carbon, but showed some deviation for the activity coefficient data.

7. A silica gel bed was more suitable for separation of aldehydes, however a molecular sieve bed could be used to remove the aldehydes together from a gas stream.

8. The lighter aldehydes were displaced by the heavier aldehydes from the adsorbent surfaces, as a consequence the gas phase concentrations of lighter aldehydes became higher than the inlet concentrations but eventually decreased to the inlet concentrations. The displacement of the lighter aldehydes by the heavier ones was more pronounced in the silica gel bed than was observed for molecular sieve.

### **RECOMMENDATIONS**

The following works are suggested for future study :

1. Attempt could be made to extend the proposed method to calculate the binary adsorption equilibria to ternary and higher mixtures.

2. The effects on the equilibrium uptake by the adsorbent particles when crushed to reduce its size should be studied.

## **APPENDICES**

## APPENDIX A

## CALCULATION FOR BUOYANCY EFFECTS ON WEIGHT MEASUREMENTS

The buoyancy effect on the sample weight in an electrobalance is given by

$$B = m (\rho_g / \rho_s) - (V_{cw} \rho_g + C) \quad (A-1)$$

where

B = buoyancy, g

m = mass of the sample, g

$\rho_g$  = density of vapor, g/cm<sup>3</sup>

$\rho_s$  = density of the sample, g/cm<sup>3</sup>

$V_{cw}$  = effective volume of counterweight, cm<sup>3</sup>

C = correction factor, g

In a typical experimental run for acetaldehyde-silica gel system when the system pressure is 130 mmHg, sample weight is 0.2476 g and temperature is 298.2 K, the above parameters have these values :

$$m = 0.2476 \text{ g}$$

$$\rho_s = 1.19 \text{ g/cm}^3$$

$$\rho_g = 3.0886 \times 10^{-4} \text{ g/cm}^3$$

$$V_{cw} = 0.2 \text{ cm}^3$$

$$C = 0$$

Therefore, the buoyance effect

$$\begin{aligned} B &= (0.2476) (3.0886 \times 10^{-4} / 1.19) - [(0.2) (3.0886 \times 10^{-4}) + 0] \\ &= 2.49 \times 10^{-6} \\ &= 0.001 \% \text{ of the sample weight} \end{aligned}$$

## APPENDIX B

## CALCULATION OF ISOTHERIC HEAT OF ADSORPTION

The isotheric heats of adsorption at a constant adsorbate loading were calculated from the following relationship :

$$\Delta H_{iso} = -R \left[ \frac{\partial (\ln P)}{\partial (1/T)} \right]_q \quad (B-1)$$

Therefore, a plot of  $\ln P$  as a function of  $(1/T)$  at constant adsorbate loading should yield a straight line. The slope of the straight line should provide the value of  $(\Delta H_{iso}/R)$ . A sample calculation for an acetaldehyde-silica gel system is shown below :

Loading (mmol/g)	P (mmHg)	lnP	T (K)	$1/T \cdot 10^3$ (K) <sup>-1</sup>
2.0429	1.65	0.501	287.0	3.484
	3.80	1.335	298.2	3.354
	6.00	1.792	306.5	3.263

A plot of above data along with other data is shown in Figure B.1. The slope of the straight line obtained from the above data set is -5880.95. Therefore the isotheric heat of adsorption is given by

$$\begin{aligned} \Delta H_{iso} &= -(-5880.95)(1.987) = 11,685 \text{ cal/gmol} \\ &= 11.685 \text{ kcal/gmol.} \end{aligned}$$



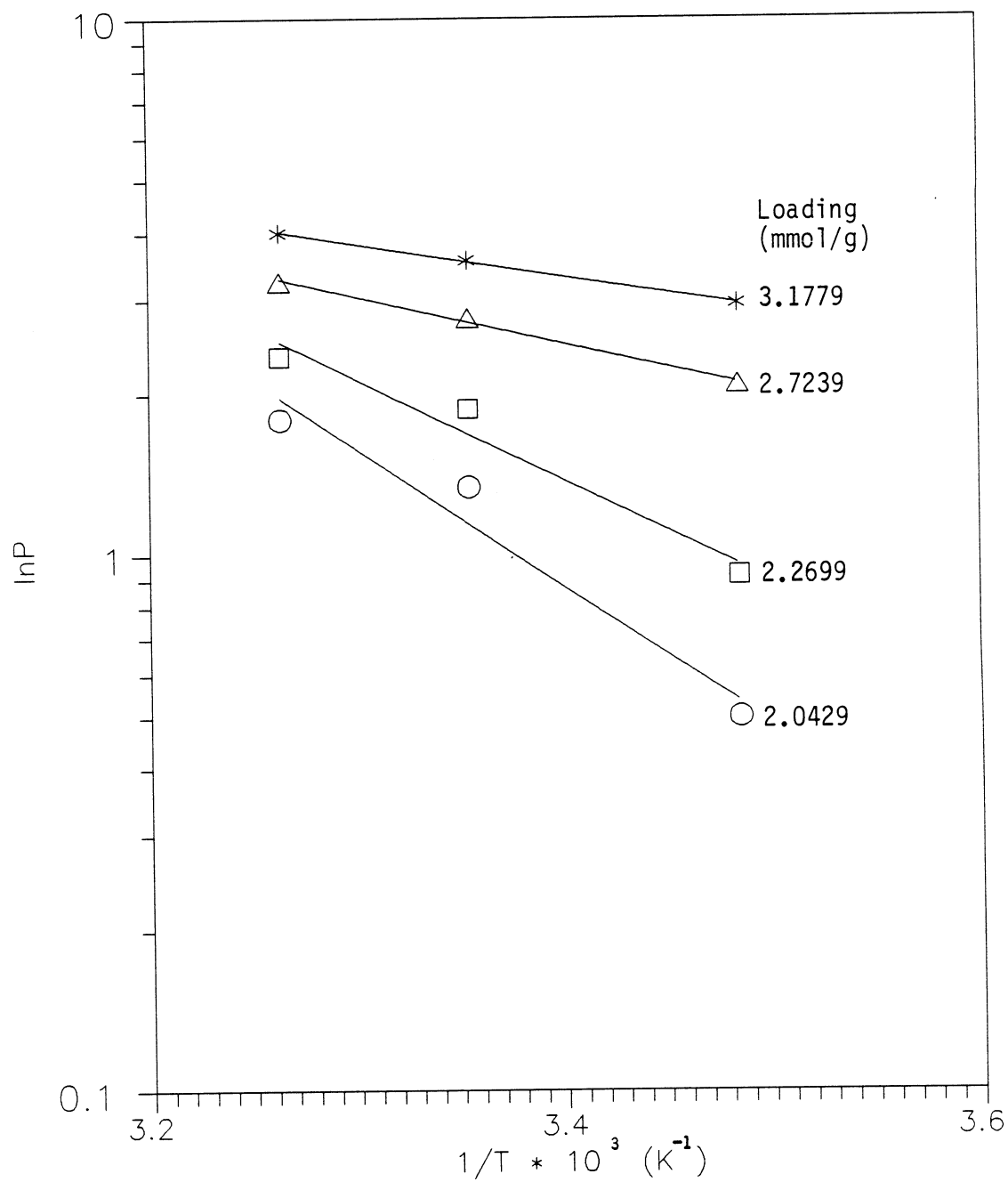


Figure B.1 Plots to Calculate Isoteric Heats of Adsorption at Different Loadings for Acetaldehyde-Silica Gel System

### APPENDIX C

#### PLOTS OF THE EXPERIMENTAL DATA ACCORDING TO THE LANGMUIR, THE BET, AND THE FREUNDLICH EQUATION

The Langmuir equation can be written as follows :

$$\frac{P}{q} = \frac{1}{q_m K} + \frac{P}{q_m} \quad (C-1)$$

The terms  $q_m$ , and  $K$  are defined earlier in the text.

According to Equation (C-1), a plot of  $P/q$  as a function of  $P$  should yield a straight line. One such plot for acetaldehyde-silica gel system is shown in Figure C.1. As can be seen from this plot that the experimental data can not be correlated according to the Langmuir model. The data can be better correlated by two straight lines, one for the low pressure data and one for the high pressure data. The slope and intercept obtained from the straight line corresponding to the low pressure data was later used used to calculate the monolayer coverages and surface areas, and is described in Appendix D.

The BET equation can be written as follows :

$$\frac{P}{q(P_s - P)} = \frac{1}{q_m C} + \frac{(C-1)P}{Cq_m P_s} \quad (C-2)$$

The constants,  $q_m$  and  $C$ , are defined earlier in the text. From Equation (C-2) it can be see, that if  $P/q(P_s - P)$  is plotted as a function of  $P/P_s$ , a straight should be obtained if the experimental data can be correlated according to the BET equation. A sample plot for the butyraldehyde-silica gel

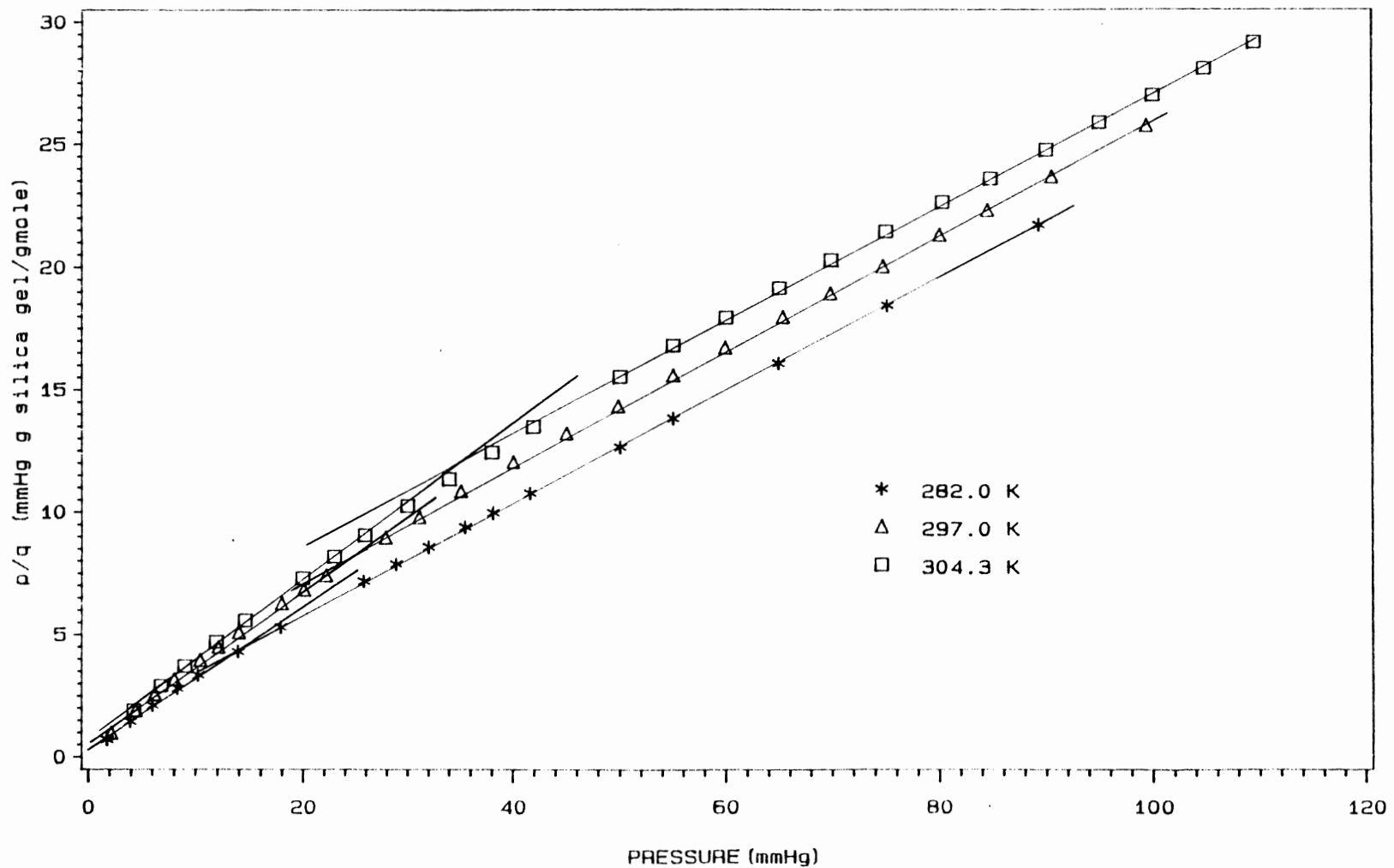


Figure C.1 The Langmuir Plots for Propionaldehyde-Silica Gel System.

system is presented in Figure C.2. As shown in the figure, a good correlation was obtained in the relative pressure range of  $0.05 \leq P/P_g \leq 0.25$ . This is the typical range within which the BET equation provides a good fit to the data. The slope and intercept obtained from such a plot are later used to estimate the BET surface area of adsorbents.

The Freundlich equation is given by

$$q = a(P)^b \quad (C-3)$$

where  $a$  and  $b$  are constants. A plot of  $\ln q$  versus  $\ln P$  in a log-log scale should result in a straight line. One such plot for butyraldehyde-molecular sieve-13X system is shown in Figure C.3. Highest deviation of the data point occurred in the high pressure region. In general the Freundlich equation provided a better fit to the experimental data than did the Langmuir and the BET equation. A comparison of these models are presented in Chapter I and II.

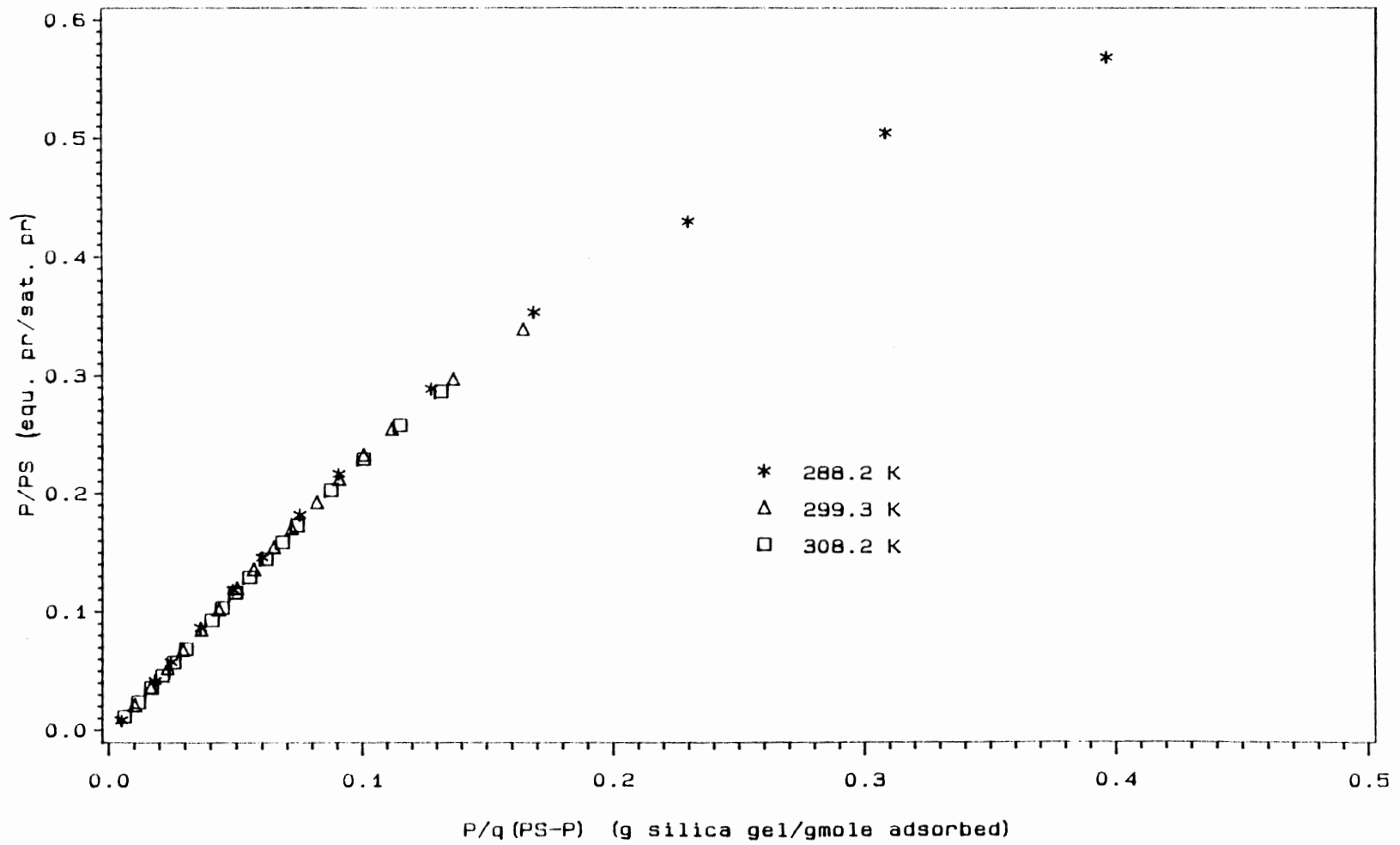


Figure C.2 The BET Plots for Butyraldehyde-Silica Gel System

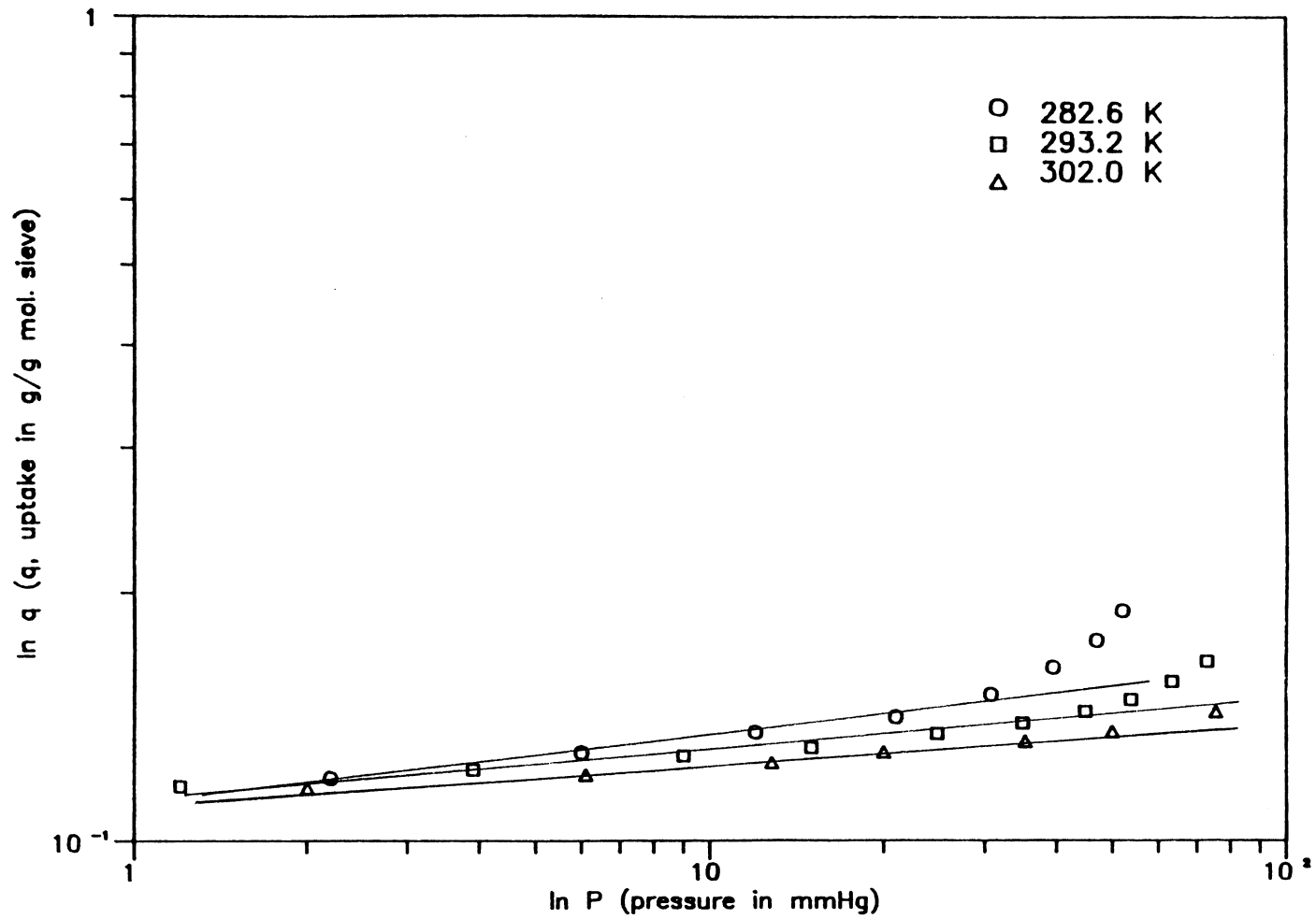


Figure C.3 The Freundlich Plots for Butyraldehyde-Molecular Sieve System

## APPENDIX D

CALCULATION OF MONOLAYER COVERAGES AND SURFACES AREAS  
FROM EQUILIBRIUM ISOTHERM DATA

The monolayer coverages and surface areas of silica gel and molecular sieve-13X are estimated by using adsorption data of aldehydes. According to the Langmuir and the BET equations, the term  $q_m$  (in both equations) is the monolayer adsorption capacity of the adsorbates on the adsorbent surface. The data used in calculation of monolayer coverage and surface area are given in Table D.I.

**Monolayer Coverages and Surface Area from the Langmuir Model**

From the slope and intercept of the straight line obtained from the Langmuir plots, the values of  $q_m$  and  $K$  can be estimated as follows. The numerical values are calculated from a acetaldehyde-silica gel system at 298.2 K.

$$\text{slope, } 1/q_m = 0.2525$$

$$\text{intercept, } K = 1.7037$$

$$\text{Monolayer coverage, } q_m = 3.9604 \text{ mmol/g} = 88.71 \text{ cm}^3/\text{g solid}$$

The projected area of a molecule on the surface can be calculated from the following expression, assuming closed hexagonal packing

$$\alpha = 1.091 \left\{ \frac{M}{N_o \rho} \right\}^{2/3} \quad (\text{D-1})$$

where  $\alpha$  is the projected area,  $M$  is the molecular weight of adsorbate,  $N_o$  is the Avogadro's number, and  $\rho$  is the density

Table D.I Data for Calculation of Monolayer Coverage and Surface Area of Silica Gel Occupied by Acetaldehyde at 298.2 K

No	P	P/q	P/q(P <sub>s</sub> -P)	P/P <sub>s</sub>
1	1.9	1.124	0.12517E-02	0.21097E-02
2	6.0	2.696	0.30146E-02	0.66621E-02
3	10.0	4.004	0.44964E-02	0.11103E-01
4	14.3	5.338	0.60230E-02	0.15878E-01
5	18.0	6.446	0.73036E-02	0.19986E-01
6	22.8	7.846	0.89385E-02	0.25316E-01
7	26.3	8.776	0.10038E-01	0.29202E-01
8	30.0	9.716	0.11161E-01	0.33310E-01
9	35.4	11.138	0.12873E-01	0.39306E-01
10	40.0	12.322	0.14317E-01	0.44414E-01
11	45.1	13.515	0.15797E-01	0.50077E-01
12	50.8	14.819	0.17438E-01	0.56406E-01
13	55.0	15.732	0.18604E-01	0.61069E-01
14	60.0	16.781	0.19963E-01	0.66621E-01
15	65.0	17.840	0.21349E-01	0.72172E-01
16	70.2	18.971	0.22845E-01	0.77946E-01
17	75.0	19.902	0.24106E-01	0.83276E-01
18	80.0	20.976	0.25561E-01	0.88828E-01
19	90.2	22.967	0.28340E-01	0.10015
20	100.0	24.747	0.30910E-01	0.11103
21	110.0	26.624	0.33674E-01	0.12214
22	120.5	28.446	0.36464E-01	0.13380

Pressure in mmHg, q in mmol/g



of liquid adsorbate.

Once the projected area,  $\alpha$ , is known, the surface area can be calculated from the following equation

$$S = \frac{V_m N_O}{V_S} \alpha \quad (D-2)$$

where  $S$  is surface area,  $V_m$  is monolayer coverage in  $\text{cm}^3/\text{g}$  of solid, and  $V_S$  is the standard volume at STP. For the system mentioned above the values of projected area and surface area are

$$\alpha = 1.091 \left[ \frac{44.04}{(6.023 \cdot 10^{23}) (0.7714)} \right]^{2/3} = 2.267 \cdot 10^{-15}$$

and,

$$\begin{aligned} S &= \frac{(88.71) (6.023 \cdot 10^{23})}{22,400} (2.267 \cdot 10^{-15}) \\ &= 5.41 \cdot 10^6 \text{ cm}^2/\text{g} = 541 \text{ m}^2/\text{g} \end{aligned}$$

#### **Monolayer Coverage and Surface Area from the BET Model**

The straight line obtained from the BET plot for acetaldehyde-silica gel system at 298.2 K provided the following values of slope and intercept :

$$\text{slope} = 0.2522$$

$$\text{intercept} = 0.0029$$

$$C = (\text{slope} + \text{intercept}) / \text{intercept} = 87.965$$

$$q_m = 1.0 / (C \times \text{intercept}) = 3.92 \text{ mmol/g} = 87.8087 \text{ cm}^3/\text{g}$$

The surface area calculated using Equations (D-1) and (D-2) is given below

$$S = \frac{(87.81) (6.023 \cdot 10^{23})}{22,400} (2.267 \cdot 10^{-15})$$
$$= 5.35 \cdot 10^6 \text{ cm}^2/\text{g} = 535 \text{ m}^2/\text{g}$$

## APPENDIX E

ESTIMATION OF THE CONSTANTS IN THE KUO-HINES  
AND THE SIRCAR MODEL

The Kuo-Hines equation can be written as

$$q = m \left[ 1 - \frac{K_3}{K_3 - K_1 K_3} \left\{ \frac{K_1}{P + K_1} - \frac{K_1 K_2}{P + K_3} \right\} \right] \quad (\text{E-1})$$

and Henry's Law constant is given by

$$K_L = m \left[ \frac{K_3^2 - K_1^2 K_2}{K_1 K_3 (K_3 - K_1 K_2)} \right] \quad (\text{E-2})$$

Equation (E-2) can be rearranged as follow

$$K_2 = \frac{(K_L K_1 - m) K_3^2}{K_L K_1 K_3 - m K_1^2} \quad (\text{E-3})$$

A trial and error procedure was used to obtain the best fit parameters. A value of  $m$  was chosen and  $K_2$  was calculated from Equation (E-3) for a value of  $K_1$ . As mentioned in the text  $K_3$  was set to unit pressure. The entire isotherm was generated for these values of  $m$ ,  $K_1$ , and  $K_2$ . If the calculated isotherm was not within  $\pm 2\%$ , a new value of  $m$  was chosen and the procedure was repeated. A sample calculation is shown below for acetaldehyde-silica gel system at 298.2 K.

$$K_L = 2.51 \text{ mmol/g mmHg}$$

$$K_3 = 1 \text{ mmHg}$$

$$m = 6.51 \text{ mmol/g}$$

$$K_2 = -0.004$$

$$K_1 = 154.1 \text{ mmHg}$$

Therefore, Equation (E-1) becomes

$$q = 6.51 \left[ 1 - 0.6186 \left\{ \frac{154.1}{P+154.1} + \frac{0.004}{P+1} \right\} \right]$$

The values of  $q$  at different pressure are given below

<u>P(mmHg)</u>	<u>q(mmol/g)</u>
1.90	1.676
6.00	2.280
10.00	2.503
30.00	3.060
40.00	3.253

The isotherm equation proposed by Sircar can be expressed as

$$q = m \left\{ 1 - \theta e^{\theta E_{n+1}(\theta)} \right\} \quad n = 0, 1, 2, \dots \quad (\text{E-4})$$

$$\theta = \frac{\alpha}{P} \quad (\text{E-5})$$

$$K_L = \frac{(n+1)m}{\alpha} \quad (\text{E-6})$$

Equation (E-6) can be rearranged as below

$$\alpha = (n+1)m/K_L \quad (\text{E-7})$$

The best fit parameters of Sircar's equation are obtained by trial and error. First,  $n$  was set to a integer value, say, zero. A value of  $m$  was chosen to calculate  $\alpha$  from Equation (E-7),  $\theta$  was obtained from Equation (E-5) and next integral exponent  $E_{n+1}(\theta)$  was obtained from a Handbook of Mathematical Functions and  $q$  was calculated from Equation (E-4) for each pressure. A numerical example is shown below

$$K_L = 12.0 ; \quad m = 3.00 ; \quad n = 0 ; \quad \alpha = 0.25$$

<u>P</u>	<u><math>\theta</math></u>	<u><math>E_{n+1}(\theta)</math></u>	<u>q</u>
3.20	0.07810	0.17300	2.481
6.00	0.04170	0.11470	2.666
25.00	0.01000	0.04070	2.850
35.00	0.00714	0.03140	2.905
75.00	0.00333	0.01715	2.948

## APPENDIX F

## CALCULATION FOR ENERGY DISTRIBUTION FUNCTION

The energy distribution on an adsorbent surface is described by the following function (See Chapter III for derivation).

$$f\left(\frac{q_A}{RT}, \frac{q_B}{RT}\right) = \frac{A_1 A_3}{A_3 - A_1 A_2} \left\{ \exp(-A_1 \epsilon_A) - A_2 \exp(-A_3 \epsilon_A) \right\} (\epsilon_A + a_0) \left\{ \frac{\epsilon_B - b_0}{\epsilon_M} \right\} \quad (\text{F-1})$$

and

$$\epsilon_A = b_0 [\exp(q_A/RT) - 1] \quad (\text{F-2})$$

The energy distribution on the adsorbent surface in  $q_A/RT$  domain are obtained by keeping other parameters constant. The fixed values of these parameters are given below :

$$\epsilon_M = 0.50 ; A_2 = -50.0 ; q_B = 0.0 ; b_0 = 0.25$$

Calculation of energy distribution proceeded as follows. A value of  $A_1$  was chosen and next  $\epsilon_A$  was calculated for different values of  $q_A/RT$  from Equation (F-2). Finally, energy distribution was calculated from Equation (F-1). Numerical values are given below for  $A_1$  equal to 0.3 :

<u><math>q_A</math></u>	<u><math>\epsilon_A</math></u>	<u><math>f(q_A/RT, q_B/RT)</math></u>
0.00	0.0000	$4.7812 \cdot 10^{-5}$
5.00	$1.4741 \cdot 10^{-2}$	$6.9935 \cdot 10^{-3}$
10.00	2.2025	0.1248

## APPENDIX G

## PROPERTIES OF THE NEW ISOTHERM EQUATION AND CALCULATION OF THE HENRY'S LAW CONSTANT FROM THE NEW ISOTHERM

New isotherm equation is given by

$$N(P, T) = \theta_m \left\{ 1 - \frac{A_1 A_3}{A_3 - A_1 A_2} \left( \frac{1}{A_1 + P} - \frac{A_2}{A_3 + P} \right) \right\} \frac{\exp(-b_0 P)}{\epsilon_M^P} \left\{ \exp(\epsilon_M^P) - 1 \right\} \quad (G-1)$$

The term  $\exp(\epsilon_M^P)$  can be expanded in a power series as follows :

$$\exp(\epsilon_M^P) = 1 + \epsilon_M^P + \frac{(\epsilon_M^P)^2}{2!} + \frac{(\epsilon_M^P)^3}{3!} + \dots \quad (G-2)$$

Therefore,

$$\frac{\exp(\epsilon_M^P) - 1}{\epsilon_M^P} = 1 + \frac{(\epsilon_M^P)}{2!} + \frac{(\epsilon_M^P)^2}{3!} + \dots \quad (G-3)$$

Hence, Equation (G-1) can be written as :

$$N(P, T) = \theta_m \left\{ 1 - \frac{A_1 A_3}{A_3 - A_1 A_2} \left( \frac{1}{A_1 + P} - \frac{A_2}{A_3 + P} \right) \right\} \exp(-b_0 P) \left\{ 1 + \frac{(\epsilon_M^P)}{2!} + \frac{(\epsilon_M^P)^2}{3!} + \dots \right\} \quad (G-4)$$

For  $P \rightarrow 0$

$$N(P, T) = \theta_m \left\{ 1 - \frac{A_1 A_3}{A_3 - A_1 A_2} \left( \frac{1}{A_1} - \frac{A_2}{A_3} \right) \right\} \exp(0) \left\{ 1 + 0 + 0 + \dots \right\} \quad (G-5)$$

$$= 0$$

For  $\epsilon_M - b_0 > 0$  and as  $p \rightarrow \infty$ , Equation (G-1) is rearranged as follow

$$N(P, T) = \theta_m \left\{ 1 - \frac{A_1 A_3}{A_3 - A_1 A_2} \left( \frac{1}{A_1 + P} - \frac{A_2}{A_3 + P} \right) \right\} \left( \frac{\exp[(\epsilon_M - b_0)P]}{\epsilon_M^P} - \frac{\exp(-b_0 P)}{\epsilon_M^P} \right) \quad (G-6)$$

or,

$$N(P, T) \Big|_{\lim P \rightarrow \infty} \rightarrow \theta_m (1-0) \left( \frac{\infty}{\infty} - \frac{\infty}{\infty} \right) \quad (G-7)$$

by applying La Hopital' rule it can be shown that

$$N(P, T) \Big|_{\lim P \rightarrow \infty} \rightarrow \theta_m \cdot \infty \rightarrow \infty \quad (G-8)$$

### Henry's Law Constant

The Henry's Law constant is defined as

$$\frac{\partial N(P, T)}{\partial P} \Big|_T \lim P \rightarrow 0 = K_L \quad (G-9)$$

The derivative of Equation (G-4) with respect to P is given by

$$\begin{aligned} \frac{\partial N}{\partial P} = & \frac{\partial}{\partial P} \left[ \theta_m \left\{ 1 - \frac{A_1 A_3}{A_3 - A_1 A_2} \left( \frac{1}{A_1 + P} - \frac{A_2}{A_3 + P} \right) \right\} \right] \cdot \left( \frac{\exp[(\epsilon_M - b_0)P]}{\epsilon_M^P} - \frac{\exp(-b_0 P)}{\epsilon_M^P} \right) \\ & + \frac{\partial}{\partial P} \left( \frac{\exp[(\epsilon_M - b_0)P]}{\epsilon_M^P} - \frac{\exp(-b_0 P)}{\epsilon_M^P} \right) \cdot \left[ \theta_m \left\{ 1 - \frac{A_1 A_3}{A_3 - A_1 A_2} \left( \frac{1}{A_1 + P} - \frac{A_2}{A_3 + P} \right) \right\} \right] \end{aligned} \quad (G-10)$$

After taking derivatives and applying La Hopital's rule to the exponential terms at limit  $P \rightarrow 0$ ,



$$\frac{\partial N}{\partial P} = \left[ \theta_m \left\{ \frac{A_3^2 - A_1 A_2^2}{A_1 A_3 (A_3 - A_1 A_3)} \right\} \right] \cdot \left\{ \frac{(\epsilon_M - b_O)}{\epsilon_M} - \frac{(-b_O)}{\epsilon_M} \right\}$$

$$+ \frac{\partial}{\partial P} \left\{ \frac{\exp[(\epsilon_M - b_O)P]}{\epsilon_M^P} - \frac{\exp(-b_O P)}{\epsilon_M^P} \right\} \cdot \left[ \theta_m \left\{ 1 - \frac{A_1 A_3}{A_3 - A_1 A_2} \left( \frac{1}{A_1 + P} - \frac{A_2}{A_3 + P} \right) \right\} \right]$$

(G-11)

or,

$$\frac{\partial N}{\partial P} = \left[ \theta_m \left\{ \frac{A_3^2 - A_1 A_2^2}{A_1 A_3 (A_3 - A_1 A_3)} \right\} \right] \equiv K_L$$

(G-12)

**APPENDIX H****EXPERIMENTAL DATA FOR BINARY AND TERNARY  
MIXTURES OF ALDEHYDES**

The experimental breakthrough curves for individual aldehydes in their binary and ternary mixtures are shown in Figures H.1 through H.18. In Figure H.19, the reproducibility of the equilibrium isotherm data are shown by plotting the data for butyraldehyde adsorption on silica gel at 288.2 K, obtained from two separate runs (Run no. 2 and 3). The experimental data in tabular form are presented in Table H.I through H.XX.

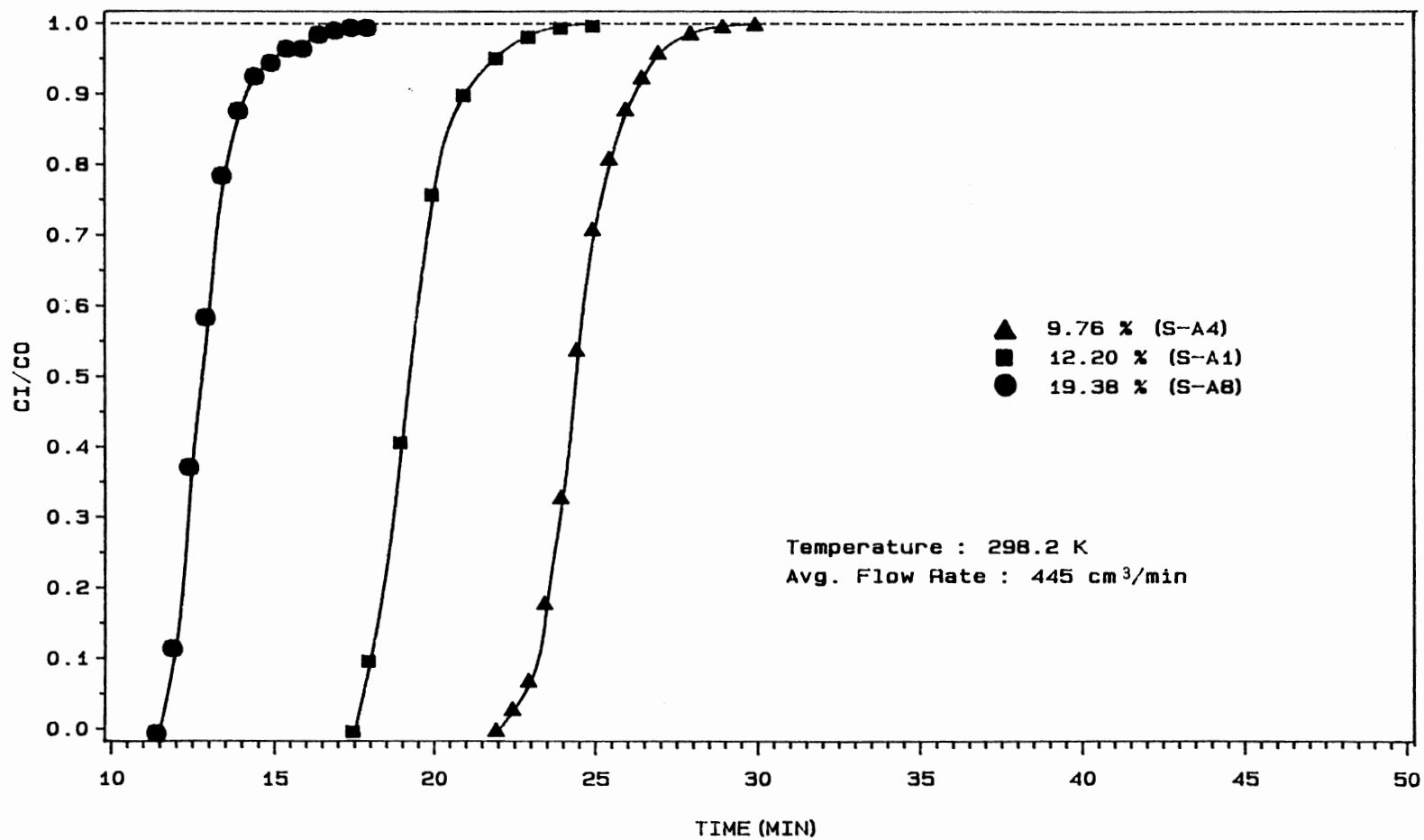


Figure H.1 Effects of Inlet Concentration on Breakthrough Curves for Acetaldehyde in a Silica Gel Bed

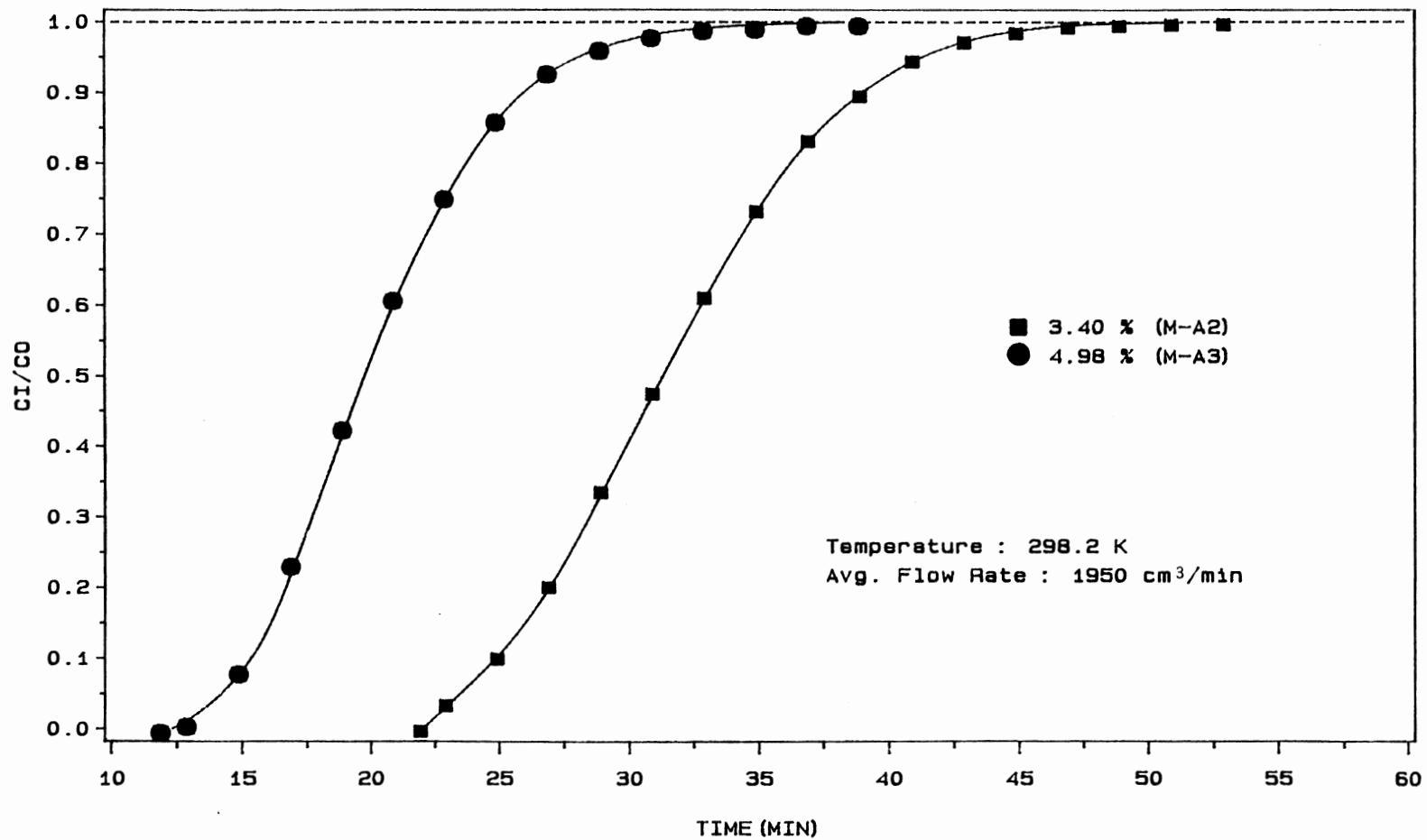


Figure H.2 Effects of Inlet Concentration on Breakthrough Curves for Acetaldehyde in a Molecular Sieve-13X Bed

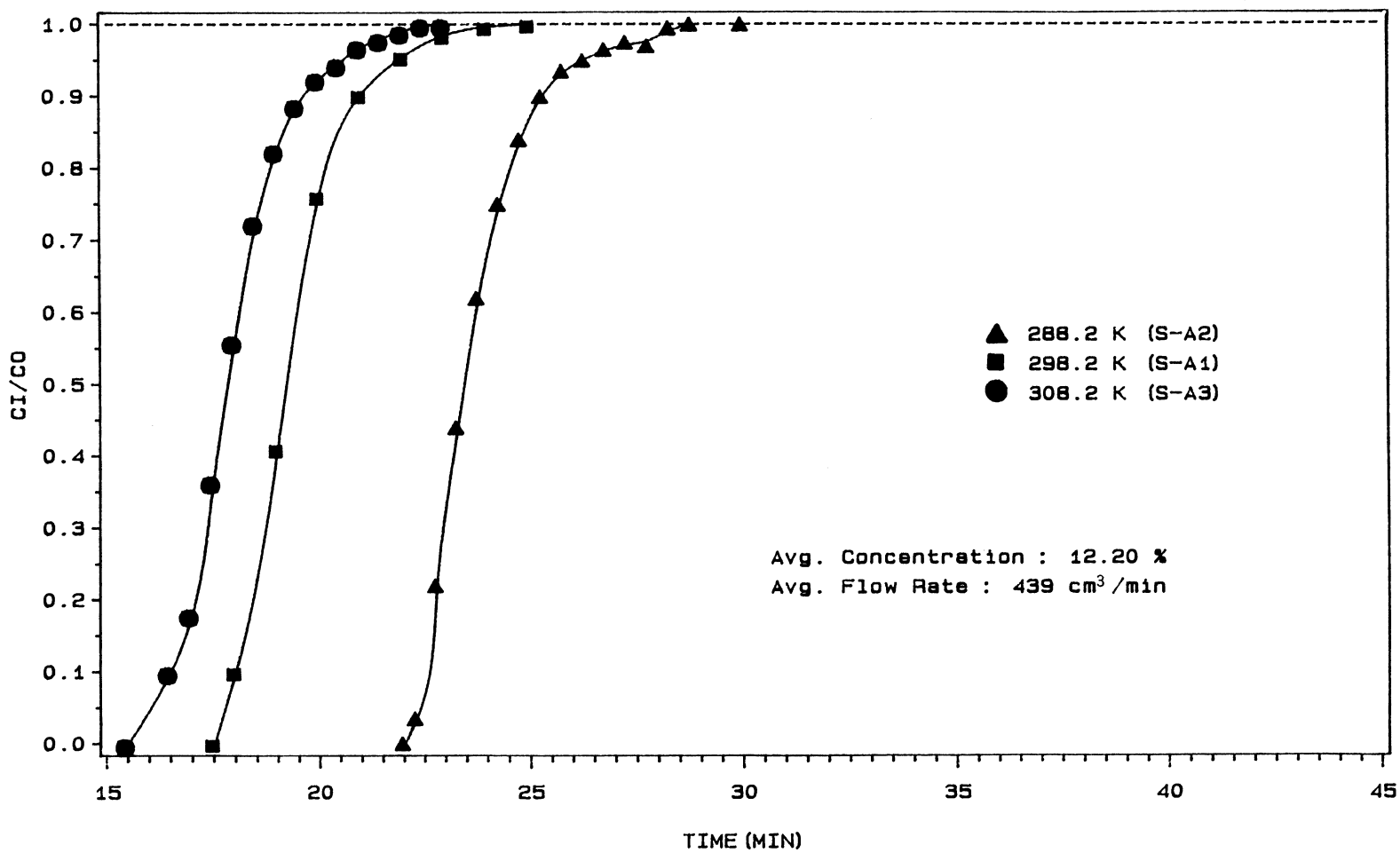


Figure H.3 Effects of Temperature on Breakthrough Curves for Acetaldehyde in a Silica Gel Bed

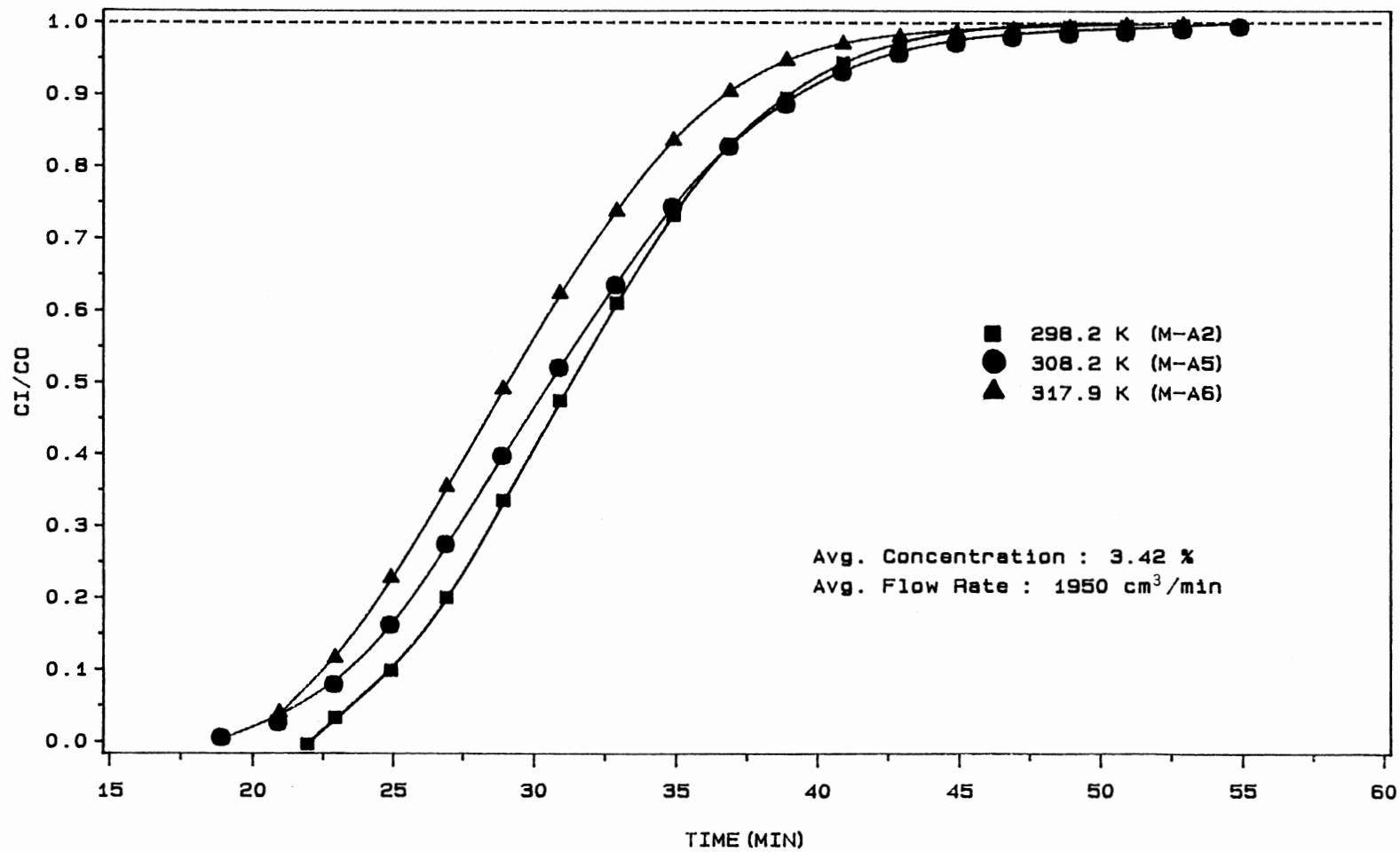


Figure H.4 Effects of Temperature on Breakthrough Curves for Acetaldehyde in a Molecular Sieve-13X Bed

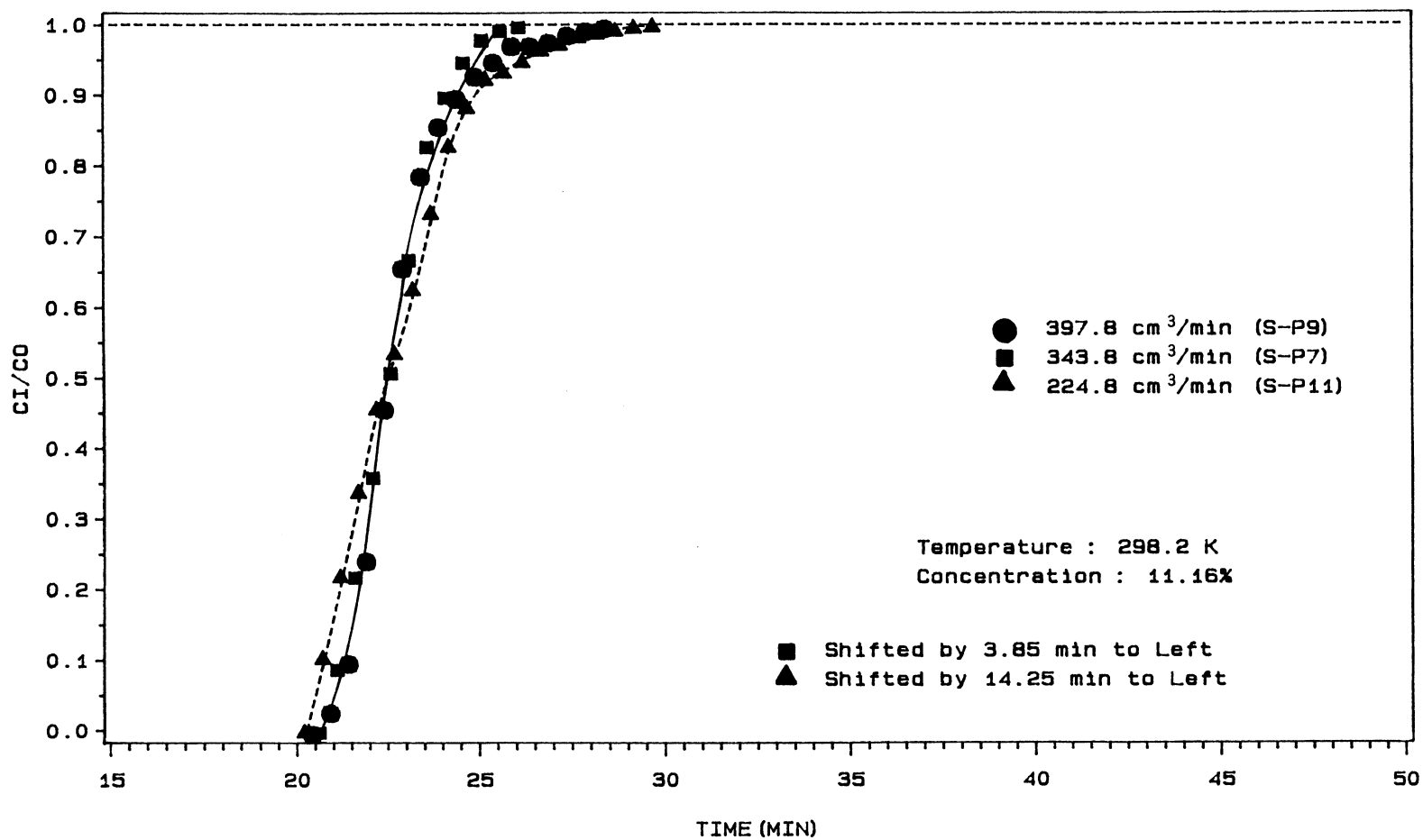


Figure H.5 Effects of Flow Rate on Breakthrough Curves for Propionaldehyde in a Silica Gel Bed

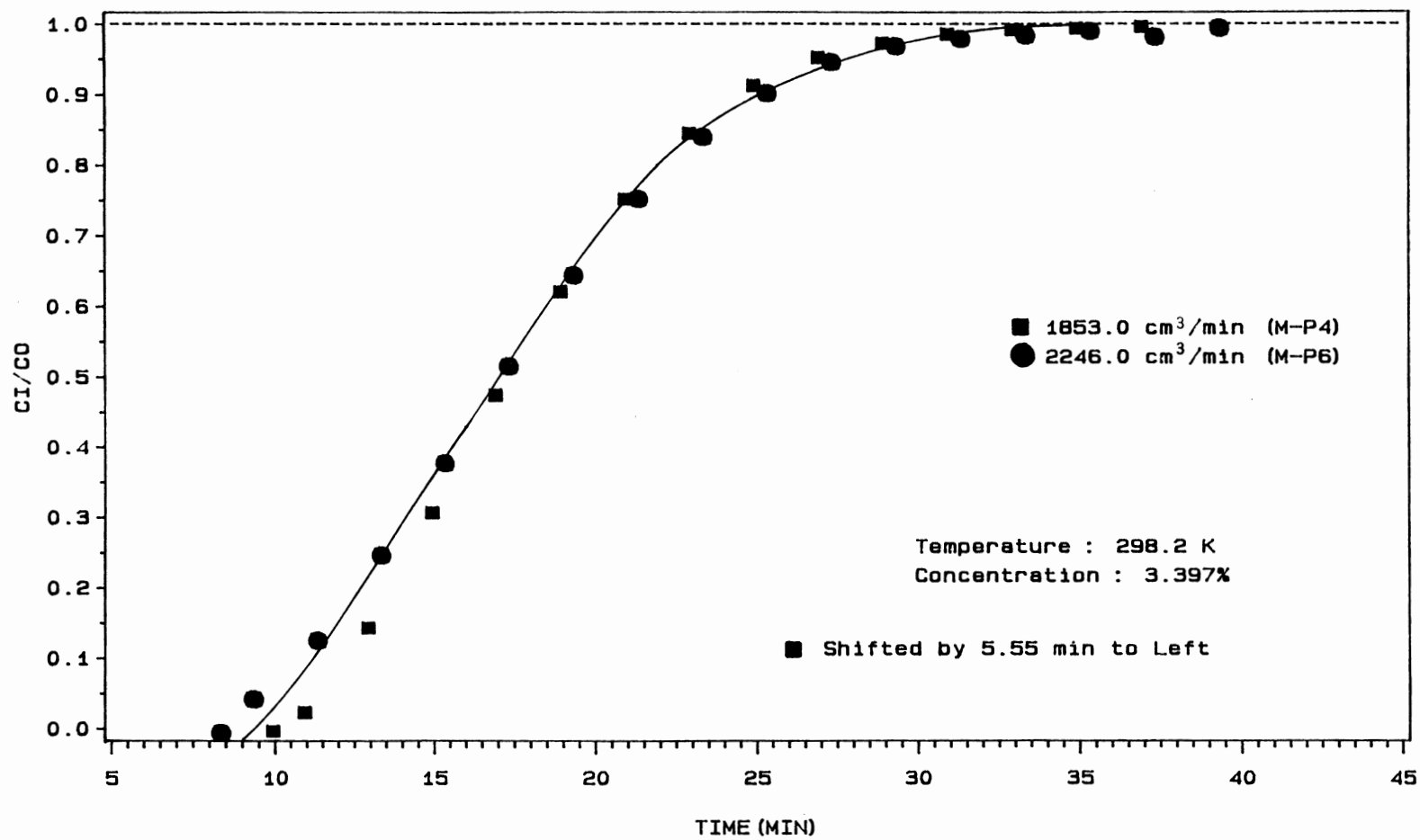


Figure H.6 Effects of Flow Rate on Breakthrough Curves for Propionaldehyde in a Molecular Sieve Bed



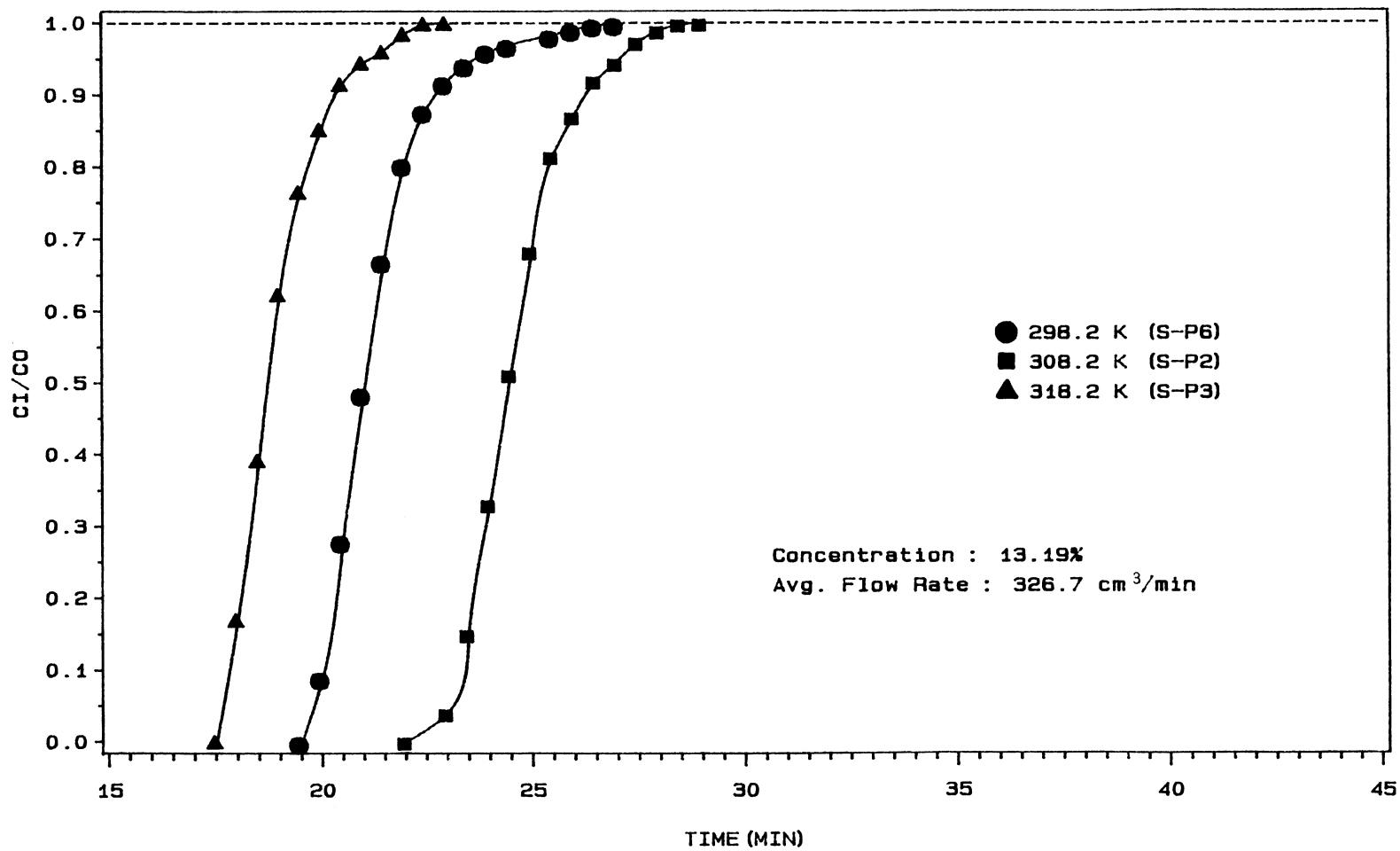


Figure H.7 Effects of Temperature on Breakthrough Curves for Propionaldehyde in a Silica Gel Bed

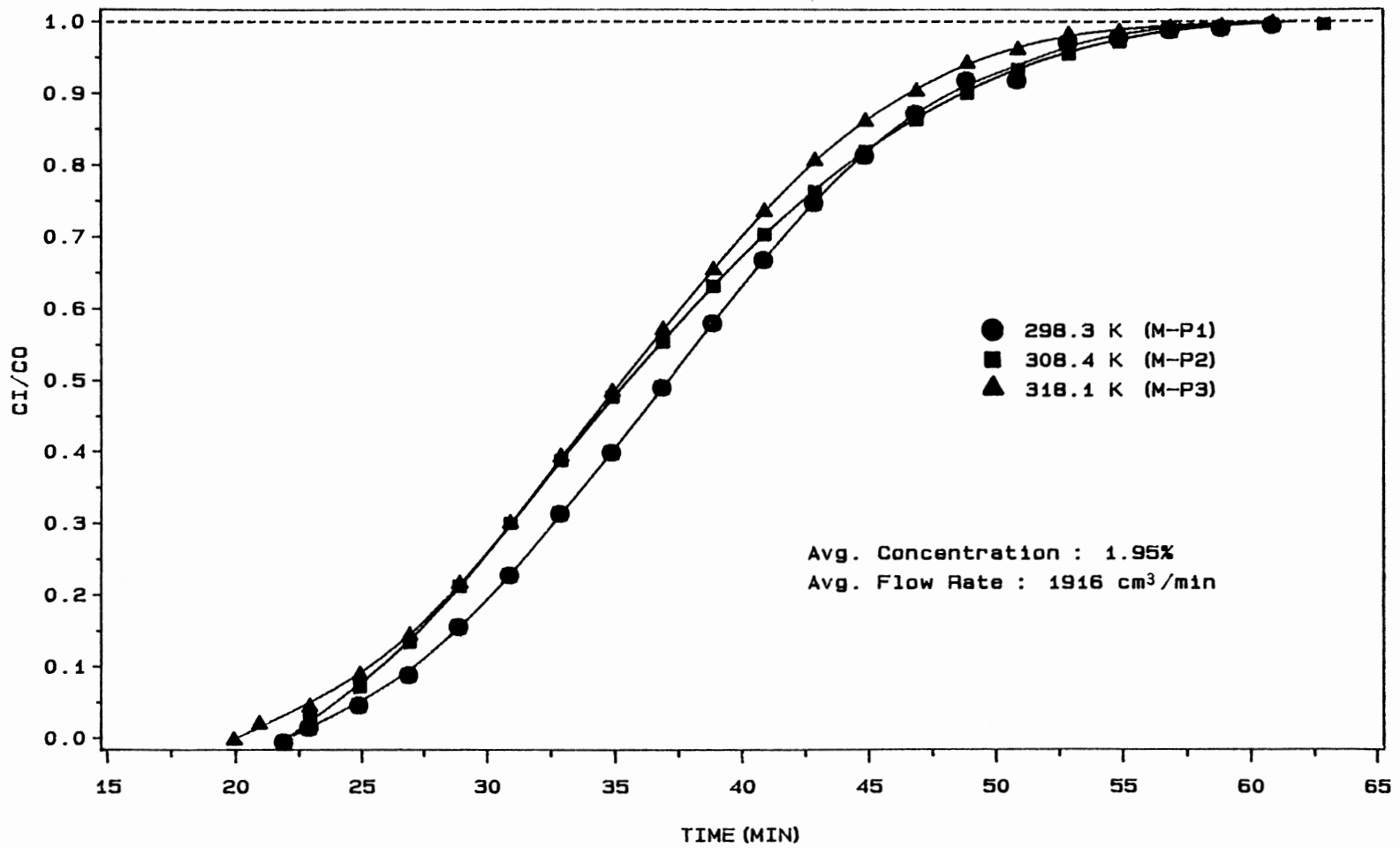


Figure H.8 Effects of Temperature on Breakthrough Curves for Propionaldehyde in a Molecular Sieve Bed

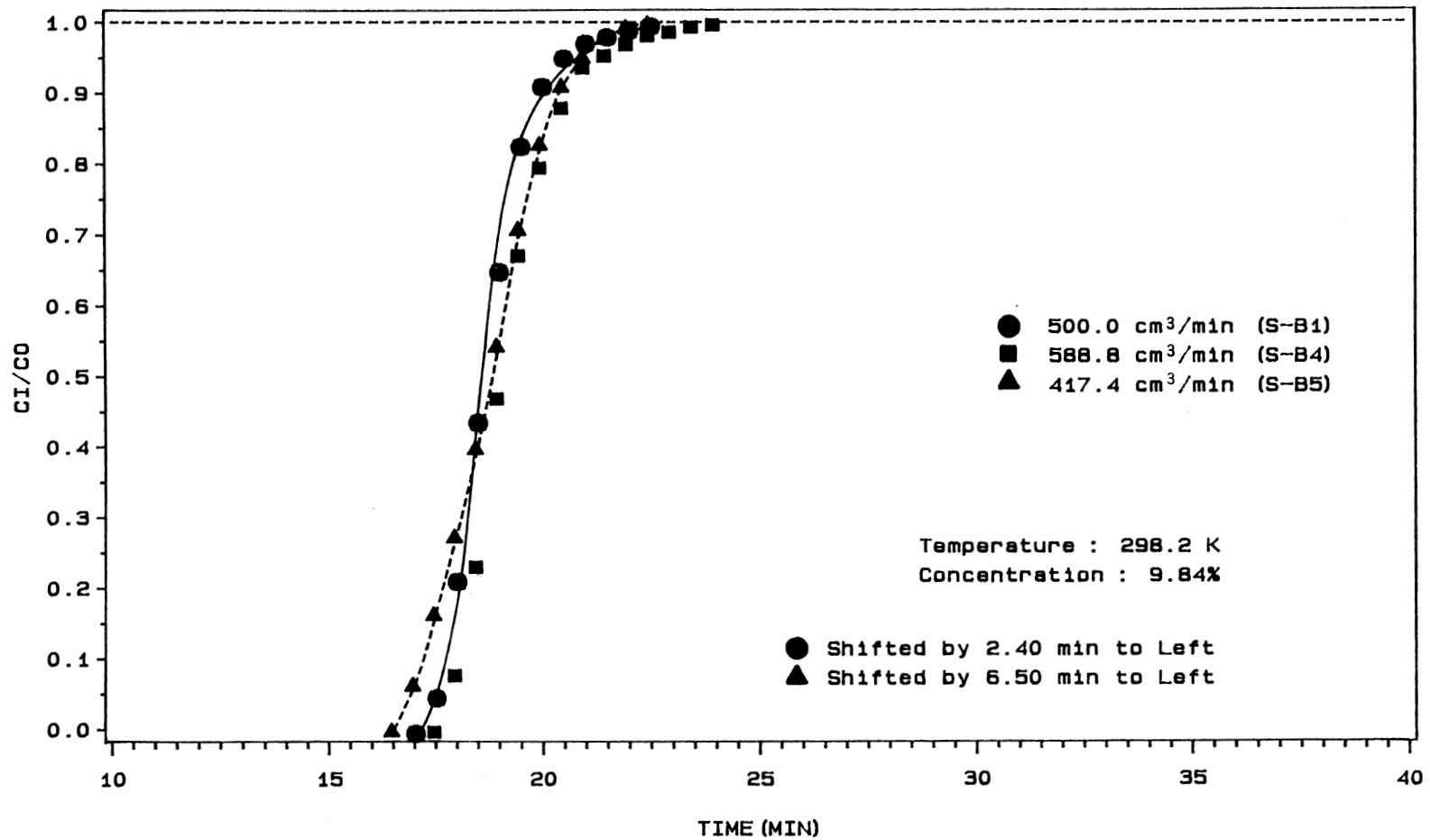


Figure H.9 Effects of Flow Rate on Breakthrough Curves for Butyraldehyde in a Silica Gel Bed in a Silica Gel Bed

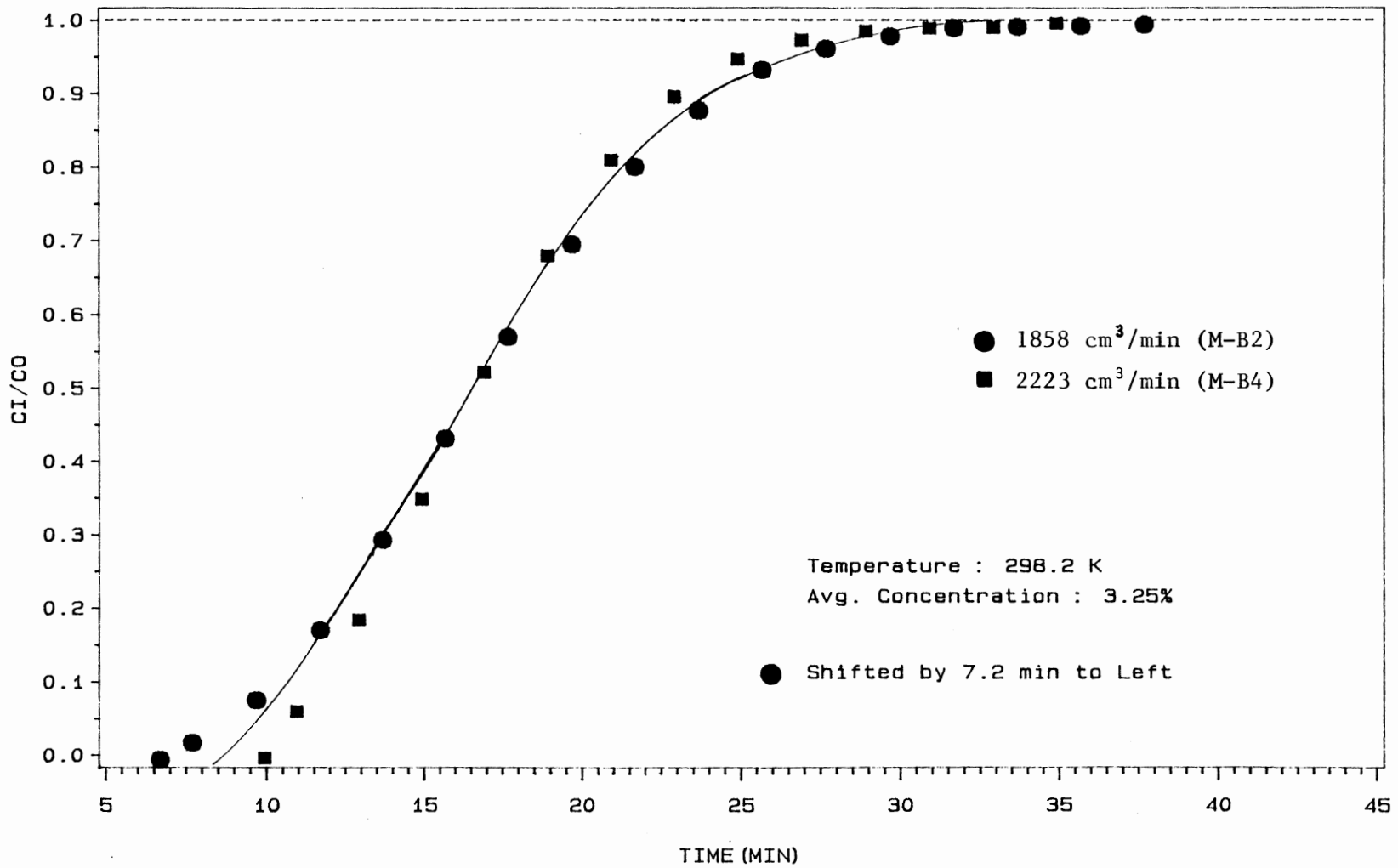


Figure H.10 Effects of Flow Rate on Breakthrough Curves for Butyraldehyde in a Molecular Sieve Bed

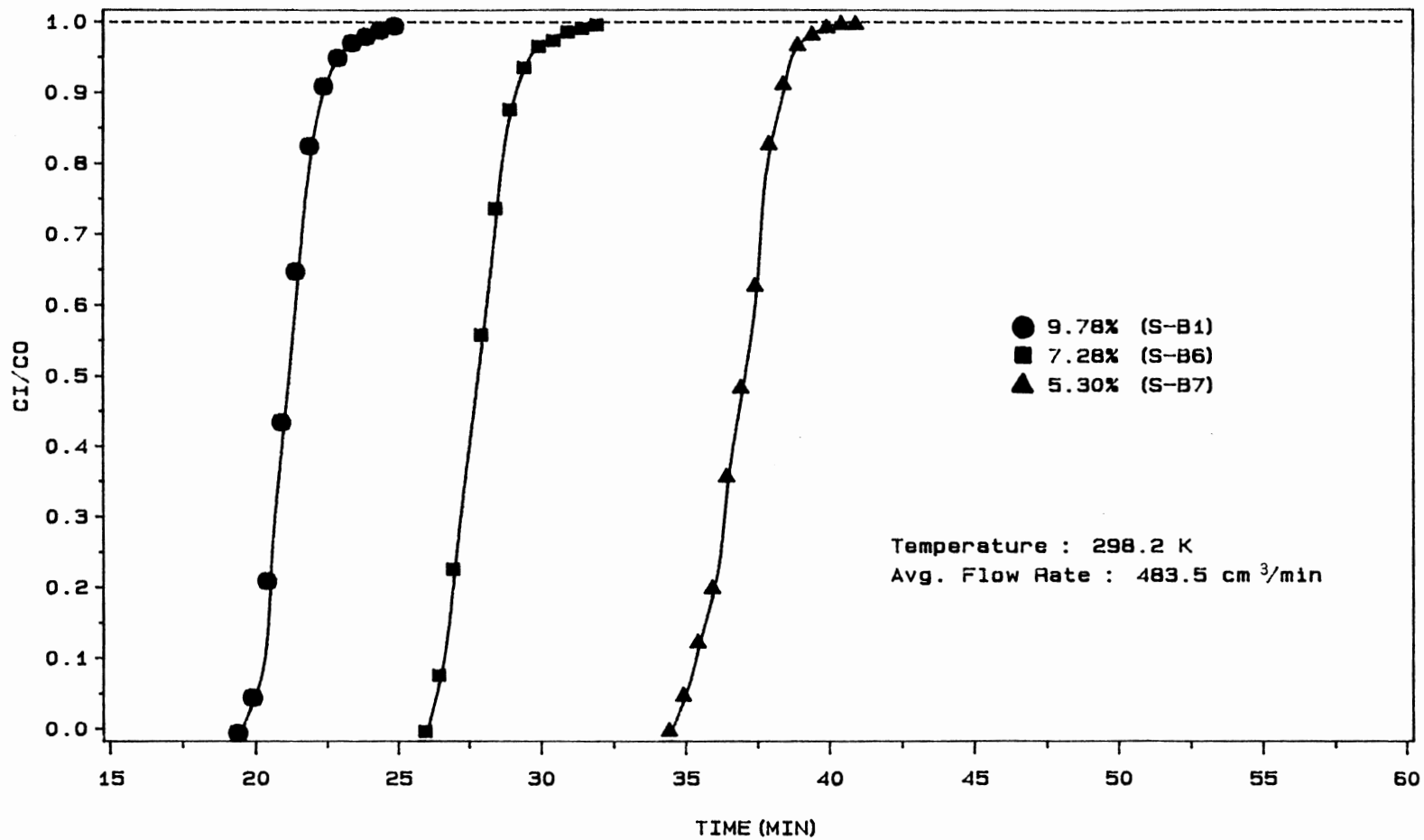


Figure H.11 Effects of Inlet Concentration on Breakthrough Curves for Butyraldehyde in a Silica Gel Bed

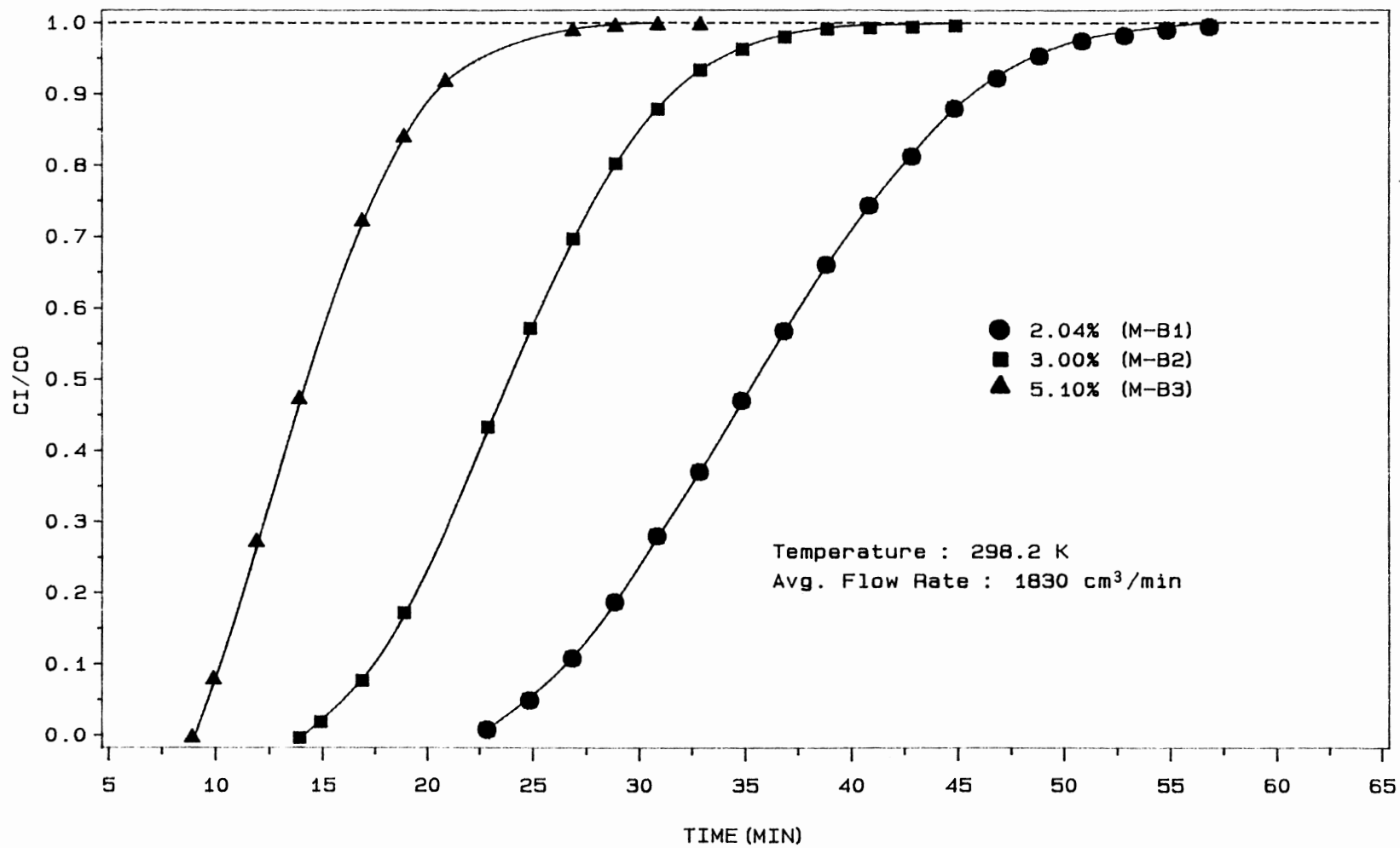


Figure H.12 Effects of Inlet Concentration on Breakthrough Curves for Butyraldehyde in a Molecular Sieve Bed

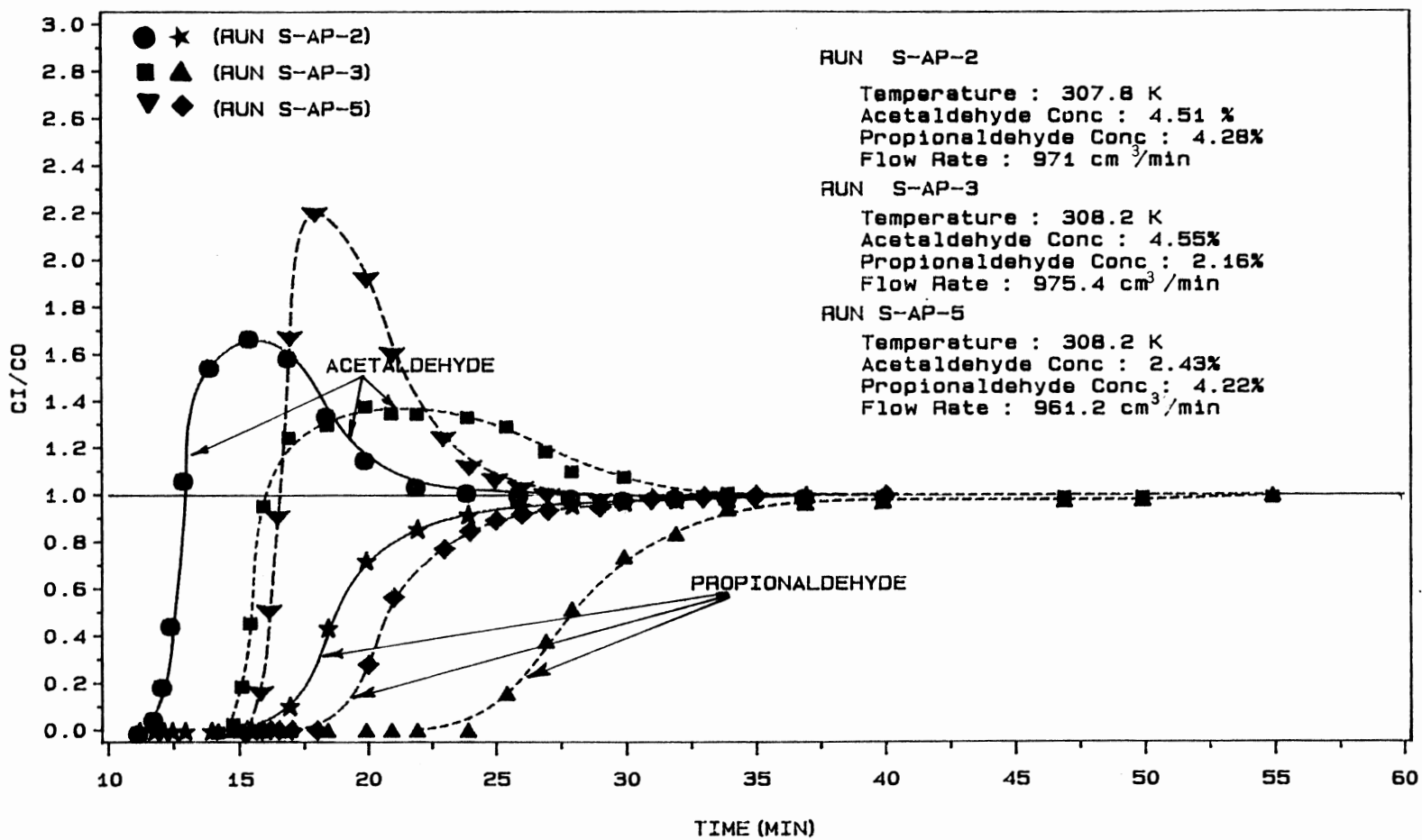


Figure H.13 Effects of Inlet Concentration on Breakthrough Curves for Acetaldehyde and Propionaldehyde in their Binary Mixtures in a Silica Gel Bed

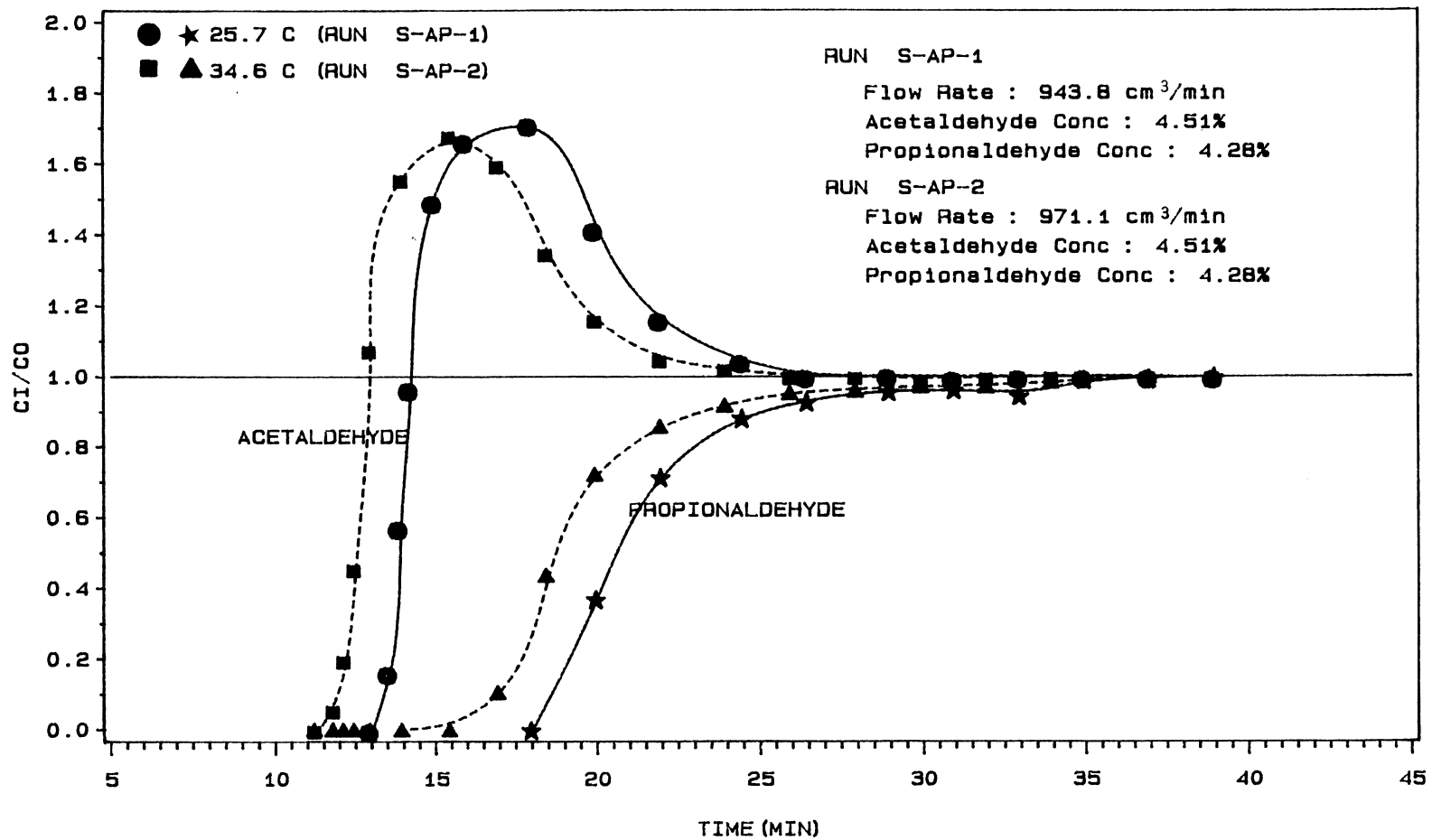


Figure H.14 Effects of Temperature on Breakthrough Curves for Acetaldehyde and Propionaldehyde in their Binary Mixture in a Silica Gel Bed



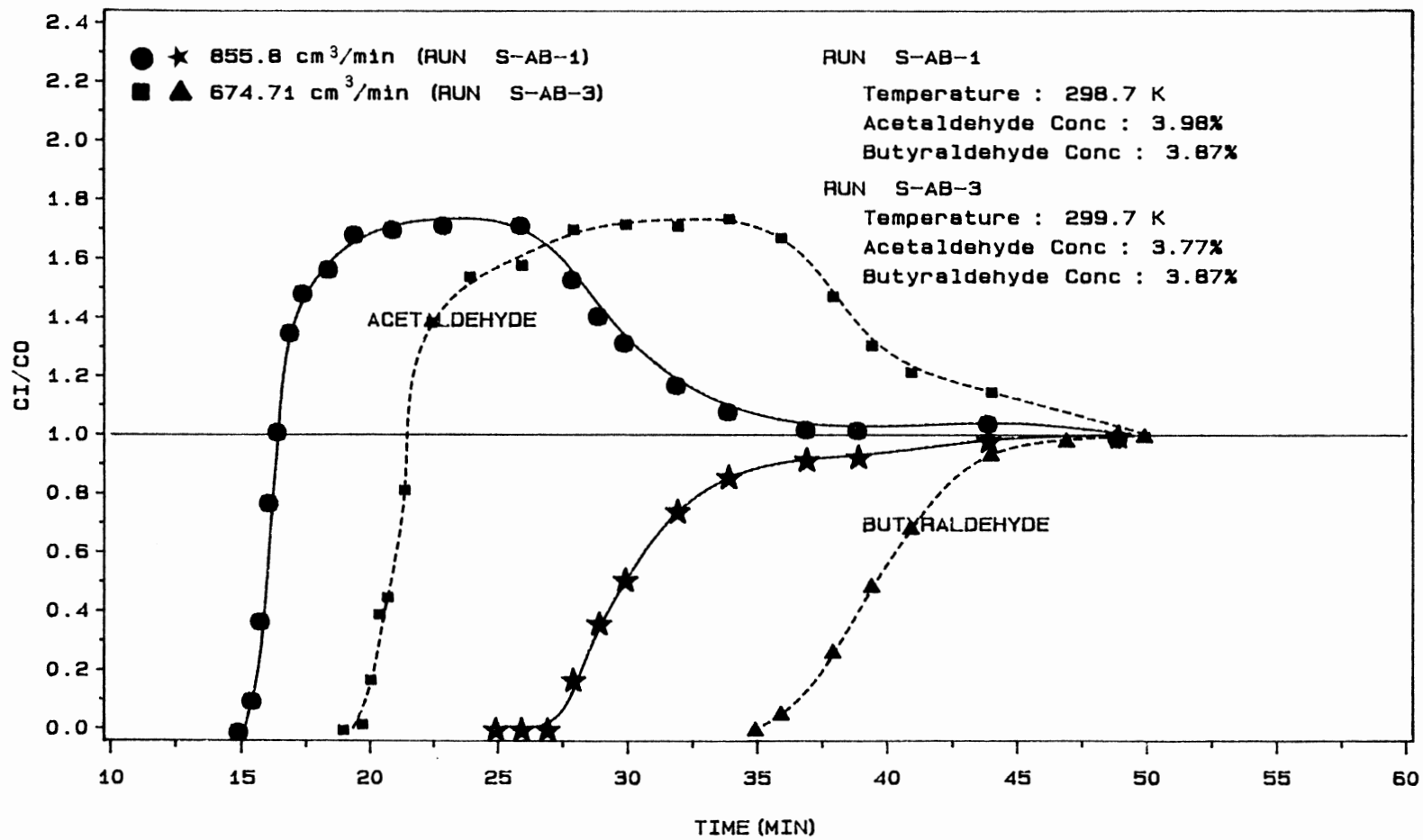


Figure H.15 Effects of Flow Rate on Breakthrough Curves for Acetaldehyde and Butyraldehyde in their Binary Mixtures in a Silica Gel Bed

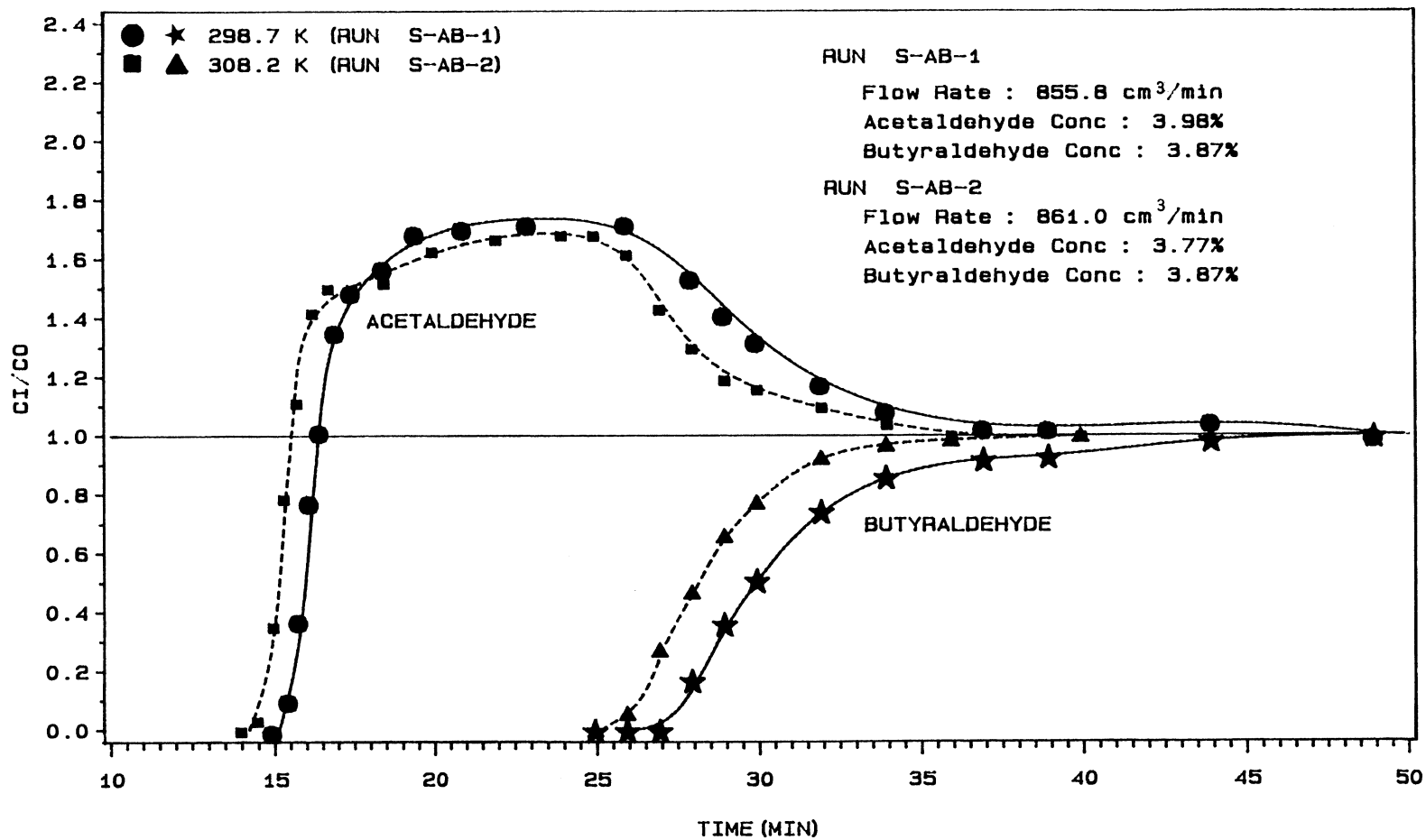


Figure H.16 Effects of Temperature on Breakthrough Curves for Acetaldehyde and Butyraldehyde in their Binary Mixtures in a Silica Gel Bed

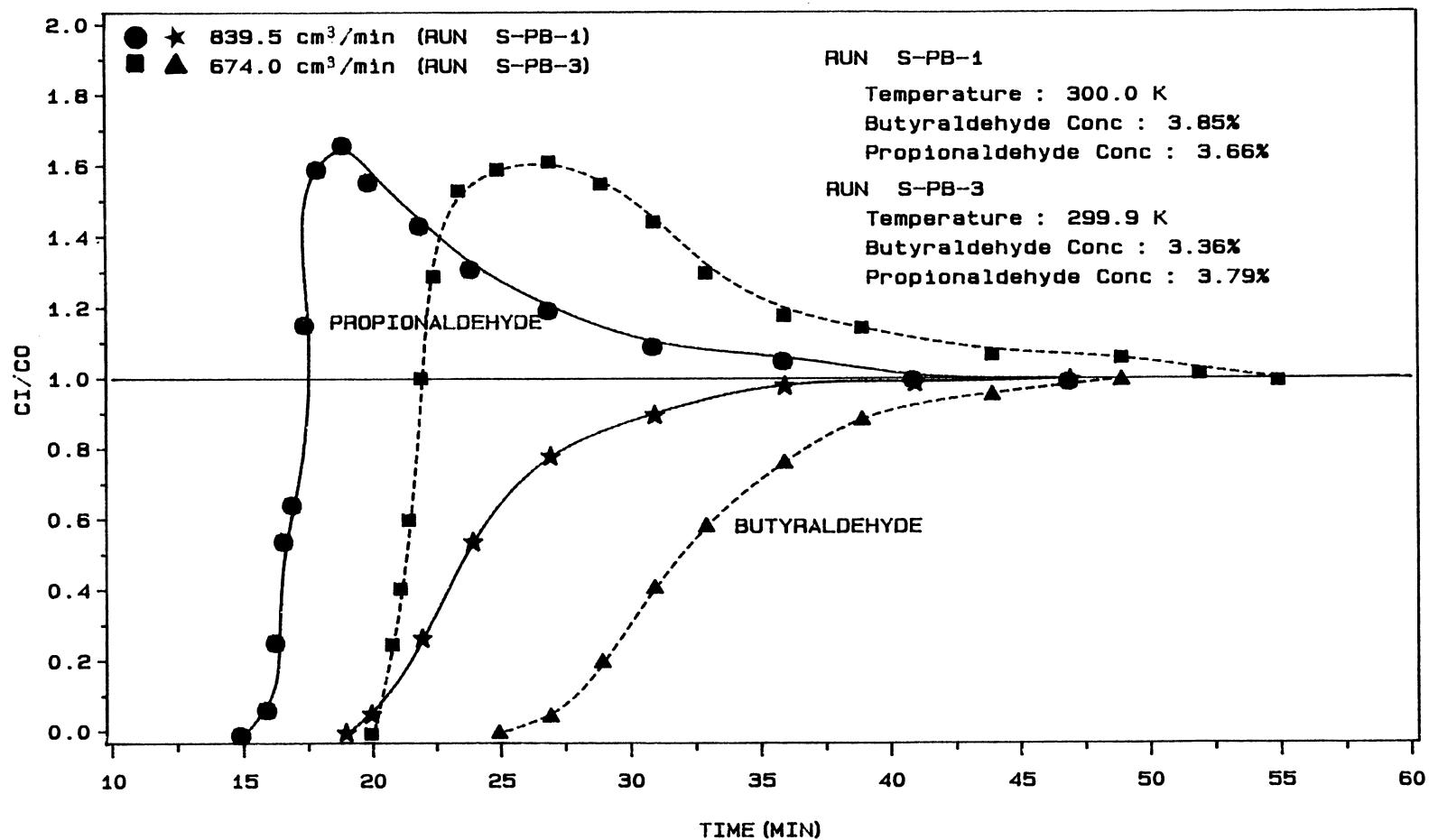


Figure H.17 Effects of Flow Rate on Breakthrough Curves for Propionaldehyde and Butyraldehyde in their Binary Mixtures in a Silica Gel Bed

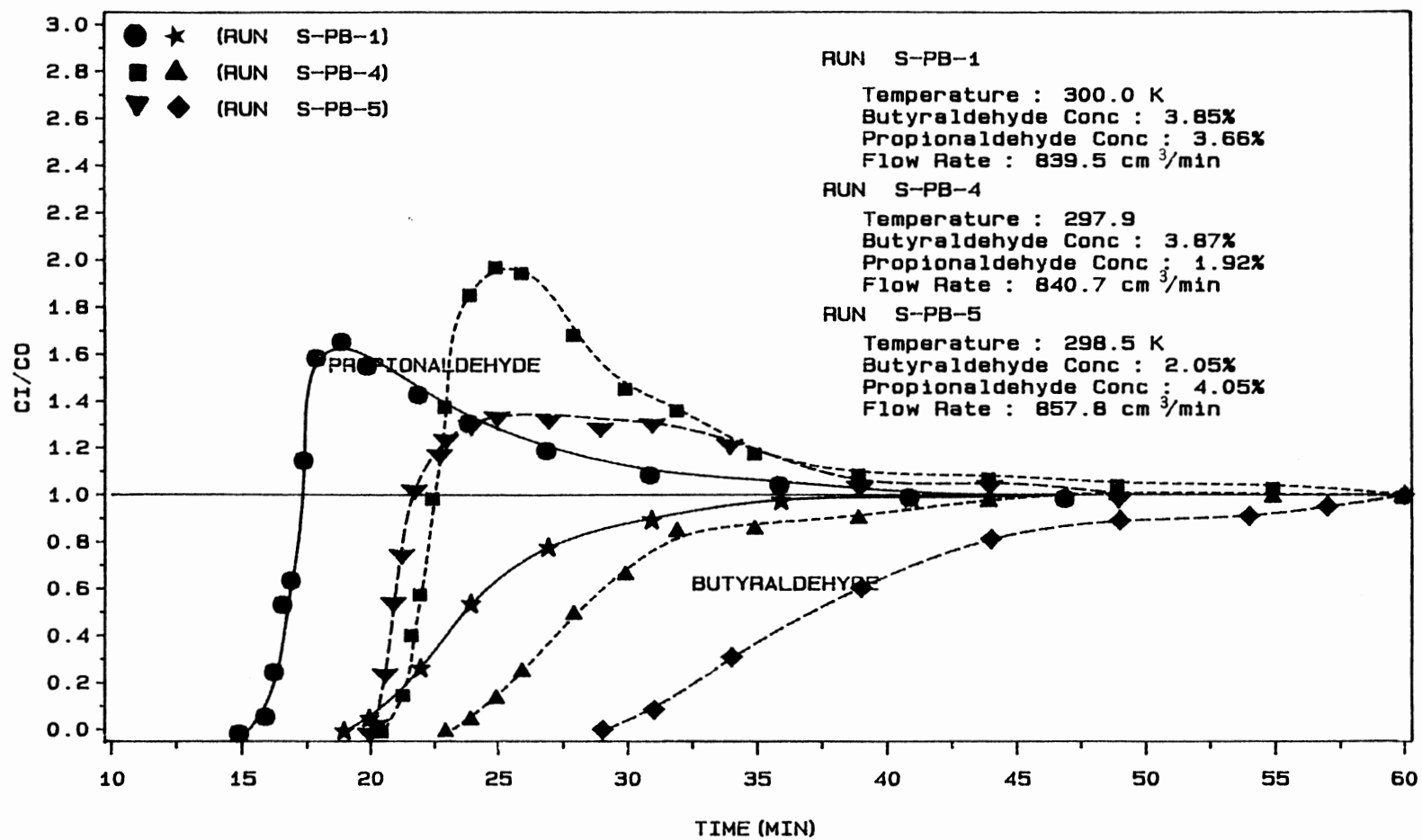


Figure H.18 Effects of Inlet Concentration on Breakthrough Curves for Propionaldehyde and Butyraldehyde in their Binary Mixtures in a Silica Gel Bed

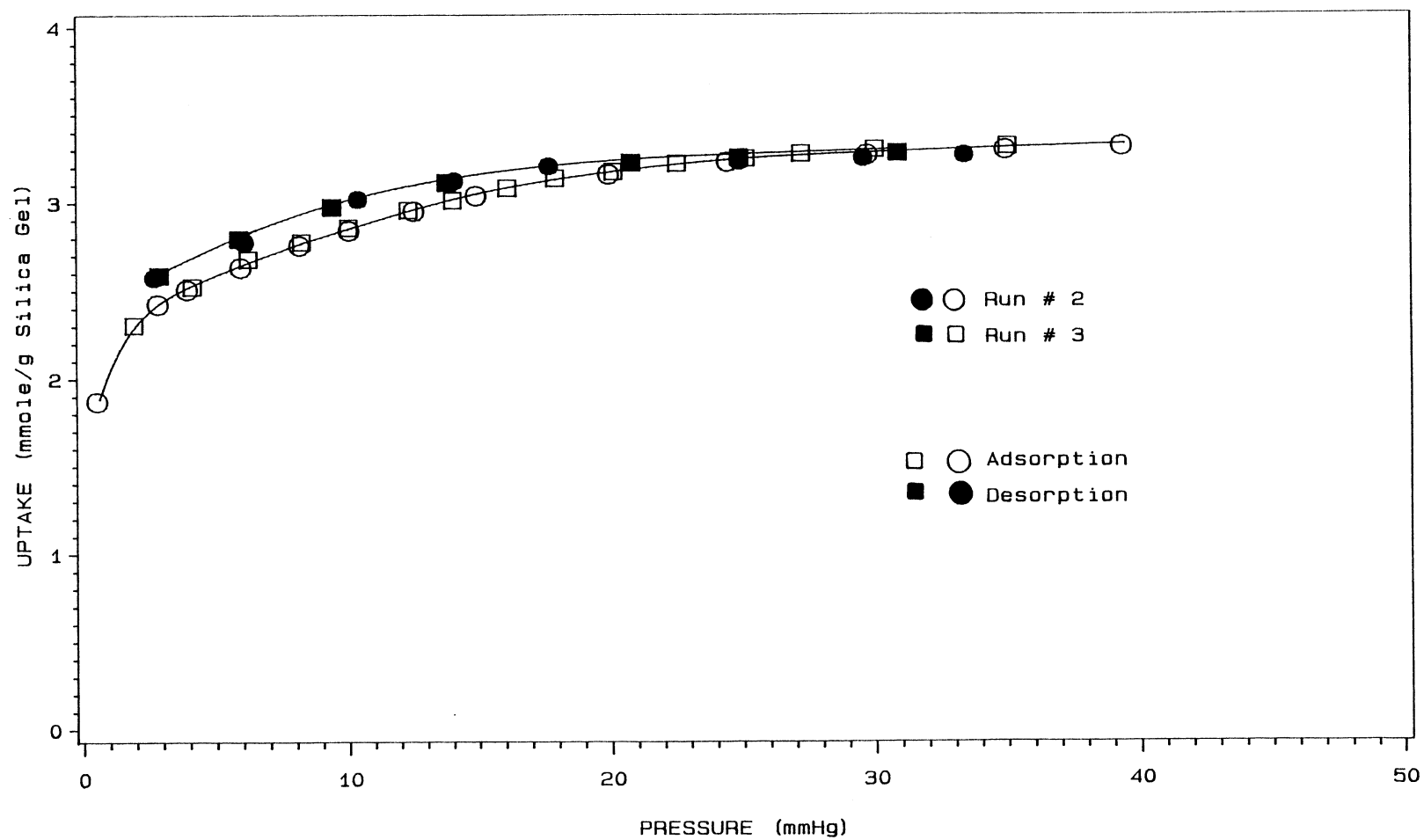


Figure H.19 Reproducibility of the Experimental Data (Butyraldehyde Adsorption on Silica Gel at 288.2 K)

Table H.I Experimental Data for Acetaldehyde Adsorption on Silica Gel

P (mmHg)	UPTAKE (mmol/g)	P (mmHg)	UPTAKE (mmol/g)	P (mmHg)	UPTAKE (mmol/g)
287.0 K		298.2 K		306.5 K	
Adsorption Data :					
1.9	1.952	1.9	1.689	2.6	1.703
4.4	2.495	6.0	2.225	5.4	2.020
8.0	2.747	10.0	2.497	8.3	2.179
12.5	2.947	14.3	2.679	11.1	2.293
16.2	3.087	18.0	2.792	14.3	2.429
20.9	3.246	22.8	2.906	16.9	2.497
25.0	3.360	26.3	2.997	20.0	2.588
30.0	3.519	30.0	3.087	28.0	2.770
35.0	3.632	35.4	3.178	32.2	2.860
40.0	3.746	40.0	3.246	36.0	2.928
50.0	3.927	45.1	3.337	40.1	2.974
60.0	4.086	50.8	3.428	46.0	3.065
70.0	4.245	55.0	3.496	58.0	3.224
80.0	4.404	60.0	3.576	64.0	3.292
90.0	4.563	65.0	3.644	70.0	3.371
99.9	4.699	70.2	3.700	80.0	3.473
114.0	4.858	75.0	3.768	90.2	3.564
129.8	5.017	80.0	3.814	100.0	3.655
149.5	5.221	90.2	3.927	110.0	3.768
174.5	5.426	100.0	4.041	120.0	3.836
199.5	5.607	110.0	4.132	130.0	3.882
225.0	5.721	120.5	4.236	140.0	3.961
250.0	5.789	130.0	4.313	149.5	4.041
		140.0	4.404	160.0	4.109
				170.0	4.154
Desorption Data :					
229.5	5.761	131.5	4.370	159.5	4.109
210.0	5.725	120.5	4.322	150.5	4.063
190.0	5.691	110.5	4.263	141.0	4.018
170.0	5.632	100.0	4.199	130.0	3.972
150.0	5.541	90.5	4.131	120.5	3.938
130.0	5.425	80.0	4.050	109.5	3.882
110.0	5.278	70.0	3.938	100.5	3.836
100.5	5.141	60.0	3.859	90.0	3.791
85.5	5.017	50.0	3.768	79.8	3.723
75.6	4.901	40.0	3.632	65.5	3.586
60.0	4.724	28.5	3.450	49.4	3.450
45.0	4.517	19.0	3.223	39.9	3.314
29.5	4.267	15.0	3.110	30.0	3.155
17.5	3.950	10.0	2.928	19.5	2.996
9.0	3.723	7.3	2.792	10.4	2.724
4.6	3.462	4.1	2.610	3.5	2.315
2.0	3.237	2.0	2.383		

Table H.II Experimental Data for Propionaldehyde Adsorption on Silica Gel

P (mmHg)	UPTAKE (mmol/g)	P (mmHg)	UPTAKE (mmol/g)	P (mmHg)	UPTAKE (mmol/g)
282.0 K		297.0 K		304.3 K	
Adsorption Data :					
1.7	2.367	2.1	2.161	4.2	2.204
3.9	2.686	4.4	2.333	6.8	2.342
6.0	2.841	6.2	2.436	9.0	2.428
8.3	2.961	8.0	2.531	11.9	2.531
10.2	3.058	10.4	2.634	14.6	2.617
13.9	3.228	12.1	2.703	20.0	2.738
17.9	3.375	14.0	2.755	23.0	2.806
25.8	3.590	18.0	2.875	25.9	2.858
28.9	3.666	20.1	2.944	30.0	2.927
32.0	3.726	22.2	2.996	34.0	2.996
35.5	3.777	27.9	3.116	38.0	3.056
38.1	3.819	31.1	3.177	41.9	3.109
41.6	3.859	35.1	3.237	50.0	3.220
50.0	3.951	40.0	3.323	55.0	3.271
55.0	3.977	45.0	3.409	60.0	3.340
64.9	4.034	49.8	3.478	65.0	3.392
75.1	4.069	55.0	3.530	69.9	3.444
89.3	4.112	59.9	3.581	75.0	3.495
		65.3	3.633	80.3	3.547
		69.8	3.685	84.8	3.593
		74.7	3.728	90.0	3.633
		80.0	3.753	95.0	3.667
		84.5	3.788	100.0	3.702
		90.5	3.822	104.8	3.728
		99.4	3.857	109.5	3.753
Desorption Data :					
79.0	4.081	89.5	3.822	100.0	3.702
70.5	4.046	80.0	3.771	90.5	3.650
60.5	4.012	70.0	3.719	81.0	3.564
50.0	3.977	60.2	3.650	71.0	3.478
40.0	3.943	49.6	3.564	61.8	3.409
34.9	3.926	40.5	3.461	52.9	3.306
25.0	3.753	30.3	3.289	44.5	3.203
20.0	3.616	23.8	3.151	37.5	3.116
15.3	3.478	18.3	3.030	26.3	2.944
9.3	3.254	12.5	2.875	19.0	2.806
6.0	3.065	5.9	2.600	14.5	2.703
3.9	2.910	1.9	2.307	9.8	2.565
1.3	2.703			5.0	2.365
				2.5	2.135

Table H.III Experimental Data for Butyraldehyde Adsorption on Silica Gel

P (mmHg)	UPTAKE (mmol/g)	P (mmHg)	UPTAKE (mmol/g)	P (mmHg)	UPTAKE (mmol/g)
288.2 K		299.3 K		308.2 K	
Adsorption Data :					
0.6	1.886	2.5	2.191	2.0	1.969
2.9	2.441	4.3	2.316	4.2	2.141
4.0	2.524	6.2	2.413	6.3	2.247
6.0	2.649	8.0	2.510	8.1	2.316
8.2	2.773	10.0	2.566	10.0	2.385
10.1	2.857	12.0	2.635	12.0	2.435
12.6	2.968	14.1	2.713	16.2	2.538
15.0	3.055	16.0	2.771	18.0	2.593
20.0	3.176	18.2	2.829	20.2	2.642
24.5	3.245	20.1	2.865	22.5	2.690
29.8	3.287	22.7	2.912	25.2	2.746
35.0	3.314	25.0	2.964	27.7	2.773
39.4	3.334	27.4	3.011	30.2	2.829
		30.0	3.048	35.4	2.907
		35.0	3.086	40.0	2.954
		40.0	3.120	45.0	3.009
				50.0	3.037
Desorption Data :					
33.5	3.294	35.0	3.102	44.0	2.995
29.7	3.277	29.6	3.081	39.5	2.954
25.0	3.259	25.8	3.048	34.5	2.926
17.8	3.231	22.2	3.000	29.8	2.871
14.2	3.148	19.0	2.936	24.9	2.773
10.5	3.045	16.5	2.886	21.0	2.704
6.2	2.801	12.8	2.773	17.0	2.621
2.8	2.600	8.9	2.663	14.5	2.566
		6.4	2.566	11.0	2.468
		4.3	2.455	8.0	2.385
		2.1	2.295	3.8	2.163
				1.2	1.976



Table H.IV Experimental Data for Acetaldehyde Adsorption on Molecular Sieve-13X

P (mmHg)	UPTAKE (mmol/g)	P (mmHg)	UPTAKE (mmol/g)	P (mmHg)	UPTAKE (mmol/g)
286.5 K		293.2 K		301.0 K	
Adsorption Data :					
3.2	2.384	2.1	2.225	2.5	2.209
6.0	2.474	6.3	2.384	5.5	2.322
14.9	2.599	10.0	2.452	10.1	2.391
19.8	2.645	20.0	2.565	15.8	2.454
25.0	2.688	30.0	2.633	20.5	2.497
35.0	2.733	40.0	2.690	30.0	2.556
45.0	2.770	55.0	2.747	40.5	2.602
59.8	2.815	70.0	2.781	54.8	2.647
75.0	2.847	90.0	2.817	69.8	2.683
94.7	2.883	115.0	2.854	89.7	2.724
115.0	2.913	160.0	2.901	115.2	2.756
139.8	2.938	200.0	2.940	144.8	2.788
170.0	2.974	251.0	2.974	180.0	2.824
199.5	3.013	305.5	3.026	220.0	2.854
239.0	3.051	356.2	3.065	270.0	2.876
280.0	3.087	401.8	3.099	360.0	2.933
300.0	3.110	450.6	3.142		
Desorption Data :					
267.5	3.087	350.0	3.064	240.0	2.860
250.0	3.076	281.0	3.030	200.5	2.837
230.0	3.062	242.0	3.012	160.0	2.803
210.0	3.051	208.0	3.000	123.5	2.792
190.5	3.042	180.0	2.983	97.0	2.747
168.0	3.026	150.0	2.962	76.0	2.724
144.0	3.008	118.0	2.928	56.5	2.678
122.0	2.996	91.5	2.883	37.0	2.610
101.0	2.969	70.5	2.837	15.5	2.497
80.0	2.949	46.5	2.769	7.0	2.383
59.5	2.919	32.0	2.724	2.2	2.270
43.5	2.892	16.5	2.633		
31.5	2.867	8.0	2.556		
22.5	2.840	4.0	2.481		
10.0	2.760	2.0	2.422		
5.2	2.697				
2.0	2.617				

Table H.V Experimental Data for Propionaldehyde Adsorption  
on Molecular Sieve-13X

P (mmHg)	UPTAKE (mmol/g)	P (mmHg)	UPTAKE (mmol/g)	P (mmHg)	UPTAKE (mmol/g)
283.2 K		293.2 K		303.2 K	
Adsorption Data :					
3.5	1.911	2.3	1.839	3.0	1.806
12.7	2.049	5.0	1.899	12.0	1.915
20.0	2.130	10.0	1.963	20.0	1.961
29.8	2.181	19.9	2.032	30.0	2.002
40.5	2.230	29.5	2.083	43.5	2.049
50.5	2.261	40.3	2.130	54.8	2.076
64.5	2.309	49.5	2.162	75.0	2.107
79.5	2.366	70.0	2.204	100.0	2.151
100.5	2.450	94.5	2.238	121.0	2.175
123.0	2.626	119.0	2.290	144.7	2.200
141.0	2.772	171.0	2.479	186.5	2.276
154.0	2.875			215.0	2.324
Desorption Data :					
130.5	2.738	135.0	2.362	195.0	2.300
110.0	2.614	114.0	2.354	170.0	2.264
95.0	2.527	96.0	2.345	148.0	2.207
80.0	2.462	81.5	2.331	126.5	2.180
65.0	2.411	64.0	2.273	101.0	2.152
50.0	2.362	45.5	2.224	84.0	2.126
35.0	2.311	25.5	2.149	65.0	2.092
20.0	2.249	16.0	2.104	39.5	2.032
8.5	2.185	9.0	2.066	29.5	1.997
3.0	2.111	3.0	1.985	21.5	1.946
				8.5	1.877
				4.0	1.825

Table H.VI Experimental Data for Butyraldehyde Adsorption on Molecular Sieve-13X

P (mmHg)	UPTAKE (mmol/g)	P (mmHg)	UPTAKE (mmol/g)	P (mmHg)	UPTAKE (mmol/g)
282.6 K		293.2 K		302.0 K	
Adsorption Data :					
2.2	1.650	1.2	1.613	2.0	1.605
6.0	1.775	3.9	1.692	6.1	1.668
12.0	1.879	9.0	1.760	12.8	1.725
21.0	1.961	15.0	1.800	20.0	1.776
30.8	2.087	24.8	1.872	35.3	1.831
39.5	2.252	35.0	1.928	50.0	1.879
47.0	2.427	45.0	1.990	75.5	1.987
52.0	2.635	54.0	2.057		
		63.5	2.163		
		73.0	2.288		
Desorption Data :					
45.0	2.385	63.0	2.163	64.9	1.928
33.0	2.149	50.0	2.011	55.0	1.900
24.0	2.044	24.0	1.858	42.5	1.861
13.0	1.941	16.0	1.825	26.3	1.786
8.5	1.886	10.0	1.793	15.0	1.747
1.9	1.761	4.2	1.746	9.1	1.706
		2.1	1.714	3.7	1.629

Table H.VII Experimental Data for Breakthrough Curves of Acetaldehyde on Silica Gel

TIME (min)	CI/CO	TIME (min)	CI/CO	TIME (min)	CI/CO
RUN # S-A1		RUN # S-A2		RUN # S-A3	
17.5	0.000	15.5	0.000	22.0	0.000
18.0	0.100	16.5	0.100	22.3	0.035
19.0	0.410	17.0	0.180	22.8	0.220
20.0	0.761	17.5	0.365	23.3	0.440
21.0	0.902	18.0	0.560	23.8	0.620
22.0	0.955	18.5	0.725	24.3	0.750
23.0	0.985	19.0	0.825	24.8	0.840
24.0	0.997	19.5	0.888	25.3	0.900
25.0	1.000	20.0	0.925	25.8	0.935
		20.5	0.945	26.3	0.950
		21.0	0.970	26.8	0.965
		21.5	0.980	27.3	0.975
		22.0	0.990	27.8	0.970
		22.5	1.000	28.3	0.995
		23.0	1.000	28.8	1.000
				30.0	1.000
RUN # S-A4		RUN # S-A6		RUN # S-A7	
22.0	0.000	16.5	0.000	24.5	0.000
22.5	0.030	17.0	0.062	25.0	0.054
23.0	0.070	17.5	0.132	25.5	0.115
23.5	0.180	18.0	0.320	26.0	0.205
24.0	0.330	18.5	0.551	26.5	0.295
24.5	0.540	19.0	0.740	27.0	0.390
25.0	0.710	19.5	0.865	27.5	0.475
25.5	0.810	20.0	0.915	28.0	0.564
26.0	0.880	20.5	0.952	28.5	0.655
26.5	0.925	21.0	0.962	29.0	0.724
27.0	0.960	21.5	0.981	29.5	0.821
28.0	0.988	22.0	0.990	30.0	0.908
29.0	0.997	22.5	0.997	30.5	0.950
30.0	1.000	23.0	1.000	31.0	0.960
				31.5	0.980
				32.0	0.975
				32.5	0.990
				33.0	1.000
RUN # S-A8		RUN # S-A9			
11.5	0.000	33.0	0.000		
12.0	0.120	33.5	0.146		
12.5	0.377	34.0	0.175		
13.0	0.590	35.0	0.262		
13.5	0.790	36.0	0.400		
14.0	0.882	37.0	0.554		
14.5	0.931	38.0	0.706		
15.0	0.950	39.0	0.821		
15.5	0.970	40.0	0.899		
16.0	0.970	41.0	0.938		
16.5	0.990	42.0	0.961		
17.0	0.996	43.0	0.963		
17.5	1.000	44.0	0.972		
18.0	1.000	45.0	0.975		
		46.0	0.975		
		47.0	0.957		
		49.0	0.990		
		53.0	1.000		

Table H.VIII Experimental Data for Breakthrough Curves of Propionaldehyde on Silica Gel

TIME (min)	CI/CO	TIME (min)	CI/CO	TIME (min)	CI/CO
RUN # S-P2		RUN # S-P3		RUN # S-P5	
19.5	0.000	17.5	0.000	21.5	0.000
20.0	0.090	18.0	0.170	22.5	0.090
20.5	0.280	18.5	0.392	23.0	0.350
21.0	0.485	19.0	0.623	23.5	0.612
21.5	0.670	19.5	0.765	24.0	0.750
22.0	0.804	20.0	0.852	24.5	0.835
22.5	0.878	20.5	0.915	25.0	0.882
23.0	0.918	21.0	0.945	25.5	0.924
23.5	0.943	21.5	0.960	26.0	0.943
24.0	0.962	22.0	0.985	26.5	0.961
24.5	0.970	22.5	0.999	27.0	0.972
25.5	0.983	23.0	1.000	27.5	0.981
26.0	0.992			28.0	0.995
26.5	0.998			28.5	0.999
27.0	1.000			29.0	1.000
RUN # S-P6		RUN # S-P7		RUN # S-P9	
22.0	0.000	24.0	0.000	20.5	0.000
23.0	0.040	25.0	0.090	21.0	0.030
23.5	0.150	25.5	0.220	21.5	0.100
24.0	0.331	26.0	0.365	22.0	0.245
24.5	0.512	26.5	0.510	22.5	0.460
25.0	0.683	27.0	0.670	23.0	0.660
25.5	0.815	27.5	0.830	23.5	0.790
26.0	0.870	28.0	0.900	24.0	0.860
26.5	0.920	28.5	0.950	24.5	0.900
27.0	0.945	29.0	0.980	25.0	0.932
27.5	0.974	29.5	0.997	25.5	0.952
28.0	0.990	30.0	1.000	26.0	0.975
28.5	0.999			26.5	0.975
29.0	1.000			27.0	0.980
27.0	1.000			27.5	0.990
				28.0	0.996
				28.5	1.000
RUN # S-p11					
34.5	0.000				
35.0	0.105				
35.5	0.220				
36.0	0.340				
36.5	0.458				
37.0	0.537				
37.5	0.627				
38.0	0.735				
38.5	0.830				
39.0	0.885				
39.5	0.925				
40.0	0.935				
40.5	0.950				
41.0	0.966				
41.5	0.974				
42.0	0.985				
42.5	0.990				
43.0	0.994				
43.5	0.998				
44.0	1.000				

Table H.IX Experimental Data for Breakthrough Curves of Butyraldehyde on Silica Gel

TIME (min)	CI/CO	TIME (min)	CI/CO	TIME (min)	CI/CO
RUN # S-B1		RUN # S-B2		RUN # S-B3	
19.5	0.000	17.5	0.000	16.5	0.000
20.0	0.052	18.0	0.030	17.0	0.100
20.5	0.213	18.5	0.163	17.5	0.240
21.0	0.443	19.0	0.345	18.0	0.450
21.5	0.655	19.5	0.540	18.5	0.660
22.0	0.830	20.0	0.722	19.0	0.772
22.5	0.915	20.5	0.808	19.5	0.862
23.0	0.958	21.0	0.930	20.0	0.920
23.5	0.976	21.5	0.970	20.5	0.950
24.0	0.985	22.0	0.985	21.0	0.972
24.5	0.995	22.5	0.999	21.5	0.992
25.0	1.000	23.0	1.000	22.0	1.000
RUN # S-B4		RUN # S-B5		RUN # S-B6	
17.5	0.000	23.0	0.000	26.0	0.000
18.0	0.080	23.5	0.065	26.5	0.080
18.5	0.234	24.0	0.165	27.0	0.230
19.0	0.472	24.5	0.275	27.5	0.400
19.5	0.674	25.0	0.400	28.0	0.562
20.0	0.798	25.5	0.545	28.5	0.740
20.5	0.883	26.0	0.710	29.0	0.880
21.0	0.940	26.5	0.830	29.5	0.940
21.5	0.957	27.0	0.912	30.0	0.970
22.0	0.973	27.5	0.953	30.5	0.978
22.5	0.985	28.0	0.980	31.0	0.990
23.0	0.990	28.5	0.995	31.5	0.995
23.5	0.997	29.0	1.000	32.0	1.000
24.0	1.000				
RUN # S-B7					
34.5	0.000				
35.0	0.050				
35.5	0.125				
36.0	0.202				
36.5	0.360				
37.0	0.486				
37.5	0.630				
38.0	0.830				
38.5	0.915				
39.0	0.970				
39.5	0.985				
40.0	0.995				
40.5	1.000				
41.0	1.000				

Table H.X Experimental Data for Breakthrough Curves of Acetaldehyde on Molecular Sieve-13X

TIME (min)	CI/CO	TIME (min)	CI/CO	TIME (min)	CI/CO
	RUN # M-A2		RUN # M-A3		RUN # M-A4
22.0	0.000	12.0	0.000	10.0	0.000
23.0	0.037	13.0	0.008	11.0	0.025
25.0	0.103	15.0	0.083	13.0	0.118
27.0	0.204	17.0	0.235	15.0	0.278
29.0	0.339	19.0	0.428	17.0	0.468
31.0	0.478	21.0	0.612	19.0	0.648
33.0	0.614	23.0	0.755	21.0	0.787
35.0	0.736	25.0	0.864	23.0	0.880
37.0	0.835	27.0	0.932	25.0	0.944
39.0	0.899	29.0	0.965	27.0	0.972
41.0	0.948	31.0	0.983	29.0	0.988
43.0	0.975	33.0	0.993	31.0	0.995
45.0	0.988	35.0	0.995	33.0	0.998
47.0	0.996	37.0	1.000	36.0	1.000
49.0	0.999	39.0	1.000	38.0	1.000
51.0	1.000				
53.0	1.000				
	RUN # M-A5		RUN # M-A6		
19.0	0.011	21.0	0.043		
21.0	0.032	23.0	0.120		
23.0	0.086	25.0	0.231		
25.0	0.168	27.0	0.358		
27.0	0.280	29.0	0.494		
29.0	0.403	31.0	0.627		
31.0	0.526	33.0	0.741		
33.0	0.641	35.0	0.840		
35.0	0.749	37.0	0.908		
37.0	0.833	39.0	0.951		
39.0	0.892	41.0	0.974		
41.0	0.937	43.0	0.984		
43.0	0.963	45.0	0.990		
45.0	0.977	47.0	0.994		
47.0	0.985	49.0	0.997		
49.0	0.990	51.0	1.000		
51.0	0.993	53.0	1.000		
53.0	0.996				
55.0	1.000				

Table H.XI Experimental Data for Breakthrough Curves of Propionaldehyde on Molecular Sieve-13X

TIME (min)	CI/CO	TIME (min)	CI/CO	TIME (min)	CI/CO
RUN # M-P1		RUN # M-P2		RUN # M-P3	
22.0	0.000	22.0	0.000	20.0	0.000
23.0	0.020	23.0	0.030	21.0	0.023
25.0	0.051	25.0	0.076	23.0	0.047
27.0	0.094	27.0	0.138	25.0	0.092
29.0	0.161	29.0	0.216	27.0	0.147
31.0	0.233	31.0	0.304	29.0	0.219
33.0	0.319	33.0	0.391	31.0	0.304
35.0	0.404	35.0	0.480	33.0	0.396
37.0	0.495	37.0	0.557	35.0	0.487
39.0	0.585	39.0	0.635	37.0	0.574
41.0	0.673	41.0	0.707	39.0	0.657
43.0	0.752	43.0	0.767	41.0	0.738
45.0	0.818	45.0	0.823	43.0	0.809
47.0	0.877	47.0	0.867	45.0	0.864
49.0	0.923	49.0	0.904	47.0	0.906
51.0	0.923	51.0	0.937	49.0	0.945
53.0	0.976	53.0	0.959	51.0	0.964
55.0	0.982	55.0	0.976	53.0	0.985
57.0	0.993	57.0	0.989	55.0	0.989
59.0	0.996	59.0	0.996	57.0	0.994
61.0	1.000	61.0	0.998	59.0	0.996
		63.0	1.000	61.0	1.000
RUN # M-P4		RUN # M-P6			
14.0	0.000	10.0	0.000		
15.0	0.048	11.0	0.027		
17.0	0.131	13.0	0.147		
19.0	0.252	15.0	0.311		
21.0	0.383	17.0	0.478		
23.0	0.521	19.0	0.625		
25.0	0.650	21.0	0.756		
27.0	0.758	23.0	0.849		
29.0	0.846	25.0	0.917		
31.0	0.908	27.0	0.957		
33.0	0.952	29.0	0.977		
35.0	0.975	31.0	0.990		
37.0	0.985	33.0	0.996		
39.0	0.990	35.0	0.998		
41.0	0.996	37.0	1.000		
43.0	0.988				
45.0	1.000				



Table H.XII Experimental Data for Breakthrough Curves of  
Butyraldehyde on Molecular Sieve-13X

TIME (min)	CI/CO	TIME (min)	CI/CO	TIME (min)	CI/CO
RUN # M-B1		RUN # M-B2		RUN # M-B3	
23.0	0.014	14.0	0.000	9.0	0.000
25.0	0.055	15.0	0.023	10.0	0.082
27.0	0.114	17.0	0.081	12.0	0.275
29.0	0.193	19.0	0.176	14.0	0.476
31.0	0.286	21.0	0.299	17.0	0.725
33.0	0.376	23.0	0.437	19.0	0.843
35.0	0.476	25.0	0.576	21.0	0.921
37.0	0.574	27.0	0.701	23.0	0.961
39.0	0.667	29.0	0.807	25.0	0.984
41.0	0.750	31.0	0.883	27.0	0.992
43.0	0.819	33.0	0.938	29.0	0.998
45.0	0.886	35.0	0.967	31.0	1.000
47.0	0.929	37.0	0.984	33.0	1.000
49.0	0.960	39.0	0.995		
51.0	0.981	41.0	0.997		
53.0	0.988	43.0	0.998		
55.0	0.995	45.0	1.000		
57.0	1.000				
RUN # M-B4		RUN # M-B5		RUN # M-B6	
10.0	0.000	8.0	0.000	8.0	0.000
11.0	0.064	9.0	0.043	9.0	0.058
13.0	0.189	11.0	0.187	11.0	0.226
15.0	0.353	13.0	0.397	13.0	0.415
17.0	0.526	15.0	0.603	15.0	0.619
19.0	0.684	17.0	0.774	17.0	0.760
21.0	0.814	19.0	0.877	19.0	0.861
23.0	0.900	21.0	0.942	21.1	0.933
25.0	0.951	23.0	0.973	23.0	0.956
27.0	0.977	25.0	0.981	25.0	0.978
29.0	0.989	27.0	0.988	27.0	0.988
31.0	0.993	29.0	0.992	29.0	0.992
33.0	0.994	31.0	0.996	31.0	0.996
35.0	1.000	33.0	0.998	33.0	0.998
		35.0	0.998	35.0	0.998
		37.0	1.000	37.0	1.000
				39.0	1.000

Table H.XIII Experimental Data for Breakthrough Curves : Binary Mixtures of Acetaldehyde and Propionaldehyde on Silica Gel

TIME (min)	CA/CAO	CP/CPD	TIME (min)	CA/CAO	CP/CPD
RUN # S-AP1			RUN # S-AP2		
13.0	0.000	0.000	11.3	0.000	0.000
13.6	0.164	0.000	11.8	0.057	0.000
13.9	0.574	0.000	12.2	0.198	0.000
14.3	0.966	0.000	12.5	0.456	0.000
15.0	1.495	0.000	13.0	1.075	0.000
16.0	1.667	0.000	14.0	1.557	0.000
18.0	1.714	0.000	15.5	1.681	0.000
20.0	1.417	0.370	17.0	1.596	0.107
22.0	1.163	0.715	18.5	1.349	0.438
24.5	1.045	0.883	20.0	1.161	0.724
26.5	1.003	0.929	22.0	1.048	0.859
29.0	1.004	0.958	24.0	1.023	0.919
31.0	0.997	0.963	26.0	1.000	0.954
33.0	1.000	0.946	28.0	1.000	0.960
35.0	1.000	0.992	30.0	0.991	0.973
37.0	1.000	0.995	32.0	0.998	0.972
39.0	1.000	1.000	34.0	1.000	0.985
			37.0	1.000	1.000
RUN # S-AP3			RUN # S-AP4		
14.3	0.000	0.000	15.5	0.000	0.000
14.8	0.035	0.000	16.1	0.326	0.000
15.2	0.196	0.000	16.4	0.711	0.000
15.5	0.465	0.000	16.8	1.039	0.000
16.0	0.963	0.000	17.3	1.457	0.000
17.0	1.255	0.000	18.5	1.691	0.000
18.5	1.309	0.000	20.0	1.773	0.000
20.0	1.388	0.000	22.0	1.529	0.101
21.0	1.357	0.000	23.0	1.506	0.302
22.0	1.354	0.000	24.0	1.337	0.525
24.0	1.340	0.000	25.0	1.195	0.671
25.5	1.300	0.158	27.0	1.080	0.845
27.0	1.194	0.379	29.0	1.009	0.905
28.0	1.108	0.515	31.0	0.970	0.944
30.0	1.085	0.738	33.0	0.999	0.984
32.0	0.994	0.836	35.0	0.980	0.972
34.0	1.016	0.942	37.0	1.000	1.000
37.0	1.000	0.965	40.0	1.010	1.018
40.0	1.000	0.973	43.0	1.000	1.000
47.0	1.000	0.977			
50.0	1.000	0.980			
55.0	1.000	1.000			
RUN # S-AP5					
15.3	0.000	0.000	25.0	1.082	0.891
15.8	0.182	0.000	26.0	1.051	0.917
16.2	0.526	0.000	27.0	1.020	0.934
16.5	0.928	0.000	29.0	0.976	0.947
17.0	1.690	0.000	31.0	0.992	0.984
18.0	2.216	0.000	33.0	1.000	0.993
20.0	1.938	0.279	35.0	1.000	1.000
21.0	1.622	0.564			
23.0	1.261	0.771			
24.0	1.139	0.846			

Table H.XIV Experimental Data for Breakthrough Curves : Binary Mixtures of Propionaldehyde and Butyraldehyde on Silica Gel

TIME (min)	CP/CPO	CB/CBO	TIME (min)	CP/CPO	CB/CBO
RUN # S-PB1			RUN # S-PB2		
15.0	0.000	0.000	14.0	0.000	0.000
16.0	0.072	0.000	14.8	0.264	0.000
16.3	0.262	0.000	15.2	0.700	0.000
16.7	0.548	0.000	15.5	1.018	0.000
17.0	0.652	0.000	16.0	1.403	0.000
17.5	1.162	0.000	16.5	1.647	0.000
18.0	1.600	0.000	17.5	1.742	0.000
19.0	1.669	0.000	19.0	1.691	0.131
20.0	1.564	0.053	21.0	1.467	0.443
22.0	1.442	0.268	23.0	1.280	0.689
24.0	1.320	0.541	26.0	1.153	0.871
27.0	1.203	0.783	29.0	1.082	0.941
31.0	1.100	0.900	34.0	1.029	0.966
36.0	1.058	0.982	39.0	1.028	0.997
41.0	1.006	0.990	44.0	1.060	1.000
47.0	1.000	1.000	49.0	1.016	1.000
			52.0	1.000	1.000
RUN # S-PB3			RUN # S-PB4		
20.0	0.000	0.000	20.5	0.000	0.000
20.8	0.254	0.000	21.3	0.157	0.000
21.2	0.412	0.000	21.7	0.413	0.000
21.5	0.607	0.000	22.0	0.585	0.000
22.0	1.008	0.000	22.5	0.993	0.000
22.5	1.297	0.000	23.0	1.384	0.000
23.5	1.538	0.000	24.0	1.862	0.051
25.0	1.598	0.000	25.0	1.980	0.143
27.0	1.619	0.048	26.0	1.954	0.257
29.0	1.556	0.202	28.0	1.691	0.501
31.0	1.449	0.411	30.0	1.461	0.670
33.0	1.305	0.586	32.0	1.369	0.856
36.0	1.185	0.765	35.0	1.185	0.864
39.0	1.150	0.887	39.0	1.097	0.910
44.0	1.073	0.957	44.0	1.080	0.982
49.0	1.065	1.000	49.0	1.050	1.010
52.0	1.020	1.000	55.0	1.038	0.999
55.0	1.000	1.000	60.0	1.000	1.000
RUN # S-PB5					
20.0	0.000	0.000	27.0	1.335	0.000
20.3	0.039	0.000	29.0	1.300	0.000
20.6	0.253	0.000	31.0	1.319	0.086
20.9	0.556	0.000	34.0	1.228	0.309
21.3	0.762	0.000	39.0	1.049	0.603
21.8	1.036	0.000	44.0	1.056	0.813
22.8	1.186	0.000	49.0	1.000	0.891
23.0	1.250	0.000	54.0	1.000	0.910
24.0	1.311	0.000	57.0	1.000	0.950
25.0	1.347	0.000	60.0	1.000	1.000

Table H.XV Experimental Data for Breakthrough Curves : Binary Mixtures of Acetaldehyde and Butyraldehyde on Silica Gel

TIME (min)	CA/CAO	CB/CBO	TIME (min)	CA/CAO	CB/CBO
RUN # S-AB1			RUN # S-AB2		
15.0	0.000	0.000	14.0	0.000	0.000
15.5	0.106	0.000	14.5	0.035	0.000
15.8	0.376	0.000	15.0	0.354	0.000
16.2	0.779	0.000	15.3	0.789	0.000
16.5	1.020	0.000	15.8	1.115	0.000
17.0	1.359	0.000	16.3	1.421	0.000
17.5	1.493	0.000	16.8	1.503	0.000
18.5	1.575	0.000	17.5	1.503	0.000
19.5	1.693	0.000	18.5	1.522	0.000
21.0	1.709	0.000	20.0	1.629	0.000
23.0	1.724	0.000	22.0	1.670	0.000
26.0	1.724	0.000	24.0	1.684	0.000
28.0	1.540	0.170	25.0	1.683	0.000
29.0	1.416	0.361	26.0	1.618	0.058
30.0	1.325	0.510	27.0	1.432	0.273
32.0	1.180	0.745	28.0	1.300	0.470
34.0	1.090	0.861	29.0	1.192	0.662
37.0	1.030	0.920	30.0	1.160	0.775
39.0	1.027	0.929	32.0	1.099	0.926
44.0	1.050	0.985	34.0	1.040	0.970
49.0	1.000	1.000	36.0	1.000	0.985
			40.0	1.000	1.000
RUN # S-AB3			RUN # S-AB4		
19.0	0.000	0.000	23.0	0.000	0.000
19.8	0.020	0.000	23.6	0.256	0.000
20.1	0.172	0.000	23.9	0.658	0.000
20.4	0.394	0.000	24.2	1.030	0.000
20.8	0.452	0.000	25.2	2.157	0.000
21.4	0.817	0.000	26.2	2.310	0.000
22.5	1.389	0.000	28.0	2.392	0.000
24.0	1.544	0.000	29.0	2.389	0.000
26.0	1.584	0.000	32.0	2.222	0.144
28.0	1.704	0.000	33.5	1.588	0.521
30.0	1.721	0.000	34.5	1.374	0.696
32.0	1.715	0.000	35.0	1.321	0.750
34.0	1.740	0.000	37.0	1.122	0.840
36.0	1.676	0.055	39.0	1.069	0.910
38.0	1.477	0.266	41.0	1.042	0.969
39.5	1.310	0.490	44.0	1.000	0.963
41.0	1.218	0.688	47.0	1.000	0.985
44.1	1.151	0.938	50.0	1.000	1.000
47.0	1.050	0.985			
50.0	1.000	1.000			

(Table H.XV continued)

TIME (min)	CA/CA0	CB/CB0
RUN # S-AB5		
17.0	0.000	0.000
17.8	0.144	0.000
18.2	0.407	0.000
18.5	0.670	0.000
19.0	0.970	0.000
20.0	1.173	0.000
22.0	1.244	0.000
24.0	1.272	0.000
26.5	1.272	0.000
29.0	1.279	0.000
31.0	1.279	0.000
33.0	1.290	0.000
35.0	1.272	0.000
37.0	1.244	0.000
40.0	1.180	0.000
42.0	1.160	0.000
45.0	1.100	0.198
46.0	1.090	0.410
48.0	1.076	0.615
51.0	1.034	0.842
54.0	1.008	0.905
57.0	1.000	0.937
60.0	1.000	0.947
63.0	1.000	0.953
66.0	1.000	0.958
69.0	1.000	0.963
72.0	1.000	0.980
75.0	1.000	1.000

Table H.XVI Experimental Data for Breakthrough Curves :  
Ternary Mixtures of Aldehydes on Silica Gel

TIME (min)	CA/CA0	CP/CP0	CB/CB0	TIME (min)	CA/CA0	CP/CP0	CB/CB0
RUN # S-APB1				RUN # S-APB2			
10.0	0.000	0.000	0.000	14.0	0.000	0.000	0.000
10.3	0.023	0.000	0.000	14.8	0.289	0.000	0.000
10.5	0.577	0.000	0.000	15.2	0.887	0.000	0.000
10.8	0.825	0.000	0.000	15.5	0.897	0.000	0.000
11.0	1.153	0.000	0.000	16.0	1.572	0.000	0.000
11.5	1.676	0.000	0.000	17.0	2.308	0.034	0.000
12.5	1.978	0.038	0.000	18.0	2.343	0.325	0.000
14.0	1.725	0.572	0.000	19.0	2.069	0.817	0.000
15.0	1.470	1.006	0.000	21.0	1.592	1.508	0.019
16.5	1.236	1.332	0.000	23.0	1.285	1.634	0.171
18.0	1.126	1.412	0.053	24.0	1.186	1.543	0.289
20.0	1.083	1.389	0.273	26.0	1.113	1.384	0.523
22.0	1.027	1.217	0.524	27.0	1.078	1.288	0.603
24.0	1.000	1.118	0.686	29.0	1.190	1.168	0.699
26.0	1.000	1.099	0.810	31.0	1.035	1.149	0.798
28.0	0.990	1.035	0.862	33.0	0.972	1.083	0.861
30.0	1.002	1.036	0.924	36.0	1.026	1.078	0.925
34.0	0.997	1.000	0.940	40.0	1.006	1.038	0.940
39.0	1.000	1.000	0.963	44.0	0.992	1.019	0.953
44.0	1.000	1.000	0.974	49.0	1.000	1.010	0.952
48.0	1.000	1.000	0.986	52.0	1.000	1.000	0.985
50.0	1.000	1.000	1.000	55.0	1.000	1.000	1.000
RUN # S-APB3				RUN # S-APB4			
12.5	0.000	0.000	0.000	17.5	0.000	0.000	0.000
13.0	0.209	0.000	0.000	18.1	0.207	0.000	0.000
13.3	0.395	0.000	0.000	18.4	0.477	0.000	0.000
13.7	0.556	0.000	0.000	18.8	0.698	0.000	0.000
14.3	1.421	0.000	0.000	19.3	1.291	0.000	0.000
15.0	1.900	0.000	0.000	20.0	1.930	0.000	0.000
16.0	2.077	0.104	0.000	21.5	2.241	0.000	0.000
17.5	1.860	0.538	0.000	23.0	2.196	0.191	0.000
19.0	1.573	0.997	0.000	24.0	1.989	0.453	0.000
21.0	1.310	1.323	0.000	26.0	1.561	0.984	0.000
22.0	1.227	1.373	0.036	28.0	1.324	1.258	0.000
24.0	1.173	1.413	0.154	30.0	1.231	1.440	0.000
26.0	1.095	1.310	0.338	32.0	1.159	1.470	0.000
28.0	1.038	1.185	0.501	34.0	1.097	1.455	0.080
30.0	1.018	1.188	0.672	36.0	1.104	1.440	0.199
32.0	1.003	1.119	0.786	39.0	1.052	1.281	0.464
34.0	1.000	1.057	0.850	41.0	1.032	1.184	0.619
39.0	1.000	1.025	0.936	45.0	1.032	1.098	0.793
44.0	1.000	1.000	0.958	49.0	1.000	1.018	0.857
49.0	1.000	1.000	0.970	53.0	0.990	0.998	0.900
52.0	1.000	1.000	0.980	57.0	1.001	1.000	0.934
55.0	1.000	1.000	0.990	61.0	1.000	1.000	0.939
60.0	1.000	1.000	1.000	65.0	1.000	1.000	0.975
				69.0	1.000	1.000	0.985
				72.0	1.000	1.000	0.990
				75.0	1.000	1.000	1.000

(Table H.XVI continued)

TIME (min)	CA/CA0	CP/CPO	CB/CBO	TIME (min)	CA/CA0	CP/CPO	CB/CBO
RUN # S-APB5				RUN # S-APB6			
16.0	0.000	0.000	0.000	12.5	0.000	0.000	0.000
16.6	0.255	0.000	0.000	13.3	0.037	0.000	0.000
16.9	0.568	0.000	0.000	13.7	0.115	0.000	0.000
17.3	0.945	0.000	0.000	14.0	0.244	0.000	0.000
17.8	1.654	0.000	0.000	14.8	0.918	0.000	0.000
18.8	2.129	0.000	0.000	15.8	1.383	0.000	0.000
20.0	2.226	0.000	0.000	17.0	1.553	0.000	0.000
21.5	2.021	0.313	0.000	18.5	1.622	0.000	0.000
22.5	1.726	0.703	0.000	20.0	1.592	0.067	0.000
24.0	1.387	1.157	0.000	22.0	1.402	0.524	0.000
26.0	1.179	1.411	0.000	24.0	1.224	1.027	0.000
28.0	1.115	1.523	0.000	26.0	1.164	1.280	0.000
30.0	1.076	1.533	0.000	28.0	1.101	1.402	0.000
32.0	1.004	1.435	0.133	30.0	1.044	1.434	0.000
34.0	1.059	1.416	0.337	32.0	1.077	1.454	0.068
37.0	1.040	1.118	0.646	34.0	1.006	1.355	0.228
39.0	1.041	1.119	0.800	36.0	1.052	1.274	0.432
43.0	1.016	1.030	0.919	40.0	1.011	1.136	0.704
47.3	1.016	1.009	0.967	44.0	1.032	1.089	0.853
51.0	1.010	1.004	0.989	48.0	0.995	1.025	0.896
53.0	1.009	1.000	1.000	52.0	1.003	1.018	0.928
55.0	1.000	1.000	1.000	56.0	1.000	1.006	0.933
60.0	1.000	1.000	1.000	60.0	1.000	1.000	0.949
				65.0	1.000	1.000	0.965
				70.0	1.000	1.000	0.990
				75.0	1.000	1.000	1.000
RUN # S-APB7							
14.3	0.000	0.000	0.000				
14.8	0.273	0.000	0.000				
15.2	0.826	0.000	0.000				
15.5	1.482	0.000	0.000				
16.0	2.243	0.000	0.000				
17.0	2.446	0.188	0.000				
18.5	1.832	0.683	0.000				
20.5	1.378	1.043	0.000				
22.0	1.234	1.165	0.000				
24.0	1.106	1.241	0.000				
26.0	1.068	1.251	0.000				
28.5	1.029	1.235	0.104				
31.0	1.012	1.184	0.295				
33.0	0.994	1.115	0.442				
35.0	1.003	1.102	0.584				
37.0	1.000	1.087	0.722				
39.0	1.000	1.050	0.805				
43.0	1.000	1.015	0.890				
47.0	1.000	1.002	0.920				
51.0	1.000	1.000	0.950				
55.0	1.000	1.000	0.972				
59.0	1.000	1.000	0.985				
65.0	1.000	1.000	1.000				

Table H.XVII Experimental Data for Breakthrough Curves :  
Binary Mixtures of Acetaldehyde and Butyraldehyde  
on Molecular Sieve-13X

TIME (min)	CA/CAO	CB/CBO	TIME (min)	CA/CAO	CB/CBO
RUN # M-AB1			RUN # M-AB2		
8.0	0.000	0.000	8.0	0.000	0.000
9.0	0.088	0.099	9.0	0.013	0.000
11.0	0.265	0.285	11.0	0.163	0.033
13.0	0.469	0.495	13.0	0.428	0.137
15.0	0.637	0.668	15.0	0.672	0.279
17.0	0.752	0.800	17.0	0.841	0.388
19.0	0.814	0.905	19.0	0.940	0.508
21.0	0.845	0.964	21.0	1.021	0.634
23.0	0.869	0.987	23.0	1.034	0.754
25.0	0.896	0.996	25.0	1.029	0.858
27.0	0.918	0.999	27.0	1.014	0.918
29.0	0.936	1.000	29.0	1.002	0.967
31.0	0.951	1.000	31.0	1.000	0.985
33.0	0.958	1.000	33.0	1.000	0.995
35.0	0.969	1.000	35.0	1.000	1.000
37.0	0.976	1.000			
39.0	0.980	1.000			
41.0	0.987	1.000			
43.0	0.996	1.000			
45.0	1.000	1.000			
RUN # M-AB3					
TIME (min)	CA/CAO	CB/CBO			
16.0	0.000	0.000			
17.0	0.049	0.014			
19.0	0.142	0.068			
21.0	0.341	0.158			
23.0	0.531	0.274			
25.0	0.704	0.391			
27.0	0.847	0.500			
29.0	0.973	0.601			
31.0	1.022	0.693			
33.0	1.062	0.774			
35.0	1.071	0.845			
37.0	1.064	0.897			
39.0	1.062	0.929			
41.0	1.033	0.954			
43.0	1.024	0.967			
45.0	1.013	0.978			
47.0	1.007	0.989			
49.0	1.000	0.992			
51.0	0.996	1.000			
53.0	0.996	1.000			



Table H.XVIII Experimental Data for Breakthrough Curves : Binary Mixtures of Acetaldehyde and Propionaldehyde on Molecular Sieve-13X

TIME (min)	CA/CAO	CP/CPO	TIME (min)	CA/CAO	CP/CPO
RUN # M-AP1			RUN # M-AP3		
14.0	0.000	0.000	10.0	0.000	0.000
15.0	0.054	0.014	11.0	0.025	0.002
17.0	0.219	0.078	13.0	0.189	0.066
19.0	0.433	0.186	15.0	0.436	0.191
21.0	0.637	0.302	17.0	0.668	0.351
23.0	0.814	0.419	19.0	0.883	0.494
25.0	0.958	0.529	21.0	1.020	0.600
27.0	1.068	0.622	23.0	1.097	0.710
29.0	1.127	0.698	25.0	1.106	0.797
32.0	1.139	0.802	27.0	1.101	0.864
34.0	1.120	0.855	29.0	1.081	0.915
36.0	1.097	0.895	31.0	1.060	0.943
38.0	1.075	0.920	33.0	1.045	0.965
40.0	1.059	0.949	35.0	1.026	0.977
42.0	1.042	0.964	37.0	1.020	0.991
44.0	1.026	0.969	39.0	1.014	1.000
46.0	1.023	0.976	41.0	1.002	1.000
48.0	1.014	0.985	43.0	1.006	1.000
50.0	1.009	0.995	45.0	1.002	1.000
52.0	1.003	0.997	47.0	1.000	1.000
54.0	1.002	1.000			
56.0	1.002	1.007			
58.0	1.000	1.000			

Table H.XIX Experimental Data for Breakthrough Curves : Binary Mixtures of Propionaldehyde and Butyraldehyde on Molecular Sieve-13X

TIME (min)	CP/CPO	CB/CBO	TIME (min)	CP/CPO	CB/CBO
RUN # M-PB2			RUN # M-PB3		
10.0	0.000	0.000	10.0	0.000	0.000
11.0	0.026	0.011	11.0	0.065	0.045
13.0	0.131	0.136	13.0	0.169	0.142
15.0	0.306	0.286	15.0	0.322	0.268
17.0	0.485	0.477	17.0	0.478	0.464
19.0	0.647	0.662	19.0	0.612	0.615
21.0	0.772	0.817	21.0	0.725	0.732
23.0	0.849	0.916	23.0	0.816	0.852
25.0	0.903	0.975	25.0	0.883	0.933
27.0	0.933	0.992	27.0	0.929	0.964
29.0	0.953	0.997	29.0	0.952	0.986
31.0	0.966	1.000	31.0	0.967	0.994
33.0	0.976	1.000	33.0	0.976	0.997
35.0	0.979	1.000	35.0	0.985	1.000
37.0	0.989	1.000	37.0	0.991	1.000
39.0	0.991	1.000	39.0	0.994	1.000
41.0	0.993	1.000	41.0	1.000	1.000
43.0	0.998	1.000			
45.0	1.000	1.000			

Table H.XX Experimental Data for Breakthrough Curves : Ternary Mixtures of Aldehydes on Molecular Sieve-13X

TIME (min)	CA/CA0	CP/CP0	CB/CB0	TIME (min)	CA/CA0	CP/CP0	CB/CB0
RUN # M-APB1				RUN # M-APB5			
6.0	0.000	0.000	0.000	6.0	0.000	0.000	0.000
7.0	0.211	0.189	0.212	7.0	0.049	0.036	0.033
9.0	0.523	0.456	0.532	9.0	0.248	0.179	0.154
11.0	0.738	0.642	0.774	11.0	0.531	0.389	0.355
13.0	0.828	0.756	0.932	13.0	0.773	0.584	0.572
15.0	0.839	0.822	1.000	15.0	0.936	0.733	0.745
17.0	0.864	0.876	1.018	17.0	1.004	0.832	0.871
19.0	0.899	0.909	1.022	19.0	1.004	0.893	0.949
21.0	0.932	0.931	1.018	21.0	1.000	0.936	0.991
23.0	0.946	0.945	1.016	23.0	0.996	0.958	1.005
25.0	0.961	0.960	1.012	25.0	0.996	0.972	1.012
27.0	0.971	0.978	1.008	28.0	1.002	0.994	1.019
29.0	0.982	0.978	1.004	30.0	0.996	0.987	1.000
31.0	0.986	0.982	1.004	32.0	0.996	0.989	0.998
33.0	0.989	0.985	1.002	34.0	0.998	0.994	1.000
35.0	0.993	0.985	1.000	36.0	1.000	0.998	1.000
37.0	0.993	0.989	1.000	38.0	1.000	1.000	1.000
39.0	1.000	0.993	1.000				
41.0	1.000	0.989	1.000				
43.0	1.000	0.993	1.000				
45.0	1.000	1.000	1.000				
RUN # M-APB6				RUN # M-APB7			
8.0	0.000	0.000	0.000	8.0	0.000	0.000	0.000
9.0	0.073	0.044	0.041	9.0	0.097	0.057	0.048
11.0	0.275	0.195	0.165	11.0	0.350	0.210	0.191
14.0	0.657	0.479	0.449	13.0	0.623	0.403	0.372
16.0	0.842	0.634	0.616	16.0	0.924	0.640	0.625
18.0	0.970	0.757	0.756	18.0	1.025	0.753	0.761
20.0	1.020	0.852	0.878	20.0	1.055	0.848	0.878
22.0	1.005	0.915	0.948	22.0	1.044	0.908	0.943
24.0	1.005	0.956	0.986	24.0	1.023	0.943	0.970
26.0	1.002	0.968	1.005	26.0	1.009	0.952	0.986
28.0	1.000	0.977	1.005	28.0	1.004	0.972	1.000
30.0	1.000	0.986	1.007	30.0	1.002	0.974	1.005
32.0	1.000	0.993	1.005	32.0	1.000	0.986	1.000
34.0	1.000	0.996	1.002	34.0	1.000	0.995	1.000
36.0	1.000	0.996	1.000	36.0	1.000	0.995	1.000
38.0	1.000	1.000	1.000	38.0	1.000	0.998	1.000
37.0	0.993	0.989	1.000	40.0	1.000	0.998	1.000
39.0	1.000	0.993	1.000	42.0	1.000	1.000	1.000

VITA

Tushar Kanti Ghosh

Candidate for the Degree of  
Doctor of Philosophy

Thesis: ADSORPTION OF ACETALDEHYDE, PROPIONALDEHYDE, AND  
BUTYRALDEHYDE ON SILICA GEL AND MOLECULAR SIEVE-13X

Major Field: Chemical Engineering

Biographical:

Personal Data: Born in West Bengal, India, January 9,  
1959, the son of Renuka and Kanai Lal Ghosh.

Education: Graduated from South Suburban School (Main),  
Calcutta, India, In August, 1975; received Bachelor  
of Chemical Engineering degree from University of  
Jadavpur, India, in August, 1980; received Master of  
Science degree in Chemical Engineering from  
University of Calgary, Alberta, Canada, in June,  
1985; completed requirements for the Doctor of  
Philosophy degree at Oklahoma State University in  
July, 1989.

Professional Experience: Teaching and Research  
Assistant, Chemical and Petroleum Engineering  
department, University of Calgary, Calgary, Alberta,  
Canada, from January, 1982, to December, 1983;  
Research Associate, Environmental Engineering  
Laboratory, Chemical and Petroleum Engineering  
Department, University of Calgary, from January,  
1984, to July, 1985. Teaching and Research Assistant,  
School of Chemical Engineering, Oklahoma State  
University, Stillwater, Oklahoma, from October, 1985,  
to present.

Membership in Professional Societies: American Institute  
of Chemical Engineering; American Chemical Society.